ParisTech
INSTITUT DES SCIENCES ET TECHNOLOGIES
PARIS INSTITUTE OF TECHNOLOGY

TELECOM ParisTech

2013-ENST-0035

EDITE - ED 130

Doctorat ParisTech

T H È S E

pour obtenir le grade de docteur délivré par

TELECOM ParisTech

Spécialité « Communication et Electronique »

présentée et soutenue publiquement par

Jinyuan Chen

le 21 Juin 2013

Communication au sein d'un canal de broadcast avec feedback limité et retardé : Limites fondamentales, nouveaux encodeurs et décodeurs

Directeur de thèse : **Petros ELIA**
Co-encadrement de la thèse : **Raymond KNOPP**

Jury

M. Dirk SLOCK, Professeur, EURECOM, France	Président
Mme Daniela TUNINETTI, Professeur, University of Illinois in Chicago, US	Rapporteur
Mme Mari KOBAYASHI, Enseignant-Chercheur, SUPELEC, France	Rapporteur
M. Syed Ali JAFAR, Professeur, University of California, Irvine, US	Examinateur
M. Sheng YANG, Enseignant-Chercheur, SUPELEC, France	Examinateur
M. David GESBERT, Professeur, EURECOM, France	Examinateur

TELECOM ParisTech
école de l'Institut Télécom - membre de ParisTech

T H È S E

ParisTech
INSTITUT DES SCIENCES ET TECHNOLOGIES
PARIS INSTITUTE OF TECHNOLOGY

TELECOM ParisTech

2012-ENST-0035

EDITE - ED 130

Doctor of Philosophy ParisTech

DISSERTATION

In Partial Fulfillment of the Requirements
for the Degree of Doctor of Philosophy from

TELECOM ParisTech

Specialization « Electronics and Communications »

publicly presented and defended by

Jinyuan Chen

on 21 June 2013

Communications over the Broadcast Channel with Limited and Delayed Feedback : Fundamental Limits and Novel Encoders and Decoders

Thesis Advisors : **Petros ELIA**
Raymond KNOPP

Jury

Dirk SLOCK, Professor, EURECOM, France	President
Daniela TUNINETTI, Professor, University of Illinois in Chicago, US	Reviewer
Mari KOBAYASHI, Assistant Prof., SUPELEC, France	Reviewer
Syed Ali JAFAR, Professor, University of California, Irvine, US	Examiner
Sheng YANG, Assistant Prof., SUPELEC, France	Examiner
David GESBERT, Professor, EURECOM, France	Examiner

TELECOM ParisTech
An Institute Telecom School - Member of ParisTech

THÈSE

Acknowledgements

It is my pleasure to express my thanks to all the people who contributed in many ways to the success of this dissertation.

Many thanks must begin with my advisers, Prof. Petros Elia and Prof. Raymond Knopp. This dissertation would not have been possible without their guidance, support and encouragement. My first and sincere appreciation goes to Prof. Petros Elia. I appreciate his continuing interactions and helps, in all stages of this thesis, which made my Ph.D. experience productive and stimulating. I remember that he used to work on a paper with me overnight in the office, and that he used to discuss on a paper with me in a McDonald's store during the weekend. His attitude and enthusiasm to research inspired me to become a better researcher. I am also thankful to Prof. Raymond Knopp, whose advices and supports were invaluable to me.

In addition, I would like to thank Prof. Sheng Yang and Prof. Syed Ali Jafar for the insightful technical discussions on my topic, as well as my thesis jury members Prof. Daniela Tuninetti, Prof. Mari Kobayashi, Prof. Dirk Slock and Prof. David Gesbert for their valuable comments and encouragement.

My warm and sincere thanks now goes to all of my friends. I would like to thank Arun Singh and Erhan Yilmaz for their helps and suggestions. I would also like to thank my office-mates Paul de Kerret and Amélie Gyrard ; my lunch-mates Fidan Mehmeti, Rajeev Gangula, Robin Thomas, Ngoc-Duy Nguyen, Tien-Thinh Nguyen, Ankit Bhamri and Rui Pedro Ferreira-Da-Costa ; as well as Tania Villa, Imran Latif, Siouar Bensaid, Miltiades Filippou, Fatma Hrizi, Maha Alodeh, Haiyong Jiang, Xueliang Liu, Jinbang Chen, Rui Min, Xuran Zhao, Lusheng Wang, Kaijie Zhou, Shengyun Liu, Xinping Yi, Xiaohu Wu and other friends. During the last three years, I have had lots of good memories together with them.

Last but not least, I wish to express my deepest gratitude to my family for their love and support throughout my life. I would like to give a special thanks to my wife, Haiwen Wang, who has been at my side and has supported me in so many ways. Also, I would like to thank my lovely son, Lucas Chen, who is an exciting and special result for us, and who is bringing us happiness and hopes.

Abstract

In many multiuser wireless communications scenarios, good feedback is a crucial ingredient that facilitates improved performance. While being useful, perfect feedback is also hard and time-consuming to obtain. With this challenge as a starting point, the main work of the thesis seeks to address the simple yet elusive and fundamental question of "HOW MUCH QUALITY of feedback, AND WHEN, must one send to achieve a certain degrees-of-freedom (DoF) performance in specific settings of multiuser communications".

Emphasis is first placed on communications over the two-user multiple-input single-output (MISO) broadcast channel (BC) with imperfect and delayed channel state information at the transmitter (CSIT); a setting for which the work explores the tradeoff between *performance* on the one hand, and *CSIT timeliness and accuracy* on the other hand. The work considers a broad setting where communication takes place in the presence of a random fading process, and in the presence of a feedback process that, at any point in time, may or may not provide CSIT estimates - of some arbitrary quality - for any past, current or future channel realization. This feedback quality may fluctuate in time across all ranges of CSIT accuracy and timeliness, ranging from perfectly accurate and instantaneously available estimates, to delayed estimates of minimal accuracy. Under standard assumptions, the work derives the DoF region, which is tight for a large range of CSIT quality. This derived DoF region concisely captures the effect of channel correlations, the accuracy of predicted, current, and delayed-CSIT, and generally captures the effect of the quality of CSIT offered at any time, about any channel.

The work also introduces novel schemes which - in the context of imperfect and delayed CSIT - employ encoding and decoding with a phase-Markov structure. The results hold for a large class of block and non-block fading channel models, and they unify and extend many prior attempts to capture the effect of imperfect and delayed feedback. This generality also allows for consideration of novel pertinent settings, such as the new *periodically evolving feedback* setting, where a gradual accumulation of feedback bits progressively improves CSIT as time progresses across a finite coherence period.

The above results are achieved for the two-user MISO-BC, and are then immediately extended to the two-user multiple-input multiple-output (MIMO)

BC and MIMO interference channel (MIMO IC) settings, again in the presence of a random fading process, and in the presence of a feedback process that, at any point in time, may or may not provide CSIT estimates - of some arbitrary quality - for any past, current or future channel realization. Under standard assumptions, and in the presence of M antennas per transmitter and N antennas per receiver, the work derives the DoF region, which is optimal for a large regime of CSIT quality. In addition to the progress towards describing the limits of using such imperfect and delayed feedback in MIMO settings, the work offers different insights that include the fact that, an increasing number of receive antennas can allow for reduced quality feedback, as well as that no CSIT is needed for the direct links in the IC.

Then, the work considers the more general setting of the K-user MISO broadcast channel, where a transmitter with M antennas transmits information to K single-antenna users, and where again, the quality and timeliness of CSIT is imperfect. In this multiuser setting, the work establishes bounds on the tradeoff between DoF performance and CSIT feedback quality. Specifically, this work provides a novel DoF region outer bound for the general K-user $M \times 1$ MISO BC with imperfect quality current-CSIT, which naturally bridges the gap between the case of having no current CSIT (only delayed CSIT, or no CSIT) and the case with full CSIT. In this setting, the work then characterizes the minimum current CSIT feedback that is necessary to achieve any sum DoF point. This characterization is optimal for the case where $M \geq K$, and the case where $M = 2,\ K = 3$.

Moving towards a different direction, the work also considers another aspect of communicating with imperfect and delayed feedback, i.e., the aspect of having additional imperfection on the receiver estimates of the channel of the other receiver (global CSIR), in addition to the imperfection on the CSIT. The work focuses on a MIMO broadcast channel with fixed-quality imperfect delayed CSIT and imperfect delayed global CSIR, and proceeds to present schemes and DoF bounds that are often tight, and to constructively reveal how even substantially imperfect delayed-CSIT and substantially imperfect delayed-global CSIR, are in fact sufficient to achieve the optimal DoF performance previously associated to perfect delayed CSIT and perfect global CSIR.

Moving towards one another different direction, the work also considers the diversity aspect of communicating - over the two-user MISO BC - with delayed CSIT. In this setting, the work proposes a novel broadcast scheme which employs delayed CSIT and a form of interference alignment to achieve both the maximum possible DoF (2/3) as well as full diversity.

In addition to the theoretical limits and novel encoders and decoders, the work applies towards gaining insights on practical questions on topics relating to how much feedback quality (delayed, current or predicted) allows for a certain DoF performance, relating to the usefulness of delayed feedback, the usefulness of predicted CSIT, the impact of imperfections in the quality

of current and delayed CSIT, the impact of feedback timeliness and the effect of feedback delays, the benefit of having feedback symmetry by employing comparable feedback links across users, the impact of imperfections in the quality of global CSIR, and relating to how to achieve both full DoF and full diversity.

Résumé

Dans des nombreux scénarios de communication sans fil multi-utilisateurs, une bonne rétroaction est un ingrédient essentiel qui facilite l'amelioration des performances. Bien qu'étant utile, une rétroaction parfaite reste difficile et fastidieuse à obtenir. En considérant ce défi comme point de départ, les présents travaux cherchent à adresser la question simple et pourtant insaisissable et fondamentale suivante : " Quel niveau de qualité de la rétroaction doit-on rechercher, et à quel moment faut-il envoyer pour atteindre une certaine performance en degrés de liberté (DoF en anglais) avec des paramètres spécifiques de communications multi-utilisateurs".

L'accent est tout d'abord mis sur les communications à travers un canal de diffusion (BC en anglais) à deux utilisateurs, multi-entrées, unique sortie (MISO en anglais) avec informations imparfaites et retardées à l'émetteur de l'état du canal (CSIT en anglais), un paramètre pour lequel la présente thèse explore le compromis entre la performance et la rapidité et la qualité de la rétroaction. La présente étude considère un cadre général dans lequel la communication a lieu en présence d'un processus d'attenuation aléatoire, et en présence d'un processus de rétroaction qui, à tout moment, peut ou non fournir des estimations CSIT - d'une qualité arbitraire - pour toute réalisation passée, actuelle ou future du canal. Sous des hypothèses standard, dans cette thèse est dérivée la région DoF qui est optimale pour un large régime de qualité CSIT. Cette région capture de manière concise l'effet des corrélations de canaux, la qualité de la valeur prédite, la valeur courante et retardée du CSIT, et capture généralement l'effet de la qualité du CSIT fourni à n'importe quel moment, sur n'importe quel canal.

Les encadrements sont obtenus à l'aide de nouveaux schémas qui - dans le contexte de CSIT imparfait et retardé - sont présentés ici pour la première fois, avec encodage et décodage sur structure de phase Markovienne. Les résultats sont validés pour une grande classe de modèles de canaux d'atténuation en bloc et non-bloc, et ils unifient et étendent de nombreuses tentatives antérieures de capture de l'effet de rétroaction imparfaite et retardée. Cette généralité permet également d'examiner de nouveaux paramètres pertinents, tels que la nouvelle technique de rétroaction à évolution périodique, où une accumulation progressive de bits de rétroaction améliore progressivement le CSIT avec le temps, ce dernier progressant à travers une période de cohérence

finie.

Les résultats ci-dessus sont atteints dans le cas du MISO-BC à deux utilisateurs, et sont ensuite immédiatement étendus aux cas entrées multiples sorties multiples (MIMO) BC à deux utilisateurs et de canaux d'interférence MIMO (MIMO IC), encore une fois en présence de processus d'atténuation aléatoire, et en présence d'un processus de rétroaction qui, à tout moment, peut ou non fournir des estimations CSIT - d'une qualité arbitraire - pour toute réalisation passée, actuelle ou future du canal. Sous les hypothèses standard, et en présence de M antennes par émetteur et N antennes par récepteur, la région DoF, qui est optimale pour un large régime de qualité CSIT, est dérivée. En plus de présenter une avancée dans la description des limites d'utilisation de telles informations imparfaites et retardées dans les milieux MIMO, la presente étude propose différentes idées dont le fait qu'un nombre croissant d'antennes de réception peuvent causer la réduction de la qualité de la rétroaction, ainsi que le fait qu'aucun CSIT n'est requis pour les liens directs dans l'IC.

Dans un deuxieme temps, la thèse considère le cadre plus général de la chaîne de diffusion K-utilisateurs MISO, où un émetteur avec M antennes transmet des informations aux K utilisateurs à une seule antenne, et où, une nouvelle fois, la qualité et la rapidité du CSIT est imparfaite. Dans ce contexte multi-utilisateurs, la thèse établit des limites sur le compromis entre la performance du DoF et la qualité de la rétroaction CSIT. Plus précisément, elle fournit une nouvelle région de la borne externe DoF dans le cas general à K - utilisateurs MISO BC avec un CSIT à qualité imparfaite courante, ce qui naturellement comble le lien entre le cas sans CSIT courant (ou le CSIT est seulement retardé, ou sans CSIT) et le cas où l'on dispose d'un CSIT complet. Dans ce contexte, la présente étude caractérise alors la rétroaction CSIT à courant minimum nécessaire pour atteindre n'importe quel état de somme DoF. Cette caractérisation est optimale dans le cas où $M \geq K$, et le cas $M = 2, K = 3$.

Dans une autre perspective, l'étude considère également un autre aspect de la communication à rétroaction imparfaite et retardée : celui où une imperfection supplémentaire sur les estimations du récepteur sur le canal d'un autre récepteur (CSIR global) est présente, en plus de l' imperfection du CSIT. L'étude se concentre sur un canal de diffusion MIMO avec un CSIT de qualité donnée, imparfait et retardé, et un CSIR global imparfait et retardé. Et des schémas, ainsi que des encadrements des DoFs, souvent précises, sont présentés. L'étude continue ensuite en révélant de manière constructive comment même des CSIT sensiblement imparfaits retardés et des CSIR globaux essentiellement imparfaits retardés sont en fait suffisants pour atteindre la performance optimale en DoF qui était précédemment associée au CSIT parfait retardé et au CSIR parfait global.

En s'aventurant plus loin encore, l'étude tient également compte de l'aspect diversité de la communication - entre deux utilisateurs MISO BC -

avec CSIT retardé. Dans ce cadre, l'ouvrage propose un nouveau système de diffusion qui fait appel au CSIT retardé et à une forme d' alignement d'interférence pour obtenir à la fois le maximum DoF possible (2/3), ainsi qu'une diversité complète.

En plus de fournir des limites théoriques et des nouveaux encodeurs et décodeurs, l'étude s'applique à obtenir une meilleure comprehension sur des questions pratiques relatives à combien la qualité de rétroaction (différée, en cours ou prévue) influe sur les performances DoF. Sur des questions relatives à l'utilité de la rétroaction retardée, l'utilité du CSIT prédit, à l'impact des imperfections s

Table of Contents

List of Figures

List of Tables

Acronyms

We provide here the main acronyms used in this dissertation. The meaning of an acronym is usually indicated once, when it first occurs in the text. The English acronyms are also used for the French summary.

AWGN	Additive White Gaussian Noise
BC	Broadcast Channel
CSI	Channel State Information
CSIR	Channel State Information at the Receiver
CSIT	Channel State Information at the Transmitter
cf.	Confer (compare to, see also)
DMT	Diversity-Multiplexing Tradeoff
DoF	Degrees-of-Freedom
e.g.	exempli gratia (for the sake of example)
et al.	et alii, et alia (and others)
FDD	Frequency Division Duplex
FDMA	Frequency Division Multiple Access
QAM	Quadrature Amplitude Modulation
IC	Interference Channel
i.i.d.	Independent and Identically Distributed
i.e.	id est (that is)
MAC	Multiple Access Channel
ML	Maximum Likelihood
MMSE	Minimum Mean Square Error
MIMO	Multi-Input Multi-Output
MISO	Multi-Input Single-Output
pdf	probability density function
resp.	Respectively
SNR	Signal-to-Noise Ratio
SISO	Single-Input Single-Output
TDD	Time Division Duplex
ZF	Zero-Forcing

Notations

We summarize here the symbols and notations that are commonly used in this dissertation, with the rest notations defined in the text where they occur.

Specifically, we use the bold uppercase letters, e.g., $\boldsymbol{H}$, to refer to matrices, while bold lowercase letters, e.g., $\boldsymbol{h}$, to refer to column vectors. We use $\doteq$ to denote *exponential equality*, i.e., we write $f(P) \doteq P^B$ to denote $\lim\limits_{P\to\infty} \dfrac{\log f(P)}{\log P} = B$. Similarly $\dot{\geq}$ and $\dot{\leq}$ denote exponential inequalities. $o(\bullet)$ and $O(\bullet)$ come from the standard Landau notation, where $f(x) = o(g(x))$ implies $\lim_{x\to\infty} f(x)/g(x) = 0$, with $f(x) = O(g(x))$ implying that $\limsup_{x\to\infty} |f(x)/g(x)| < \infty$.

We also use $\boldsymbol{A} \succeq \boldsymbol{0}$ to denote that $\boldsymbol{A}$ is positive semidefinite, and use $\boldsymbol{A} \preceq \boldsymbol{B}$ to mean that $\boldsymbol{B} - \boldsymbol{A} \succeq \boldsymbol{0}$. $\boldsymbol{e}^{\perp}$ denotes a unit-norm vector orthogonal to $\boldsymbol{e}$. Logarithms are of base 2.

Other notational conventions are summarized as follows :

$\mathbb{R}, \mathbb{C}$	The sets of real and complex numbers, respectively
$\mathbb{R}^+$	The set of positive real numbers
$\lvert \bullet \rvert$	Either the magnitude of a scalar or the cardinality of a set
$(\bullet)^+$	The operation $\max(0, \bullet)$
$\lvert\lvert\boldsymbol{x}\rvert\rvert$	The Euclidian (l^2) norm of a vector
$\boldsymbol{x}^{\perp}$	A unit-norm vector orthogonal to vector $\boldsymbol{x}$
$\boldsymbol{X}^{\perp}$	A unit-norm matrix orthogonal to matrix $\boldsymbol{X}$
$\mathrm{diag}(\boldsymbol{x})$	The diagonal matrix whose diagonal entries are represented by the elements of a vector $\boldsymbol{x}$ in order
$\mathcal{CN}(\mu, \sigma^2)$	The circularly symmetric complex Gaussian distribution with mean μ and variance σ^2
$\mathbb{E}_X[\bullet]$	The expectation operator over the random variable X
$\boldsymbol{X}^*$	The conjugate operation on $\boldsymbol{X}$
$\boldsymbol{X}^{\mathsf{H}}$	The complex conjugate (Hermitian) operation on $\boldsymbol{X}$
$\boldsymbol{X}^{\mathsf{T}}$	The transpose operation on $\boldsymbol{X}$
$\lvert\lvert\boldsymbol{X}\rvert\rvert_F$	The Frobenius norm of $\boldsymbol{X}$
$\mathrm{rank}(\boldsymbol{X})$	The rank of $\boldsymbol{X}$
$\mathrm{tr}(\boldsymbol{X})$	The trace of $\boldsymbol{X}$
$\det(\boldsymbol{X})$	The determinant of $\boldsymbol{X}$

$\boldsymbol{X}^{-1}$	The inverse of $\boldsymbol{X}$
I_m	The $m \times m$ identity matrix
$\mathbf{0}$	The all-zeros matrix of appropriate dimensions

Chapter 1

Introduction

In many multiuser wireless communications scenarios, the capacity performance depends heavily on the timeliness and quality of channel state information at the transmitter (CSIT). This timeliness and quality of CSIT though may be reduced, due to the time-varying nature of wireless fading channel, as well as limited-capacity feedback links. With this challenge as a starting point, the main work of the thesis seeks to address the simple yet elusive and fundamental question of "How much quality of feedback, and when, must one send to achieve a certain performance in specific settings of multiuser communications".

1.1 Channel model

With the rapid growth of wireless connectivity, multiuser communications have received a tremendous amount of interest in the literature. In the context of multiuser communications scenarios (see for example in Fig 1.1 and in Fig 1.2), we will consider multiple-input single-output broadcast channel (MISO BC), multiple-input multiple-output BC (MIMO BC), as well as MIMO interference channel (MIMO IC).

1.1.1 MISO BC channel model

We first focus on the multiuser broadcast channel with a transmitter communicating to K receiving users, in the presence of imperfect and delayed CSIT feedback.

We begin with two user MISO BC where an M-transmit antenna transmitter communicates to two ($K = 2$) single-antenna users. For $\boldsymbol{h}_t$ and $\boldsymbol{g}_t$

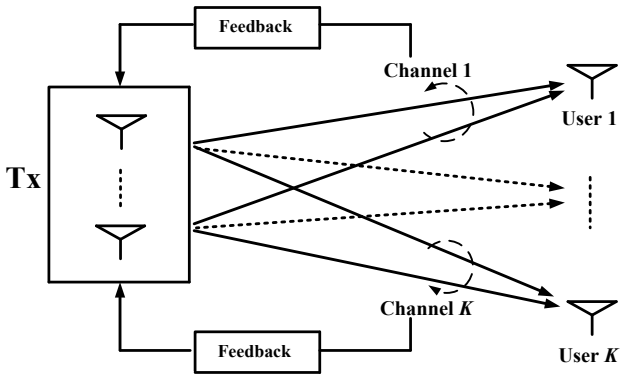

FIGURE 1.1 – System model of K-user MISO BC with CSIT feedback.

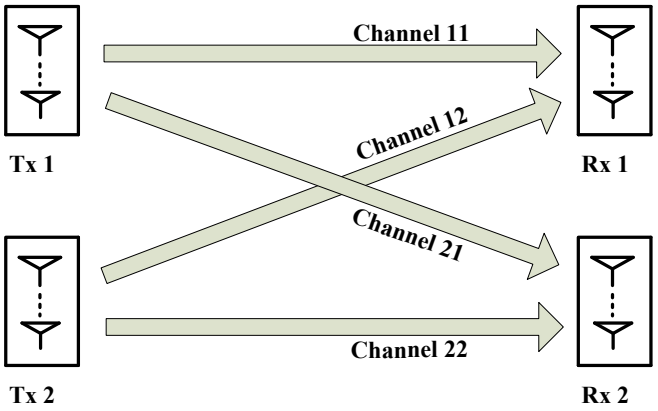

FIGURE 1.2 – System model of two-user interference channel.

denoting this channel at time t for the first and second user respectively, and for $\boldsymbol{x}_t$ denoting the transmitted vector at time t, the corresponding received signals at the first and second user take the form

$$y_t^{(1)} = \boldsymbol{h}_t^{\mathsf{T}} \boldsymbol{x}_t + z_t^{(1)} \tag{1.1}$$

$$y_t^{(2)} = \boldsymbol{g}_t^{\mathsf{T}} \boldsymbol{x}_t + z_t^{(2)} \tag{1.2}$$

$(t = 1, 2, \cdots)$, where $z_t^{(1)}, z_t^{(2)}$ denote the unit power AWGN noise at the receivers. The above transmit vectors accept a power constraint $\mathbb{E}[||\boldsymbol{x}_t||^2] \leq P = \rho$, for some power P (or ρ) which also here takes the role of the signal-to-noise ratio (SNR).

1.1.2 MIMO BC channel model

For the setting of the MIMO BC, we consider the case where an M-antenna transmitter, sends information to two receivers with N receive an-

tennas each. In this setting, the received signals at the two receivers take the form

$$\boldsymbol{y}_t^{(1)} = \boldsymbol{H}_t^{(1)}\boldsymbol{x}_t + \boldsymbol{z}_t^{(1)} \tag{1.3}$$

$$\boldsymbol{y}_t^{(2)} = \boldsymbol{H}_t^{(2)}\boldsymbol{x}_t + \boldsymbol{z}_t^{(2)} \tag{1.4}$$

where $\boldsymbol{H}_t^{(1)} \in \mathbb{C}^{N\times M}, \boldsymbol{H}_t^{(2)} \in \mathbb{C}^{N\times M}$ respectively represent the first and second receiver channels at time t, where $\boldsymbol{z}_t^{(1)}, \boldsymbol{z}_t^{(2)}$ represent unit power AWGN noise at the two receivers, where $\boldsymbol{x}_t \in \mathbb{C}^{M\times 1}$ is the input signal with power constraint $\mathbb{E}[||\boldsymbol{x}_t||^2] \leq P$.

1.1.3 MIMO IC channel model

For the setting of the MIMO IC, we consider a case where two transmitters, each with M transmit antennas, send information to their respective receivers, each having N receive antennas. In this setting, the received signals at the two receivers take the form

$$\boldsymbol{y}_t^{(1)} = \boldsymbol{H}_t^{(11)}\boldsymbol{x}_t^{(1)} + \boldsymbol{H}_t^{(12)}\boldsymbol{x}_t^{(2)} + \boldsymbol{z}_t^{(1)} \tag{1.5}$$

$$\boldsymbol{y}_t^{(2)} = \boldsymbol{H}_t^{(21)}\boldsymbol{x}_t^{(1)} + \boldsymbol{H}_t^{(22)}\boldsymbol{x}_t^{(2)} + \boldsymbol{z}_t^{(2)} \tag{1.6}$$

where $\boldsymbol{H}_t^{(11)} \in \mathbb{C}^{N\times M}, \boldsymbol{H}_t^{(22)} \in \mathbb{C}^{N\times M}$ represent the fading matrices of the direct links of the two pairs, while $\boldsymbol{H}_t^{(12)} \in \mathbb{C}^{N\times M}, \boldsymbol{H}_t^{(21)} \in \mathbb{C}^{N\times M}$, represent the fading matrices of the cross links at time t.

1.2 Degrees-of-freedom

The main work of thesis will focus on the degrees-of-freedom (DoF) performance. In the high-SNR setting of interest, for an achievable rate tuple $(R_1, R_2, \cdots, R_K)$, the corresponding degrees-of-freedom tuple $(d_1, d_2, \cdots, d_K)$ is given by

$$d_i = \lim_{P\to\infty} \frac{R_i}{\log P},\ i = 1, 2, \cdots, K.$$

The corresponding DoF region $\mathcal{D}$ is then the set of all achievable DoF tuples $(d_1, d_2, \cdots, d_K)$.

Although the main work will focus on the high-SNR regime, there is substantial evidence that, the high-SNR analysis offers good insight on the performance at moderate SNR regime.

1.3 Delay-and-quality effects of feedback

As in many multiuser wireless communications scenarios, the performance of the broadcast channel depends on the timeliness and quality of

CSIT. This timeliness and quality though may be reduced by limited-capacity feedback links, which may offer consistently low feedback quality, or may offer good quality feedback which though comes late in the communication process and can thus be used for only a fraction of the communication duration. The corresponding performance degradation, as compared to the case of having perfect feedback without delay, forces the delay-and-quality question of how much feedback is necessary, and when, in order to achieve a certain performance.

These delay-and-quality effects of feedback, naturally fall between the two extreme cases of no CSIT and of full CSIT (immediately available and perfect CSIT), for the two-user MISO BC setting, with full CSIT allowing for the optimal 1 degrees-of-freedom per user (cf., [1]), while the absence of any CSIT reduces this to just 1/2 DoF per user (cf., [2, 3]).

A valuable tool towards bridging this gap and further understanding the delay-and-quality effects of feedback, came with [4] showing that arbitrarily delayed feedback can still allow for performance improvement over the no-CSIT case. In a setting that differentiated between current and delayed CSIT - delayed CSIT being that which is available after the channel elapses, i.e., after the end of the coherence period corresponding to the channel described by this delayed feedback, while current CSIT corresponded to feedback received during the channel's coherence period - the work in [4] showed that perfect delayed CSIT, even without any current CSIT, allows for an improved 2/3 DoF per user.

Within the same context of delayed vs. current CSIT, the work in [5–8] introduced feedback quality considerations, and managed to quantify the usefulness of combining perfect delayed CSIT with immediately available imperfect CSIT of a certain quality that remained unchanged throughout the entire coherence period. In this setting the above work showed a further bridging of the gap from 2/3 to 1 DoF (two-user MISO BC case.), as a function of this current CSIT quality.

Further progress came with the work in [9] which, in addition to exploring the effects of the quality of current CSIT, also considered the effects of the quality of delayed CSIT, thus allowing for consideration of the possibility that the overall number of feedback bits (corresponding to delayed plus current CSIT) may be reduced. Focusing again on the specific setting where the current CSIT quality remained unchanged for the entirety of the coherence period, this work revealed among other things that imperfect delayed CSIT can achieve the same optimality that was previously attributed to perfect delayed CSIT, thus equivalently showing how the amount of delayed feedback required, is proportional to the amount of current feedback.

A useful generalization of the delayed vs. current CSIT paradigm, came with the work in [10] which deviated from the assumption of having invariant CSIT quality throughout the coherence period, and allowed for the possibility that current CSIT may be available only after some delay, and

specifically only after a certain fraction of the coherence period. Under these assumptions, in the presence of more than two users, and in the presence of perfect delayed CSIT, the above work showed that for up to a certain delay, one can achieve the optimal performance corresponding to full (and immediate) CSIT.

Another interesting generalization came with the work in [11] which, for the setting of the time-selective two-user MISO BC, the CSIT for the channel of user 1 and of user 2, alternate between the three extreme states of perfect current CSIT, perfect delayed CSIT, and no CSIT.

The above settings, and many other settings with imperfect and delayed CSIT, such as those in [12–32], addressed different instances of the more general problem of communicating in the presence of feedback with different delay-and-quality properties, with each of these settings being motivated by the fact that perfect CSIT may be generally hard and time-consuming to obtain, that CSIT precision may be improved over time, and that feedback delays and imperfections generally cost in terms of performance. The generalization here to the setting with general imperfect, delayed and limited CSIT, incorporates the above considerations and motivations, and allows for insight on pertinent questions such as :

- How much CSIT quality (delayed, current or predicted) allows for a certain DoF performance ?
- Can imperfect delayed CSIT achieve the same optimality that was previously attributed to perfect delayed CSIT ?
- When is delayed feedback unnecessary ?
- Is predicted CSIT useful in terms of the DoF performance ?
- Can symmetric feedback offer DoF benefit over the asymmetric feedback ?
- What is the impact of imperfect global CSIR (imperfect receiver estimates of the channel of the other receiver) ?
- Can a communication scheme achieve both full diversity and full DoF for the setting with only delayed CSIT ?

1.4 Channel and CSIT feedback process

We will first focus on the two-user MISO BC, and will consider communication of an infinite duration n (unless with specific argument), a random channel fading process $\{\boldsymbol{h}_t, \boldsymbol{g}_t\}_{t=1}^{n}$ drawn from a statistical distribution, and a feedback process that provides CSIT estimates $\{\hat{\boldsymbol{h}}_{t,t'}, \hat{\boldsymbol{g}}_{t,t'}\}_{t,t'=1}^{n}$ (of channel $\boldsymbol{h}_t, \boldsymbol{g}_t$) at any time t' - before, during, or after materialization of $\boldsymbol{h}_t, \boldsymbol{g}_t$ at time t - and does so with a certain quality

$$\{\mathbb{E}[||\boldsymbol{h}_t - \hat{\boldsymbol{h}}_{t,t'}||^2], \mathbb{E}[||\boldsymbol{g}_t - \hat{\boldsymbol{g}}_{t,t'}||^2]\}_{t,t'=1}^{n}.$$

1.5 Early, current, and delayed CSIT

For the channel $\boldsymbol{h}_t, \boldsymbol{g}_t$ at time t, the estimates $\{\hat{\boldsymbol{h}}_{t,t}, \hat{\boldsymbol{g}}_{t,t}\}$, estimates $\{\hat{\boldsymbol{h}}_{t,t'}, \hat{\boldsymbol{g}}_{t,t'}\}_{t'>t}$, and estimates $\{\hat{\boldsymbol{h}}_{t,t'}, \hat{\boldsymbol{g}}_{t,t'}\}_{t'<t}$ form what can be described as current CSIT estimates, delayed CSIT estimates and early CSIT estimates, respectively. Unlike the current CSIT estimates available at time t, the delayed CSIT estimates are available at time $t' > t$ due to the delay, while the early CSIT estimates are available at time $t' < t$ attributed to prediction.

1.6 Examples

Here let us consider some examples that are incorporated and considered in our generalization.

Example 1 (Delayed CSIT)**.** *One of the incorporated setting is the delayed CSIT (without any current CSIT) setting in [4]. Extended from the delayed CSIT setting in [4], our generalization follows and reveals that imperfect delayed CSIT can be as useful as perfect delayed CSIT.*

Example 2 (Imperfect current and delayed CSIT)**.** *Another incorporated setting is the imperfect current and delayed CSIT setting in [6, 7].*

Example 3 (Asymmetric CSIT)**.** *One another incorporated setting is the asymmetric CSIT setting in [33], where both users offered perfect delayed CSIT, but where only one user offered perfect current CSIT. Such asymmetry could reflect feedback links with different capacity or different delays.*

Example 4 (Not-so-delayed CSIT)**.** *Not-so-delayed CSIT setting in [10] is one of the incorporated setting, which corresponds to the block fading channel with periodic feedback.*

Example 5 (Alternating CSIT)**.** *Alternating CSIT setting in [11] is one of the incorporated setting, where CSIT alternates between perfect, delayed and no CSIT states.*

Example 6 (Evolving CSIT)**.** *One of the novel setting considered is the periodically evolving feedback setting over the quasi-static block fading channel, where a gradual accumulation of feedback bits results in a progressively increasing CSIT quality as time progresses across a finite coherence period. This powerful setting captures many of the engineering options relating to feedback, as well as captured many interesting settings previously considered.*

1.7 Diversity

In additon to the DoF aspect, the thesis also considers the *diversity* aspect of communicating with imperfect and delayed CSIT feedback. For P_e denoting the probability that at least one user has decoded erroneously, we recall the notion of diversity to be

$$\mathbb{d} = -\lim_{P\to\infty} \frac{\log P_e}{\log P}$$

(cf. [34]).

1.8 Global CSIR

In addition to the challenge of communicating CSIT over feedback channels with limited capacity and limited reliability, another known bottleneck is the non-negligible cost of distributing global CSIR (receiver estimates of the channel of the other receiver) across the different receiving nodes (see [35], [36]). For this reason, we explore the case where, in addition to limited and imperfect CSIT, we also have the additional imperfection of the global CSIR, which means that each user has imperfect estimates of the other user's channel, as well as, in this case, no access to the estimates of the transmitter.

1.9 Contributions and outline of the thesis

As stated, the main work of thesis seeks to address the simple yet elusive and fundamental question of "How much quality of feedback, and when, must one send to achieve a certain performance in specific settings of multiuser communications".

In Chapter 2, the work considers two-user MISO BC with imperfect and delayed CSIT, and explores the tradeoff between performance, and feedback timeliness and quality. The work considers a broad setting where communication takes place in the presence of a random fading process, and in the presence of a feedback process that, at any point in time, may or may not provide CSIT estimates - of some arbitrary quality - for any past, current or future channel realization. Under standard assumptions, the work derives the DoF region, which is optimal for a large regime of CSIT quality. This region concisely captures the effect of channel correlations, the quality of predicted, current, and delayed-CSIT, and generally captures the effect of the quality of CSIT offered at any time, about any channel. The bounds are met with novel schemes which - in the context of imperfect and delayed CSIT - introduce here for the first time, encoding and decoding with a phase-Markov structure. The results hold for a large class of block and non-block

fading channel models, and they unify and extend many prior attempts to capture the effect of imperfect and delayed feedback. This generality also allows for consideration of novel pertinent settings, such as the new periodically evolving feedback setting, where a gradual accumulation of feedback bits progressively improves CSIT as time progresses across a finite coherence period. The results were published in part at

- Jinyuan Chen and Petros Elia, "**Can Imperfect Delayed CSIT be as Useful as Perfect Delayed CSIT ? DoF Analysis and Constructions for the BC**", in *Proc. of 50th Annual Allerton Conf. Communication, Control and Computing (Allerton'12)*, October 2012.
- Jinyuan Chen and Petros Elia, "**Degrees-of-Freedom Region of the MISO Broadcast Channel with General Mixed-CSIT**", in *Proc. Information Theory and Applications Workshop (ITA'13)*, February 2013.
- Jinyuan Chen and Petros Elia, "**MISO Broadcast Channel with Delayed and Evolving CSIT**", in *Proc. IEEE Int. Symp. Information Theory (ISIT'13)*, July 2013.

and will be published in part at

- Jinyuan Chen and Petros Elia, "**Toward the Performance vs. Feedback Tradeoff for the Two-User MISO Broadcast Channel**", to appear in *IEEE Trans. Inf. Theory*, available on arXiv :1306.1751.
- Jinyuan Chen and Petros Elia, "**Optimal DoF Region of the Two-User MISO-BC with General Alternating CSIT**", to appear in *Proc. 47th Asilomar Conference on Signals, Systems and Computers (Asilomar'13)*, 2013, available on arXiv :1303.4352.

In Chapter 3, extending the results of two-user MISO BC setting, the work explores the performance of the two user multiple-input multiple-output (MIMO) BC and the two user MIMO interference channel (MIMO IC), in the presence of feedback with evolving quality and timeliness. Under standard assumptions, and in the presence of M antennas per transmitter and N antennas per receiver, the work derives the DoF region, which is optimal for a large regime of CSIT quality. This region concisely captures the effect of having predicted, current and delayed-CSIT, as well as concisely captures the effect of the quality of CSIT offered at any time, about any channel. In addition to the progress towards describing the limits of using such imperfect and delayed feedback in MIMO settings, the work offers different insights that include the fact that, an increasing number of receive antennas can allow for reduced quality feedback, as well as that no CSIT is needed for the direct links in the IC. The results were published in part at

- Jinyuan Chen and Petros Elia, "**Symmetric Two-User MIMO BC and IC with Evolving Feedback**", June 2013, available on arXiv : 1306.3710.
- Jinyuan Chen and Petros Elia, "**MIMO BC with Imperfect and Delayed Channel State Information at the Transmitter and**

Receivers", in *Proc. IEEE 14th Workshop on Signal Processing Advances in Wireless Communications (SPAWC'13)*, June 2013.

In Chapter 4, the work considers the K-user MISO BC, and establishes bounds on the tradeoff between DoF performance and CSIT feedback quality. Specifically, for the general MISO BC with imperfect current CSIT, a novel DoF region outer bound is provided, which naturally bridges the gap between the case of having no current CSIT and the case with full CSIT. The work then characterizes the minimum CSIT feedback that is necessary for any point of the sum DoF, which is optimal for many cases. The results will be published in part at

– Jinyuan Chen, Sheng Yang, and Petros Elia, "**On the Fundamental Feedback-vs-Performance Tradeoff over the MISO-BC with Imperfect and Delayed CSIT**", in *Proc. IEEE Int. Symp. Information Theory (ISIT'13)*, July 2013.

In Chapter 5, the work further considers the other fundamental aspects on the communications with imperfect and delayed feedback. One further work focuses on a MIMO broadcast channel with fixed-quality imperfect delayed CSIT and imperfect delayed global CSIR (the receiver estimates of the channel of the other receiver), and proceeds to present schemes and DoF bounds that are often tight, and to constructively reveal how even substantially imperfect delayed-CSIT and substantially imperfect delayed-global CSIR, are in fact sufficient to achieve the optimal DoF performance previously associated to perfect delayed CSIT and perfect global CSIR. Another further work studies the diversity aspect of the communication with delayed CSIT. The work proposes a novel broadcast scheme which, over broadcast channel with delayed CSIT, employs a form of interference alignment to achieve both full DoF as well as full diversity. The results were published in part at

– Jinyuan Chen, Raymond Knopp, and Petros Elia, "**Interference Alignment for Achieving both Full DOF and Full Diversity in the Broadcast Channel with Delayed CSIT**", in *Proc. IEEE Int. Symp. Information Theory (ISIT'12)*, July 2012.
– Jinyuan Chen and Petros Elia, "**MIMO BC with Imperfect and Delayed Channel State Information at the Transmitter and Receivers**", in *Proc. IEEE 14th Workshop on Signal Processing Advances in Wireless Communications (SPAWC'13)*, June 2013.

Chapter 6 finally describes the conclusions and future work.

In addition to the theoretical limits and novel encoders and decoders, the work applies towards gaining insights on practical questions on topics relating to how much feedback quality (delayed, current or predicted) allows for a certain DoF performance, relating to the usefulness of delayed feedback, the usefulness of predicted CSIT, the impact of imperfections in the quality of current and delayed CSIT, the impact of feedback timeliness and the effect of feedback delays, the benefit of having feedback symmetry by employing comparable feedback links across users, the impact of imperfections in the

quality of global CSIR, and relating to how to achieve both full DoF and full diversity.

Furthermore, in additon to the above results, some other results achieved in my PhD study were published in part at

- Jinyuan Chen, Petros Elia, and Raymond Knopp, "**Relay-Aided Interference Neutralization for the Multiuser Uplink-Downlink Asymmetric Setting**", in *Proc. IEEE Int. Symp. Information Theory (ISIT'12)*, July 2011.
- Jinyuan Chen, Arun Singh, Petros Elia and Raymond Knopp, "**Interference Neutralization for Separated Multiuser Uplink - Downlink with Distributed Relays**", in *Proc. Information Theory and Applications Workshop (ITA)*, February 2011.

Chapter 2

Fundamental Performance and Feedback Tradeoff over the Two-User MISO BC

For the two-user MISO broadcast channel with imperfect and delayed channel state information at the transmitter (CSIT), the work explores the tradeoff between *performance* on the one hand, and *CSIT timeliness and accuracy* on the other hand. The work considers a broad setting where communication takes place in the presence of a random fading process, and in the presence of a feedback process that, at any point in time, may provide CSIT estimates - of some arbitrary accuracy - for any past, current or future channel realization. This feedback quality may fluctuate in time across all ranges of CSIT accuracy and timeliness, ranging from perfectly accurate and instantaneously available estimates, to delayed estimates of minimal accuracy. Under standard assumptions, the work derives the degrees-of-freedom (DoF) region, which is tight for a large range of CSIT quality. This derived DoF region concisely captures the effect of channel correlations, the accuracy of predicted, current, and delayed-CSIT, and generally captures the effect of the quality of CSIT offered at any time, about any channel.

The work also introduces novel schemes which - in the context of imperfect and delayed CSIT - employ encoding and decoding with a phase-Markov structure. The results hold for a large class of block and non-block fading channel models, and they unify and extend many prior attempts to capture the effect of imperfect and delayed feedback. This generality also allows for consideration of novel pertinent settings, such as the new *periodically evolving feedback* setting, where a gradual accumulation of feedback bits progressively

improves CSIT as time progresses across a finite coherence period.

2.1 Introduction

2.1.1 Channel model

We consider the multiple-input single-output broadcast channel (MISO BC) with an M-transmit antenna ($M \geq 2$) transmitter communicating to two receiving users with a single receiving antenna each. Let $\boldsymbol{h}_t, \boldsymbol{g}_t$ denote the channel of the first and second user respectively at time t, and let $\boldsymbol{x}_t$ denote the transmitted vector at time t, satisfying a power constraint $\mathbb{E}[||\boldsymbol{x}_t||^2] \leq P$, for some power P which also here takes the role of the signal-to-noise ratio (SNR). Here $\boldsymbol{h}_t$ and $\boldsymbol{g}_t$ are drawn from a random distribution, such that each has zero mean and identity covariance (spatially - but not necessarily temporally - uncorrelated), and such that $\boldsymbol{h}_t$ is linearly independent of $\boldsymbol{g}_t$ with probability 1.

In this setting, the corresponding received signals at the first and second user take the form

$$y_t^{(1)} = \boldsymbol{h}_t^\mathsf{T} \boldsymbol{x}_t + z_t^{(1)} \tag{2.1}$$

$$y_t^{(2)} = \boldsymbol{g}_t^\mathsf{T} \boldsymbol{x}_t + z_t^{(2)} \tag{2.2}$$

($t = 1, 2, \cdots$), where $z_t^{(1)}, z_t^{(2)}$ denote the unit power AWGN noise at the receivers.

In the high-SNR setting of interest, for an achievable rate pair (R_1, R_2) for the first and second user respectively, the corresponding degrees-of-freedom (DoF) pair (d_1, d_2) is given by

$$d_i = \lim_{P \to \infty} \frac{R_i}{\log P}, \ i = 1, 2$$

and the corresponding DoF region is then the set of all achievable DoF pairs.

2.1.2 Delay-and-quality effects of feedback

As in many multiuser wireless communications scenarios, the performance of the broadcast channel depends on the timeliness and precision of channel state information at the transmitter (CSIT). This timeliness and precision though may be reduced by limited-capacity feedback links, which may offer CSIT with consistently low precision and high delays, i.e., feedback that offers an inaccurate representation of the true state of the channel, as well feedback that can only be used for an insufficient fraction of the communication duration. The corresponding performance degradation, as compared to the case of having perfect feedback without delay, forces the delay-and-quality question of how much CSIT precision is necessary, and when, in order to achieve a certain performance.

2.1.3 Channel process and feedback process with predicted, current, and delayed CSIT

We here consider communication of an infinite duration n, a channel fading process $\{\boldsymbol{h}_t, \boldsymbol{g}_t\}_{t=1}^n$ drawn from a statistical distribution, and a feedback process that provides CSIT estimates

$$\{\hat{\boldsymbol{h}}_{t,t'}, \hat{\boldsymbol{g}}_{t,t'}\}_{t,t'=1}^n$$

(of channel $\boldsymbol{h}_t, \boldsymbol{g}_t$) at any time t' - before, during, or after materialization of $\boldsymbol{h}_t, \boldsymbol{g}_t$ at time t - and does so with precision/quality defined by the statistics of

$$\{(\boldsymbol{h}_t - \hat{\boldsymbol{h}}_{t,t'}), (\boldsymbol{g}_t - \hat{\boldsymbol{g}}_{t,t'})\}_{t,t'=1}^n \tag{2.3}$$

where we consider these estimation errors to have zero-mean circularly-symmetric complex Gaussian entries. Naturally any attempt to capture and meet the tradeoff between performance, and feedback timeliness and quality, must consider the full effect of the statistics of the channel and of CSIT precision $\{(\boldsymbol{h}_t - \hat{\boldsymbol{h}}_{t,t'}), (\boldsymbol{g}_t - \hat{\boldsymbol{g}}_{t,t'})\}_{t,t'=1}^n$ at any point in time, about any channel.

Predicted, current, and delayed CSIT

For the channel $\boldsymbol{h}_t, \boldsymbol{g}_t$ at time t, the set of all estimates $\{\hat{\boldsymbol{h}}_{t,t'}, \hat{\boldsymbol{g}}_{t,t'}\}_{t'=1}^n$ is formed by what can be described as the set of *predicted estimates* $\{\hat{\boldsymbol{h}}_{t,t'}, \hat{\boldsymbol{g}}_{t,t'}\}_{t'<t}$, by the *current estimates* $\hat{\boldsymbol{h}}_{t,t}, \hat{\boldsymbol{g}}_{t,t}$ at time t, and by the set of *delayed CSIT* $\{\hat{\boldsymbol{h}}_{t,t'}, \hat{\boldsymbol{g}}_{t,t'}\}_{t'>t}$ comprising of estimates that are not available at time t. Predicted CSIT may potentially allow for reduction of the effect of future interference, current CSIT may be used to 'separate' the current signals of the users, while delayed CSIT may facilitate retrospective compensation for the lack of perfect quality feedback ([4]).

2.1.4 Notation, conventions and assumptions

We will use the notation

$$\alpha_t^{(1)} \triangleq -\lim_{P\to\infty} \frac{\log \mathbb{E}[||\boldsymbol{h}_t - \hat{\boldsymbol{h}}_{t,t}||^2]}{\log P} \tag{2.4}$$

$$\alpha_t^{(2)} \triangleq -\lim_{P\to\infty} \frac{\log \mathbb{E}[||\boldsymbol{g}_t - \hat{\boldsymbol{g}}_{t,t}||^2]}{\log P} \tag{2.5}$$

to describe the *current quality exponent* for the current estimate of the channel of each user at time t ($\alpha_t^{(1)}$ is for user 1), while we will use

$$\beta_t^{(1)} \triangleq -\lim_{P\to\infty} \frac{\log \mathbb{E}[||\boldsymbol{h}_t - \hat{\boldsymbol{h}}_{t,t+\eta}||^2]}{\log P} \tag{2.6}$$

$$\beta_t^{(2)} \triangleq -\lim_{P\to\infty} \frac{\log \mathbb{E}[||\boldsymbol{g}_t - \hat{\boldsymbol{g}}_{t,t+\eta}||^2]}{\log P} \tag{2.7}$$

- for any sufficiently large but finite integer $\eta > 0$ - to denote the *delayed quality exponent* for each user. To clarify, with delayed CSIT consisting of all channel estimates that arrive after the channel materializes, the above use of a finite η, reflects the fact that we here only consider delayed CSIT that arrives up to a finite time of η channel uses from the moment the channel materializes. In words, $\alpha_t^{(1)}$ measures the precision/quality of the CSIT (about $\boldsymbol{h}_t$) that is available at time t, while $\beta_t^{(1)}$ measures the (best) quality of the CSIT (again about $\boldsymbol{h}_t$) which arrives strictly after the channel appears, i.e., strictly after time t (similarly $\alpha_t^{(2)}, \beta_t^{(2)}$ for the channel $\boldsymbol{g}_t$ of the second user).

It is easy to see that without loss of generality, in the DoF setting of interest, we can restrict our attention to the range [1]

$$0 \leq \alpha_t^{(i)} \leq \beta_t^{(i)} \leq 1 \tag{2.8}$$

where $\beta_t^{(1)} = \beta_t^{(2)} = 1$ corresponds to being able to eventually gather (asymptotically) perfect delayed CSIT for $\boldsymbol{h}_t, \boldsymbol{g}_t$, while $\alpha_t^{(1)} = \alpha_t^{(2)} = 1$, simply corresponds to having instantaneously available CSIT of asymptotically perfect precision.

Furthermore we will use the notation

$$\bar{\alpha}^{(i)} \triangleq \lim_{n\to\infty} \frac{1}{n}\sum_{t=1}^{n} \alpha_t^{(i)}, \quad \bar{\beta}^{(i)} \triangleq \lim_{n\to\infty} \frac{1}{n}\sum_{t=1}^{n} \beta_t^{(i)}, \quad i = 1, 2 \tag{2.9}$$

to denote the average of the quality exponents.

Assumptions

Our results, specifically the achievability part, will hold under the soft assumption that any sufficiently long subsequence $\{\alpha_t^{(1)}\}_{t=\tau}^{\tau+T}$ (resp. $\{\alpha_t^{(2)}\}_{t=\tau}^{\tau+T}$, $\{\beta_t^{(1)}\}_{t=\tau}^{\tau+T}$, $\{\beta_t^{(2)}\}_{t=\tau}^{\tau+T}$) has an average that approaches the long term average $\bar{\alpha}^{(1)}$ (resp. $\bar{\alpha}^{(2)}, \bar{\beta}^{(1)}, \bar{\beta}^{(2)}$), for some finite T that can be chosen to be sufficiently large to allow for the above convergence. Such an assumption - which has also been employed in works like [11] - essentially imply that the long term statistics of the feedback process, remains the same in time, i.e., that the average feedback behavior - averaged over large amounts of time - remains the same throughout the communication process.

1. To see this, we recall from [16, 17] that under a peak-power constraint of P, having CSIT estimation error in the order of P^{-1} causes no DoF reduction as compared to the perfect CSIT case. In our DoF high-SNR setting of interest where $P >> n$, this same observation also holds under an average power constraint of P. The fact that $\alpha_t^{(i)} \leq \beta_t^{(i)}$ comes naturally from the fact that one can recall, at a later time, statistically good estimates.

We also adhere to the common convention (see [4, 6, 7, 33]) of assuming perfect and global knowledge of channel state information at the receivers (perfect global CSIR), where the receivers know all channel states and all estimates. We further adopt the common assumption (see [5–7, 15]) that the current *estimation error* is statistically independent of current and past *estimates*, and consequently that the input signal is a function of the message and of the CSIT. This assumption fits well with many channel models spanning from the fast fading channel (i.i.d. in time), to the correlated channel model as this is considered in [5], to the quasi-static block fading model where the CSIT estimates are successively refined while the channel remains static (see [16], see also the discussion in the appendix in Section 2.8). Additionally we consider the entries of each estimation error vector $\boldsymbol{h}_t - \hat{\boldsymbol{h}}_{t,t'}$ (similarly of $\boldsymbol{g}_t - \hat{\boldsymbol{g}}_{t,t'}$) to be i.i.d. Gaussian, clarifying though that we are just referring to the M entries in each such specific vector $\boldsymbol{h}_t - \hat{\boldsymbol{h}}_{t,t'}$, and that we do *not* suggest that the error entries are i.i.d. in time or across users. The appendix in Section 2.8 offers further details and justification on the above assumptions and conventions.

Finally we safely assume that $\mathbb{E}[||\boldsymbol{h}_t - \hat{\boldsymbol{h}}_{t,t'}||^2] \dot{\leq} \mathbb{E}[||\boldsymbol{h}_t - \hat{\boldsymbol{h}}_{t,t''}||^2]$ (similarly $\mathbb{E}[||\boldsymbol{g}_t - \hat{\boldsymbol{g}}_{t,t'}||^2] \dot{\leq} \mathbb{E}[||\boldsymbol{g}_t - \hat{\boldsymbol{g}}_{t,t''}||^2]$), for any $t' > t''$. This assumption - which simply suggests that one can revert back to past estimates of statistically better quality - is used here for simplicity of notation, and can be removed, after a small change in the definition of the quality exponents, without an effect to the main result.

2.1.5 Prior work

The delay-and-quality effects of feedback, naturally fall between the two extreme cases of no CSIT and of full CSIT (immediately available, perfect-quality CSIT), with full CSIT allowing for the optimal 1 DoF per user (cf. [1]), while the absence of any CSIT reduces this to just 1/2 DoF per user (cf. [2, 3]).

Toward bridging this gap, different works have considered the use of imperfect and delayed feedback. For example, the work by Lapidoth, Shamai and Wigger in [15] considered the case where the amount of feedback is limited to the extent that the channel-estimation error power does not vanish with increasing SNR, in the sense that $\lim_{P\to\infty}(\log \mathbb{E}[||\boldsymbol{h}_t - \hat{\boldsymbol{h}}_{t,t}||^2])/\log P = \lim_{P\to\infty}(\log \mathbb{E}[||\boldsymbol{g}_t - \hat{\boldsymbol{g}}_{t,t}||^2])/\log P = 0$. In this setting - which corresponds to the case here where $\alpha_t^{(1)} = \alpha_t^{(2)} = \beta_t^{(1)} = \beta_t^{(2)} = 0,\ \forall t$ - the work in [15] showed that the symmetric DoF is upper bounded by 2/3 DoF per user, again under the assumption placed here that the input signaling is independent of the estimation error. It is worth noting that finding the exact DoF in this zero-exponent setting, currently remains an open problem.

At the other extreme, the work by Caire et al. [17] (see also the work

of Jindal [16], as well as of Lapidoth and Shamai [37]) showed that having immediately available CSIT estimates with estimation error power that is in the order of P^{-1} - i.e., having $-\lim_{P\to\infty}(\log \mathbb{E}[||\boldsymbol{h}_t - \hat{\boldsymbol{h}}_{t,t}||^2])/\log P = -\lim_{P\to\infty}(\log \mathbb{E}[||\boldsymbol{g}_t - \hat{\boldsymbol{g}}_{t,t}||^2])/\log P = 1,\ \forall t$, corresponding here to having $\alpha_t^{(1)} = \alpha_t^{(2)} = 1,\ \forall t$ - causes no DoF reduction as compared to the perfect CSIT case, and can thus achieve the optimal 1 DoF per user.

A valuable tool toward bridging this gap and further understanding the delay-and-quality effects of feedback, came with the work by Maddah-Ali and Tse in [4] which showed that arbitrarily delayed feedback can still allow for performance improvement over the no-CSIT case. In a fast-fading block-fading setting, the work differentiated between current and delayed CSIT - with delayed CSIT defined in [4] as the CSIT which is available after the channel's coherence period - and showed that delayed and completely obsolete CSIT, even without any current CSIT, allows for an improved optimal 2/3 DoF per user. This setting - which in principle corresponded to perfect delayed CSIT - is here represented by current-CSIT exponents of the form $\alpha_t^{(1)} = \alpha_t^{(2)} = 0,\ \forall t$.

Within the same block-fading context of delayed vs. current CSIT, the work by Kobayashi et al., Yang et al., and Gou and Jafar [5–7], quantified the usefulness of combining delayed and completely obsolete CSIT with immediately available but imperfect CSIT of a certain quality $\alpha = -\lim_{P\to\infty}(\log \mathbb{E}[||\boldsymbol{h}_t - \hat{\boldsymbol{h}}_{t,t}||^2])/\log P = -\lim_{P\to\infty}(\log \mathbb{E}[||\boldsymbol{g}_t - \hat{\boldsymbol{g}}_{t,t}||^2])/\log P$ that remained unchanged throughout the communication process. This work - which again in principle assumed perfect delayed CSIT, and which is here represented by current-CSIT exponents of the form $\alpha_t^{(1)} = \alpha_t^{(2)} = \alpha,\ \forall t$ - derived the optimal DoF region to be that with a symmetric DoF of $(2+\alpha)/3$ DoF per user. Interestingly, despite the fact that in principle, the above settings in [4–7] corresponded to perfect delayed CSIT, the actual schemes in these works in fact achieved the optimal DoF, by using delayed CSIT for only a fraction of the channels. This possibility that imperfect and sparse delayed CSIT may be as good as perfect and omnipresent delayed CSIT (cf. [9]), is one of the many facets that are explored in detail in Sections 2.2-2.3.

Another interesting approach was introduced by Tandon et al. in [11] who considered the fast-fading two-user MISO BC setting, where each user's CSIT changes every coherence period by alternating between the three extreme states of perfect current CSIT, perfect delayed CSIT, and no CSIT.

Additionally, Lee and Heath in [10] considered, in the setting of the quasi-static block-fading channel, the possibility that current CSIT may be available only after a certain fraction γ of a finite-duration coherence period T_c.

Other work such as that by Maleki et al. in [33] considered, again in the MISO BC context, an asymmetric setting where both users offered perfect delayed CSIT, but where only one user offered perfect current CSIT while

the other user offered no current CSIT. In this setting, the optimal DoF corner point was calculated to be $(1, 1/2)$ (sum-DoF $d_1 + d_2 = 3/2$). Another asymmetric-feedback setting was considered in [8].

In addition to the above works that are immediately related to our own result, many other works that have provided interesting results in the context of delayed or imperfect feedback, include [12, 13, 18–32, 38].

2.1.6 Structure

Section 2.2 will give the main result of this work by describing, under the aforementioned common assumptions, the DoF offered by a CSIT process $\{\hat{\boldsymbol{h}}_{t,t'}, \hat{\boldsymbol{g}}_{t,t'}\}_{t=1,t'=1}^{n}$ of a certain quality $\{(\boldsymbol{h}_t - \hat{\boldsymbol{h}}_{t,t'}), (\boldsymbol{g}_t - \hat{\boldsymbol{g}}_{t,t'})\}_{t=1,t'=1}^{n}$. Specifically Proposition 1 and Lemma 1 lower and upper bound the DoF region, and the resulting Theorem 1 provides the optimal DoF for a large range of 'sufficiently good' delayed CSIT. The results capture specific existing cases of interest, such as the Maddah-Ali and Tse setting in [4], the Yang et al. and Gou and Jafar setting in [6, 7], the Lee and Heath 'not-so-delayed CSIT' setting in [10] for two users, the Maleki et al. asymmetric setting in [33], and in the range of sufficiently good delayed CSIT, also capture the results in the Tandon et al. setting of alternating CSIT [11] .

Towards gaining further insight, we then proceed to provide different corollaries for specific cases of interest. Again in Section 2.2, Corollary 1a distills the main result down to the symmetric feedback case where $\bar{\alpha}^{(1)} = \bar{\alpha}^{(2)}$ and $\bar{\beta}^{(1)} = \bar{\beta}^{(2)}$, and immediately after that, Corollary 1b explores the benefits of such feedback symmetry, by quantifying the extent to which having similar feedback quality for the two users, offers a gain over the asymmetric case where one user has generally more feedback than the other. One of the outcomes here is that such 'symmetry gains' are often nonexistent. Corollary 1c generalizes the pertinent result in the setting in [33] corresponding to feedback asymmetry ; a setting which we consider to be important as it captures the inherent non-homogeneity of feedback quality of different users. Corollary 1d offers insight on the need for delayed CSIT, and shows how, reducing $\bar{\alpha}^{(1)}, \bar{\alpha}^{(2)}$ allows - to a certain extent - for further reducing of $\bar{\beta}^{(1)}, \bar{\beta}^{(2)}$, without an additional DoF penalty. It will be surprising to note that the expressions from Corollary 1d, match the amount of delayed CSIT used by different previous schemes which were designed for settings that in principle offered perfect delayed CSIT, and which were thus designed without an expressed purpose of reducing the amount of delayed CSIT. At the other extreme, Corollary 1e offers insight on the need for using predicted channel estimates (forecasting channel states in advance), by showing that - at least in the range of sufficiently good delayed CSIT - employing predicted CSIT is unnecessary.

Section 2.3 highlights the newly considered *periodically evolving feedback* setting over the quasi-static block fading channel, where a gradual accu-

mulation of feedback, results in a progressively increasing CSIT quality as time progresses across a finite coherence period. This setting is powerful as it captures the many feedback options that one may have in a block-fading environment where the *statistical* nature of feedback may remain largely unchanged across coherence periods. To offer further understanding, we provide examples which - under very clearly specified assumptions - describe how many feedback bits to introduce, and when, in order to achieve a certain DoF performance. In the same section, smaller results and examples offer further insight - again in the context of periodically evolving feedback over a quasi-static channel - like for example the result in Corollary 1g which bounds the quality of current and of delayed CSIT needed to achieve a certain target symmetric DoF, and in the process offers intuition on when delayed feedback is entirely unnecessary, in the sense that there is no need to wait for feedback that arrives after the end of the coherence period of the channel. Similarly Corollary 1h provides insight on the feedback delays that allow for a given target symmetric DoF in the presence of constraints on current and delayed CSIT qualities. This quantifies to a certain extent the intuitive argument that, with a target DoF in mind, feedback delays must be compensated for, with high quality feedback estimates.

Section 2.4 corresponds to the achievability part of the proof of the main result, and presents the general communication scheme that utilizes the available information of a CSIT process $\{\hat{\boldsymbol{h}}_{t,t'}, \hat{\boldsymbol{g}}_{t,t'}\}_{t=1,t'=1}^{n}$, to achieve the corresponding DoF corner points. This is done - by properly employing different combinations of zero forcing, superposition coding, interference compressing and broadcasting, as well as specifically tailored power and rate allocation - in order to transmit private information, using currently available CSIT estimates to reduce interference, and using delayed CSIT estimates to alleviate the effect of past interference. The scheme has a forward-backward phase-Markov structure which, in the context of imperfect and delayed CSIT, was first introduced in [8,9] to consist of four main ingredients that include, block-Markov encoding, spatial precoding, interference quantization, and backward decoding.
After the description of the scheme in its general form, and the explicit description of how the scheme achieves the different DoF corner points, Section 2.4.4 provides example schemes - distilled from the general scheme - for specific settings such as the imperfect-delayed CSIT setting, the (extended) alternating CSIT setting of Tandon et al. [11], as well as discusses schemes with small delay.

Section 2.5 offers concluding remarks, the appendix in Section 2.6 provides the details of the outer bound, the appendix in Section 2.7 offers details on the proofs, while the appendix in Section 2.8 offers a discussion on some of the assumptions employed in this work.

In the end, the above results provide insight on pertinent questions such

as :

- What CSIT feedback precision should be provided, and when, in order to achieve a certain target DoF performance ? (Theorem 1)
- When is delayed feedback unnecessary ? (Corollary 1g)
- Is there any gain in early prediction of future channels ? (Corollary 1e)
- What current-CSIT and delayed-CSIT qualities suffice to achieve a certain performance ? (Corollary 1g)
- Can delayed CSIT that is sparse and of imperfect-quality, achieve the same DoF performance that was previously attributed to sending perfect delayed CSIT ? (Corollary 1d)
- How much more valuable are feedback bits that are sent early, than those sent late ? (Section 2.3)
- In the quasi-static block-fading case, is it better to send less feedback early, or more feedback later ? (Section 2.3)
- What is the effect of having asymmetric feedback links, and when can we have a 'symmetry gain' ? (Corollary 1b)

2.2 DoF region of the MISO BC

We proceed with the main DoF results, which are proved in Section 2.4 (inner bound) and Section 2.6 (outer bound).

We here remind the reader of the sequences $\{\alpha_t^{(1)}\}_{t=1}^n$, $\{\alpha_t^{(2)}\}_{t=1}^n$, $\{\beta_t^{(1)}\}_{t=1}^n$, $\{\beta_t^{(2)}\}_{t=1}^n$ of quality exponents, as these were defined in (2.4)-(2.7), as well as of the corresponding averages $\bar{\alpha}^{(1)}, \bar{\alpha}^{(2)}, \bar{\beta}^{(1)}, \bar{\beta}^{(2)}$ from (2.9). We also remind the reader that we consider communication over an asymptotically large time duration n. We henceforth label the users so that $\bar{\alpha}^{(2)} \leq \bar{\alpha}^{(1)}$.

We start with the following proposition, the proof of which can be found in Section 2.4 which describes the scheme that achieves the corresponding DoF corner points.

Proposition 1. *The DoF region of the two-user MISO BC with a CSIT process* $\{\hat{\boldsymbol{h}}_{t,t'}, \hat{\boldsymbol{g}}_{t,t'}\}_{t=1,t'=1}^n$ *of quality* $\{(\boldsymbol{h}_t - \hat{\boldsymbol{h}}_{t,t'}), (\boldsymbol{g}_t - \hat{\boldsymbol{g}}_{t,t'})\}_{t=1,t'=1}^n$*, is inner bounded by the polygon described by*

$$d_1 \leq 1, \quad d_2 \leq 1 \tag{2.10}$$

$$2d_1 + d_2 \leq 2 + \bar{\alpha}^{(1)} \tag{2.11}$$

$$2d_2 + d_1 \leq 2 + \bar{\alpha}^{(2)} \tag{2.12}$$

$$d_1 + d_2 \leq 1 + \min\{\bar{\beta}^{(1)}, \bar{\beta}^{(2)}\}. \tag{2.13}$$

Figure 2.1 corresponds to the result in Proposition 1.

Towards tightening the above inner bound, we here draw from the DoF outer bound in [6] that focused on CSIT with invariant and symmetric quality and non-static channels, and employ techniques that allow for the new bound to hold for a broad range of channels including the static-channel case that is of particular interest here. The proof of the new bound can be found in Section 2.6.

Lemma 1. *The DoF region of the two-user MISO BC with a CSIT process* $\{\hat{\boldsymbol{h}}_{t,t'}, \hat{\boldsymbol{g}}_{t,t'}\}_{t=1,t'=1}^n$ *of quality* $\{(\boldsymbol{h}_t - \hat{\boldsymbol{h}}_{t,t'}), (\boldsymbol{g}_t - \hat{\boldsymbol{g}}_{t,t'})\}_{t=1,t'=1}^n$*, is upper bounded as*

$$d_1 \leq 1, \quad d_2 \leq 1 \tag{2.14}$$

$$2d_1 + d_2 \leq 2 + \bar{\alpha}^{(1)} \tag{2.15}$$

$$2d_2 + d_1 \leq 2 + \bar{\alpha}^{(2)}. \tag{2.16}$$

Comparing the above inner and outer bounds, and observing that the last bound in Proposition 1 becomes inactive in the range of sufficiently good delayed-CSIT where $\min\{\bar{\beta}^{(1)}, \bar{\beta}^{(2)}\} \geq \min\{\frac{1+\bar{\alpha}^{(1)}+\bar{\alpha}^{(2)}}{3}, \frac{1+\bar{\alpha}^{(2)}}{2}\}$, gives the main result of this work in the form of the following theorem that provides the optimal DoF for this large range of 'sufficiently good' delayed CSIT.

Theorem 1. *The optimal DoF region of the two-user MISO BC with a CSIT process* $\{\hat{\boldsymbol{h}}_{t,t'}, \hat{\boldsymbol{g}}_{t,t'}\}_{t=1,t'=1}^{n}$ *of quality* $\{(\boldsymbol{h}_t - \hat{\boldsymbol{h}}_{t,t'}), (\boldsymbol{g}_t - \hat{\boldsymbol{g}}_{t,t'})\}_{t=1,t'=1}^{n}$ *is given by*

$$d_1 \leq 1, \quad d_2 \leq 1 \tag{2.17}$$

$$2d_1 + d_2 \leq 2 + \bar{\alpha}^{(1)} \tag{2.18}$$

$$2d_2 + d_1 \leq 2 + \bar{\alpha}^{(2)} \tag{2.19}$$

for any sufficiently good delayed-CSIT process such that $\min\{\bar{\beta}^{(1)}, \bar{\beta}^{(2)}\} \geq \min\{\frac{1+\bar{\alpha}^{(1)}+\bar{\alpha}^{(2)}}{3}, \frac{1+\bar{\alpha}^{(2)}}{2}\}$.

As mentioned, the achievability part of the proof can be found in Section 2.4.

Figure 2.2 corresponds to the main result in the theorem.

Before proceeding to specific corollaries that offer further insight, it is worth making a comment on the fact that the entire complexity of the problem is captured by the quality exponents.

Remark 1. *The results suggest that the quality exponents capture - in the DoF setting of interest, and under our assumptions - the effect of the statistics of the CSIT precision* $\{(\boldsymbol{h}_t - \hat{\boldsymbol{h}}_{t,t'}), (\boldsymbol{g}_t - \hat{\boldsymbol{g}}_{t,t'})\}_{t,t'=1}^{n}$. *This is indeed the case since the following two hold. Firstly, given the Gaussianity of the estimation errors, the statistics of* $\{(\boldsymbol{h}_t - \hat{\boldsymbol{h}}_{t,t'}), (\boldsymbol{g}_t - \hat{\boldsymbol{g}}_{t,t'})\}_{t,t'=1}^{n}$ *are captured by the* $2n^2 \times 2n^2$ *covariance matrix*[2] *of the* $2n^2$*-length vector consisting of the elements* $\{(\boldsymbol{h}_t - \hat{\boldsymbol{h}}_{t,t'}), (\boldsymbol{g}_t - \hat{\boldsymbol{g}}_{t,t'})\}_{t,t'=1}^{n}$. *The diagonal entries of this covariance matrix are simply* $\{\frac{1}{M}\mathbb{E}[||\boldsymbol{h}_t - \hat{\boldsymbol{h}}_{t,t'}||^2], \frac{1}{M}\mathbb{E}[||\boldsymbol{g}_t - \hat{\boldsymbol{g}}_{t,t'}||^2]\}_{t,t'=1}^{n}$. *With the above in mind, we also note that the outer bound has kept open the possibility of having arbitrary off-diagonal elements in this covariance matrix (this is specifically seen in the steps in* (2.95), (2.96)*), thus allowing for the outer bound to hold irrespective of the off-diagonal elements of this covariance matrix. Consequently, under our assumptions, the essence of the statistics is captured by* $\{\mathbb{E}[||\boldsymbol{h}_t - \hat{\boldsymbol{h}}_{t,t'}||^2], \mathbb{E}[||\boldsymbol{g}_t - \hat{\boldsymbol{g}}_{t,t'}||^2]\}_{t,t'=1}^{n}$*, and its effect is captured - in the high-SNR DoF regime - by the quality exponents.*

Symmetric vs. asymmetric feedback

We proceed to explore the special case of symmetric feedback where the long-term accumulated feedback quality at the two users is similar, in the sense that the feedback links of user 1 and user 2 share the same long-term

2. This size of the covariance matrix reflects the fact that the M entries of each $\boldsymbol{h}_t - \hat{\boldsymbol{h}}_{t,t'}$ are i.i.d. (similarly of $\boldsymbol{g}_t - \hat{\boldsymbol{g}}_{t,t'}$). Please note that we refer to independence across the *spatial* dimensions of the channel of one user, and certainly do not refer to independence across time or across users.

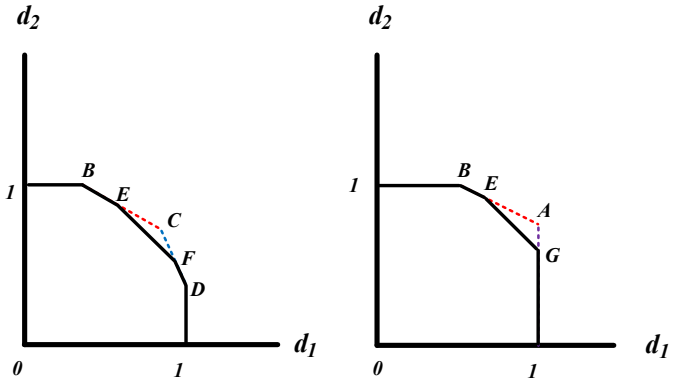

FIGURE 2.1 – DoF region inner bound for the two-user MISO BC. The corner points take the following values : $E = (2\bar{\delta} - \bar{\alpha}^{(2)}, 1 + \bar{\alpha}^{(2)} - \bar{\delta})$, $F = (1 + \bar{\alpha}^{(1)} - \bar{\delta}, 2\bar{\delta} - \bar{\alpha}^{(1)})$, and $G = (1, \bar{\delta})$, where $\bar{\delta} \triangleq \min\{\bar{\beta}^{(1)}, \bar{\beta}^{(2)}, \frac{1+\bar{\alpha}^{(1)}+\bar{\alpha}^{(2)}}{3}, \frac{1+\bar{\alpha}^{(2)}}{2}\}$.

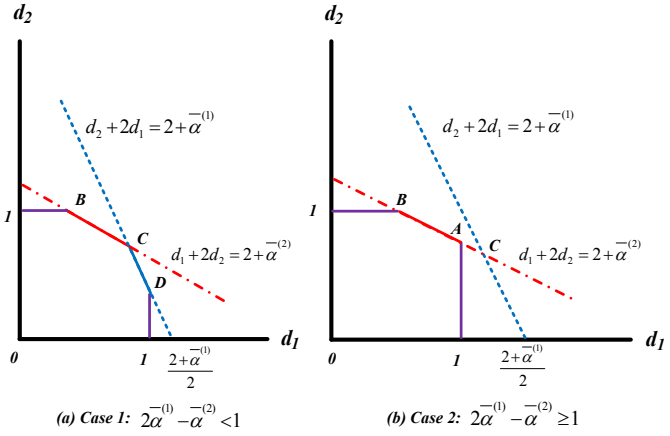

FIGURE 2.2 – Optimal DoF region for the two-user MISO BC, for the case of $\min\{\bar{\beta}^{(1)}, \bar{\beta}^{(2)}\} \geq \min\{\frac{1+\bar{\alpha}^{(1)}+\bar{\alpha}^{(2)}}{3}, \frac{1+\bar{\alpha}^{(2)}}{2}\}$. The corner points take the following values : $A = (1, \frac{1+\bar{\alpha}^{(2)}}{2})$, $B = (\bar{\alpha}^{(2)}, 1)$, $C = (\frac{2+2\bar{\alpha}^{(1)}-\bar{\alpha}^{(2)}}{3}, \frac{2+2\bar{\alpha}^{(2)}-\bar{\alpha}^{(1)}}{3})$, and $D = (1, \bar{\alpha}^{(1)})$.

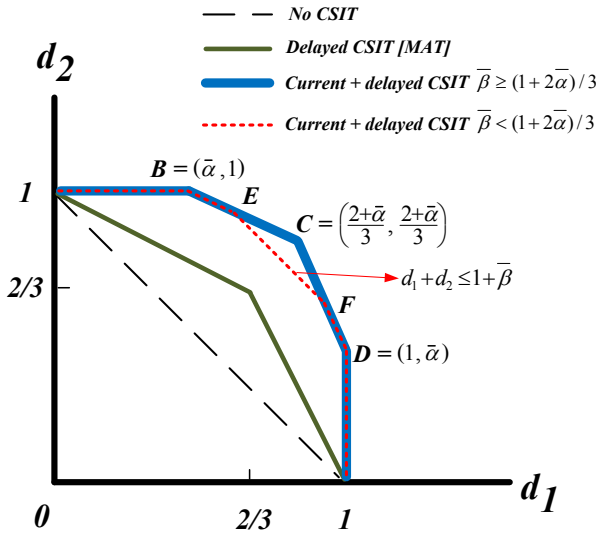

FIGURE 2.3 – DoF region of two-user MISO BC with symmetric feedback, $\bar{\alpha}^{(1)} = \bar{\alpha}^{(2)} = \bar{\alpha}, \bar{\beta}^{(1)} = \bar{\beta}^{(2)} = \bar{\beta}$. The optimal region takes the form of a polygon with corner points $\{(0,0),(0,1),(\bar{\alpha},1),(\frac{2+\bar{\alpha}}{3},\frac{2+\bar{\alpha}}{3}),(1,\bar{\alpha}),(1,0)\}$ for $\bar{\beta} \geq \frac{1+2\bar{\alpha}}{3}$. For $\bar{\beta} < \frac{1+2\bar{\alpha}}{3}$, the derived region takes the form of a polygon with corner points $\{(0,0),(0,1),(\bar{\alpha},1),(2\bar{\beta}-\bar{\alpha},1+\bar{\alpha}-\bar{\beta}),(1+\bar{\alpha}-\bar{\beta},2\bar{\beta}-\bar{\alpha}),(1,\bar{\alpha}),(1,0)\}$.

exponent *averages* $\bar{\alpha}^{(1)} = \bar{\alpha}^{(2)} =: \bar{\alpha}$ and $\bar{\beta}^{(1)} = \bar{\beta}^{(2)} =: \bar{\beta}$. Most existing works, with an exception in [33] and [8], fall under this symmetric feedback setting. The following holds directly from Theorem 1 and Proposition 1.

Corollary 1a (DoF with symmetric feedback)**.** *The optimal DoF region for the symmetric feedback case, takes the form*

$$d_1 \leq 1, \quad d_2 \leq 1, \quad 2d_1 + d_2 \leq 2 + \bar{\alpha}, \quad 2d_2 + d_1 \leq 2 + \bar{\alpha}$$

when $\bar{\beta} \geq \frac{1+2\bar{\alpha}}{3}$*, while when* $\bar{\beta} < \frac{1+2\bar{\alpha}}{3}$ *this region is inner bounded by the achievable region*

$$d_1 \leq 1, \quad d_2 \leq 1 \tag{2.20}$$
$$2d_1 + d_2 \leq 2 + \bar{\alpha} \tag{2.21}$$
$$2d_2 + d_1 \leq 2 + \bar{\alpha} \tag{2.22}$$
$$d_2 + d_1 \leq 1 + \bar{\beta}. \tag{2.23}$$

Figure 2.3 depicts the DoF region of the two-user MISO BC in the presence of CSIT feedback with long-term symmetry.

We now quantify the extent to which having symmetric feedback offers a benefit over the asymmetric case where one user accumulates - in the long

term - better feedback than the other. Such 'symmetry gains' have been recorded in different instances (cf. [11], [33]).

The following broad comparison focuses on the case of perfect delayed CSIT ($\bar{\beta} = 1$), and contrasts the symmetric feedback case $\bar{\alpha}^{(1)} = \bar{\alpha}^{(2)}$, to the asymmetric case $\bar{\alpha}^{(1)} \neq \bar{\alpha}^{(2)}$. Naturally such comparison is performed under an overall feedback constraint, which - reflecting the spirit of previous works that have identified symmetry gains - is here chosen to be in the form of a fixed sum $\bar{\alpha}^{(1)} + \bar{\alpha}^{(2)}$. The comparison is in terms of the optimal sum DoF d_1+d_2, where again we recall that the users are labeled so that $\bar{\alpha}^{(1)} \geq \bar{\alpha}^{(2)}$. To clarify, the symmetry gain will be the difference in the sum-DoF performance of two cases; the symmetric case where the two exponent averages are the same and are equal to $\frac{1}{2}(\bar{\alpha}^{(1)} + \bar{\alpha}^{(2)})$, and the asymmetric case where the two distinct exponent averages are $\bar{\alpha}^{(1)}$ and $\bar{\alpha}^{(2)}$. The proof is direct from Theorem 1 and Corollary 1a.

Corollary 1b (Symmetric vs. asymmetric feedback)**.** *The symmetry sum-DoF gain is equal to* $\frac{1}{6}(2\bar{\alpha}^{(1)} - \bar{\alpha}^{(2)} - 1)^+$*, i.e., if* $2\bar{\alpha}^{(1)} - \bar{\alpha}^{(2)} - 1 > 0$*, the symmetric sum-DoF gain is* $\frac{2\bar{\alpha}^{(1)} - \bar{\alpha}^{(2)} - 1}{6} > 0$*, else there is no symmetry gain.*

Example 7. *For example, consider the asymmetric feedback option* $\bar{\alpha}^{(1)} = 1, \bar{\alpha}^{(2)} = 0$ *which corresponds to an optimal sum-DoF of* $d_1 + d_2 = 3/2$ *(see Theorem 1, and consider perfect delayed CSIT), and compare this with the symmetric option where both exponent averages are equal to* $1/2$*. The symmetric option provides a sum-DoF of* $d_1+d_2 = 5/3$*, and a symmetry gain of* $5/3 - 3/2 = 1/6$*. As expected, the gain is positive since* $2\bar{\alpha}^{(1)} - \bar{\alpha}^{(2)} - 1 = 2 - 0 - 1 = 1 > 0$.

On the other hand, an asymmetric option $\bar{\alpha}^{(1)} = 3/5, \bar{\alpha}^{(2)} = 2/5$ *corresponds to an optimal sum DoF of* $d_1 + d_2 = 5/3$*, which matches the aforementioned DoF performance of the symmetric option. The symmetry gain here is zero, since* $2\bar{\alpha}^{(1)} - \bar{\alpha}^{(2)} - 1 = 6/5 - 2/5 - 1 = -1/5 < 0$.

Finally, before concluding our discussion on feedback symmetry/asymmetry, it is worth noting that the asymmetric setting here - where $\bar{\alpha}^{(1)} \neq \bar{\alpha}^{(2)}$ and where $\bar{\beta}^{(1)}$ and $\bar{\beta}^{(2)}$ need not be equal - yields a natural generalization for the asymmetric setting of Maleki et al. in [33] which, as we have mentioned, in the presence of abundant delayed CSIT, had an optimal DoF corresponding to DoF corner point $(1, 1/2)$ (and a sum-DoF $d_1 + d_2 = 3/2$). The following corollary - which again corresponds to the range of sufficiently good delayed CSIT where $\min\{\beta^{(1)}, \beta^{(2)}\} \geq \min\{\frac{1+\bar{\alpha}^{(1)}+\bar{\alpha}^{(2)}}{3}, \frac{1+\bar{\alpha}^{(2)}}{2}\}$ - offers a broad generalization of the corresponding result in [33]. The proof is direct from the main result.

Corollary 1c (Asymmetric and periodic CSIT)**.** *In the range of sufficiently good delayed CSIT, the optimal DoF region is defined by corner points* $B =$

$(\bar{\alpha}^{(2)}, 1)$, $C = (\frac{2+2\bar{\alpha}^{(1)}-\bar{\alpha}^{(2)}}{3}, \frac{2+2\bar{\alpha}^{(2)}-\bar{\alpha}^{(1)}}{3})$ *and* $D = (1, \bar{\alpha}^{(1)})$ *whenever* $2\bar{\alpha}^{(1)} - \bar{\alpha}^{(2)} < 1$, *else by corner points* $A = (1, \frac{1+\bar{\alpha}^{(2)}}{2})$ *and* B.

As an example we can see that the same DoF corner point $A = (1, 1/2)$ - derived in [33] under the general principle of perfect delayed CSIT for both users, and perfect current CSIT for the first user - can in fact be achieved with a plethora of options with lesser current and delayed CSIT, such as

$$\alpha_t^{(1)} = 1/2,\ \alpha_t^{(2)} = 0,\ \beta_t^{(1)} = \beta_t^{(2)} = 1/2,\ \forall t.$$

Need for delayed feedback : Imperfect vs. perfect delayed CSIT

We now shift emphasis to explore the fact that imperfect delayed CSIT ($\bar{\beta} < 1$) can - in some cases - be as useful as (asymptotically) perfect delayed CSIT ($\bar{\beta} = 1$), and to provide insight on the overall feedback quality (timely and delayed) that is necessary to achieve a certain DoF performance.

Before proceeding with the result, we briefly motivate our interest in imperfect and sparse *delayed* CSIT. Towards this we recall that $\bar{\alpha}^{(1)}, \bar{\alpha}^{(2)}$ are more representative of the quality (and inevitably of the amount) of *timely* feedback, while $\bar{\beta}^{(1)}, \bar{\beta}^{(2)}$ are more representative of the quality of the *entirety* of feedback (timely plus delayed). In this sense, any attempt to limit the total amount and quality of feedback - that is communicated during a certain communication process - must include reducing $\bar{\beta}^{(1)}, \bar{\beta}^{(2)}$, rather than just focusing on reducing $\bar{\alpha}^{(1)}, \bar{\alpha}^{(2)}$. For example, even if we removed entirely all current CSIT ($\alpha_t^{(1)} = \alpha_t^{(2)} = 0, \forall t$), but insisted on always sending perfect delayed CSIT ($\beta_t^{(1)} = \beta_t^{(2)} = 1, \forall t$), we would achieve little towards reducing the total amount of feedback, and we would mainly shift the time-frame of the problem, again irrespective of the drastic reduction in $\bar{\alpha}^{(1)}, \bar{\alpha}^{(2)}$.

As we will see though, having reduced $\bar{\alpha}^{(1)}, \bar{\alpha}^{(2)}$ can in fact translate to having overall reduced feedback because, interestingly, having reduced $\bar{\alpha}^{(1)}, \bar{\alpha}^{(2)}$, can translate - to a certain extent - to needing lesser quality delayed feedback, i.e., can translate to further reductions in $\bar{\beta}^{(1)}, \bar{\beta}^{(2)}$. This is quantified in the following, the proof of which is direct, because it simply restates part of what is in the theorem.

Corollary 1d (Imperfect vs. perfect delayed CSIT)**.** *A CSIT process* $\{\hat{\boldsymbol{h}}_{t,t'}, \hat{\boldsymbol{g}}_{t,t'}\}_{t=1,t'=1}^{n}$ *that offers*

$$\min\{\bar{\beta}^{(1)}, \bar{\beta}^{(2)}\} \geq \min\{\frac{1+\bar{\alpha}^{(1)}+\bar{\alpha}^{(2)}}{3}, \frac{1+\bar{\alpha}^{(2)}}{2}\} \tag{2.24}$$

gives the same DoF as a CSIT process that offers perfect delayed CSIT for each channel realization ($\beta_t^{(1)} = \beta_t^{(2)} = 1, \forall t$, *i.e.,* $\bar{\beta}^{(1)} = \bar{\beta}^{(2)} = 1$).
For the symmetric case, having

$$\bar{\beta} \geq \frac{1+2\bar{\alpha}}{3} \tag{2.25}$$

guarantees the same.

It is interesting to observe that the expressions in the above corollary match the amount of delayed CSIT used by schemes in the past, even though such schemes were not designed with the expressed purpose of reducing the amount of delayed CSIT. For example, the Maddah-Ali and Tse scheme in [4] (feedback with $\alpha_t^{(1)} = \alpha_t^{(2)} = 0, \forall t$, over an i.i.d fast-fading channel), while in principle corresponding to abundant delayed CSIT, in fact was based on a precoding design that only needed delayed CSIT only for every third channel realization, corresponding to

$$\beta_t^{(i)} = \begin{cases} 1 & \text{if } t = i \ (\text{ mod } 3) \\ 0 & \text{otherwise} \end{cases}, \text{ user } i = 1, 2 \tag{2.26}$$

and [3] thus corresponding to $\bar{\beta}^{(i)} = 1/3,\ i = 1, 2$, which happens to match the above expression in (2.25) ($\bar{\alpha} = 0$). This same general expression in (2.25) additionally tells us that, in the Maddah-Ali and Tse setting, any combination of CSIT quality exponents that allows for $\bar{\beta}^{(1)} = \bar{\beta}^{(2)} \geq 1/3$, will allow for the same optimal DoF region in [4]. For example, one such choice would be to use $\beta_t^{(1)} = \beta_t^{(2)} = 1/3, \forall t$.

A similar observation holds for the optimal schemes in [6, 7] ($\alpha_t^{(1)} = \alpha_t^{(2)} = \alpha, \forall t$) which again operated in a setting that in principle allowed for unlimited delayed CSIT, but which in fact asked for delayed CSIT only for every third channel realization

$$\beta_t^{(i)} = \begin{cases} 1 & \text{if } t = i \ (\text{ mod } 3) \\ \alpha & \text{otherwise} \end{cases} \tag{2.27}$$

corresponding to $\bar{\beta}^{(i)} = (1 + 2\alpha)/3,\ i = 1, 2$. This again can be seen as a special instance of the general expression in (2.25), which is powerful enough to reveal that any combination of CSIT quality exponents that allows for $\bar{\beta}^{(1)} = \bar{\beta}^{(2)} \geq (1 + 2\bar{\alpha})/3$, will achieve the same optimal DoF in [6, 7]. One such choice would be to have $\beta_t^{(1)} = \beta_t^{(2)} = \frac{1+2\alpha}{3}, \forall t$.

Along the same lines, the optimal asymmetric scheme in [33] which operated under the general principle of perfect delayed CSIT for both users, and perfect current CSIT for the first user, in fact employed a scheme that used lesser feedback. In this scheme, which had duration of two channel uses, the actual required CSIT corresponded to $\alpha_1^{(1)} = \beta_1^{(1)} = \beta_1^{(2)} = 1$, and $\alpha_1^{(2)} = \alpha_2^{(1)} = \alpha_2^{(2)} = \beta_2^{(1)} = \beta_2^{(2)} = 0$, thus corresponding to $\bar{\alpha}^{(1)} = 1/2, \bar{\alpha}^{(2)} = 0, \bar{\beta}^{(1)} = 1/2, \bar{\beta}^{(2)} = 1/2$, which matches the expression in (2.24) since $\min\{\bar{\beta}^{(1)}, \bar{\beta}^{(2)}\} = \min\{1/2, 1/2\} = \min\{\frac{1+\bar{\alpha}^{(1)}+\bar{\alpha}^{(2)}}{3}, \frac{1+\min\{\bar{\alpha}^{(1)},\bar{\alpha}^{(2)}\}}{2}\} =$

3. Here when we say $t = i$ (mod 3), we refer to the modulo operation, i.e., we mean that $t = 3k + i$ for some integer k.

$\min\{\frac{1+1/2+0}{3}, \frac{1+0}{2}\} = 1/2$. This same expression in (2.24) further reveals other CSIT options that allow for the same optimal DoF.

Need for predicted CSIT

We now shift emphasis from delayed CSIT to the other extreme of predicted CSIT. As we recall, we considered a channel process $\{\boldsymbol{h}_t, \boldsymbol{g}_t\}_t$ and a CSIT process $\{\hat{\boldsymbol{h}}_{t,t'}, \hat{\boldsymbol{g}}_{t,t'}\}_{t,t'}$, consisting of estimates $\hat{\boldsymbol{h}}_{t,t'}$ - available at any time t' - of the channel $\boldsymbol{h}_t$ that materializes at any time t. We also advocated that we can safely assume that $\mathbb{E}[||\boldsymbol{h}_t - \hat{\boldsymbol{h}}_{t,t'}||^2] \leq \mathbb{E}[||\boldsymbol{h}_t - \hat{\boldsymbol{h}}_{t,t''}||^2]$ (similarly $\mathbb{E}[||\boldsymbol{g}_t - \hat{\boldsymbol{g}}_{t,t'}||^2] \leq \mathbb{E}[||\boldsymbol{g}_t - \hat{\boldsymbol{g}}_{t,t''}||^2]$), for any $t' > t''$, simply because one can revert back to past estimates of statistically better quality. This assumption though does not preclude the possible usefulness of early (predicted) estimates, even if such estimates are generally of lesser quality (statistically) than current estimates (i.e., of lesser quality than estimates that appear during or after the channel materializes). It is still conceivable that transmission at a certain time t^*, can benefit from being a function of an estimate $\hat{\boldsymbol{h}}_{t,t'}$ of a future channel $t > t^*$, where this estimate became available - naturally by prediction - at any time $t' \leq t^* < t$. The following addresses this, in the range of sufficiently good delayed CSIT where $\min\{\bar{\beta}^{(1)}, \bar{\beta}^{(2)}\} \geq \min\{\frac{1+\bar{\alpha}^{(1)}+\bar{\alpha}^{(2)}}{3}, \frac{1+\bar{\alpha}^{(2)}}{2}\}$.

Corollary 1e (Need for predicted CSIT)**.** *In the range of sufficiently good delayed CSIT, transmission need not consider predicted estimates of future channels, to achieve the optimal DoF.*

Proof. The proof is by construction ; the designed schemes do not use predicted estimates, while the tight outer bound does not preclude the use of such predicted estimates. □

2.3 Periodically evolving CSIT

We here focus on the block fading setting with a finite coherence period of T_c channel uses, during which the channel remains fixed, and during which a gradual accumulation of feedback provides a progressively increasing CSIT quality, as time progresses across the coherence period (partially delayed current CSIT), or at any time after the end of the coherence period (delayed and potentially obsolete CSIT) [4].

Such gradual improvement could be sought in FDD (frequency division duplex) settings with limited-capacity feedback links that can be used more than once during the coherence period to progressively refine CSIT, as well as in TDD (time division duplex) settings that use reciprocity-based estimation that progressively improves over time.

In this setting, where the channel remains the same for a finite duration of T_c channel uses, the time index is arranged so that

$$\boldsymbol{h}_{\ell T_c+1} = \boldsymbol{h}_{\ell T_c+2} = \cdots = \boldsymbol{h}_{(\ell+1)T_c}$$

$$\boldsymbol{g}_{\ell T_c+1} = \boldsymbol{g}_{\ell T_c+2} = \cdots = \boldsymbol{g}_{(\ell+1)T_c}$$

for a non-negative integer ℓ. As a result, in the presence of a periodic feedback process which repeats with period T_c, we are presented with a periodic sequence of current-CSIT quality exponents

$$\alpha_t^{(i)} = \alpha_{\ell T_c+t}^{(i)}, \forall \ell = 0, 1, 2, \cdots, \ i = 1, 2. \tag{2.28}$$

We focus here - simply for the sake of clarity of exposition - on the symmetric feedback case ($\bar{\alpha}^{(1)} = \bar{\alpha}^{(2)} =: \bar{\alpha}$). In this setting - and after adopting a periodic time index corresponding to having $\ell = 0$ (cf. (2.28)) - the time horizon of interest spans $t = 1, 2, \cdots, T_c$, and the feedback quality is now represented by the T_c current CSIT quality exponents $\{\alpha_t\}_{t=1}^{T_c}$ and by the delayed CSIT exponent β. Specifically each α_t describes the high SNR precision of the current CSIT estimates at time $t \leq T_c$, whereas β captures the precision of the best CSIT estimate received after the channel has elapsed, i.e., after the coherence period of the channel. In this setting we have that

$$0 \leq \alpha_1 \leq \cdots \leq \alpha_{T_c} \leq \beta \leq 1 \tag{2.29}$$

where - since the channel remains fixed during the coherence period - any difference between two consecutive exponents is attributed to feedback that was received during that time slot.

One of the utilities of this setting is that it concisely captures practical timing issues, capturing the effects of feedback that offers an inaccurate representation of the true state of the channel, as well the effects of feedback

4. This definition of current vs. delayed CSIT, originates from [4], and is the standard definition adopted by most existing works on the topic.

that can only be used for a small fraction of the communication duration. Having for example $\alpha_1 = 1$ simply refers to the case of asymptotically perfect and immediately available (full) CSIT, whereas having $\alpha_{T_c} = 0$ simply means that no (or very limited) current feedback is sent during the coherence period of the channel. Similarly having $\alpha_{\gamma T_c} = 0$, for some $\gamma \in [0, 1]$, simply means that no (or very limited) current feedback is sent during the first γ fraction of the coherence period [5].

Example 8. *Having a periodic feedback process that sends refining feedback, let's say, two times per coherence period, at times $t = \gamma_1 T_c + 1, t = \gamma_2 T_c + 1$ and never again about that same channel, will result in having*

$$\overbrace{0 = \alpha_1 = \cdots = \alpha_{\gamma_1 T_c}}^{\textit{Before feedback}} \leq \overbrace{\alpha_{\gamma_1 T_c + 1} = \cdots = \alpha_{\gamma_2 T_c}}^{\textit{After first feedback}} \leq \underbrace{\alpha_{\gamma_2 T_c + 1} = \cdots = \alpha_{T_c} = \beta}_{\textit{After second feedback}} \quad (2.30)$$

whereas if the same feedback system is modified to further add some delayed feedback after the channel elapses, may allow for $\beta > \alpha_{T_c}$.

One can note that reducing α_{T_c}, implies a reduced amount of feedback - about a specific channel - that is sent during the coherence period of that same channel. On the other hand, reducing β implies a reduced amount of feedback, during and after the channel's coherence period. Along these lines, reducing $(\beta - \alpha_{T_c})$ implies a reduced amount of feedback, about a specific fading coefficient, that is sent after the coherence period of the channel.

The results here hold directly from the previous results in this work, where directly from (2.9), we now simply have that

$$\bar{\alpha} = \frac{1}{T_c} \sum_{t=1}^{T_c} \alpha_t. \quad (2.31)$$

The following - which is placed here for completeness - holds directly from Corollary 1a, for the case of a periodically evolving feedback process over a quasi-static channel.

Corollary 1f (Periodically evolving feedback)**.** *For a periodic feedback process with $\{\alpha_t\}_{t=1}^{T_c}$ and perfect delayed CSIT (received at any time after the end of the coherence period), the optimal DoF region over a block-fading channel is the polygon with corner points*

$$\{(0,0), (0,1), (\bar{\alpha}, 1), (\frac{2+\bar{\alpha}}{3}, \frac{2+\bar{\alpha}}{3}), (1, \bar{\alpha}), (1,0)\}. \quad (2.32)$$

5. Our ignoring here of integer rounding is an abuse of notation that is only done for the sake of clarity of notation, and it carries no real effect on the result.

This same optimal region can in fact be achieved even with imperfect-quality delayed CSIT, as long as $\beta \geq \frac{1+2\bar{\alpha}}{3}$.

Remark 2 (Feedback quality vs. quantity)**.** *While all the results here are in terms of feedback* quality *rather than in terms of feedback* quantity*, there are distinct cases where the relationship between the two is well defined. Such is the case when CSIT estimates are derived using basic - and not necessarily optimal - scalar quantization techniques [39]. In such cases, which we mention here simply to offer some insight*[6] *- and remaining in the high SNR regime - dedicating* $\alpha \log P$ *quantization bits, per scalar, to quantize* $\boldsymbol{h}$ *into an estimate* $\hat{\boldsymbol{h}}$*, allows for a mean squared error [39]*

$$\mathbb{E}\|\boldsymbol{h} - \hat{\boldsymbol{h}}\|^2 \doteq P^{-\alpha}.$$

Drawing from this, and going back to our previous example, let us consider a similar example.

Example 9. *Consider a periodic feedback process that sends refining feedback two times per coherence period, by first sending* $\alpha' \log P$ *bits of feedback per scalar at time* $t = \gamma_1 T_c + 1$*, then by sending extra* $\alpha'' \log P$ *bits of feedback per scalar at time* $t = \gamma_2 T_c + 1$*, and where it finally sends* $(\beta - (\alpha' + \alpha'')) \log P$ *extra bits of refining feedback per scalar, at some fixed point in time after the end of the coherence period of the channel. This would result in having*

$$\begin{aligned} \overbrace{0 = \alpha_1 = \cdots = \alpha_{\gamma_1 T_c}}^{\textit{Before feedback}} &\leq \overbrace{\alpha' = \alpha_{\gamma_1 T_c + 1} = \cdots = \alpha_{\gamma_2 T_c}}^{\textit{After first feedback}} \\ &\leq \underbrace{\alpha' + \alpha'' = \alpha_{\gamma_2 T_c + 1} = \cdots = \alpha_{T_c}}_{\textit{After second feedback, before } T_c} \leq \underbrace{\beta}_{\textit{After coherence period}} . \end{aligned} \tag{2.33}$$

For instance, if this periodic feedback process sends $\frac{4}{9} \log P$ *feedback bits per scalar, at time* $t = \frac{1}{3} T_c + 1$*, and then sends extra* $\frac{1}{9} \log P$ *bits of feedback at time* $t = \frac{2}{3} T_c + 1$*, it will allow for*

$$\begin{aligned} \overbrace{0 = \alpha_1 = \cdots = \alpha_{\frac{1}{3} T_c}}^{\textit{Before feedback}} &\leq \overbrace{\frac{4}{9} = \alpha_{\frac{1}{3} T_c + 1} = \cdots = \alpha_{\frac{2}{3} T_c}}^{\textit{After first feedback}} \\ &\leq \underbrace{\frac{5}{9} = \alpha_{\frac{2}{3} T_c + 1} = \cdots = \alpha_{T_c}}_{\textit{After second feedback, before } T_c} \end{aligned} \tag{2.34}$$

6. We clarify that this relationship between CSIT quality and feedback quantity, plays no role in the development of the results, and is simply mentioned in the form of comments that offer intuition. Our focus is on quality exponents, and we make no optimality claim regarding the number of quantization bits.

which gives $\bar{\alpha} = (0 + 4/9 + 5/9)/3 = 1/3$*, which in turn gives (Corollary 1f) an optimal DoF region which is defined by the polygon with corner points*

$$\{(0,0),(0,1),(1/3,1),(7/9,7/9),(1,1/3),(1,0)\}. \tag{2.35}$$

Note that in this example, there is no need for extra bits of (delayed) feedback after the end of the coherence period, because the existing amount and timing of feedback bits - again under scalar quantization - guarantees that

$$\beta = \alpha_{T_c} = 5/9 = \frac{1 + 2\bar{\alpha}}{3} = \frac{1 + 2/3}{3}$$

which we have seen (Corollary 1f) to already be as good as perfect delayed feedback ($\beta = 1$).

Placing our focus back on feedback quality, and remaining on the setting of periodically evolving feedback, we proceed with a corollary that offers insight on the question of what CSIT quality and timing, suffice to achieve a certain DoF performance. For ease of exposition, we focus on the hardest-to-achieve DoF point $d_1 = d_2 = d$. The proof is again direct.

Corollary 1g (Sufficient feedback for target DoF)**.** *Having* $\bar{\alpha} \geq 3d - 2$ *with* $\beta \geq 2d - 1$*, or having* $\bar{\alpha} \geq 3d - 2$ *with* $\alpha_{T_c} \geq 2d - 1$ *(and no extra delayed feedback), suffices to achieve a symmetric target DoF* $d_1 = d_2 = d$*.*

One can see that having $\bar{\alpha} \geq 3d - 2$ with $\alpha_{T_c} \geq 2d - 1$ simply means that there is no need to send delayed feedback, i.e., there is no need to send feedback after the end of the coherence period.

Another practical aspect that is addressed here - again in the context of periodically evolving feedback - has to do with feedback delays. Such delays might cause performance degradation, which might be mitigated if the feedback - albeit with delays - has higher precision. The following corollary provides some insight on these aspects, by describing the feedback delays that allow a given target symmetric DoF d in the presence of constraints on current and delayed CSIT qualities. We will be specifically interested in the allowable fractional delay of feedback (cf. [10])

$$\gamma \triangleq \arg\max_{\gamma'} \{\alpha_{\gamma' T_c} = 0\} \tag{2.36}$$

i.e., the fraction $\gamma \leq 1$ for which $\alpha_1 = \cdots = \alpha_{\gamma T_c} = 0, \alpha_{\gamma T_c + 1} > 0$. We are also interested to see how this allowable delay reduces in the presence of a constraint $\alpha_t \leq \alpha_{\max} \forall t$ on timely feedback, or in the presence of a constraint on β.

Corollary 1h (Allowable feedback delay)**.** *Under a current CSIT quality constraint* $\alpha_t \leq \alpha_{\max}$ $\forall t$*, a symmetric target DoF* d *can be achieved with any*

fractional delay

$$\gamma \leq \begin{cases} 1-\frac{3d-2}{\alpha_{\max}} & \text{if } \ d \in [2/3, (2+\alpha_{\max})/3] \\ 1 & \text{if } \ d \in [0, 2/3] \end{cases}$$

while under a constraint $\beta \leq \beta_{\max}$*, it can be achieved with any*

$$\gamma \leq \begin{cases} 1 & \text{if } \ d \in [0, \frac{1+\min\{\beta_{\max},1/3\}}{2}] \\ \frac{1}{2}\big(\frac{1}{2d-1}-1\big) & \text{else if } \ d \in [\frac{1+\min\{\beta_{\max},1/3\}}{2}, \frac{1+\beta_{\max}}{2}] \end{cases}$$

Finally since $\alpha_{\max} \leq \beta_{\max} \leq 1$*, the above reveals that under no specific constraint on CSIT quality,* d *can be achieved with*

$$\gamma \leq \begin{cases} 3(1-d) & \text{if } \ d \in [2/3, 1] \\ 1 & \text{if } \ d \in [0, 2/3]. \end{cases}$$

To see the above, we first note that in the first case ($\alpha_t \leq \alpha_{\max}$), $d \in [0, 2/3]$ can be achieved by using perfect but delayed feedback sent at any point in time after $t = T_c$

$$\underbrace{\alpha_1 = \cdots = \alpha_{T_c} = 0}_{\text{No feedback}}, \qquad \underbrace{\beta = 1}_{\text{delayed CSIT at } t > T_c}$$

(cf. [4]), while $d \in (2/3, (2+\alpha_{\max})/3]$ can be achieved by setting $\alpha_1 = \cdots = \alpha_{\gamma T_c} = 0, \alpha_{\gamma T_c+1} = \cdots = \alpha_{T_c} = \alpha_{\max}$, $\gamma = 1 - \frac{3d-2}{\alpha_{\max}}$, $\beta \geq 2d-1$ (cf. Corollary 1a).

In the second case ($\beta \leq \beta_{\max}$), if $d \in [0, \frac{1+\min\{\beta_{\max},1/3\}}{2}]$, then d can be achieved by using imperfect and delayed feedback sent at any point in time after $t = T_c$

$$\underbrace{\alpha_1 = \cdots = \alpha_{T_c} = 0}_{\text{No feedback}}, \qquad \underbrace{\beta = \beta_{\max}}_{\text{delayed CSIT at } t > T_c}$$

(cf. Corollary 1a), else if $d \in [\frac{2}{3}, \frac{1+\beta_{\max}}{2}]$ and $\beta_{\max} \geq 1/3$, then d can be achieved by setting $\alpha_1 = \cdots = \alpha_{\gamma T_c} = 0, \alpha_{\gamma T_c+1} = \cdots = \alpha_{T_c} = \beta = 2d-1$, $\gamma = \frac{1}{2}\big(\frac{1}{2d-1}-1\big)$.

Finally, in the unconstrained case, $d \in [0, 2/3]$ can be achieved by setting $\alpha_1 = \cdots = \alpha_{T_c} = 0$ and $\beta = 1$, while $d \in [2/3, 1]$ can be achieved by using perfect (but partially delayed) feedback sent at $t = \gamma T_c + 1$

$$\underbrace{\alpha_1 = \cdots = \alpha_{\gamma T_c} = 0}_{\text{No feedback}}, \underbrace{\alpha_{\gamma T_c+1} = \cdots \alpha_{T_c} = \beta = 1}_{\text{Perfect quality CSIT}}.$$

Example 10. *Consider a symmetric target DoF of* $d_1 = d_2 = d = \frac{7}{9}$*. This can be achieved with* $\gamma = 3(1-d) = 2/3$ *if there is no bound on the quality exponents, and with* $\gamma = 1 - (3d-2)/\alpha_{\max} = 1/3$ *if the feedback*

link only allows for $\alpha_t \leq \alpha_{\max} = 1/2,\ \forall t$. *If on the other hand, feedback timeliness is easily obtained, we can substantially reduce the amount of CSIT and achieve the same* $d = \frac{7}{9}$ *with* $\alpha_1 = \cdots = \alpha_{T_c} = \bar{\alpha} = 3d - 2 = 1/3$ *(*$\gamma = 0, \beta = \frac{1+2\bar{\alpha}}{3} = 2d - 1 = 5/9$*).*

2.4 Universal encoding-decoding scheme

We proceed to describe the universal scheme that achieves the aforementioned DoF corner points. The challenge entails designing a scheme of an asymptotically large duration n, that utilizes a CSIT process $\{\hat{\boldsymbol{h}}_{t,t'}, \hat{\boldsymbol{g}}_{t,t'}\}_{t=1,t'=1}^{n}$ of quality defined by the statistics of $\{(\boldsymbol{h}_t - \hat{\boldsymbol{h}}_{t,t'}), (\boldsymbol{g}_t - \hat{\boldsymbol{g}}_{t,t'})\}_{t=1,t'=1}^{n}$. This will be achieved by focusing on the corresponding quality-exponent sequences $\{\alpha_t^{(1)}\}_{t=1}^{n}, \{\alpha_t^{(2)}\}_{t=1}^{n}, \{\beta_t^{(1)}\}_{t=1}^{n}, \{\beta_t^{(2)}\}_{t=1}^{n}$, as these were defined in (2.4)-(2.7). The optimal DoF region in Theorem 1 and the additional corner points in Proposition 1, will be achieved by properly utilizing different combinations of zero forcing, superposition coding, interference compressing and broadcasting, as well as proper power and rate allocation.

Phase-Markov forward-backward scheme The scheme has a forward-backward phase-Markov structure which, in the context of imperfect and delayed CSIT, was first introduced in [8,9] to consist of four main ingredients that include

- block-Markov encoding
- spatial precoding
- interference quantization
- backward decoding.

The scheme asks that the accumulated quantized interference bits of a certain (current) phase, be broadcasted to both users inside the common information symbols of the next phase, while also a certain amount of common information can be transmitted to both users during the current phase, which will then help resolve the accumulated interference of the previous phase.

As previously suggested, this causal scheme does not require knowledge of future quality exponents, nor does it use predicted CSIT estimates of future channels. The transmitter must know though the long term averages $\bar{\alpha}^{(1)}, \bar{\alpha}^{(2)}, \bar{\beta}^{(1)}, \bar{\beta}^{(2)}$, which - as is commonly assumed of long term statistics - can be derived.

By 'feeding' this universal scheme with the proper parameters, we can get schemes that are tailored to the different specific settings we have discussed. We will see such examples later in this section.

We remind the reader that the users are labeled so that $\bar{\alpha}^{(2)} \leq \bar{\alpha}^{(1)}$. We also remind the reader of the soft assumption that any sufficiently long subsequence $\{\alpha_t^{(1)}\}_{t=\tau}^{\tau+T}$ (resp. $\{\alpha_t^{(2)}\}_{t=\tau}^{\tau+T}, \{\beta_t^{(1)}\}_{t=\tau}^{\tau+T}, \{\beta_t^{(2)}\}_{t=\tau}^{\tau+T}$) is assumed to have an average that converges to the long term average $\bar{\alpha}^{(1)}$ (resp. $\bar{\alpha}^{(2)}, \bar{\beta}^{(1)}, \bar{\beta}^{(2)}$), for a finite T that can be sufficiently large to allow for this convergence. We briefly note that, as we will see later, in periodic settings such as those described in Section 2.3, T need not be large.

We proceed to describe in Section 2.4.1 the encoding part, and in Section 2.4.2 the decoding part. In Section 2.4.3 we show how the scheme

achieves the different DoF corner points of interest. Finally in Section 2.4.4 we provide example instances of our general scheme, for specific cases of particular interest.

For notational convenience, we will use

$$\hat{\boldsymbol{h}}_t \triangleq \hat{\boldsymbol{h}}_{t,t}, \quad \hat{\boldsymbol{g}}_t \triangleq \hat{\boldsymbol{g}}_{t,t}$$

$$\check{\boldsymbol{h}}_t \triangleq \hat{\boldsymbol{h}}_{t,t+\eta}, \quad \check{\boldsymbol{g}}_t \triangleq \hat{\boldsymbol{g}}_{t,t+\eta}$$

to denote the current and delayed estimates of $\boldsymbol{h}_t$ and $\boldsymbol{g}_t$, respectively [7], with corresponding estimation errors being

$$\tilde{\boldsymbol{h}}_t \triangleq \boldsymbol{h}_t - \hat{\boldsymbol{h}}_t, \quad \tilde{\boldsymbol{g}}_t \triangleq \boldsymbol{g}_t - \hat{\boldsymbol{g}}_t \tag{2.37}$$

$$\ddot{\boldsymbol{h}}_t \triangleq \boldsymbol{h}_t - \check{\boldsymbol{h}}_t, \quad \ddot{\boldsymbol{g}}_t \triangleq \boldsymbol{g}_t - \check{\boldsymbol{g}}_t. \tag{2.38}$$

2.4.1 Scheme $\mathcal{X}$: encoding

Scheme $\mathcal{X}$ is designed to have S phases, where each phase has a duration of T channel uses, and where T is finite but - unless stated otherwise - sufficiently large. Specifically each phase s ($s = 1, 2, \cdots, S$) will take place over all time slots t belonging to the set

$$\mathcal{B}_s = \{\mathcal{B}_{s,\ell} \triangleq (s-1)2T + \ell\}_{\ell=1}^{T}, \quad s = 1, \cdots, S. \tag{2.39}$$

As stated, T is sufficiently large so that

$$\frac{1}{T}\sum_{t\in\mathcal{B}_s} \alpha_t^{(i)} \to \bar{\alpha}^{(i)}, \ \frac{1}{T}\sum_{t\in\mathcal{B}_s} \beta_t^{(i)} \to \bar{\beta}^{(i)}, \ s = 1, \cdots, S \tag{2.40}$$

$i = 1, 2$. The above allocation in (2.39) guarantees that there are T channel uses in between any two neighboring phases. Having T being sufficiently large allows for the delayed CSIT corresponding to the channels appearing during phase s, to be available before the beginning of the phase that we label as phase $s + 1$. This implies that $T > \eta$ (cf. (2.6),(2.7)), although this assumption can be readily removed [8]. Naturally there is no silent time, and over the remaining channel uses

$$t \in \{(2s-1)T + \ell\}_{\ell=1,s=1}^{\ell=T,s=S}$$

7. Recall that η is a sufficiently large but finite integer, corresponding to the maximum delay allowed for waiting for delayed CSIT.

8. The assumption can be removed because we can, instead of splitting time into two interleaved halves and identifying each half to a message, to instead split time into more parts, each corresponding to a different message. For a sufficiently large number of parts, this would allow for the removal of the assumption that $T \geq \eta$, and the only assumption that would remain would be that T is large enough so that (2.40) is satisfied. In periodic settings, such T can be small.

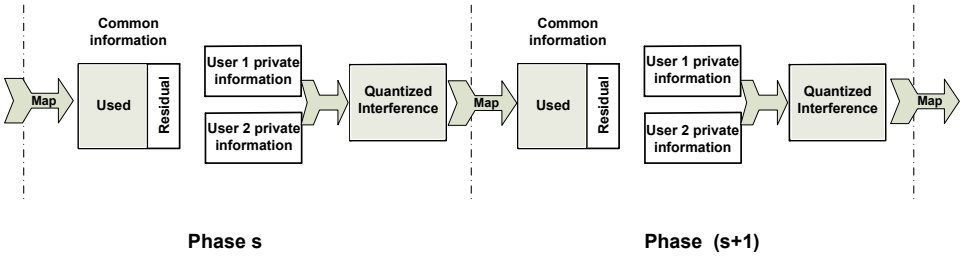

FIGURE 2.4 – Illustration of coding across phases.

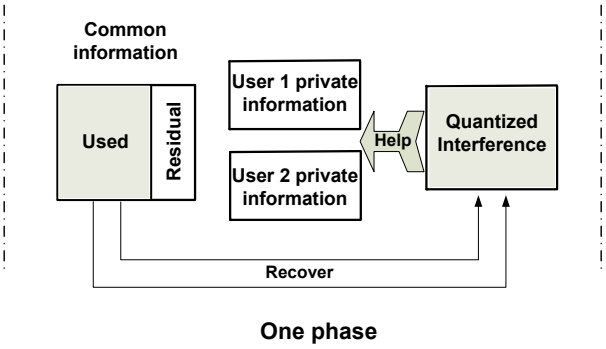

FIGURE 2.5 – Illustration of coding over a single phase.

we simply repeat scheme $\mathcal{X}$ with a different message. With n being generally infinite, S is also infinite (except for specific instances, some of which are highlighted in Section 2.4.4).

We proceed to give the general description that holds for all phases $s = 1, 2, \cdots, S-1$, except for the last phase S, which we describe separately afterwards. A brief corresponding illustration can be found in Figure 2.4 and Figure 2.5.

Phase s, for $s = 1, 2, \cdots, S-1$

We proceed to describe the way the scheme, in each phase $s \in [1, S-1]$, combines zero forcing and superposition coding, power and rate allocation, and interference compressing and broadcasting, in order to transmit private information, using currently available CSIT estimates to reduce interference, and using delayed CSIT estimates to alleviate the effect of past interference.

Zero forcing and superposition coding During phase s, $t \in \mathcal{B}_s$, the transmitter sends

$$\boldsymbol{x}_t = \boldsymbol{w}_t c_t + \hat{\boldsymbol{g}}_t^{\perp} a_t + \hat{\boldsymbol{h}}_t a_t^{'} + \hat{\boldsymbol{h}}_t^{\perp} b_t + \hat{\boldsymbol{g}}_t b_t^{'} \tag{2.41}$$

where $a_t, a_t^{'}$ are the symbols meant for user 1, $b_t, b_t^{'}$ for user 2, where c_t is a common symbol, where $\boldsymbol{e}^{\perp}$ denotes a unit-norm vector orthogonal to $\boldsymbol{e}$, and where $\boldsymbol{w}_t$ is a predetermined randomly-generated vector known by all the nodes.

Power and rate allocation policy In describing the power and rates of the symbols in (2.41), we use the notation

$$P_t^{(x)} \triangleq \mathbb{E}|x_t|^2 \tag{2.42}$$

to denote the power of x_t corresponding to time-slot t, and we use $r_t^{(x)}$ to denote the prelog factor of the number of bits $r_t^{(x)} \log P - o(\log P)$ carried by symbol x_t at time t.

When in phase s, during time-slot t, the powers and (normalized) rates are set as

$$\begin{array}{rl} P_t^{(c)} \doteq P, & \\ P_t^{(a)} \doteq P^{\delta_t^{(2)}}, & r_t^{(a)} = \delta_t^{(2)} \\ P_t^{(b)} \doteq P^{\delta_t^{(1)}}, & r_t^{(b)} = \delta_t^{(1)} \\ P_t^{(a')} \doteq P^{\delta_t^{(2)} - \alpha_t^{(2)}}, & r_t^{(a')} = (\delta_t^{(2)} - \alpha_t^{(2)})^+ \\ P_t^{(b')} \doteq P^{\delta_t^{(1)} - \alpha_t^{(1)}}, & r_t^{(b')} = (\delta_t^{(1)} - \alpha_t^{(1)})^+ \end{array} \tag{2.43}$$

where $(\bullet)^+ \triangleq \max\{\bullet, 0\}$.

We design the scheme so that the entirety of common information symbols $\{c_{\mathcal{B}_s,t}\}_{t=1}^T$, carry

$$T(1-\bar{\delta}) \log P - o(\log P) \tag{2.44}$$

bits, and design the power parameters $\{\delta_t^{(1)}, \delta_t^{(2)}\}_{t \in \mathcal{B}_s}$ to satisfy

$$\beta_t^{(i)} \geq \delta_t^{(i)} \quad i = 1, 2, \ t \in \mathcal{B}_s \tag{2.45}$$

$$\frac{1}{T} \sum_{t \in \mathcal{B}_s} \delta_t^{(1)} = \frac{1}{T} \sum_{t \in \mathcal{B}_s} \delta_t^{(2)} = \bar{\delta} \tag{2.46}$$

$$\frac{1}{T} \sum_{t \in \mathcal{B}_s} (\delta_t^{(i)} - \alpha_t^{(i)})^+ = (\bar{\delta} - \bar{\alpha}^{(i)})^+ \quad i = 1, 2, \tag{2.47}$$

for some $\bar{\delta}$ that will be bounded by

$$\bar{\delta} \leq \min\{\bar{\beta}^{(1)}, \bar{\beta}^{(2)}, \frac{1 + \bar{\alpha}^{(1)} + \bar{\alpha}^{(2)}}{3}, \frac{1 + \bar{\alpha}^{(2)}}{2}\}. \tag{2.48}$$

There indeed exist solutions $\{\delta_t^{(1)}, \delta_t^{(2)}\}_{t \in \mathcal{B}_s}$ that satisfy the above, and an explicit solution is shown in Appendix 2.7.1. Our solution for power and rate allocation allows that, at time t, the transmitter needs only acquire

knowledge of $\{\alpha_t^{(1)}, \beta_t^{(1)}; \alpha_t^{(2)}, \beta_t^{(2)}\}$, in addition to the derived long-term averages $\bar{\alpha}^{(1)}, \bar{\alpha}^{(2)}, \bar{\beta}^{(1)}, \bar{\beta}^{(2)}$. This nature of the derived solutions is crucial for handling asymmetry ($\alpha_t^{(1)} \neq \alpha_t^{(2)}$, $\beta_t^{(1)} \neq \beta_t^{(2)}$).

After transmission, the received signals take the form

$$\begin{aligned} y_t^{(1)} &= \underbrace{\boldsymbol{h}_t^{\mathsf{T}}\boldsymbol{w}_t c_t}_{P} + \underbrace{\boldsymbol{h}_t^{\mathsf{T}}\hat{\boldsymbol{g}}_t^{\perp} a_t}_{P^{\delta_t^{(2)}}} + \underbrace{\boldsymbol{h}_t^{\mathsf{T}}\hat{\boldsymbol{h}}_t a_t^{'}}_{P^{\delta_t^{(2)}-\alpha_t^{(2)}}} + \underbrace{z_t^{(1)}}_{P^0} \\ &\quad + \underbrace{\overbrace{\check{\boldsymbol{h}}_t^{\mathsf{T}}(\hat{\boldsymbol{h}}_t^{\perp} b_t + \hat{\boldsymbol{g}}_t b_t^{'})}^{\check{\iota}_t^{(1)}}}_{P^{\delta_t^{(1)}-\alpha_t^{(1)}}} + \underbrace{\overbrace{\ddot{\boldsymbol{h}}_t^{\mathsf{T}}(\hat{\boldsymbol{h}}_t^{\perp} b_t + \hat{\boldsymbol{g}}_t b_t^{'})}^{\iota_t^{(1)}-\check{\iota}_t^{(1)}}}_{P^{\delta_t^{(1)}-\beta_t^{(1)}} \leq P^0} \end{aligned} \tag{2.49}$$

$$\begin{aligned} y_t^{(2)} &= \underbrace{\boldsymbol{g}_t^{\mathsf{T}}\boldsymbol{w}_t c_t}_{P} + \underbrace{\boldsymbol{g}_t^{\mathsf{T}}\hat{\boldsymbol{h}}_t^{\perp} b_t}_{P^{\delta_t^{(1)}}} + \underbrace{\boldsymbol{g}_t^{\mathsf{T}}\hat{\boldsymbol{g}}_t b_t^{'}}_{P^{\delta_t^{(1)}-\alpha_t^{(1)}}} + \underbrace{z_t^{(2)}}_{P^0} \\ &\quad + \underbrace{\overbrace{\check{\boldsymbol{g}}_t^{\mathsf{T}}(\hat{\boldsymbol{g}}_t^{\perp} a_t + \hat{\boldsymbol{h}}_t a_t^{'})}^{\check{\iota}_t^{(2)}}}_{P^{\delta_t^{(2)}-\alpha_t^{(2)}}} + \underbrace{\overbrace{\ddot{\boldsymbol{g}}_t^{\mathsf{T}}(\hat{\boldsymbol{g}}_t^{\perp} a_t + \hat{\boldsymbol{h}}_t a_t^{'})}^{\iota_t^{(2)}-\check{\iota}_t^{(2)}}}_{P^{\delta_t^{(2)}-\beta_t^{(2)}} \leq P^0} \end{aligned} \tag{2.50}$$

where

$$\iota_t^{(1)} \triangleq \boldsymbol{h}_t^{\mathsf{T}}(\hat{\boldsymbol{h}}_t^{\perp} b_t + \hat{\boldsymbol{g}}_t b_t^{'}),\ \iota_t^{(2)} \triangleq \boldsymbol{g}_t^{\mathsf{T}}(\hat{\boldsymbol{g}}_t^{\perp} a_t + \hat{\boldsymbol{h}}_t a_t^{'}) \tag{2.51}$$

denote the interference at user 1 and user 2 respectively, and where

$$\check{\iota}_t^{(1)} \triangleq \check{\boldsymbol{h}}_t^{\mathsf{T}}(\hat{\boldsymbol{h}}_t^{\perp} b_t + \hat{\boldsymbol{g}}_t b_t^{'}),\ \check{\iota}_t^{(2)} \triangleq \check{\boldsymbol{g}}_t^{\mathsf{T}}(\hat{\boldsymbol{g}}_t^{\perp} a_t + \hat{\boldsymbol{h}}_t a_t^{'}) \tag{2.52}$$

denote the transmitter's delayed estimates of the scalar interference terms $\iota_t^{(1)}, \iota_t^{(2)}$. In the above - where under each term we noted the order of the summand's average power - we considered that

$$\begin{aligned} \mathbb{E}|\check{\iota}_t^{(1)}|^2 &= \mathbb{E}|\check{\boldsymbol{h}}_t^{\mathsf{T}}\hat{\boldsymbol{h}}_t^{\perp} b_t|^2 + \mathbb{E}|\check{\boldsymbol{h}}_t^{\mathsf{T}}\hat{\boldsymbol{g}}_t b_t^{'}|^2 \\ &= \mathbb{E}|(\hat{\boldsymbol{h}}_t^{\mathsf{T}} + \tilde{\boldsymbol{h}}_t^{\mathsf{T}} - \ddot{\boldsymbol{h}}_t^{\mathsf{T}})\hat{\boldsymbol{h}}_t^{\perp} b_t|^2 + \mathbb{E}|\check{\boldsymbol{h}}_t^{\mathsf{T}}\hat{\boldsymbol{g}}_t b_t^{'}|^2 \\ &= \mathbb{E}|(\tilde{\boldsymbol{h}}_t^{\mathsf{T}} - \ddot{\boldsymbol{h}}_t^{\mathsf{T}})\hat{\boldsymbol{h}}_t^{\perp} b_t|^2 + \mathbb{E}|\check{\boldsymbol{h}}_t^{\mathsf{T}}\hat{\boldsymbol{g}}_t b_t^{'}|^2 \\ &\doteq P^{\delta_t^{(1)}-\alpha_t^{(1)}} \\ \mathbb{E}|\check{\iota}_t^{(2)}|^2 &= \mathbb{E}|(\tilde{\boldsymbol{g}}_t^{\mathsf{T}} - \ddot{\boldsymbol{g}}_t^{\mathsf{T}})\hat{\boldsymbol{g}}_t^{\perp} a_t|^2 + \mathbb{E}|\check{\boldsymbol{g}}_t^{\mathsf{T}}\hat{\boldsymbol{h}}_t a_t^{'}|^2 \\ &\doteq P^{\delta_t^{(2)}-\alpha_t^{(2)}}. \end{aligned} \tag{2.53}$$

Quantizing and broadcasting the accumulated interference After the end of phase s and before the beginning of the next phase - which starts

TABLE 2.1 – Bits carried by private symbols, common symbols, and by the quantized interference, for phase s, $s = 1, 2, \cdots, S-1$.

	Total bits ($\times \log P$)
Private symbols for user 1	$T(\bar{\delta} + (\bar{\delta} - \bar{\alpha}^{(2)})^+)$
Private symbols for user 2	$T(\bar{\delta} + (\bar{\delta} - \bar{\alpha}^{(1)})^+)$
Common symbols	$T(1 - \bar{\delta})$
Quantized interference	$T((\bar{\delta} - \bar{\alpha}^{(1)})^+ + (\bar{\delta} - \bar{\alpha}^{(2)})^+)$

T channel uses after the end of phase s, i.e., after the accumulation of all delayed CSIT - the transmitter reconstructs $\check{\iota}_t^{(1)}, \check{\iota}_t^{(2)}, t \in \mathcal{B}_s$ using its knowledge of delayed CSIT, and quantizes these into

$$\bar{\check{\iota}}_t^{(1)} = \check{\iota}_t^{(1)} - \tilde{\iota}_t^{(1)}, \quad \bar{\check{\iota}}_t^{(2)} = \check{\iota}_t^{(2)} - \tilde{\iota}_t^{(2)} \tag{2.54}$$

with $(\delta_t^{(1)} - \alpha_t^{(1)})^+ \log P$ and $(\delta_t^{(2)} - \alpha_t^{(2)})^+ \log P$ quantization bits respectively, allowing for bounded power of quantization noise $\tilde{\iota}_t^{(1)}, \tilde{\iota}_t^{(2)}$, i.e, allowing for

$$\mathbb{E}|\tilde{\iota}_t^{(2)}|^2 \doteq \mathbb{E}|\tilde{\iota}_t^{(1)}|^2 \doteq 1$$

since $\mathbb{E}|\tilde{\iota}_t^{(2)}|^2 \doteq P^{\delta_t^{(2)} - \alpha_t^{(2)}}$, $\mathbb{E}|\tilde{\iota}_t^{(1)}|^2 \doteq P^{\delta_t^{(1)} - \alpha_t^{(1)}}$ (cf. [39]). Then the transmitter evenly splits the

$$\sum_{t \in \mathcal{B}_s} \left((\delta_t^{(1)} - \alpha_t^{(1)})^+ + (\delta_t^{(2)} - \alpha_t^{(2)})^+ \right) \log P \tag{2.55}$$

quantization bits into the common symbols $\{c_t\}_{t \in \mathcal{B}_{s+1}}$ that will be transmitted during the next phase (phase $s+1$), conveying these quantization bits together with other new information bits for the users.

This transmission of $\{c_t\}_{t \in \mathcal{B}_{s+1}}$ in the next phase, will help each of the users cancel the dominant part of the interference, and it will also serve as an extra observation (see (2.67) later on) that allows for decoding of all private information of that same user. Table 2.1 summarizes the number of bits carried by private symbols, common symbols, and by the quantized interference, for phase s, $s = 1, 2, \cdots, S-1$.

We now proceed with the description of encoding over the last phase S.

Phase S

The last phase, in addition to communicating new private symbols, conveys the remaining accumulated interference from the previous phase, and does so in a manner that allows for termination at the end of this phase.

During this last phase, the transmitter sends

$$\boldsymbol{x}_t = \boldsymbol{w}_t c_t + \hat{\boldsymbol{g}}_t^{\perp} a_t + \hat{\boldsymbol{h}}_t^{\perp} b_t \tag{2.56}$$

$t \in \mathcal{B}_S$, with power and rates set as

$$\begin{array}{lll} P_t^{(c)} \doteq P, & P_t^{(a)} \doteq P^{\alpha_t^{(2)}}, & P_t^{(b)} \doteq P^{\delta_t^{(1)}} \\ & r_t^{(a)} = \alpha_t^{(2)}, & r_t^{(b)} = \delta_t^{(1)}. \end{array} \tag{2.57}$$

With the entirety of common information symbols $\{c_{\mathcal{B}_{S,\ell}}\}_{\ell=1}^{T}$ now carrying [9]

$$T(1-\bar{\alpha}^{(2)}) \log P - o(\log P) \tag{2.58}$$

bits, the power parameters $\{\delta_t^{(1)}\}_{t\in\mathcal{B}_S}$ are designed such that

$$\alpha_t^{(1)} \geq \delta_t^{(1)} \quad \forall t \tag{2.59}$$

$$\frac{1}{T}\sum_{t\in\mathcal{B}_S} \delta_t^{(1)} = \bar{\alpha}^{(2)}. \tag{2.60}$$

The solution to the above problem is similar to that in (2.45),(2.46),(2.47).

This concludes the part of encoding. After transmission, the received signals are then of the form

$$y_t^{(1)} = \underbrace{\boldsymbol{h}_t^{\mathsf{T}} \boldsymbol{w}_t c_t}_{P} + \underbrace{\boldsymbol{h}_t^{\mathsf{T}} \hat{\boldsymbol{g}}_t^{\perp} a_t}_{P^{\alpha_t^{(2)}}} + \underbrace{\tilde{\boldsymbol{h}}_t^{\mathsf{T}} \hat{\boldsymbol{h}}_t^{\perp} b_t}_{\leq P^0} + \underbrace{z_t^{(1)}}_{P^0} \tag{2.61}$$

$$y_t^{(2)} = \underbrace{\boldsymbol{g}_t^{\mathsf{T}} \boldsymbol{w}_t c_t}_{P} + \underbrace{\tilde{\boldsymbol{g}}_t^{\mathsf{T}} \hat{\boldsymbol{g}}_t^{\perp} a_t}_{P^0} + \underbrace{\boldsymbol{g}_t^{\mathsf{T}} \hat{\boldsymbol{h}}_t^{\perp} b_t}_{P^{\delta_t^{(1)}}} + \underbrace{z_t^{(2)}}_{P^0}. \tag{2.62}$$

We now move to describe decoding at both receivers, where this decoding part has a phase Markov structure (see Figure 2.6), similar to the encoding part.

2.4.2 Scheme $\mathcal{X}$: decoding

As it may be apparent (more details will be shown in Section 2.4.3), the power and rate allocation in (2.45),(2.46),(2.47) guarantees that the quantized interference accumulated during phase s ($s = 1, \cdots, S-1$) has fewer bits than the load of the common symbols transmitted during the next phase (cf. (2.55)). Consequently decoding of the common symbols during a certain phase, helps recover the interference accumulated during the previous phase. As a result, decoding moves backwards, from the last to the first phase.

9. We remind the reader of the definition of $\mathcal{B}_{s,\ell}$ (cf. (2.39)) which denotes the ℓth element of set $\mathcal{B}_s$ consisting of all time indexes of phase s. For example, saying that $t = \mathcal{B}_{1,\ell}$ simply means that $t = \ell$.

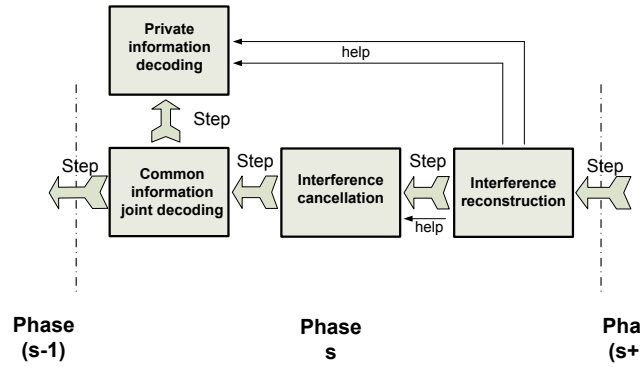

FIGURE 2.6 – Illustration of decoding steps.

Phase S

At the end of phase S, we consider *joint* decoding of all common symbols $[c_{\mathcal{B}_{S,1}}, \cdots, c_{\mathcal{B}_{S,T}}]^{\mathsf{T}}$. Specifically user i, $i = 1, 2$, decodes the corresponding common-information vector using its received signal vector $[y^{(i)}_{\mathcal{B}_{S,1}}, y^{(i)}_{\mathcal{B}_{S,2}}, \cdots, y^{(i)}_{\mathcal{B}_{S,T}}]^{\mathsf{T}}$, and does so by treating the other signals as noise. We now note that the accumulated mutual information satisfies

$$\begin{aligned} I([c_{\mathcal{B}_{S,1}}, \cdots, c_{\mathcal{B}_{S,T}}]^{\mathsf{T}}; [y^{(1)}_{\mathcal{B}_{S,1}}, \cdots, y^{(1)}_{\mathcal{B}_{S,T}}]^{\mathsf{T}}) \\ = \log \prod_{t \in \mathcal{B}_S} P^{1-\alpha_t^{(2)}} - o(\log P) \\ = T(1 - \bar{\alpha}^{(2)}) \log P - o(\log P) \\ I([c_{\mathcal{B}_{S,1}}, \cdots, c_{\mathcal{B}_{S,T}}]^{\mathsf{T}}; [y^{(2)}_{\mathcal{B}_{S,1}}, \cdots, y^{(2)}_{\mathcal{B}_{S,T}}]^{\mathsf{T}}) \\ = \log \prod_{t \in \mathcal{B}_S} P^{1-\delta_t^{(1)}} - o(\log P) \\ = T(1 - \bar{\alpha}^{(2)}) \log P - o(\log P) \end{aligned} \tag{2.63}$$

(cf. (2.59),(2.60)), to conclude that both users can reliably decode all

$$T(1 - \bar{\alpha}^{(2)}) \log P - o(\log P) \tag{2.64}$$

bits in the common information vector $[c_{\mathcal{B}_{S,1}}, \cdots, c_{\mathcal{B}_{S,T}}]^{\mathsf{T}}$. This is proved in Lemma 2 in the appendix of Section 2.7.2, which in fact guarantees that both users will be able to decode the amount of feedback bits described in (2.64), even for finite and small T. This is done to ensure the validity of the schemes also for finite T, and is achieved by employing specific lattice codes that have good properties in the finite-duration high-SNR regime. The details for this step can be found in the aforementioned appendix.

After decoding $[c_{\mathcal{B}_{S,1}}, \cdots, c_{\mathcal{B}_{S,T}}]^\mathsf{T}$, user 1 removes $\boldsymbol{h}_t^\mathsf{T}\boldsymbol{w}_t c_t$ from the received signal in (2.61), to decode a_t. Similarly user 2 removes $\boldsymbol{g}_t^\mathsf{T}\boldsymbol{w}_t c_t$ from its received signal in (2.62), to decode b_t.

Now we go back one phase and utilize knowledge of $\{c_t\}_{t\in\mathcal{B}_S}$, to decode the corresponding symbols.

Phase s, $s = S-1, S-2, \cdots, 1$

We here describe, for phase s, the actions of interference reconstruction, interference cancelation, joint decoding of common information symbols, and decoding of private information symbols, in the order they happen.

Interference reconstruction In this phase (phase s), each user employs knowledge of $\{c_t\}_{t\in\mathcal{B}_{s+1}}$ from phase $s+1$, to reconstruct the delayed estimates of all the interference accumulated in phase s, i.e., to reconstruct $\{\bar{\iota}_t^{(2)}, \bar{\iota}_t^{(1)}\}_{t\in\mathcal{B}_s}$.

Interference cancelation Now with knowledge of $\{\bar{\iota}_t^{(2)}, \bar{\iota}_t^{(1)}\}_{t\in\mathcal{B}_s}$, each user can remove - up to noise level - all the interference $\iota_t^{(i)}$, $t \in \mathcal{B}_s$, by subtracting the delayed interference estimates $\bar{\iota}_t^{(i)}$ from $y_t^{(i)}$.

Joint decoding of common information symbols At this point, user i decodes the common information vector $\boldsymbol{c}_s \triangleq [c_{\mathcal{B}_{s,1}}, \cdots, c_{\mathcal{B}_{s,T}}]^\mathsf{T}$ from its (modified) received signal vector $[y^{(i)}_{\mathcal{B}_{s,1}} - \bar{\iota}^{(i)}_{\mathcal{B}_{s,1}}, \cdots, y^{(i)}_{\mathcal{B}_{s,T}} - \bar{\iota}^{(i)}_{\mathcal{B}_{s,T}}]^\mathsf{T}$ by treating the other signals as noise. The accumulated mutual information then satisfies

$$\begin{aligned}
&I(\boldsymbol{c}_s; [y^{(1)}_{\mathcal{B}_{s,1}} - \bar{\iota}^{(1)}_{\mathcal{B}_{s,1}}, \cdots, y^{(1)}_{\mathcal{B}_{s,T}} - \bar{\iota}^{(1)}_{\mathcal{B}_{s,T}}]^\mathsf{T}) \\
&= \log \prod_{t\in\mathcal{B}_s} P^{1-\delta_t^{(2)}} - o(\log P) = T(1-\bar{\delta})\log P - o(\log P) \\
&I(\boldsymbol{c}_s; [y^{(2)}_{\mathcal{B}_{s,1}} - \bar{\iota}^{(2)}_{\mathcal{B}_{s,1}}, \cdots, y^{(2)}_{\mathcal{B}_{s,T}} - \bar{\iota}^{(2)}_{\mathcal{B}_{s,T}}]^\mathsf{T}) \\
&= \log \prod_{t\in\mathcal{B}_s} P^{1-\delta_t^{(1)}} - o(\log P) = T(1-\bar{\delta})\log P - o(\log P)
\end{aligned} \tag{2.65}$$

(cf. (2.45)-(2.50)), and we conclude that both users can reliably decode all

$$T(1-\bar{\delta})\log P - o(\log P) \tag{2.66}$$

bits of the common information vector $\boldsymbol{c}_s$. The details for this step, can again be found in the appendix of Section 2.7.2.

After decoding $\boldsymbol{c}_s$, user 1 removes $\boldsymbol{h}_t^\mathsf{T}\boldsymbol{w}_t c_t$ from $y_t^{(1)} - \bar{\iota}_t^{(1)}$, while user 2 removes $\boldsymbol{g}_t^\mathsf{T}\boldsymbol{w}_t c_t$ from $y_t^{(2)} - \bar{\iota}_t^{(1)}$, $t \in \mathcal{B}_s$.

Decoding of private information symbols After removing the interference, and decoding and subtracting out the common symbols, each user now decodes its private information symbols of phase s. Using knowledge of $\{\bar{\bar{\iota}}_t^{(2)}, \bar{\bar{\iota}}_t^{(1)}\}_{t\in\mathcal{B}_s}$, user 1 will use the estimate $\bar{\bar{\iota}}_t^{(2)}$ (of $\iota_t^{(2)}$) as an extra observation which, together with the observation $y_t^{(1)} - \boldsymbol{h}_t^{\mathsf{T}}\boldsymbol{w}_t c_t - \bar{\bar{\iota}}_t^{(1)}$, will allow for decoding of both a_t and $a_t^{'}$, $t \in \mathcal{B}_s$. Specifically user 1, at each instance t, can 'see' a 2×2 MIMO channel of the form

$$\begin{bmatrix} y_t^{(1)} - \boldsymbol{h}_t^{\mathsf{T}}\boldsymbol{w}_t c_t - \bar{\bar{\iota}}_t^{(1)} \\ \bar{\bar{\iota}}_t^{(2)} \end{bmatrix} = \begin{bmatrix} \boldsymbol{h}_t^{\mathsf{T}} \\ \check{\boldsymbol{g}}_t^{\mathsf{T}} \end{bmatrix} \begin{bmatrix} \hat{\boldsymbol{g}}_t^{\perp} & \hat{\boldsymbol{h}}_t \end{bmatrix} \begin{bmatrix} a_t \\ a_t^{'} \end{bmatrix} + \begin{bmatrix} \tilde{z}_t^{(1)} \\ -\tilde{\iota}_t^{(2)} \end{bmatrix} \tag{2.67}$$

where

$$\tilde{z}_t^{(1)} = \ddot{\boldsymbol{h}}_t^{\mathsf{T}}(\hat{\boldsymbol{h}}_t^{\perp} b_t + \hat{\boldsymbol{g}}_t b_t^{'}) + z_t^{(1)} + \tilde{\iota}_t^{(1)}.$$

The fact that $\mathbb{E}|\tilde{z}_t^{(1)}|^2 \doteq 1$, allows for decoding of a_t and $a_t^{'}$, corresponding to the aforementioned rates $r_t^{(a)} = \delta_t^{(2)}$, $r_t^{(a')} = (\delta_t^{(2)} - \alpha_t^{(2)})^+$, $t \in \mathcal{B}_s$. Similar actions are taken by user 2, allowing for decoding of b_t and $b_t^{'}$, again with $r_t^{(b)} = \delta_t^{(1)}$, $r_t^{(a')} = (\delta_t^{(1)} - \alpha_t^{(1)})^+$, $t \in \mathcal{B}_s$.

At this point, each user has decoded all the information symbols (common and private) corresponding to phase s, goes back one phase (to phase $s-1$) to utilize its knowledge of $\{c_t\}_{t\in\mathcal{B}_s}$, and decodes the common and private symbols of that phase. The whole decoding effort naturally terminates after decoding of the symbols in the first phase.

2.4.3 Scheme $\mathcal{X}$: Calculating the achieved DoF

In the following DoF calculation we will consider two separate cases. Case 1 will correspond to

$$2\bar{\alpha}^{(1)} - \bar{\alpha}^{(2)} < 1 \tag{2.68}$$

which in turn implies that $\bar{\alpha}^{(1)} \leq \frac{1+\bar{\alpha}^{(1)}+\bar{\alpha}^{(2)}}{3} \leq \frac{1+\bar{\alpha}^{(2)}}{2}$, while case 2 will correspond to

$$2\bar{\alpha}^{(1)} - \bar{\alpha}^{(2)} \geq 1 \tag{2.69}$$

which in turn implies that $\bar{\alpha}^{(1)} \geq \frac{1+\bar{\alpha}^{(1)}+\bar{\alpha}^{(2)}}{3} \geq \frac{1+\bar{\alpha}^{(2)}}{2}$. We recall that the users are labeled so that $\bar{\alpha}^{(1)} \geq \bar{\alpha}^{(2)}$.

Generic DoF point

To calibrate the DoF performance, we first note that for any fixed $\bar{\delta} \leq \min\{\bar{\beta}^{(1)}, \bar{\beta}^{(2)}, \frac{1+\bar{\alpha}^{(1)}+\bar{\alpha}^{(2)}}{3}, \frac{1+\bar{\alpha}^{(2)}}{2}\}$ (cf. (2.48)), the rate and power allocation in (2.45),(2.46),(2.47) (as this policy is explicitly described in the appendix

of Section 2.7.1) tells us that, the total amount of information, for user 1, in the *private symbols* of a certain phase $s < S$, is equal to

$$\big(\bar{\delta} + (\bar{\delta} - \bar{\alpha}^{(2)})^+\big)T \log P \tag{2.70}$$

bits, while for user 2 this is

$$\big(\bar{\delta} + (\bar{\delta} - \bar{\alpha}^{(1)})^+\big)T \log P \tag{2.71}$$

bits.

The next step is to see how much interference there is to load onto common symbols. Given the power and rate allocation in (2.45),(2.46),(2.47),(2.48), it is guaranteed that the accumulated quantized interference in a phase $s < S$ (cf. (2.55)) has $\big((\bar{\delta} - \bar{\alpha}^{(1)})^+ + (\bar{\delta} - \bar{\alpha}^{(2)})^+\big)T \log P$ bits, which can be carried by the common symbols of the next phase $(s+1)$ since they can carry a total of $\big(1 - \bar{\delta}\big)T \log P$ bits (cf. (2.44)). This leaves an extra space of $\Delta_{\text{com}} T \log P$ bits in the common symbols, where

$$\Delta_{\text{com}} \triangleq 1 - \bar{\delta} - (\bar{\delta} - \bar{\alpha}^{(1)})^+ - (\bar{\delta} - \bar{\alpha}^{(2)})^+ \tag{2.72}$$

is guaranteed to be non-negative for any given $\bar{\delta} \leq \min\{\bar{\beta}^{(1)}, \bar{\beta}^{(2)}, \frac{1+\bar{\alpha}^{(1)}+\bar{\alpha}^{(2)}}{3}, \frac{1+\bar{\alpha}^{(2)}}{2}\}$. This extra space can be split between the two users, by allocating $\omega\Delta_{\text{com}} T \log P$ bits for the message of user 1, and the remaining $(1-\omega)\Delta_{\text{com}} T \log P$ bits for the message of user 2, for some $\omega \in [0, 1]$.

Consequently the above, combined with the information stored in private symbols (cf. (2.70),(2.71)), allows for

$$d_1 = \bar{\delta} + (\bar{\delta} - \bar{\alpha}^{(2)})^+ + \omega\Delta_{\text{com}} \tag{2.73}$$

$$d_2 = \bar{\delta} + (\bar{\delta} - \bar{\alpha}^{(1)})^+ + (1-\omega)\Delta_{\text{com}}. \tag{2.74}$$

The above considers that S is large, and thus removes the effect of having a last phase that carries less new message information. In the following, we will achieve different corner points by accordingly setting the value of $\omega \in [0, 1]$ and of $\bar{\delta} \leq \min\{\bar{\beta}^{(1)}, \bar{\beta}^{(2)}, \frac{1+\bar{\alpha}^{(1)}+\bar{\alpha}^{(2)}}{3}, \frac{1+\bar{\alpha}^{(2)}}{2}\}$.

DoF corner points in Theorem 1

To achieved the DoF region in Theorem 1, we will show how to achieve the following DoF corner points (see also Table 2.2)

$$A = \big(1, \frac{1+\bar{\alpha}^{(2)}}{2}\big) \tag{2.75}$$

$$B = \big(\bar{\alpha}^{(2)}, 1\big) \tag{2.76}$$

$$C = \big(\frac{2+2\bar{\alpha}^{(1)}-\bar{\alpha}^{(2)}}{3}, \frac{2+2\bar{\alpha}^{(2)}-\bar{\alpha}^{(1)}}{3}\big) \tag{2.77}$$

$$D = \big(1, \bar{\alpha}^{(1)}\big). \tag{2.78}$$

To achieve the DoF region of Theorem 1 we need sufficiently good (but certainly not perfect) delayed CSIT such that

$$\min\{\bar{\beta}^{(1)}, \bar{\beta}^{(2)}\} \geq \min\{\frac{1+\bar{\alpha}^{(1)}+\bar{\alpha}^{(2)}}{3}, \frac{1+\bar{\alpha}^{(2)}}{2}\} \tag{2.79}$$

(cf. Theorem 1), which in turn implies that (cf. (2.48))

$$\bar{\delta} \leq \min\{\frac{1+\bar{\alpha}^{(1)}+\bar{\alpha}^{(2)}}{3}, \frac{1+\bar{\alpha}^{(2)}}{2}\}.$$

Under the condition of (2.79), the DoF corner points are achievable by setting the value of $\omega \in [0,1]$ and of $\bar{\delta} \leq \min\{\frac{1+\bar{\alpha}^{(1)}+\bar{\alpha}^{(2)}}{3}, \frac{1+\bar{\alpha}^{(2)}}{2}\}$ as in Table 2.2.

Specifically when (2.79) and (2.68) hold, we achieve DoF point B by setting $\omega = 0, \bar{\delta} = \bar{\alpha}^{(2)}$ which indeed gives (cf. (2.72),(2.73),(2.74))

$$\begin{aligned} d_1 &= \bar{\delta} + (\bar{\delta} - \bar{\alpha}^{(2)})^+ = \bar{\alpha}^{(2)} \\ d_2 &= \bar{\delta} + (\bar{\delta} - \bar{\alpha}^{(1)})^+ + \Delta_{\text{com}} = \bar{\alpha}^{(2)} + 1 - \bar{\alpha}^{(2)} = 1. \end{aligned}$$

To achieve DoF point D we set $\omega = 1$ and $\bar{\delta} = \bar{\alpha}^{(1)}$ and get

$$\begin{aligned} d_1 &= \bar{\delta} + (\bar{\delta} - \bar{\alpha}^{(2)})^+ + \Delta_{\text{com}} = \bar{\alpha}^{(1)} + 1 - \bar{\alpha}^{(1)} = 1 \\ d_2 &= \bar{\delta} + (\bar{\delta} - \bar{\alpha}^{(1)})^+ = \bar{\alpha}^{(1)} \end{aligned}$$

while to achieve DoF point C we set $\omega = 0$ and $\bar{\delta} = \frac{1+\bar{\alpha}^{(1)}+\bar{\alpha}^{(2)}}{3}$ and get

$$\begin{aligned} d_1 &= \bar{\delta} + (\bar{\delta} - \bar{\alpha}^{(2)})^+ = \frac{2+2\bar{\alpha}^{(1)}-\bar{\alpha}^{(2)}}{3} \\ d_2 &= \bar{\delta} + (\bar{\delta} - \bar{\alpha}^{(1)})^+ + \Delta_{\text{com}} = \frac{2+2\bar{\alpha}^{(2)}-\bar{\alpha}^{(1)}}{3}. \end{aligned}$$

On the other hand, when (2.69) (case 2) and (2.79) hold, to achieve DoF point B we set $\omega = 0$ and $\bar{\delta} = \bar{\alpha}^{(2)}$ as before, while to achieve DoF point A, we set $\omega = 0$ and $\bar{\delta} = \frac{1+\bar{\alpha}^{(2)}}{2}$.

Finally the entire DoF region of Theorem 1 is achieved using time sharing between these corner points.

DoF corner points of Proposition 1

Now we focus on the DoF points of Proposition 1 (see Table 2.3). These are the points we label as DoF points B and D, as these were defined in (2.76) and (2.78), as well as three new DoF points

$$E = \big(2\min\{\bar{\beta}^{(1)}, \bar{\beta}^{(2)}\} - \bar{\alpha}^{(2)}, 1 + \bar{\alpha}^{(2)} - \min\{\bar{\beta}^{(1)}, \bar{\beta}^{(2)}\}\big) \tag{2.80}$$

$$F = \big(1 + \bar{\alpha}^{(1)} - \min\{\bar{\beta}^{(1)}, \bar{\beta}^{(2)}\}, 2\min\{\bar{\beta}^{(1)}, \bar{\beta}^{(2)}\} - \bar{\alpha}^{(1)}\big) \tag{2.81}$$

$$G = \big(1, \min\{\bar{\beta}^{(1)}, \bar{\beta}^{(2)}\}\big). \tag{2.82}$$

TABLE 2.2 – Optimal corner points summary, for sufficiently good delayed CSIT such that $\min\{\bar{\beta}^{(1)}, \bar{\beta}^{(2)}\} \geq \min\{\frac{1+\bar{\alpha}^{(1)}+\bar{\alpha}^{(2)}}{3}, \frac{1+\bar{\alpha}^{(2)}}{2}\}$.

Cases	Corner points	$\bar{\delta}$	ω
Case 1	C	$\frac{1+\bar{\alpha}^{(1)}+\bar{\alpha}^{(2)}}{3}$	0
	D	$\bar{\alpha}^{(1)}$	1
	B	$\bar{\alpha}^{(2)}$	0
Case 2	B	$\bar{\alpha}^{(2)}$	0
	A	$\frac{1+\bar{\alpha}^{(2)}}{2}$	0

TABLE 2.3 – DoF inner bound corner points, for delayed CSIT such that $\min\{\bar{\beta}^{(1)}, \bar{\beta}^{(2)}\} < \min\{\frac{1+\bar{\alpha}^{(1)}+\bar{\alpha}^{(2)}}{3}, \frac{1+\bar{\alpha}^{(2)}}{2}\}$.

Cases	Corner points
Case 1 and case of $\min\{\bar{\beta}^{(1)}, \bar{\beta}^{(2)}\} \geq \bar{\alpha}^{(1)}$	E, F, B, D
Case 1 and case of $\min\{\bar{\beta}^{(1)}, \bar{\beta}^{(2)}\} < \bar{\alpha}^{(1)}$	B, E, G
Case 2	B, E, G

As stated in the proposition, we are interested in the range of reduced-quality delayed CSIT, as this is defined by

$$\min\{\bar{\beta}^{(1)}, \bar{\beta}^{(2)}\} < \min\{\frac{1+\bar{\alpha}^{(1)}+\bar{\alpha}^{(2)}}{3}, \frac{1+\bar{\alpha}^{(2)}}{2}\} \tag{2.83}$$

and which implies that $\bar{\delta} \leq \min\{\bar{\beta}^{(1)}, \bar{\beta}^{(2)}\}$ (cf. (2.48)). In addition to the two cases in (2.68),(2.69), we now additionally consider the cases where

$$\min\{\bar{\beta}^{(1)}, \bar{\beta}^{(2)}\} \geq \bar{\alpha}^{(1)} \tag{2.84}$$

$$\min\{\bar{\beta}^{(1)}, \bar{\beta}^{(2)}\} < \bar{\alpha}^{(1)}. \tag{2.85}$$

When (2.68),(2.83) and (2.84) hold, we set $\omega = 0, \bar{\delta} = \bar{\alpha}^{(2)}$ as before to achieve DoF point B. To achieve point D, we set $\omega = 1$ and $\bar{\delta} = \bar{\alpha}^{(1)}$ as before, whereas to achieve point E, we set $\omega = 0, \bar{\delta} = \min\{\bar{\beta}^{(1)}, \bar{\beta}^{(2)}\}$ to get (cf. (2.72), (2.73), (2.74))

$$d_1 = \bar{\delta} + (\bar{\delta} - \bar{\alpha}^{(2)})^+ = 2\min\{\bar{\beta}^{(1)}, \bar{\beta}^{(2)}\} - \bar{\alpha}^{(2)}$$
$$d_2 = \bar{\delta} + (\bar{\delta} - \bar{\alpha}^{(1)})^+ + \Delta_{\text{com}} = 1 + \bar{\alpha}^{(2)} - \min\{\bar{\beta}^{(1)}, \bar{\beta}^{(2)}\}.$$

Finally to achieve DoF point F, we set $\omega = 1$ and $\bar{\delta} = \min\{\bar{\beta}^{(1)}, \bar{\beta}^{(2)}\}$.

When (2.68),(2.83) and (2.85) hold, we achieve points B and E with the same parameters as before, while to achieve point G, we set $\omega = 1, \bar{\delta} = \min\{\bar{\beta}^{(1)}, \bar{\beta}^{(2)}\}$.

Similarly when (2.69) and (2.83) hold, we achieve points B, E, G by setting ω and $\bar{\delta}$ as above.

Finally the entire DoF region of Proposition 1 is achieved with time sharing between the corner points.

2.4.4 Scheme $\mathcal{X}$: examples

We proceed to provide example instances of our general scheme, for specific cases of particular interest.

Fixed and imperfect quality delayed CSIT, no current CSIT

We consider the case of no current CSIT ($\alpha_t^{(i)} = 0,\ \forall t, i$) and of imperfect delayed CSIT of an unchanged quality $\beta_t^{(1)} = \beta_t^{(2)} \leq 1, \forall t$. We focus on the case of $\beta_t^{(1)} = \beta_t^{(2)} = 1/3, \forall t$. The universal scheme - with these parameters - achieves the optimal DoF by achieving the optimal DoF corner point ($d_1 = \frac{2}{3}, d_2 = \frac{2}{3}$), as in the case of [4] which assumed that the delayed feedback of a channel could be sent with perfect quality.

For this case of $\beta_t^{(i)} = 1/3, \alpha_t^{(i)} = 0$, we have $\bar{\alpha}^{(1)} = \bar{\alpha}^{(2)} = 0$, $\bar{\beta}^{(1)} = \bar{\beta}^{(2)} = 1/3$. Toward designing the scheme, we set $\bar{\delta} = 1/3$ (cf. (2.48)). For the case of block fading where we can rewrite the time index to reflect a unit

TABLE 2.4 – Bits carried by private symbols, common symbols, and by the quantized interference, for phase $s = 1, 2, \cdots, S-1$.

	Total bits ($\log P$)
Private symbols for user 1	2/3
Private symbols for user 2	2/3
Common symbols	2/3
Quantized interference	2/3

coherence period, delayed CSIT is simply the CSIT that comes during the next coherence period, i.e., during the next time slot. Given the i.i.d. fast fading assumption ([4]), we can set $\eta = 1$ (cf. (2.6),(2.7)), which allows for a simpler variant of our scheme where now the phases have duration $T = 1$. In this simplified variant, the transmitted signal (cf. (2.41)) takes the simple form

$$\boldsymbol{x}_t = \boldsymbol{w}_t c_t + \begin{bmatrix} a_t \\ a_t' \end{bmatrix} + \begin{bmatrix} b_t \\ b_t' \end{bmatrix}$$

with the power and rates of the symbols (cf. (2.43)) set as

$$\begin{gathered} P_t^{(c)} \doteq P, \; r_t^{(c)} = 1 - 1/3 \\ P_t^{(a)} \doteq P_t^{(a')} \doteq P_t^{(b)} \doteq P_t^{(b')} \doteq P^{1/3} \\ r_t^{(a)} = r_t^{(a')} = r_t^{(b)} = r_t^{(b')} = 1/3. \end{gathered} \tag{2.86}$$

During each phase, the transmitter quantizes - as instructed in (2.55) - the interference accumulated in that phase, with a quantization rate of $2/3 \log P$, which is mapped into the common symbol c_{t+1} that will be transmitted in the next phase (at time-slot $t+1$). For large enough communication length, simple calculations can show that this can achieve the optimal DoF ($d_1 = \frac{2}{3}, d_2 = \frac{2}{3}$), and can do so with imperfect quality CSIT. Table 2.4 summarizes the rates associated to the symbols in this scheme.

Alternating between two current-CSIT states

In the context of the two-user MISO BC with spatially and temporally i.i.d. fading and $M = 2$, the work in [11] considered the *alternating CSIT* setting where CSIT for the two users, alternates between perfect current CSIT (labeled here as state P), perfect delayed CSIT (D), or no CSIT (N). In this setting where I_i denoted the CSIT state for the channel of user i at any given time ($I_1, I_2 \in \{P, D, N\}$), the work in [11] considered communication where, for a fraction $\lambda_{I_1 I_2}$ of the time, the CSIT states are equal to I_1, I_2 (state I_1 for the first user, state I_2 for the second user).

The same work focused on the symmetric case where $\lambda_{I_1 I_2} = \lambda_{I_2 I_1}$. For $\lambda_P \triangleq \sum_{I_2 \in \{P,D,N\}} \lambda_{P I_2}$ being the fraction of the time where one user has perfect CSIT, and $\lambda_D \triangleq \sum_{I_2 \in \{P,D,N\}} \lambda_{D I_2}$ being the fraction of the time where one user had delayed CSIT, the work in [11] characterized the optimal DoF region to take the form

$$\begin{aligned} d_1 \leq 1, \quad d_1 \leq 1, \\ d_1 + 2d_2 \leq 2 + \lambda_P \\ d_2 + 2d_1 \leq 2 + \lambda_P \\ d_1 + d_2 \leq 1 + \lambda_P + \lambda_D. \end{aligned}$$

The above setting corresponds to our symmetric setting where $\alpha_t^{(1)}, \beta_t^{(1)}, \alpha_t^{(2)}, \beta_t^{(2)} \in \{0, 1\}$, $\forall t$, and where

$$\lambda_P = \bar{\alpha}^{(1)} = \bar{\alpha}^{(2)} \tag{2.87}$$

$$\lambda_D = \bar{\beta}^{(1)} - \bar{\alpha}^{(1)} = \bar{\beta}^{(2)} - \bar{\alpha}^{(2)} \tag{2.88}$$

in which case our DoF inner bound matches the above, and as a result, for any $\bar{\beta} \geq \frac{1+2\bar{\alpha}}{3}$, Theorem 1 generalizes [11] to any set of quality exponents, avoiding the symmetry assumption, as well as easing on the i.i.d. block-fading assumption.

The universal scheme described in this section, can be directly applied to optimally implement more general alternating CSIT settings. We here offer an example where, in the presence of sufficiently good delayed CSIT, the current CSIT of the two users alternates between two quality exponents equal to $\frac{1}{2}$ and $\frac{3}{4}$, i.e.,

	$t=1$	$t=2$	$t=3$	$t=4$	$\cdots$
$\alpha_t^{(1)} =$	$\frac{1}{2}$	$\frac{3}{4}$	$\frac{1}{2}$	$\frac{3}{4}$	$\cdots$
$\alpha_t^{(2)} =$	$\frac{3}{4}$	$\frac{1}{2}$	$\frac{3}{4}$	$\frac{1}{2}$	$\cdots$

In this case, which corresponds to having $\bar{\alpha}^{(1)} = \bar{\alpha}^{(2)} = 5/8$, we can choose any delayed CSIT process that gives $\bar{\beta}^{(1)} = \bar{\beta}^{(2)} = 3/4$ which suffices (see Corollary 1d) to achieve the optimal DoF region by achieving the optimal DoF point $(d_1 = \frac{7}{8}, d_2 = \frac{7}{8})$.

Toward designing the scheme, we set $\bar{\delta} = 3/4$. For this example, and again considering a block-fading fast-fading setting (unit-length coherence period), the scheme can have phases with duration $T = 2$. The transmitted signal (cf. (2.41)) now takes the form

$$\boldsymbol{x}_t = \boldsymbol{w}_t c_t + \hat{\boldsymbol{g}}_t^{\perp} a_t + \hat{\boldsymbol{h}}_t a_t' + \hat{\boldsymbol{h}}_t^{\perp} b_t + \hat{\boldsymbol{g}}_t b_t'$$

with power and rates of the symbols being set as instructed in (2.43). Again as instructed by the general description of the scheme, at the end of phase $s =$

TABLE 2.5 – Bits carried by private symbols, common symbols, and by the quantized interference, for phase s, $s = 1, 2, \cdots, S-1$, of the alternating CSIT scheme.

	Total bits ($\times \log P$)
Private symbols for user 1	$(7 \times 2)/8$
Private symbols for user 2	$(7 \times 2)/8$
Common symbols	$(1 \times 2)/4$
Quantized interference	$(1 \times 2)/4$

$1, 2, \cdots, S-1$, the transmitter quantizes the interference accumulated during that phase, and does so using a total of $2(1/8 + 1/8) \log P$ quantization bits (cf. (2.55)). These bits are then mapped into the common symbols that will be transmitted in the next phase. For a large number of phases, the proposed scheme achieves the optimal DoF point $(d_1 = \frac{7}{8}, d_2 = \frac{7}{8})$. Table 2.5 summarizes the rates associated to the symbols in this scheme.

Schemes with short duration

We recall that the Maddah-Ali and Tse scheme [4] uses (under the employed assumption in [4] of a unit coherence period) $T = 3$ channel uses, during which it employs[10] $\beta_1^{(1)} = 1, \beta_1^{(2)} = 1$ (the rest of the exponents are zero). The scheme manages to have the information bits of the quantized interference, 'fit' inside the common symbols in the above three time slots.

A similar setting where again the information bits of the quantized interference, can fit in the common symbols of a single, short phase, would be if

$$\begin{array}{rccccc} & t=1 & t=2 & t=3 & t=4 & \cdots \\ \alpha_t^{(1)} = & 0 & 0 & \frac{1}{4} & 0 & \cdots \\ \beta_t^{(1)} = & 1 & \frac{1}{4} & \frac{1}{4} & 0 & \cdots \\ \alpha_t^{(2)} = & 0 & \frac{1}{4} & 0 & 0 & \cdots \\ \beta_t^{(2)} = & 1 & \frac{1}{4} & \frac{1}{4} & 0 & \cdots \end{array}$$

where the corresponding single-phase ($T = 4$ time-slots) scheme, can achieve the optimal DoF corner point $(d_1 = \frac{11}{16}, d_2 = \frac{11}{16})$.

10. We here refer to an equivalent MAT scheme that can be seen as a special case of the scheme in [6] for $\alpha = 0$.

2.5 Conclusions

The work made progress toward establishing and meeting the limits of using imperfect and delayed feedback. Considering a general CSIT process and a primitive measure of CSIT quality, the work provided DoF expressions that are simple and insightful functions of easy to calculate parameters which concisely capture the problem complexity. The derived insight addresses practical questions on topics relating to the usefulness of predicted, current and delayed CSIT, the impact of estimate precision, the effect of feedback delays, and the benefit of having feedback symmetry by employing comparable feedback links across users. Further insight was derived from the introduced *periodically evolving feedback* setting, which captures many of the engineering options in practical feedback settings.

In terms of the applicability of the DoF high-SNR asymptotic approach, for our chosen setting of a small number of users (two in this case), we expect the high-SNR insights to hold for SNR values of operational interest. The nature of the improved bounds and novel constructions, allows for this same insight to hold for a broad family of block fading and non-block fading channel models.

We believe that the adopted approach is fundamental, in the sense that it considers a general fading process, a general CSIT process, and a primitive measure of feedback quality in the form of the precision of estimates at any time about any channel, i.e., in the form of the entire set of estimation errors $\{(\boldsymbol{h}_t - \hat{\boldsymbol{h}}_{t,t'}), (\boldsymbol{g}_t - \hat{\boldsymbol{g}}_{t,t'})\}_{t,t'=1}^{n}$ at any time about any channel. As we have seen, this set of errors naturally fluctuates depending on the instance of the problem, and as expected, the overall optimal performance is defined by the statistics of this error set. These statistics are mildly constrained to the case of having Gaussian estimation errors which are independent of the prior and current channel estimates [11]. Under these assumptions, the results capture the performance effect of the statistics of feedback. Interestingly this effect - at least for sufficiently good delayed CSIT, and for high SNR - is captured by the averages of the quality exponents. As noted, this can be traced back to the assumption that the estimation errors are Gaussian, which means that the statistics of $\{(\boldsymbol{h}_t - \hat{\boldsymbol{h}}_{t,t'}), (\boldsymbol{g}_t - \hat{\boldsymbol{g}}_{t,t'})\}_{t,t'=1}^{n}$ are captured by a covariance matrix that has diagonal (block) entries of the form $\{\frac{1}{M}\mathbb{E}[||\boldsymbol{h}_t - \hat{\boldsymbol{h}}_{t,t'}||_F^2], \frac{1}{M}\mathbb{E}[||\boldsymbol{g}_t - \hat{\boldsymbol{g}}_{t,t'}||_F^2]\}_{t,t'=1}^{n}$, and whose off-diagonal entries are not used by the scheme, but where this scheme though meets an outer bound that has kept open the possibility of any off-diagonal elements. Hence, as stated, under our assumptions, the essence of the CSIT error statistics is captured by the diagonal block elements (of the aforementioned covariance matrix) whose effects are in turn captured - in the high-SNR regime - by the quality

11. Again we caution the reader that this is not an assumption about independence between errors, but rather between errors and estimates.

exponents.

This general approach allows for consideration of many facets of the performance-vs-feedback question in the two-user MISO BC setting, accentuating some important facets while revealing the reduced role of other facets. For example, while the approach allows for consideration of predicted CSIT - i.e., of estimates for future channels - the result at the end reveals that such estimates do not provide DoF gains, again under our assumptions. In a similar manner, the result leaves open the possibility of a role in the off-diagonal elements of the aforementioned covariance matrix of estimation errors, but in the end again reveals that these can be neglected without a DoF effect. Similarly, the approach allows for any 'typical' sequence of quality exponents - thus avoiding the need to assume periodic or static feedback processes or a block-fading structure - but despite this generality in the range of the considered exponents, in the end the result reveals that what really matters is the long-term average of each of these sequences of current and delayed CSIT exponents.

Finally we believe the main assumptions here to be mild. Regarding the high SNR assumption, there is substantial evidence that for primitive networks (such as the BC and the IC) with a reasonably small number of users, DoF analysis offers good insight on the performance at moderate SNR. Any possible extensions though to the setting of larger cellular networks, may need to consider saturation effects on the high-SNR spectral efficiency, as these were recently revealed in [29] to hold for settings where communication involves clusters of large size. Furthermore the assumption of having global CSIR, allowed us to focus on the question of feedback to the transmitters, which is a fundamental question on its own. While the overhead of gathering global CSIR must not be neglected, it has been repeatedly shown (cf. [35,36]) that this overhead is manageable in the presence of a reduced number of users. When considering extensions to other multiuser networks with potentially more users, such analysis may have to be combined with finding ways to disseminate imperfect global CSIR (cf. [35,36,38], see also [30,40]) whose effect increases as the number of users increases. Additionally asking that current estimation errors are independent of current estimates, is a widely accepted assumption. Similarly accepted is the assumption that the estimation error is independent of the past estimates, as this assumption suggests good feedback processes that utilize possible correlations to improve current channel estimates. Finally the requirement that the running average of the quality exponents of a single user, converges to a fixed value after a sufficiently long time, is also believed to be reasonable, as it would hold even if these exponents were themselves treated as random variables from an ergodic process.

2.6 Appendix - Proof of outer bound Lemma

Proof. Let W_1, W_2 respectively denote the messages for the first and second user, and let R_1, R_2 denote the two users' rates. Each user sends their message over n channel uses, where n is large. For ease of exposition we introduce the following notation.

$$\begin{aligned}
\boldsymbol{S}_t &\triangleq \begin{bmatrix} \boldsymbol{h}_t^\mathsf{T} \\ \boldsymbol{g}_t^\mathsf{T} \end{bmatrix}, \quad \check{\boldsymbol{S}}_t \triangleq \begin{bmatrix} \check{\boldsymbol{h}}_t^\mathsf{T} \\ \check{\boldsymbol{g}}_t^\mathsf{T} \end{bmatrix}, \quad \hat{\boldsymbol{S}}_t \triangleq \begin{bmatrix} \hat{\boldsymbol{h}}_t^\mathsf{T} \\ \hat{\boldsymbol{g}}_t^\mathsf{T} \end{bmatrix}, \quad \boldsymbol{z}_t \triangleq \begin{bmatrix} z_t^{(1)} \\ z_t^{(2)} \end{bmatrix} \\
y_{[n]}^{(i)} &\triangleq \{y_t^{(i)}\}_{t=1}^n, \quad i = 1, 2 \\
\Omega_{[n]} &\triangleq \{\boldsymbol{S}_t, \check{\boldsymbol{S}}_t, \hat{\boldsymbol{S}}_t\}_{t=1}^n.
\end{aligned}$$

The first step is to construct a degraded BC by providing the first user with complete and immediately available information on the second user's received signal. In this improved scenario, the following bounds hold.

$$\begin{aligned}
&nR_1 \\
&= H(W_1) \\
&= H(W_1|\Omega_{[n]}) \\
&\leq I(W_1; y_{[n]}^{(1)}, y_{[n]}^{(2)}|\Omega_{[n]}) + n\epsilon_n \qquad (2.89) \\
&\leq I(W_1; W_2, y_{[n]}^{(1)}, y_{[n]}^{(2)}|\Omega_{[n]}) + n\epsilon_n \\
&= I(W_1; y_{[n]}^{(1)}, y_{[n]}^{(2)}|W_2, \Omega_{[n]}) + n\epsilon_n \\
&= h(y_{[n]}^{(1)}, y_{[n]}^{(2)}|W_2, \Omega_{[n]}) - \underbrace{h(y_{[n]}^{(1)}, y_{[n]}^{(2)}|W_1, W_2, \Omega_{[n]})}_{no(\log P)} + n\epsilon_n \\
&= \sum_{t=1}^{n} h(y_t^{(1)}, y_t^{(2)}|y_{[t-1]}^{(1)}, y_{[t-1]}^{(2)}, W_2, \Omega_{[n]}) + no(\log P) + n\epsilon_n \qquad (2.90)
\end{aligned}$$

where (2.89) results from Fano's inequality, where $y_0^{(i)}$ was set to zero by convention, and where the last equality follows from the entropy chain rule and the fact that the knowledge of $\{W_1, W_2, \Omega_{[n]}\}$ implies knowledge of $\{y_{[n]}^{(1)}, y_{[n]}^{(2)}\}$ up to noise level.

Similarly

$$
\begin{aligned}
& nR_2 \\
& = H(W_2) \\
& \leq I(W_2; y_{[n]}^{(2)}|\Omega_{[n]}) + n\epsilon_n && (2.91) \\
& = \underbrace{h(y_{[n]}^{(2)}|\Omega_{[n]})}_{\leq n\log P + no(\log P)} - h(y_{[n]}^{(2)}|W_2, \Omega_{[n]}) + n\epsilon_n && (2.92) \\
& \leq -\sum_{t=1}^{n} h(y_t^{(2)}|y_{[t-1]}^{(2)}, W_2, \Omega_{[n]}) + n\log P + no(\log P) + n\epsilon_n && (2.93) \\
& \leq -\sum_{t=1}^{n} h(y_t^{(2)}|y_{[t-1]}^{(1)}, y_{[t-1]}^{(2)}, W_2, \Omega_{[n]}) \\
& \qquad + n\log P + no(\log P) + n\epsilon_n && (2.94)
\end{aligned}
$$

where (2.93) follows from the entropy chain rule and from the fact that received signals are scalars, while the last step is due to the fact that conditioning reduces entropy.

Now given (2.90) and (2.94), we upper bound $R_1 + 2R_2$ as

$$
\begin{aligned}
& n(R_1 + 2R_2) \leq 2n\log P + no(\log P) + 3n\epsilon_n \\
& + \sum_{t=1}^{n} \Big(h(y_t^{(1)}, y_t^{(2)}|U, S_t, \hat{S}_t) - 2h(y_t^{(2)}|U, S_t, \hat{S}_t) \Big) && (2.95)
\end{aligned}
$$

where

$$
U \triangleq \{y_{[t-1]}^{(1)}, y_{[t-1]}^{(2)}, W_2, \Omega_{[n]}\} \setminus S_t, \hat{S}_t
$$

and where each term $h(y_t^{(1)}, y_t^{(2)}|U, S_t, \hat{S}_t) - 2h(y_t^{(2)}|U, S_t, \hat{S}_t)$ in the summa-

tion, can be upper bounded as

$$
\begin{aligned}
&h(y_t^{(1)}, y_t^{(2)}|U, S_t, \hat{S}_t) - 2h(y_t^{(2)}|U, S_t, \hat{S}_t) \\
&\leq \max_{\substack{P_{X_t} \\ \mathbb{E}[\mathrm{tr}(X_t X_t^{\mathsf{H}})]\leq P}} \Big[h(y_t^{(1)}, y_t^{(2)}|U, S_t, \hat{S}_t) - 2h(y_t^{(2)}|U, S_t, \hat{S}_t)\Big] \\
&\leq \mathbb{E}_{\hat{S}_t} \max_{\substack{P_{X_t} \\ \mathbb{E}[\mathrm{tr}(X_t X_t^{\mathsf{H}})]\leq P}} \mathbb{E}_{S_t|\hat{S}_t}\Big[h(y_t^{(1)}, y_t^{(2)}|U, S_t = \boldsymbol{S}_t, \hat{S}_t = \hat{\boldsymbol{S}}_t) \\
&\qquad\qquad - 2h(y_t^{(2)}|U, S_t = \boldsymbol{S}_t, \hat{S}_t = \hat{\boldsymbol{S}}_t)\Big] \\
&= \mathbb{E}_{\hat{S}_t} \max_{\substack{P_{X_t} \\ \mathbb{E}[\mathrm{tr}(X_t X_t^{\mathsf{H}})]\leq P}} \mathbb{E}_{\tilde{S}_t}\Big[h(\boldsymbol{S}_t\boldsymbol{x}_t + \boldsymbol{z}_t|U) - 2h(\boldsymbol{g}_t^{\mathsf{T}}\boldsymbol{x}_t + z_t^{(2)}|U)\Big] \\
&= \mathbb{E}_{\hat{S}_t} \max_{\boldsymbol{\Psi}\succeq 0:\mathrm{tr}(\boldsymbol{\Psi})\leq P} \mathbb{E}_{\tilde{S}_t}\big[\log\det(I + \boldsymbol{S}_t\boldsymbol{\Psi}\boldsymbol{S}_t^{\mathsf{H}}) - 2\log\left(1 + \boldsymbol{g}_t^{\mathsf{H}}\boldsymbol{\Psi}\boldsymbol{g}_t\right)\Big] \qquad (2.96) \\
&\leq \mathbb{E}_{\hat{S}_t} \max_{\boldsymbol{\Psi}\succeq 0:\mathrm{tr}(\boldsymbol{\Psi})\leq P} \mathbb{E}_{\tilde{S}_t}\Big[\log\left(1 + \boldsymbol{h}_t^{\mathsf{H}}\boldsymbol{\Psi}\boldsymbol{h}_t\right) - \log\left(1 + \boldsymbol{g}_t^{\mathsf{H}}\boldsymbol{\Psi}\boldsymbol{g}_t\right)\Big]. \qquad (2.97)
\end{aligned}
$$

In the above, (2.96) uses the results in [41, Corollary 4] that tell us that Gaussian input maximizes the weighted difference of two differential entropies [12], as long as : 1) $y_t^{(2)}$ is a degraded version of $\{y_t^{(1)}, y_t^{(2)}\}$; 2) U is independent of $z_t^{(1)}, z_t^{(2)}$; 3) the input maximization is done given a fixed fading realization $\hat{\boldsymbol{S}}_t$, and is independent of $\tilde{\boldsymbol{S}}_t$ [13]. Furthermore, in the above, (2.97) comes from Fischer's inequality which gives that $\det(I + \boldsymbol{S}_t\boldsymbol{\Psi}\boldsymbol{S}_t^{\mathsf{H}}) \leq (1 + \boldsymbol{h}_t^{\mathsf{H}}\boldsymbol{\Psi}\boldsymbol{h}_t)(1 + \boldsymbol{g}_t^{\mathsf{H}}\boldsymbol{\Psi}\boldsymbol{g}_t)$.

At this point we follow the steps involving equation (25) in [6], to upper bound the right hand side of (2.97) as

$$
\begin{aligned}
&\mathbb{E}_{\hat{S}_t} \max_{\boldsymbol{\Psi}\succeq 0:\mathrm{tr}(\boldsymbol{\Psi})\leq P} \mathbb{E}_{\tilde{S}_t}\Big[\log\left(1 + \boldsymbol{h}_t^{\mathsf{H}}\boldsymbol{\Psi}\boldsymbol{h}_t\right) - \log\left(1 + \boldsymbol{g}_t^{\mathsf{H}}\boldsymbol{\Psi}\boldsymbol{g}_t\right)\Big] \\
&\leq \alpha_t^{(2)}\log P + o(\log P). \qquad (2.98)
\end{aligned}
$$

Combining (2.95) and (2.97), gives that

$$
n(R_1 + 2R_2) \leq \sum_{t=1}^{n}\Big((2 + \alpha_t^{(2)})\log P + o(\log P) + 3\epsilon_n\Big)
$$

12. We note that the results in [41, Corollary 4] are described for the non-fading channel model, however, as argued in the same work in [41, Section V], the results can be readily extended to the fading channel model by linearly transforming the fading channel into an equivalent non-fading channel, with the new channel actually maintaining the same capacity and the same degradedness order.

13. We recall that $\boldsymbol{x}_t$ is only a function of the messages and of the CSIT (current and delayed) estimates up to time t, and that these CSIT estimates are assumed to be independent of the current estimate errors at time t.

and consequently that

$$d_1 + 2d_2 \leq 2 + \bar{\alpha}^{(2)}.$$

Similarly, interchanging the roles of the two users, allows for

$$d_2 + 2d_1 \leq 2 + \bar{\alpha}^{(1)}.$$

Finally the fact that each user has a single receive antenna, gives that $d_1 \leq 1, d_2 \leq 1$. □

2.7 Appendix - Further details on the scheme

2.7.1 Explicit power allocation solutions under constraints in equations (2.45),(2.46),(2.47)

We remind the reader that, in designing the power allocation policy of the scheme, we must design the power parameters $\{\delta_t^{(1)}, \delta_t^{(2)}\}_{t\in\mathcal{B}_s}$ to satisfy equations (2.45),(2.46),(2.47) which asked that

$$\begin{aligned} \beta_t^{(i)} &\geq \delta_t^{(i)} \quad i=1,2,\ t\in\mathcal{B}_s \\ \frac{1}{T}\sum_{t\in\mathcal{B}_s}\delta_t^{(1)} &= \frac{1}{T}\sum_{t\in\mathcal{B}_s}\delta_t^{(2)} = \bar{\delta} \\ \frac{1}{T}\sum_{t\in\mathcal{B}_s}(\delta_t^{(i)}-\alpha_t^{(i)})^+ &= (\bar{\delta}-\bar{\alpha}^{(i)})^+ \quad i=1,2 \end{aligned}$$

for a given $\bar{\delta}\in[0,1]$. For each phase s, we here explicitly describe such sequence $\{\delta_t^{(1)}, \delta_t^{(2)}\}_{t\in\mathcal{B}_s}$, which is constructed using a waterfilling-like approach.

We first consider the case where $\bar{\delta}\geq\bar{\alpha}^{(i)}$. At any given time $t=\mathcal{B}_{s,1}, \mathcal{B}_{s,2}, \cdots, \mathcal{B}_{s,T}$, we set

$$\delta_t^{(i)}=\begin{cases} T(\bar{\delta}-\bar{\alpha}^{(i)})-\Delta_{\delta,t}+\alpha_t^{(i)} & \text{if } \beta_t^{(i)}\geq T(\bar{\delta}-\bar{\alpha}^{(i)})-\Delta_{\delta,t}+\alpha_t^{(i)} \\ \beta_t^{(i)} & \text{if } \beta_t^{(i)}< T(\bar{\delta}-\bar{\alpha}^{(i)})-\Delta_{\delta,t}+\alpha_t^{(i)} \end{cases}$$

where $\Delta_{\delta,t}$ is initialized to zero ($\Delta_{\delta,\mathcal{B}_{s,1}}=0$), and is updated each time, so that the calculation of $\delta_{t+1}^{(i)}$, uses

$$\Delta_{\delta,t+1}=\Delta_{\delta,t}+\delta_t^{(i)}-\alpha_t^{(i)}.$$

In the end, the solution takes the form

$$\delta_t^{(i)}=\begin{cases} \beta_t^{(i)}, & t=\mathcal{B}_{s,1},\cdots,\mathcal{B}_{s,\tau'-1} \\ T(\bar{\delta}-\bar{\alpha}^{(i)})+\alpha_t^{(i)}-\sum_{\ell=1}^{\tau'-1}(\beta_{\mathcal{B}_{s,\ell}}^{(i)}-\alpha_{\mathcal{B}_{s,\ell}}^{(i)}), & t=\mathcal{B}_{s,\tau'} \\ \alpha_t^{(i)}, & t=\mathcal{B}_{s,\tau'+1},\cdots,\mathcal{B}_{s,T} \end{cases}$$

where τ' is a function [14] of the quality exponents during phase s. This design of $\{\delta_t^{(i)}\}_{t\in\mathcal{B}_s}$ satisfies (2.45),(2.46), as well as (2.47), since, for the case where $\bar{\delta}-\bar{\alpha}^{(i)}\geq 0$, we deliberately force $\delta_t^{(i)}-\alpha_t^{(i)}\geq 0,\ t\in\mathcal{B}_s$.

Similarly for $\bar{\delta}\leq\bar{\alpha}^{(i)}$, we set

$$\delta_t^{(i)}=\begin{cases} \alpha_t^{(i)} & \text{if} \quad \alpha_t^{(i)}\leq T\bar{\delta}-\Delta_{\delta,t} \\ T\bar{\delta}-\Delta_{\delta,t} & \text{if} \quad \alpha_t^{(i)}> T\bar{\delta}-\Delta_{\delta,t} \end{cases}$$

14. Note that there is no need to explicitly describe τ', because the schemes are explicitly described as a function of the above $\delta_t^{(i)}$, which - after calculation - also reveal τ' which - by design - falls within the proper range.

where $\Delta_{\delta,t}$ is initialized to zero, and is updated as

$$\Delta_{\delta,t+1} = \Delta_{\delta,t} + \delta_t^{(i)}.$$

In the end, in this case, the solution takes the form

$$\delta_t^{(i)} = \begin{cases} \alpha_t^{(i)}, & t = \mathcal{B}_{s,1}, \cdots, \mathcal{B}_{s,\tau'-1} \\ T\bar{\delta} - \sum_{\ell=1}^{\tau'-1} \alpha_{\mathcal{B}_{s,\ell}}^{(i)}, & t = \mathcal{B}_{s,\tau'} \\ 0, & t = \mathcal{B}_{s,\tau'+1}, \cdots, \mathcal{B}_{s,T} \end{cases}$$

where again τ' is a function of the quality exponents during phase s. This satisfies (2.45),(2.46), as well as (2.47) since, for the case where $\bar{\delta} - \bar{\alpha}^{(i)} \leq 0$, we again have $\delta_t^{(i)} - \alpha_t^{(i)} \leq 0,\ t \in \mathcal{B}_s$.

2.7.2 Encoding and decoding details for equations (2.64),(2.66)

We here elaborate on how the users will be able to decode the amount of feedback bits described in equations (2.64) and (2.66). We first provide the following lemma, which holds for any T.

Lemma 2. *Let*

$$\bar{y}_t^{(1)} = c_t + P^{\frac{\delta_t^{(2)}}{2}} \bar{z}_t^{(1)}, \tag{2.99}$$

$$\bar{y}_t^{(2)} = c_t + P^{\frac{\delta_t^{(1)}}{2}} \bar{z}_t^{(2)}, \quad t = 1, 2, \cdots, T \tag{2.100}$$

where $\mathbb{E}[|c_t|^2] \leq P$, $Pr(|\bar{z}_t^{(i)}|^2 > P^{\epsilon}) \doteq 0$, *and* $\frac{1}{T}\sum_{t=1}^{T} \delta_t^{(i)} \leq \bar{\delta}^*$ *for a given* $\bar{\delta}^* \in [0,1]$, $i = 1, 2$. *Also let* $r \triangleq 1 - \bar{\delta}^* - \epsilon$ *for a vanishingly small but positive* $\epsilon > 0$, *and consider communication over* T *channel uses. Then for any rate up to* $R = r \log P - o(\log P)$ *(bits/channel use), the probability of error can be made to vanish with asymptotically increasing SNR.*

Proof. We will draw each T-length codevector

$$\boldsymbol{c} \triangleq [c_1, \cdots, c_T]^{\mathsf{T}}$$

from a lattice code of the form

$$\{\theta \boldsymbol{M} \boldsymbol{q} \mid \boldsymbol{q} \in \aleph\} \tag{2.101}$$

where $\aleph \subset \mathbb{C}^T$ is the T-dimensional 2^R-QAM constellation, where $\boldsymbol{M} \in \mathbb{C}^{T \times T}$ is a specifically constructed unitary matrix of algebraic conjugates that allows for the *non vanishing product distance* property (to be described later on - see for example [42]), and where

$$\theta = P^{\frac{1-r}{2}} = P^{(\bar{\delta}^* + \epsilon)/2} \tag{2.102}$$

is designed to guarantee that $\mathbb{E}||\boldsymbol{c}||^2 \doteq P$ (to derive this value of θ, just recall the QAM property that $\mathbb{E}||\boldsymbol{q}||^2 \doteq 2^R \doteq P^r$). Specifically for any two codevectors $\boldsymbol{c} = [c_1, \cdots, c_T]^\mathsf{T}, \boldsymbol{c}^\star = [c_1^\star, \cdots, c_T^\star]^\mathsf{T}$, $\boldsymbol{M}$ is designed to guarantee that

$$\prod_{t=1}^{T} |(c_t - c_t^\star)|^2 \dot{\geq} \theta^{2T}. \tag{2.103}$$

This can be readily done for all dimensions T by, for example, using the proper roots of unity as entries of a circulant $\boldsymbol{M}$ (cf. [42]), which in turn allows for the above product - before normalization with θ - to take non-zero integer values.

In the post-whitened channel model at user $i = 1, 2$, we have

$$\begin{aligned}
\bar{\bar{\boldsymbol{y}}}^{(1)} &\triangleq \mathrm{diag}(P^{-\delta_1^{(2)}/2}, \cdots, P^{-\delta_T^{(2)}/2})\bar{\boldsymbol{y}}^{(1)} \\
&= \mathrm{diag}(P^{-\delta_1^{(2)}/2}, \cdots, P^{-\delta_T^{(2)}/2})\boldsymbol{c} + \bar{\boldsymbol{z}}^{(1)} \\
\bar{\bar{\boldsymbol{y}}}^{(2)} &\triangleq \mathrm{diag}(P^{-\delta_1^{(1)}/2}, \cdots, P^{-\delta_T^{(1)}/2})\boldsymbol{c} + \bar{\boldsymbol{z}}^{(2)}
\end{aligned}$$

where, as we have stated, the noise $\bar{\boldsymbol{z}}^{(i)}$ has finite power in the sense that

$$Pr(||\bar{\boldsymbol{z}}^{(i)}||^2 > P^\epsilon) \to 0. \tag{2.104}$$

At the same time, after whitening at each user, the codeword distance for any two codewords $\boldsymbol{c}, \boldsymbol{c}^\star$, is lower bounded as

$$\begin{aligned}
&||\mathrm{diag}(P^{-\delta_1^{(i)}/2}, \cdots, P^{-\delta_T^{(i)}/2})(\boldsymbol{c} - \boldsymbol{c}^\star)||^2 \\
&= \sum_{t=1}^{T} |P^{-\delta_t^{(i)}/2}(c_t - c_t^\star)|^2 \\
&\dot{\geq} \prod_{t=1}^{T} |P^{-\delta_t^{(i)}/2}(c_t - c_t^\star)|^{2/T} && (2.105) \\
&= P^{-\frac{1}{T}\sum_{t=1}^{T}\delta_t^{(i)}} \prod_{t=1}^{T} |(c_t - c_t^\star)|^{2/T} \\
&\dot{\geq} P^{-\frac{1}{T}\sum_{t=1}^{T}\delta_t^{(i)}}\theta^2 && (2.106) \\
&\geq P^{-\bar{\delta}^*}P^{\bar{\delta}^*+\epsilon} = P^\epsilon && (2.107)
\end{aligned}$$

for $i = 1, 2$, where (2.105) results from the arithmetic-mean geometric-mean inequality, (2.106) is due to (2.103), and where (2.107) uses the assumption that $\frac{1}{T}\sum_{t=1}^{T}\delta_t^{(i)} \leq \bar{\delta}^*$. Setting ϵ positive but vanishingly small, combined with (2.104), proves the result. □

At this point, we use the lattice code of the above lemma, to design the T-length vector $\boldsymbol{c}$ transmitted during phase s. This encoding guarantees successful decoding of this vector, at both users, at a rate $R = r \log P - o(\log P)$, where $r = 1 - \bar{\alpha}^{(2)}$ for phase S, else $r = 1 - \bar{\delta}$ (ϵ is set positive but vanishingly small, recall (2.64), (2.66)). We note that for phase S, user $i = 1, 2$ can linearly transform their signal observations $\{y_t^{(i)}\}_{t \in \mathcal{B}_S}$ (cf. (2.61),(2.62)) to take the form in (2.99),(2.100), while for phase $s = 1, 2, \cdots, S-1$, user $i = 1, 2$ can linearly transform their signal observations $\{y_t^{(i)} - \bar{\imath}_t^{(i)}\}_{t \in \mathcal{B}_s}$ (after removing the interference $\bar{\imath}_t^{(i)}$, cf. (2.65),(2.49),(2.50)), again to take the form in (2.99),(2.100).

Finally we note that the achievable rate is determined by the exponent average $\frac{1}{T}\sum_{t=1}^{T} \delta_t^{(i)}$ and not by the instantaneous exponents $\delta_t^{(i)}$.

2.8 Appendix - Discussion on independence of estimation error and past estimates

The assumption on independence of estimation error and past estimates, is consistent with a large family of channel models ranging from the fast fading channel (i.i.d in time), to the correlated channel as this was presented in [6] [15], and even the quasi-static slow fading model where the CSIT estimates are successively refined over time. Successive CSIT refinement - as this is treated in [16] - considers an incremental amount of quantization bits that progressively improve the CSIT estimates. For example, focusing on the estimates of channel $\boldsymbol{h}_1$, the quality of this estimate would improve in time, with a successive refinement that would entail

$$\begin{aligned}\boldsymbol{h}_1 &= \hat{\boldsymbol{h}}_{1,1} + \tilde{\boldsymbol{h}}_{1,1} \\ &= \underbrace{\hat{\boldsymbol{h}}_{1,1} + \hat{\tilde{\boldsymbol{h}}}_{1,1,2}}_{\hat{\boldsymbol{h}}_{1,2}} + \tilde{\boldsymbol{h}}_{1,2} \\ &= \underbrace{\hat{\boldsymbol{h}}_{1,1} + \hat{\tilde{\boldsymbol{h}}}_{1,1,2} + \hat{\tilde{\boldsymbol{h}}}_{1,2,3}}_{\hat{\boldsymbol{h}}_{1,3}} + \tilde{\boldsymbol{h}}_{1,3} \\ &\vdots\end{aligned}$$

where

$$\tilde{\boldsymbol{h}}_{1,t'} \triangleq \hat{\tilde{\boldsymbol{h}}}_{1,t',t''} + \tilde{\boldsymbol{h}}_{1,t''}$$

and where $\hat{\tilde{\boldsymbol{h}}}_{1,t',t''}$ denotes the estimate correction that happens between time t' and t''.

Generalizing this to the estimate of any channel $\boldsymbol{h}_t$, and accepting that the estimate correction $\hat{\tilde{\boldsymbol{h}}}_{t,t',t''}$ and estimate error $\tilde{\boldsymbol{h}}_{t,t''}$ are statistically independent, allows that the estimation error $\tilde{\boldsymbol{h}}_{t,t''}$ of $\boldsymbol{h}_t$ is independent of the previous and current estimates $\{\hat{\boldsymbol{h}}_{t,\tau}\}_{\tau \leq t''}$, which in turn allows for the aforementioned assumption to hold even for the block fading channel model.

As a side note, even though we consider the quantification of CSIT quality as in (2.37), we note that our results can be readily extended to the case where we estimate channel directions (phases), in which case we would simply consider $\frac{1}{||\boldsymbol{h}_t||}\boldsymbol{h}_t = \hat{\boldsymbol{h}}_t + \tilde{\boldsymbol{h}}_t$, $\frac{1}{||\boldsymbol{g}_t||}\boldsymbol{g}_t = \hat{\boldsymbol{g}}_t + \tilde{\boldsymbol{g}}_t$ (cf. [23]).

15. Note that our assumption is softer than the assumption in [6] where $\{\{\hat{\boldsymbol{h}}_{t,t'}, \hat{\boldsymbol{g}}_{t,t'}\}_{t'=1}^{t}, \boldsymbol{h}_t, \boldsymbol{g}_t\}_{t=1}^{t^*-1} \leftrightarrow \{\hat{\boldsymbol{h}}_{t^*,t^*}, \hat{\boldsymbol{g}}_{t^*,t^*}\} \leftrightarrow \{\boldsymbol{h}_{t^*}, \boldsymbol{g}_{t^*}\}$ was assumed to be a Markov chain; an assumption which may not directly hold in block fading settings where for example, having $\boldsymbol{h}_{t^*-1} = \boldsymbol{h}_{t^*}$ (resp. $\boldsymbol{g}_{t^*-1} = \boldsymbol{g}_{t^*}$), breaks the chain $\{\boldsymbol{h}_{t^*-1}, \boldsymbol{g}_{t^*-1}\} \leftrightarrow \{\hat{\boldsymbol{h}}_{t^*,t^*}, \hat{\boldsymbol{g}}_{t^*,t^*}\} \leftrightarrow \{\boldsymbol{h}_{t^*}, \boldsymbol{g}_{t^*}\}$ because, given $\boldsymbol{h}_{t^*-1} = \boldsymbol{h}_{t^*}$, the following conditional probability density functions hold $f_{\boldsymbol{h}_{t^*-1},\boldsymbol{h}_{t^*}|\hat{\boldsymbol{h}}_{t^*}} = f_{\boldsymbol{h}_{t^*}|\hat{\boldsymbol{h}}_{t^*}} \neq f_{\boldsymbol{h}_{t^*}|\hat{\boldsymbol{h}}_{t^*}} f_{\boldsymbol{h}_{t^*-1}|\hat{\boldsymbol{h}}_{t^*}}$ as long as $\hat{\boldsymbol{h}}_{t^*} \neq \boldsymbol{h}_{t^*}$ (naturally for two random variables X_1 and X_2, then $X_1|X_2$ cannot be independent of $X_1|X_2$ no matter what X_1 and X_2 are, unless $X_1 = X_2$).

2.9 Appendix - Another Outer Bound Proof

We here provide another outer bound proof (cf. Lemma 1), remaining in the general setting of having general CSIT feedback qualities ($\alpha_t^{(1)} \neq \alpha_t^{(2)}$), except that now the channel coefficients are assumed to be i.i.d. temporal variations, and that $M = 2$. Adopting the outer bound approach in [7], we first linearly convert the original BC in (2.1),(2.2) to an equivalent BC (see (2.108a),(2.108b)) having the same DoF region as the original BC (cf. [7]), and we then consider the degraded version of the equivalent BC in the absence of delayed feedback, which matches in capacity the degraded BC with feedback (for the memoryless case), and which exceeds the capacity of the equivalent BC. The final step considers the compound and degraded version of the equivalent BC without delayed feedback, whose DoF region will serve as an outer bound on the DoF region of the original BC.

The equivalent degraded compound BC Towards the equivalent BC, directly from (2.1),(2.2) we have that

$$\begin{aligned} y_t^{(1)} &= \boldsymbol{h}_t^{\mathsf{T}} \boldsymbol{x}_t + z_t^{(1)} \\ &= \boldsymbol{h}_t^{\mathsf{T}} \sqrt{P} \boldsymbol{Q}_t \frac{1}{\sqrt{P}} \boldsymbol{Q}_t^{-1} \boldsymbol{x}_t + z_t^{(1)} \\ &= \boldsymbol{h}_t^{\mathsf{T}} \sqrt{P} \boldsymbol{Q}_t \boldsymbol{x}_t^{'} + z_t^{(1)} \\ &= \sqrt{P} \boldsymbol{h}_t^{\mathsf{T}} \hat{\boldsymbol{g}}_t^{\perp} x_t^1 + \sqrt{P} \tilde{\boldsymbol{h}}_t^{\mathsf{T}} \hat{\boldsymbol{h}}_t^{\perp} x_t^2 + z_t^{(1)} \qquad (2.108a) \\ y_t^{(2)} &= \boldsymbol{g}_t^{\mathsf{T}} \boldsymbol{x}_t + z_t^{(2)} \\ &= \boldsymbol{g}_t^{\mathsf{T}} \sqrt{P} \boldsymbol{Q}_t \boldsymbol{x}_t^{'} + z_t^{(2)} \\ &= \sqrt{P} \tilde{\boldsymbol{g}}_t^{\mathsf{T}} \hat{\boldsymbol{g}}_t^{\perp} x_t^1 + \sqrt{P} \boldsymbol{g}_t^{\mathsf{T}} \hat{\boldsymbol{h}}_t^{\perp} x_t^2 + z_t^{(2)}, \qquad (2.108b) \end{aligned}$$

where

$$\boldsymbol{x}_t^{'} \triangleq [x_t^1 \ x_t^2]^T \triangleq \frac{1}{\sqrt{P}} \boldsymbol{Q}_t^{-1} \boldsymbol{x}_t,$$

where $\boldsymbol{Q}_t \triangleq[\hat{\boldsymbol{g}}_t^{\perp}\ \hat{\boldsymbol{h}}_t^{\perp}] \in \mathbb{C}^{2\times 2}$ is, with probability 1, an invertible matrix. Furthermore each receiver normalizes to get

$$\begin{aligned} y_t^{'(1)} &= \frac{y_t^{(1)}}{\boldsymbol{h}_t^{\mathsf{T}}\hat{\boldsymbol{g}}_t^{\perp}} \\ &= \sqrt{P}x_t^1 + \frac{\sqrt{P}\tilde{\boldsymbol{h}}_t^{\mathsf{T}}\hat{\boldsymbol{h}}_t^{\perp}x_t^2}{\boldsymbol{h}_t^{\mathsf{T}}\hat{\boldsymbol{g}}_t^{\perp}} + \frac{z_t^{(1)}}{\boldsymbol{h}_t^{\mathsf{T}}\hat{\boldsymbol{g}}_t^{\perp}} \\ &= \sqrt{P}x_t^1 + \sqrt{P^{1-\alpha_t^{(1)}}}h_t^{'}x_t^2 + z_t^{'(1)}, \end{aligned} \tag{2.109a}$$

$$\begin{aligned} y_t^{'(2)} &= \frac{y_t^{(2)}}{\boldsymbol{g}_t^{\mathsf{T}}\hat{\boldsymbol{h}}_t^{\perp}} \\ &= \sqrt{P}x_t^2 + \frac{\sqrt{P}\tilde{\boldsymbol{g}}_t^{\mathsf{T}}\hat{\boldsymbol{g}}_t^{\perp}x_t^1}{\boldsymbol{g}_t^{\mathsf{T}}\hat{\boldsymbol{h}}_t^{\perp}} + \frac{z_t^{(2)}}{\boldsymbol{g}_t^{\mathsf{T}}\hat{\boldsymbol{h}}_t^{\perp}} \\ &= \sqrt{P}x_t^2 + \sqrt{P^{1-\alpha_t^{(2)}}}g_t^{'}x_t^1 + z_t^{'(2)}, \end{aligned} \tag{2.109b}$$

where $z_t^{'(1)} = \frac{z_t^{(1)}}{\boldsymbol{h}_t^{\mathsf{T}}\hat{\boldsymbol{g}}_t^{\perp}}$, $h_t^{'} = \frac{\sqrt{P^{\alpha_t^{(1)}}}\tilde{\boldsymbol{h}}_t^{\mathsf{T}}\hat{\boldsymbol{h}}_t^{\perp}}{\boldsymbol{h}_t^{\mathsf{T}}\hat{\boldsymbol{g}}_t^{\perp}}$, $z_t^{'(2)} = \frac{z_t^{(2)}}{\boldsymbol{g}_t^{\mathsf{T}}\hat{\boldsymbol{h}}_t^{\perp}}$, $g_t^{'} = \frac{\sqrt{P^{\alpha_t^{(2)}}}\tilde{\boldsymbol{g}}_t^{\mathsf{T}}\hat{\boldsymbol{g}}_t^{\perp}}{\boldsymbol{g}_t^{\mathsf{T}}\hat{\boldsymbol{h}}_t^{\perp}}$. Consequently $\sqrt{P^{\alpha_t^{(1)}}}\tilde{\boldsymbol{h}}_t$ and $\sqrt{P^{\alpha_t^{(2)}}}\tilde{\boldsymbol{g}}_t$ have identity covariance matrices, and the average power of $h_t^{'}$, $g_t^{'}$, $z_t^{'(1)}$ and $z_t^{'(2)}$ does not scale with P, i.e., in the high-SNR region this power is of order P^0. With the same CSIT knowledge mapped from the original BC, it can be shown (see [7]) that the DoF region of the equivalent BC in (2.109a)(2.109b) matches the DoF region of the original BC in (2.1)(2.2).

Towards designing the degraded version of the above equivalent BC, we supply the second user with knowledge of $y_t^{'(1)}$, and towards designing the compound version of the above degraded equivalent BC, we add two extra users (user 3 and 4). In this compound version, the received signals for the first two users are as in (2.109a)(2.109b), while the received signals of the added (virtual) users are given by

$$y_t^{''(1)} = \sqrt{P}x_t^1 + \sqrt{P^{1-\alpha_t^{(1)}}}h_t^{''}x_t^2 + z_t^{''(1)}, \tag{2.110a}$$

$$y_t^{''(2)} = \sqrt{P}x_t^2 + \sqrt{P^{1-\alpha_t^{(2)}}}g_t^{''}x_t^1 + z_t^{''(2)}. \tag{2.110b}$$

We here note that by definition, $h_t^{''}$ and $g_t^{''}$ are statistically equivalent to the original $h_t^{'}$ and $g_t^{'}$ respectively, and that $z_t^{''(1)}$ and $z_t^{''(2)}$ are statistically equivalent to the original $z_t^{'(1)}$ and $z_t^{'(2)}$. Furthermore we note that user 3 is interested in the same message as user 1, while user 4 is interested in the same message as user 2. Also we recall that in the specific degraded compound BC, user 1 knows $y_t^{'(1)}$, user 2 knows $y_t^{'(2)}$ and $y_t^{'(1)}$, user 3 knows

$y_t^{''(1)}$, and user 4 knows $y_t^{''(2)}$ and $y_t^{''(1)}$. Finally we remove delayed feedback - a removal known to not affect the capacity of the degraded BC without memory [43].

We now proceed to calculate an outer bound on the DoF region of this degraded compound BC which at least matches the DoF of the previous degraded BC and which serves as an outer bound on the DoF region of the original BC.

Outer bound We consider communication over the described equivalent degraded compound BC, letting n be the large number of fading realizations over which communication takes place, and letting R_1, R_2 be the rates of the first and second user. We also let $\Omega_{[n]} \triangleq \{\boldsymbol{h}_t, \boldsymbol{g}_t, \hat{\boldsymbol{h}}_t, \hat{\boldsymbol{g}}_t\}_{t=1}^n$, $y_{[n]}^{'(i)} \triangleq \{y_t^{'(i)}\}_{t=1}^n$ and $y_{[n]}^{''(i)} \triangleq \{y_t^{''(i)}\}_{t=1}^n$ for $i = 1, 2$.

Using Fano's inequality, we have

$$\begin{aligned} nR_1 &\leq I(W_1; y_{[n]}^{'(1)} | \Omega_{[n]}) + no(n) \\ &\leq n \log P + no(\log P) - h(y_{[n]}^{'(1)} | W_1, \Omega_{[n]}) + no(n), \end{aligned} \tag{2.111}$$

as well as

$$\begin{aligned} nR_1 &\leq I(W_1; y_{[n]}^{''(1)} | \Omega_{[n]}) + no(n) \\ &\leq n \log P + no(\log P) - h(y_{[n]}^{''(1)} | W_1, \Omega_{[n]}) + no(n), \end{aligned} \tag{2.112}$$

which is added to (2.111) to give

$$\begin{aligned} 2nR_1 &\leq 2n \log P + 2no(\log P) - h(y_{[n]}^{'(1)} | W_1, \Omega_{[n]}) \\ &\quad - h(y_{[n]}^{''(1)} | W_1, \Omega_{[n]}) + 2no(n) \\ &\leq 2n \log P + 2no(\log P) \\ &\quad - h(y_{[n]}^{'(1)}, y_{[n]}^{''(1)} | W_1, \Omega_{[n]}) + 2no(n). \end{aligned} \tag{2.113}$$

Let

$$\begin{aligned} \bar{\boldsymbol{y}}_t &\triangleq \operatorname{diag}(1, \sqrt{P^{\alpha_t^{(1)}}}) \begin{bmatrix} 1 & h_t^{'} \\ 1 & h_t^{''} \end{bmatrix}^{-1} \begin{bmatrix} y_t^{'(1)} \\ y_t^{''(1)} \end{bmatrix} \\ &= \begin{bmatrix} \sqrt{P} x_t^1 \\ \sqrt{P} x_t^2 \end{bmatrix} + \begin{bmatrix} \frac{z_t^{'(1)} h_t^{''} - z_t^{''(1)} h_t^{'}}{h_t^{''} - h_t^{'}} \\ \sqrt{P^{\alpha_t^{(1)}}} \frac{z_t^{''(1)} - z_t^{'(1)}}{h_t^{''} - h_t^{'}} \end{bmatrix} \\ &= \begin{bmatrix} \sqrt{P} x_t^1 \\ \sqrt{P} x_t^2 \end{bmatrix} + \begin{bmatrix} \bar{z}_t \\ 0 \end{bmatrix} + \begin{bmatrix} 0 \\ z_t \end{bmatrix} \end{aligned} \tag{2.114}$$

where $\bar{z}_t = \frac{z_t^{'(1)} h_t'' - z_t^{''(1)} h_t'}{h_t'' - h_t'}$, $z_t = \sqrt{P^{\alpha_t^{(1)}}} \frac{z_t^{''(1)} - z_t^{'(1)}}{h_t'' - h_t'}$, and let $z_{[n]} \triangleq \{z_t\}_{t=1}^n$. Consequently

$$\begin{aligned} nR_1 + nR_2 &= H(W_1, W_2) \\ &= I(W_1, W_2; y_{[n]}^{'(1)}, y_{[n]}^{''(1)}, z_{[n]} | \Omega_{[n]}) \\ &\quad + H(W_1, W_2 | y_{[n]}^{'(1)}, y_{[n]}^{''(1)}, z_{[n]}, \Omega_{[n]}) \\ &= I(W_1, W_2; y_{[n]}^{'(1)}, y_{[n]}^{''(1)}, z_{[n]} | \Omega_{[n]}) \\ &\quad + no(\log P) + no(n) \qquad (2.115) \\ &= I(W_1; y_{[n]}^{'(1)}, y_{[n]}^{''(1)}, z_{[n]} | \Omega_{[n]}) \\ &\quad + I(W_2; y_{[n]}^{'(1)}, y_{[n]}^{''(1)}, z_{[n]} | \Omega_{[n]}, W_1) \\ &\quad + no(\log P) + no(n), \qquad (2.116) \end{aligned}$$

where the transition to (2.115) uses the fact that the high SNR variance of $\bar{z}_t$ and z_t scales as P^0 and $P^{\alpha_t^{(1)}}$ respectively, which in turn means that knowledge of $\{y_t^{'(1)}, y_t^{''(1)}, z_t, \Omega_{[n]}\}_{t=1}^n$, implies knowledge of W_1, W_2 and of $\{x_t^1, x_t^2\}_{t=1}^n$, up to bounded noise level.

Furthermore

$$\begin{aligned} nR_1 &= H(W_1) \\ &= I(W_1; y_{[n]}^{'(1)}, y_{[n]}^{''(1)}, z_{[n]} | \Omega_{[n]}) + H(W_1 | y_{[n]}^{'(1)}, y_{[n]}^{''(1)}, z_{[n]}, \Omega_{[n]}) \\ &= I(W_1; y_{[n]}^{'(1)}, y_{[n]}^{''(1)}, z_{[n]} | \Omega_{[n]}) + no(\log P) + no(n), \qquad (2.117) \end{aligned}$$

since again knowledge of $\{y_t^{'(1)}, y_t^{''(1)}, z_t, \Omega_{[n]}\}_{t=1}^n$ provides for W_1 up to bounded noise level.

Now combining (2.116) and (2.117), gives

$$\begin{aligned}
nR_2 &= I(W_2; y_{[n]}^{'(1)}, y_{[n]}^{''(1)}, z_{[n]}|\Omega_{[n]}, W_1) + no(\log P) + no(n) \\
&= I(W_2; y_{[n]}^{'(1)}, y_{[n]}^{''(1)}|\Omega_{[n]}, W_1) \\
&\quad + I(W_2; z_{[n]}|y_{[n]}^{'(1)}, y_{[n]}^{''(1)}, \Omega_{[n]}, W_1) + no(\log P) + no(n) \\
&= h(y_{[n]}^{'(1)}, y_{[n]}^{''(1)}|\Omega_{[n]}, W_1) - \underbrace{h(y_{[n]}^{'(1)}, y_{[n]}^{''(1)}|\Omega_{[n]}, W_1, W_2)}_{no(\log P)} \\
&\quad - \underbrace{h(z_{[n]}|y_{[n]}^{'(1)}, y_{[n]}^{''(1)}, \Omega_{[n]}, W_1, W_2)}_{no(\log P)} \\
&\quad + \underbrace{h(z_{[n]}|y_{[n]}^{'(1)}, y_{[n]}^{''(1)}, \Omega_{[n]}, W_1)}_{\leq h(z_{[n]})} + no(\log P) + no(n) \\
&\leq h(y_{[n]}^{'(1)}, y_{[n]}^{''(1)}|\Omega_{[n]}, W_1) + h(z_{[n]}) + no(\log P) + no(n) \\
&\leq h(y_{[n]}^{'(1)}, y_{[n]}^{''(1)}|W_1, \Omega_{[n]}) + n\bar{\alpha}^{(1)} \log P \\
&\quad + no(\log P) + no(n),
\end{aligned}$$

which is combined with (2.113) to give

$$2nR_1 + nR_2 \leq 2n \log P + n\bar{\alpha}^{(1)} \log P + no(\log P) + no(n), \tag{2.118}$$

which in turn proves the outer bound

$$2d_1 + d_2 \leq 2 + \bar{\alpha}^{(1)}. \tag{2.119}$$

Finally interchanging the roles of the two users and of $\alpha_t^{(1)}, \alpha_t^{(2)}$, gives

$$d_1 + 2d_2 \leq 2 + \bar{\alpha}^{(2)}. \tag{2.120}$$

Naturally the single antenna constraint gives that $d_1 \leq 1, d_2 \leq 1$. □

Chapter 3

Fundamental Performance and Feedback Tradeoff over the MIMO BC and IC

Extending recent findings on the two-user MISO broadcast channel (BC) with imperfect and delayed channel state information at the transmitter (CSIT), the work here explores the performance of the two user MIMO BC and the two user MIMO interference channel (MIMO IC), in the presence of feedback with evolving quality and timeliness. Under standard assumptions, and in the presence of M antennas per transmitter and N antennas per receiver, the work derives the DoF region, which is optimal for a large regime of sufficiently good (but potentially imperfect) delayed CSIT. This region concisely captures the effect of having predicted, current and delayed-CSIT, as well as concisely captures the effect of the quality of CSIT offered at any time, about any channel. In addition to the progress towards describing the limits of using such imperfect and delayed feedback in MIMO settings, the work offers different insights that include the fact that, an increasing number of receive antennas can allow for reduced quality feedback, as well as that no CSIT is needed for the direct links in the IC.

3.1 Introduction

3.1.1 MIMO BC and MIMO IC channel models

For the setting of the multiple-input multiple-output broadcast channel (MIMO BC), we consider the case where an M-antenna transmitter, sends

information to two receivers with N receive antennas each. In this setting, the received signals at the two receivers take the form

$$\boldsymbol{y}_t^{(1)} = \boldsymbol{H}_t^{(1)}\boldsymbol{x}_t + \boldsymbol{z}_t^{(1)} \tag{3.1}$$

$$\boldsymbol{y}_t^{(2)} = \boldsymbol{H}_t^{(2)}\boldsymbol{x}_t + \boldsymbol{z}_t^{(2)} \tag{3.2}$$

where $\boldsymbol{H}_t^{(1)} \in \mathbb{C}^{N\times M}, \boldsymbol{H}_t^{(2)} \in \mathbb{C}^{N\times M}$ respectively represent the first and second receiver channels at time t, where $\boldsymbol{z}_t^{(1)}, \boldsymbol{z}_t^{(2)}$ represent unit power AWGN noise at the two receivers, where $\boldsymbol{x}_t \in \mathbb{C}^{M\times 1}$ is the input signal with power constraint $\mathbb{E}[||\boldsymbol{x}_t||^2] \leq P$.

For the setting of the MIMO interference channel (MIMO IC), we consider a case where two transmitters, each with M transmit antennas, send information to their respective receivers, each having N receive antennas. In this setting, the received signals at the two receivers take the form

$$\boldsymbol{y}_t^{(1)} = \boldsymbol{H}_t^{(11)}\boldsymbol{x}_t^{(1)} + \boldsymbol{H}_t^{(12)}\boldsymbol{x}_t^{(2)} + \boldsymbol{z}_t^{(1)} \tag{3.3}$$

$$\boldsymbol{y}_t^{(2)} = \boldsymbol{H}_t^{(21)}\boldsymbol{x}_t^{(1)} + \boldsymbol{H}_t^{(22)}\boldsymbol{x}_t^{(2)} + \boldsymbol{z}_t^{(2)} \tag{3.4}$$

where $\boldsymbol{H}_t^{(11)} \in \mathbb{C}^{N\times M}, \boldsymbol{H}_t^{(22)} \in \mathbb{C}^{N\times M}$ represent the fading matrices of the direct links of the two pairs, while $\boldsymbol{H}_t^{(12)} \in \mathbb{C}^{N\times M}, \boldsymbol{H}_t^{(21)} \in \mathbb{C}^{N\times M}$, represent the fading matrices of the cross links at time t.

3.1.2 Degrees-of-freedom as a function of feedback quality

In the presence of perfect channel state information at the transmitter (CSIT), the degrees-of-freedom (DoF) performance [1] for the case of the MIMO BC, is given by (cf. [1])

$$\{d_1 \leq \min\{M,N\},\ d_2 \leq \min\{M,N\},\ d_1+d_2 \leq \min\{M,2N\}\} \tag{3.5}$$

whereas for the MIMO IC, this DoF region with perfect CSIT, is given by (cf. [44])

$$\{d_1 \leq \min\{M,N\},\ d_2 \leq \min\{M,N\},\ d_1+d_2 \leq \min\{2M,2N,\max\{M,N\}\}\}. \tag{3.6}$$

In the absence of any CSIT though, the BC performance reduces, from that in (3.5), to the DoF region

$$\{d_1+d_2 \leq \min\{M,N\}\} \tag{3.7}$$

1. We remind the reader that in the high-SNR setting of interest, for an achievable rate pair (R_1,R_2) for the first and second receiver respectively, the corresponding DoF pair (d_1,d_2) is given by $d_i = \lim_{P\to\infty} \frac{R_i}{\log P},\ i=1,2$ and the corresponding DoF region is then the set of all achievable DoF pairs.

corresponding to a symmetric DoF corner point ($d_1 = d_2 = \min\{M, N\}/2$) (cf. [3, 45]). Similarly the performance of the MIMO IC without any CSIT, reduces from the DoF region in (3.6), to the DoF region

$$\{d_1 \leq \min\{M, N\}, d_2 \leq \min\{M, N\}, d_1 + d_2 \leq \min\{N, 2M\}\} \tag{3.8}$$

corresponding to a symmetric DoF corner point ($d_1 = d_2 = \min\{N, 2M\}/2$) (cf. [3, 45]).

This gap necessitates the use of imperfect and delayed feedback, as this was studied in works like [12, 13, 19–30, 38] for specific instances. The work here makes progress towards describing the limits of this use of imperfect and delayed feedback.

3.1.3 Predicted, current and delayed CSIT

As in [14], we consider communication of an infinite duration n.

For the case of the BC, we consider a random fading process $\{\boldsymbol{H}_t^{(1)}, \boldsymbol{H}_t^{(2)}\}_{t=1}^n$, and a feedback process that provides CSIT estimates

$$\{\hat{\boldsymbol{H}}_{t,t'}^{(1)}, \hat{\boldsymbol{H}}_{t,t'}^{(2)}\}_{t,t'=1}^n$$

(of channel $\boldsymbol{H}_t^{(1)}, \boldsymbol{H}_t^{(2)}$) at any time $t' = 1, \cdots, n$. For the channel $\boldsymbol{H}_t^{(1)}, \boldsymbol{H}_t^{(2)}$ at a specific time t, the set of all available estimates $\{\hat{\boldsymbol{H}}_{t,t'}^{(1)}, \hat{\boldsymbol{H}}_{t,t'}^{(2)}\}_{t'}$, can be naturally split in the *predicted estimates* $\{\hat{\boldsymbol{H}}_{t,t'}^{(1)}, \hat{\boldsymbol{H}}_{t,t'}^{(2)}\}_{t'<t}$ that are offered before the channel materializes, the *current estimate* $\hat{\boldsymbol{H}}_{t,t}^{(1)}, \hat{\boldsymbol{H}}_{t,t}^{(2)}$ at time t, and the *delayed estimates* $\{\hat{\boldsymbol{H}}_{t,t'}^{(1)}, \hat{\boldsymbol{H}}_{t,t'}^{(2)}\}_{t'>t}$ that may allow for retrospective compensation for the lack of perfect quality feedback. Naturally the fundamental measure of feedback quality is given by the precision of estimates at any time about any channel, i.e., is given by

$$\{(\boldsymbol{H}_t^{(1)} - \hat{\boldsymbol{H}}_{t,t'}^{(1)}), (\boldsymbol{H}_t^{(2)} - \hat{\boldsymbol{H}}_{t,t'}^{(2)})\}_{t,t'=1}^n. \tag{3.9}$$

These estimation-error sets of course fluctuate depending on the instance of the problem, and as expected, the overall optimal performance is defined by the statistics of the above estimation errors. We here only assume that these errors have zero-mean circularly-symmetric complex Gaussian entries, that are *spatially* uncorrelated, and that at any time t, the current estimation error is independent of the channel estimates up to that time.

Similarly for the case of the IC, we consider a fading process $\{\boldsymbol{H}_t^{(11)}, \boldsymbol{H}_t^{(12)}, \boldsymbol{H}_t^{(21)}, \boldsymbol{H}_t^{(22)}\}_{t=1}^n$, a set of CSIT estimates

$$\{\hat{\boldsymbol{H}}_{t,t'}^{(11)}, \hat{\boldsymbol{H}}_{t,t'}^{(12)}, \hat{\boldsymbol{H}}_{t,t'}^{(21)}, \hat{\boldsymbol{H}}_{t,t'}^{(22)}\}_{t,t'=1}^n$$

and an overall feedback quality which, at any instance, is defined by

$$\{(\boldsymbol{H}_t^{(ij)} - \hat{\boldsymbol{H}}_{t,t'}^{(ij)})\}_{t,t'=1}^{n},\ i,j=1,2 \tag{3.10}$$

where again, the statistics of the above error sets define the optimal performance. We will here seek to capture this relationship between performance and feedback.

3.1.4 Notation, conventions and assumptions

We will generally follow the notations and assumptions in [14], and will adapt them to the MIMO and IC settings. When addressing the BC, we will use the notation

$$\alpha_t^{(i)} \triangleq -\lim_{P\to\infty} \frac{\log \mathbb{E}[||\boldsymbol{H}_t^{(i)} - \hat{\boldsymbol{H}}_{t,t}^{(i)}||_F^2]}{\log P},\quad \beta_t^{(i)} \triangleq -\lim_{P\to\infty} \frac{\log \mathbb{E}[||\boldsymbol{H}_t^{(i)} - \hat{\boldsymbol{H}}_{t,t+\eta}^{(i)}||_F^2]}{\log P} \tag{3.11}$$

where $\alpha_t^{(i)}$ is used to describe the *current quality exponent* for the CSIT for channel $\boldsymbol{H}_t^{(i)}$ of receiver $i,\ i=1,2$, while $\beta_t^{(i)}$ is used to describe the *delayed quality exponents* for each user. In the above, η can be as large as necessary, but it must be finite, as we here consider delayed CSIT that arrives after a finite delay from the channel it describes. The above used $||\bullet||_F$ to denote the Frobenius norm of a matrix.

Similarly when considering the MIMO IC, we will use the same notation, except that now

$$\begin{aligned}\alpha_t^{(i)} &\triangleq -\lim_{P\to\infty} \frac{\log \mathbb{E}[||\boldsymbol{H}_t^{(ij)} - \hat{\boldsymbol{H}}_{t,t}^{(ij)}||_F^2]}{\log P},\\ \beta_t^{(i)} &\triangleq -\lim_{P\to\infty} \frac{\log \mathbb{E}[||\boldsymbol{H}_t^{(ij)} - \hat{\boldsymbol{H}}_{t,t+\eta}^{(ij)}||_F^2]}{\log P},\quad i\neq j\end{aligned} \tag{3.12}$$

where $\alpha_t^{(1)}, \beta_t^{(1)}$ will correspond to the CSIT quality for the cross link $\boldsymbol{H}_t^{(12)}$ where this CSIT is available at transmitter 2, and where $\alpha_t^{(2)}, \beta_t^{(2)}$ will correspond to the CSIT quality for the cross link $\boldsymbol{H}_t^{(21)}$ where this CSIT is available at transmitter 1 [2]

As argued in [14], the results in [16, 17] easily show that without loss of generality, in the DoF setting of interest, we can restrict our attention to the range

$$0 \le \alpha_t^{(i)} \le \beta_t^{(i)} \le 1. \tag{3.13}$$

2. When treating the IC case, emphasis is placed on the CSIT of the cross links because, as it will turn out, the DoF region will be achieved without any knowledge of the direct links. This is a small improvement over [25] where both transmitters were assumed to have static-quality CSIT for all the channels $(\boldsymbol{H}_t^{(21)}, \boldsymbol{H}_t^{(21)}, \boldsymbol{H}_t^{(11)}, \boldsymbol{H}_t^{(22)})$.

Here having $\alpha_t^{(1)} = \alpha_t^{(2)} = 1$, corresponds to the highest quality CSIT with perfect timing (full CSIT) for the specific channel at time t, while having $\beta_t^{(i)} = 1$ corresponds to having perfect delayed CSIT for the same channel, i.e., it corresponds to the case where at some point $t' > t$, the transmitter has perfect estimates of the channel that materialized at time t.

Furthermore we will use the notation

$$\bar{\alpha}^{(i)} \triangleq \lim_{n\to\infty} \frac{1}{n} \sum_{t=1}^{n} \alpha_t^{(i)}, \quad \bar{\beta}^{(i)} \triangleq \lim_{n\to\infty} \frac{1}{n} \sum_{t=1}^{n} \beta_t^{(i)}, \quad i = 1, 2 \tag{3.14}$$

to denote the average of the quality exponents. As in [14] we will adopt the mild assumption that any sufficiently long subsequence $\{\alpha_t^{(1)}\}_{t=\tau}^{\tau+T}$ (resp. $\{\alpha_t^{(2)}\}_{t=\tau}^{\tau+T}, \{\beta_t^{(1)}\}_{t=\tau}^{\tau+T}, \{\beta_t^{(2)}\}_{t=\tau}^{\tau+T}$) has an average that converges to the long term average $\bar{\alpha}^{(1)}$ (resp. $\bar{\alpha}^{(2)}, \bar{\beta}^{(1)}, \bar{\beta}^{(2)}$), for any τ and for some finite T that can be chosen to be sufficiently large to allow for the above convergence.

Implicit in our definition of the quality exponents, is our assumption that $\mathbb{E}[||\boldsymbol{H}_t^{(1)} - \hat{\boldsymbol{H}}_{t,t'}^{(1)}||_F^2] \leq \mathbb{E}[||\boldsymbol{H}_t^{(1)} - \hat{\boldsymbol{H}}_{t,t''}^{(1)}||_F^2]$, $\mathbb{E}[||\boldsymbol{H}_t^{(2)} - \hat{\boldsymbol{H}}_{t,t'}^{(2)}||_F^2] \leq \mathbb{E}[||\boldsymbol{H}_t^{(2)} - \hat{\boldsymbol{H}}_{t,t''}^{(2)}||_F^2]$, for any $t' > t''$, (similarly for the IC case) which simply reflects the fact that one can revert back to past estimates of statistically better quality. This assumption can be removed - after a small change in the definition of the quality exponents - without an effect to the main result.

We adhere to the common convention (see [4, 6, 7, 25, 33]) of assuming perfect and global knowledge of channel state information at the receivers (perfect global CSIR), where the receivers know all channel states and all estimates. We will also adopt the common convention (see [5–7, 15]) of assuming that the current estimation error is statistically independent of current and past estimates. A discussion on this can be found in [14] which argues that this assumption fits well with many channel models, spanning from the fast fading channel (i.i.d. in time), to the correlated channel model as this is considered in [5], to the quasi-static block fading model where the CSIT estimates are successively refined while the channel remains static. Additionally we consider the entries of each estimation error matrix $\boldsymbol{H}_t^{(i)} - \hat{\boldsymbol{H}}_{t,t'}^{(i)}$ to be i.i.d. Gaussian[3]. Finally we will refer to a CSIT process with 'sufficiently good delayed CSIT', to be a process for which $\min\{\bar{\beta}^{(1)}, \bar{\beta}^{(2)}\} \geq \min\{1, M - \min\{M, N\}, \frac{N(1+\bar{\alpha}^{(1)}+\bar{\alpha}^{(2)})}{\min\{M,2N\}+N}, \frac{N(1+\min\{\bar{\alpha}^{(1)}+\bar{\alpha}^{(2)}\})}{\min\{M,2N\}}\}$.

3.1.5 Existing results directly relating to the current work

The work here builds on the ideas of [4] on using delayed CSIT to retrospectively compensate for interference due to lack of current CSIT, on

3. We here make it clear that we are simply referring to the MN entries in each such specific matrix $\boldsymbol{H}_t^{(i)} - \hat{\boldsymbol{H}}_{t,t'}^{(i)}$, and that we certainly do not suggest that the error entries are i.i.d. in time or across users.

the ideas in [5] and later in [6, 7] on exploiting perfect delayed and imperfect current CSIT, as well as the work in [8, 9] which - in the context of imperfect and delayed CSIT - introduced encoding and decoding with a phase-Markov structure that will be used later on. The work here is also motivated by the work in [19] which considered the use of delayed feedback in different MIMO BC settings, as well as by recent progress in [25] that considered MIMO BC and MIMO IC settings that enjoyed perfect delayed feedback as well as imperfect current feedback of a quality that remained unchanged throughout the communication process ($\alpha^{(1)} = -\lim_{P\to\infty} \frac{\log \mathbb{E}[||\boldsymbol{H}_t^{(1)} - \hat{\boldsymbol{H}}_{t,t}^{(1)}||_F^2]}{\log P}, \alpha^{(2)} = -\lim_{P\to\infty} \frac{\log \mathbb{E}[||\boldsymbol{H}_t^{(2)} - \hat{\boldsymbol{H}}_{t,t}^{(2)}||_F^2]}{\log P}, \ \forall t$). The work is finally motivated by the recent approach in [14] that employed sequences of evolving quality exponents to address a more fundamental problem of deriving the performance limits given a general CSIT process of a certain quality.

3.2 DoF region of the MIMO BC and MIMO IC

We proceed with the main DoF results, which are proved in Section 3.3 that describes the outer bound, and in Section 3.4 that describes an inner bound by extending the schemes from [14] to the symmetric MIMO BC and MIMO IC cases of interest. We recall that we consider communication of large duration n, a possibly correlated channel process $\{\boldsymbol{H}_t^{(1)}, \boldsymbol{H}_t^{(2)}\}_{t=1}^n$ ($\{\boldsymbol{H}_t^{(11)}, \boldsymbol{H}_t^{(12)}, \boldsymbol{H}_t^{(21)}, \boldsymbol{H}_t^{(22)}\}_{t=1}^n$ for the IC), and a feedback process of quality defined by the statistics of $\{(\boldsymbol{H}_t^{(1)} - \hat{\boldsymbol{H}}_{t,t'}^{(1)}), (\boldsymbol{H}_t^{(2)} - \hat{\boldsymbol{H}}_{t,t'}^{(2)})\}_{t=1,t'=1}^n$ ($\{(\boldsymbol{H}_t^{(ij)} - \hat{\boldsymbol{H}}_{t,t'}^{(ij)})\}_{t,t'=1}^n, \ \ i,j = 1,2$ for the IC). We henceforth, without loss of generality, label the users so that $\bar{\alpha}^{(2)} \leq \bar{\alpha}^{(1)}$.

We proceed with the DoF region for any CSIT process with sufficiently good delayed CSIT.

Theorem 2. *The optimal DoF region of the two-user $(M \times (N,N))$ MIMO BC with a CSIT process $\{\hat{\boldsymbol{H}}_{t,t'}^{(1)}, \hat{\boldsymbol{H}}_{t,t'}^{(2)}\}_{t=1,t'=1}^n$ of quality $\{(\boldsymbol{H}_t^{(1)} - \hat{\boldsymbol{H}}_{t,t'}^{(1)}), (\boldsymbol{H}_t^{(2)} -$*

$\hat{\boldsymbol{H}}_{t,t'}^{(2)})\}_{t=1,t'=1}^{n}$ *that has sufficiently good delayed CSIT, is given by*

$$d_1 \leq \min\{M, N\} \tag{3.15}$$

$$d_2 \leq \min\{M, N\} \tag{3.16}$$

$$d_1 + d_2 \leq \min\{M, 2N\} \tag{3.17}$$

$$\frac{d_1}{\min\{M,N\}} + \frac{d_2}{\min\{M,2N\}} \leq 1 + \frac{\min\{M,2N\} - \min\{M,N\}}{\min\{M,2N\}}\ \bar{\alpha}^{(1)} \tag{3.18}$$

$$\frac{d_1}{\min\{M,2N\}} + \frac{d_2}{\min\{M,N\}} \leq 1 + \frac{\min\{M,2N\} - \min\{M,N\}}{\min\{M,2N\}}\ \bar{\alpha}^{(2)} \tag{3.19}$$

while for the $(M, M) \times (N, N)$ *MIMO IC with feedback quality* $\{(\boldsymbol{H}_t^{(ij)} - \hat{\boldsymbol{H}}_{t,t'}^{(ij)})\}_{t,t'=1}^{n}$, $i, j = 1, 2$, *the above holds after substituting* (3.17) *with*

$$d_1 + d_2 \leq \min\{2M, 2N, \max\{M, N\}\}. \tag{3.20}$$

The following proposition provides the DoF region inner bound for the regime of low-quality delayed CSIT. The proof is shown in Section 3.4.

Proposition 2. *The DoF region of the two-user* $(M \times (N, N))$ *MIMO BC with a CSIT process of quality* $\{(\boldsymbol{H}_t^{(1)} - \hat{\boldsymbol{H}}_{t,t'}^{(1)}), (\boldsymbol{H}_t^{(2)} - \hat{\boldsymbol{H}}_{t,t'}^{(2)})\}_{t=1,t'=1}^{n}$ *such that* $\min\{\bar{\beta}^{(1)}, \bar{\beta}^{(2)}\} < \min\{1, M - \min\{M,N\}, \frac{N(1+\bar{\alpha}^{(1)}+\bar{\alpha}^{(2)})}{\min\{M,2N\}+N}, \frac{N(1+\bar{\alpha}^{(2)})}{\min\{M,2N\}}\}$, *is inner bounded by the polygon described by*

$$d_1 \leq \min\{M, N\} \tag{3.21}$$

$$d_2 \leq \min\{M, N\} \tag{3.22}$$

$$d_1 + d_2 \leq \min\{M, 2N\} \tag{3.23}$$

$$d_1 + d_2 \leq \min\{M,N\} + (\min\{M,2N\} - \min\{M,N\}) \min\{\bar{\beta}^{(1)}, \bar{\beta}^{(2)}\} \tag{3.24}$$

$$\frac{d_1}{\min\{M,N\}} + \frac{d_2}{\min\{M,2N\}} \leq 1 + \frac{\min\{M,2N\} - \min\{M,N\}}{\min\{M,2N\}}\ \bar{\alpha}^{(1)} \tag{3.25}$$

$$\frac{d_1}{\min\{M,2N\}} + \frac{d_2}{\min\{M,N\}} \leq 1 + \frac{\min\{M,2N\} - \min\{M,N\}}{\min\{M,2N\}}\ \bar{\alpha}^{(2)}. \tag{3.26}$$

while for the $(M, M) \times (N, N)$ *MIMO IC with feedback quality* $\{(\boldsymbol{H}_t^{(ij)} - \hat{\boldsymbol{H}}_{t,t'}^{(ij)})\}_{t,t'=1}^{n}$, $i, j = 1, 2$, *the above holds after substituting* (3.23) *with*

$$d_1 + d_2 \leq \min\{2M, 2N, \max\{M, N\}\}. \tag{3.27}$$

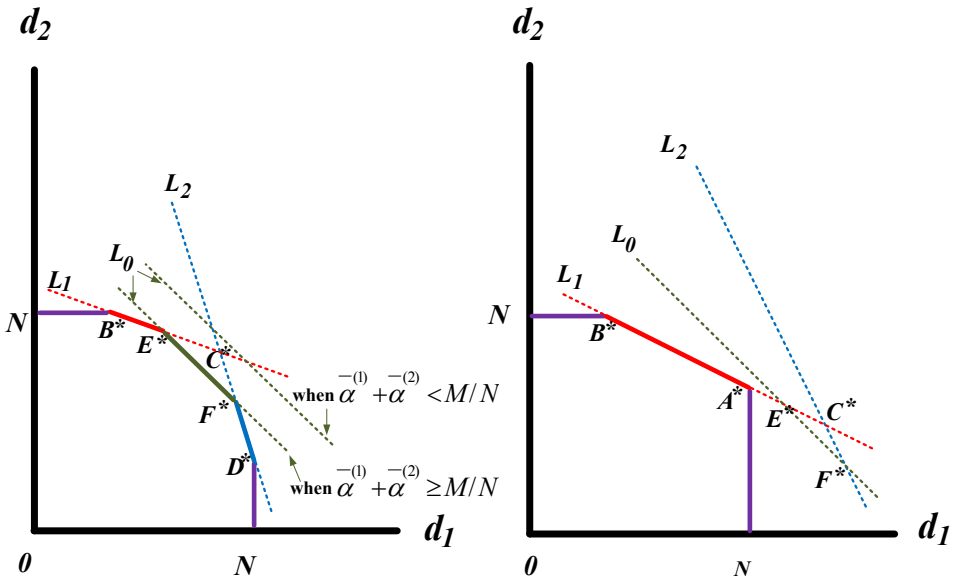

(a) Case: $N(1+\bar{\alpha}^{(2)})/M \geq \bar{\alpha}^{(1)}$ and $M>N$ **(b) Case:** $N(1+\bar{\alpha}^{(2)})/M \leq \bar{\alpha}^{(1)}$ and $M>N$

FIGURE 3.1 – Optimal DoF regions for two different cases for the two-user MIMO BC and MIMO IC, with $M > N$ and $\min\{\bar{\beta}^{(1)}, \bar{\beta}^{(2)}\} \geq \min\{1, M - \min\{M, N\}, \frac{N(1+\bar{\alpha}^{(1)}+\bar{\alpha}^{(2)})}{\min\{M,2N\}+N}, \frac{N(1+\bar{\alpha}^{(2)})}{\min\{M,2N\}}\}$. The corner points take the following values : $A^* = \big(N, \frac{(M-N)N(1+\bar{\alpha}^{(2)})}{M}\big)$, $B^* = \big((M-N)\bar{\alpha}^{(2)}, N\big)$, $C^* = \big(\frac{MN}{M+N}(1+\bar{\alpha}^{(1)} - \frac{N}{M}\bar{\alpha}^{(2)}), \frac{MN}{M+N}(1+\bar{\alpha}^{(2)} - \frac{N}{M}\bar{\alpha}^{(1)})\big)$, $D^* = \big(N, (M-N)\bar{\alpha}^{(1)}\big)$, $E^* = \big(M - N\bar{\alpha}^{(2)},\ N\bar{\alpha}^{(2)}\big)$, $F^* = \big(N\bar{\alpha}^{(1)},\ M - N\bar{\alpha}^{(1)}\big)$. Line L_0 corresponds to the bound in (3.17), Line L_1 corresponds to the bound in (3.19), while line L_2 corresponds to the bound in (3.18).

Remark 3. *As a small comment, and to place the above proposition in the context of previous work, we briefly note that deriving the DoF for even the simplest instance in the setting of low-quality delayed CSIT - corresponding to the case of* $\beta^{(1)} = \beta^{(2)} = \alpha^{(1)} = \alpha^{(2)} = 0$ *- has been a long lasting open problem. In this simple setting of all-zero quality exponents, the conjectured DoF of* $d_1 = d_2 = 1/2$ *in [15], matches the above inner bound.*

3.2.1 Imperfect current CSIT can be as useful as perfect current CSIT

The above results allow for direct conclusions on the amount of CSIT that is necessary to achieve the optimal DoF performance associated to perfect and immediately available CSIT. The following corollary holds for the BC and the IC case, for which we also remember that there is no need for CSIT when $M \leq N$ (cf. [3, 45]). The proofs for the following corollary, and of the corollary immediately after that, are direct from the above theorems.

Corollary 2a. *Having a CSIT process that offers* $\bar{\alpha}^{(1)}+\bar{\alpha}^{(2)} \geq \min\{M, 2N\}/N$*, allows for the optimal sum-DoF associated to having perfect and immediately (full) CSIT (*$\bar{\alpha}^{(1)} = \bar{\alpha}^{(2)} = 1$*).*

The above suggests a reduction in the required feedback quality $\bar{\alpha}^{(1)}, \bar{\alpha}^{(2)}$, as the number of receive antennas increases. Furthermore as stated before, when applied to the IC case, the above also reveals that no CSIT is needed for the direct links.

3.2.2 Imperfect delayed CSIT can be as useful as perfect delayed CSIT

Along the same lines, the following describes the amount of delayed CSIT that suffices to achieve the DoF associated to perfect delayed CSIT.

Corollary 2b. *Any CSIT process that offers* $\min\{\bar{\beta}^{(1)}, \bar{\beta}^{(2)}\} \geq \min\{1, M - \min\{M, N\}, \frac{N(1+\bar{\alpha}^{(1)}+\bar{\alpha}^{(2)})}{\min\{M,2N\}+N}, \frac{N(1+\bar{\alpha}^{(2)})}{\min\{M,2N\}}\}$*, can achieve the same DoF region as a CSIT process that offers perfect delayed CSIT (*$\bar{\beta}^{(1)} = \bar{\beta}^{(2)} = 1$*).*

3.3 Outer bound for the MIMO BC and MIMO IC with evolving feedback

We proceed to first describe the outer bound for the BC case. The bound, presented in the following lemma, draws from [13] and [14], and for this we here mainly focus on the proof steps that are important in the MIMO case.

3.3.1 Outer bound proof for the BC

Lemma 3. *The DoF region of the two-user MIMO BC with a CSIT process* $\{\hat{\boldsymbol{H}}_{t,t'}^{(1)}, \hat{\boldsymbol{H}}_{t,t'}^{(2)}\}_{t=1,t'=1}^{n}$ *of quality* $(\boldsymbol{H}_t^{(1)} - \hat{\boldsymbol{H}}_{t,t'}^{(1)}), (\boldsymbol{H}_t^{(2)} - \hat{\boldsymbol{H}}_{t,t'}^{(2)})\}_{t=1,t'=1}^{n}$, *is upper bounded as*

$$d_1 \leq \min\{M, N\} \tag{3.28}$$

$$d_2 \leq \min\{M, N\} \tag{3.29}$$

$$d_1 + d_2 \leq \min\{M, 2N\} \tag{3.30}$$

$$\frac{d_1}{\min\{M,N\}} + \frac{d_2}{\min\{M,2N\}} \leq 1 + \frac{\min\{M,2N\} - \min\{M,N\}}{\min\{M,2N\}}\ \bar{\alpha}^{(1)} \tag{3.31}$$

$$\frac{d_1}{\min\{M,2N\}} + \frac{d_2}{\min\{M,N\}} \leq 1 + \frac{\min\{M,2N\} - \min\{M,N\}}{\min\{M,2N\}}\ \bar{\alpha}^{(2)}. \tag{3.32}$$

Proof. For notational convenience we define $\langle \bullet \rangle' \triangleq \min\{\bullet, M\}$, $\Omega_{[n]} \triangleq \{\boldsymbol{H}_t^{(1)}, \boldsymbol{H}_t^{(2)}, \hat{\boldsymbol{H}}_{t,t'}^{(1)}, \hat{\boldsymbol{H}}_{t,t'}^{(2)}, \}_{t=1}^{n}{}_{t'=1}^{n}$, $\boldsymbol{y}_{[n]}^{(1)} \triangleq \{\boldsymbol{y}_t^{(1)}\}_{t=1}^{n}$ and $\boldsymbol{y}_{[n]}^{(2)} \triangleq \{\boldsymbol{y}_t^{(2)}\}_{t=1}^{n}$.

We first design a degraded version of the BC by giving the observations and messages of receiver 1 to receiver 2. This allows for

$$nR_1 \leq I(W_1; \boldsymbol{y}_{[n]}^{(1)} | \Omega_{[n]}) + n\epsilon \tag{3.33}$$

$$nR_2 \leq I(W_2; \boldsymbol{y}_{[n]}^{(1)}, \boldsymbol{y}_{[n]}^{(2)} | W_1, \Omega_{[n]}) + n\epsilon \tag{3.34}$$

due to Fano's inequality, due to the basic chain-rule of mutual information, and due to the fact that messages from different users are independent. This now gives that

$$nR_1 \leq h(\boldsymbol{y}_{[n]}^{(1)} \,|\, \Omega_{[n]}) - h(\boldsymbol{y}_{[n]}^{(1)} \,|\, W_1, \Omega_{[n]}) + n\epsilon \tag{3.35}$$

$$nR_2 \leq h(\boldsymbol{y}_{[n]}^{(1)}, \boldsymbol{y}_{[n]}^{(2)} \,|\, W_1, \Omega_{[n]}) - h(\boldsymbol{y}_{[n]}^{(1)}, \boldsymbol{y}_{[n]}^{(2)} \,|\, W_1, W_2, \Omega_{[n]}) + n\epsilon \tag{3.36}$$

and that

$$\frac{nR_1}{\langle N\rangle'}+\frac{nR_2}{\langle 2N\rangle'}-\big(\frac{n}{\langle N\rangle'}+\frac{n}{\langle 2N\rangle'}\big)\epsilon$$

$$\leq \frac{1}{\langle N\rangle'}h(\boldsymbol{y}_{[n]}^{(1)}\,|\,\Omega_{[n]})+\frac{1}{\langle 2N\rangle'}h(\boldsymbol{y}_{[n]}^{(1)},\boldsymbol{y}_{[n]}^{(2)}\,|\,W_1,\Omega_{[n]})-\frac{1}{\langle N\rangle'}h(\boldsymbol{y}_{[n]}^{(1)}\,|\,W_1,\Omega_{[n]})$$
$$-\frac{1}{\langle 2N\rangle'}h(\boldsymbol{y}_{[n]}^{(1)},\boldsymbol{y}_{[n]}^{(2)}\,|\,W_1,W_2,\Omega_{[n]})$$

$$=\frac{1}{\langle N\rangle'}h(\boldsymbol{y}_{[n]}^{(1)}\,|\,\Omega_{[n]})+\frac{1}{\langle 2N\rangle'}h(\boldsymbol{y}_{[n]}^{(1)},\boldsymbol{y}_{[n]}^{(2)}\,|\,W_1,\Omega_{[n]})-\frac{1}{\langle N\rangle'}h(\boldsymbol{y}_{[n]}^{(1)}\,|\,W_1,\Omega_{[n]})$$
$$+no(\log P) \tag{3.37}$$

$$\leq n\log P+no(\log P)+\frac{1}{\langle 2N\rangle'}h(\boldsymbol{y}_{[n]}^{(1)},\boldsymbol{y}_{[n]}^{(2)}\,|\,W_1,\Omega_{[n]})-\frac{1}{\langle N\rangle'}h(\boldsymbol{y}_{[n]}^{(1)}\,|\,W_1,\Omega_{[n]})$$
$$+no(\log P) \tag{3.38}$$

$$=\sum_{t=1}^{n}\left(\frac{h(\boldsymbol{y}_t^{(1)},\boldsymbol{y}_t^{(2)}\,|\,\boldsymbol{y}_{[t-1]}^{(1)},\boldsymbol{y}_{[t-1]}^{(2)},W_1,\Omega_{[n]})}{\langle 2N\rangle'}-\frac{h(\boldsymbol{y}_t^{(1)}\,|\,\boldsymbol{y}_{[t-1]}^{(1)},W_1,\Omega_{[n]})}{\langle N\rangle'}\right)$$
$$+n\log P+no(\log P) \tag{3.39}$$

$$\leq\sum_{t=1}^{n}\left(\frac{h(\boldsymbol{y}_t^{(1)},\boldsymbol{y}_t^{(2)}\,|\,\boldsymbol{y}_{[t-1]}^{(1)},\boldsymbol{y}_{[t-1]}^{(2)},W_1,\Omega_{[n]})}{\langle 2N\rangle'}-\frac{h(\boldsymbol{y}_t^{(1)}\,|\,\boldsymbol{y}_{[t-1]}^{(1)},\boldsymbol{y}_{[t-1]}^{(2)},W_1,\Omega_{[n]})}{\langle N\rangle'}\right)$$
$$+n\log P+no(\log P) \tag{3.40}$$

$$\leq\frac{1}{\langle 2N\rangle'\langle N\rangle'}\sum_{t=1}^{n}\Big((\langle 2N\rangle'-\langle N\rangle')\,\langle N\rangle'\,\alpha_t^{(1)}\log P+o(\log P)\Big)+n\log P+no(\log P) \tag{3.41}$$

$$=\frac{n}{\langle 2N\rangle'\,\langle N\rangle'}\Big((\langle 2N\rangle'-\langle N\rangle')\,\langle N\rangle'\,\bar{\alpha}^{(1)}\log P+o(\log P)\Big)+n\log P+no(\log P)$$

$$=\frac{n(\langle 2N\rangle'-\langle N\rangle')}{\langle 2N\rangle'}\bar{\alpha}^{(1)}\log P+n\log P+no(\log P). \tag{3.42}$$

In the above, (3.37) is due to the fact that knowledge of $\{W_1,W_2,\Omega_{[n]}\}$ allows for reconstruction of $\boldsymbol{y}_{[n]}^{(1)},\boldsymbol{y}_{[n]}^{(2)}$ up to noise level, while (3.38) is due to the fact that $h(\boldsymbol{y}_{[n]}^{(1)}\,|\,\Omega_{[n]})\leq\langle N\rangle'\log P+o(\log P)$. Additionally (3.39) is due to the chain rule of differential entropy, (3.40) is due to the fact that conditioning reduces differential entropy, and (3.41) is directly from Proposition 6 of Chapter 4, after setting $U=\{\boldsymbol{y}_{[t-1]}^{(1)},\boldsymbol{y}_{[t-1]}^{(2)},W_1,\Omega_{[n]}\}\setminus\{\boldsymbol{H}_t^{(1)},\boldsymbol{H}_t^{(2)},\hat{\boldsymbol{H}}_{t,t}^{(1)},\hat{\boldsymbol{H}}_{t,t}^{(2)}\}$ [4].

The above gives the bound in (3.31). Interchanging the roles of the users gives the bound in (3.32). The bounds in (3.28),(3.29) are basic single-user

4. We note that the result in Proposition 6 of Chapter 4, holds for a large family of channel models, under the assumption that the CSIT estimates up to time t are independent of the current estimate errors at time t.

constraints, while the bound in (3.30) corresponds to an assumption of user cooperation. □

3.3.2 Outer bound proof for the IC

The task is to show that the above bounds (3.28),(3.29),(3.31),(3.32) hold for the case of the IC. First let us set $\boldsymbol{y}_t^{(1)}, \boldsymbol{y}_t^{(2)}$ to take the form in (3.3),(3.4), and let us denote

$$\Omega_{[n]} \triangleq \{\boldsymbol{H}_t^{(11)}, \boldsymbol{H}_t^{(12)}, \boldsymbol{H}_t^{(22)}, \boldsymbol{H}_t^{(21)}, \hat{\boldsymbol{H}}_{t,t'}^{(12)}, \hat{\boldsymbol{H}}_{t,t'}^{(21)}, \hat{\boldsymbol{H}}_{t,t'}^{(11)}, \hat{\boldsymbol{H}}_{t,t'}^{(22)}\}_{t=1}^{n}{}_{t'=1}^{n}.$$

Focusing on the bound in (3.31), we note that the transition from (3.40) to (3.41) holds in the IC setting, because knowledge of $\{W_1, \Omega_{[n]}\}$ implies knowledge of $\boldsymbol{H}_t^{(11)}\boldsymbol{x}_t^{(1)}$ and $\boldsymbol{H}_t^{(21)}\boldsymbol{x}_t^{(1)}$, which in turn implies that

$$\begin{aligned}
&\frac{h(\boldsymbol{y}_t^{(1)}, \boldsymbol{y}_t^{(2)} \,|\, \boldsymbol{y}_{[t-1]}^{(1)}, \boldsymbol{y}_{[t-1]}^{(2)}, W_1, \Omega_{[n]})}{\langle 2N\rangle'} - \frac{h(\boldsymbol{y}_t^{(1)} \,|\, \boldsymbol{y}_{[t-1]}^{(1)}, \boldsymbol{y}_{[t-1]}^{(2)}, W_1, \Omega_{[n]})}{\langle N\rangle'} \\
&= \frac{h(\boldsymbol{H}_t^{(12)}\boldsymbol{x}_t^{(2)} + \boldsymbol{z}_t^{(1)}, \boldsymbol{H}_t^{(22)}\boldsymbol{x}_t^{(2)} + \boldsymbol{z}_t^{(2)} \,|\, \boldsymbol{y}_{[t-1]}^{(1)}, \boldsymbol{y}_{[t-1]}^{(2)}, W_1, \Omega_{[n]})}{\langle 2N\rangle'} \\
&\quad - \frac{h(\boldsymbol{H}_t^{(12)}\boldsymbol{x}_t^{(2)} + \boldsymbol{z}_t^{(1)} \,|\, \boldsymbol{y}_{[t-1]}^{(1)}, \boldsymbol{y}_{[t-1]}^{(2)}, W_1, \Omega_{[n]})}{\langle N\rangle'}
\end{aligned}$$

which has the form of the difference of the differential entropies corresponding to a BC setting, where the role of the BC transmitter is replaced now by the second IC transmitter. This implies that (3.31) holds for the IC. Bounds (3.28),(3.29),(3.32) follow easily. Finally, the bound $d_1 + d_2 \leq \min\{2M, 2N, \max\{M, N\}, \max\{M, N\}\}$ is directly from [44].

3.4 Phase-Markov transceiver for imperfect and delayed feedback

We proceed to extend the MISO BC scheme in [14], to the current setting of the MIMO BC and MIMO IC.

While part of the extension of the schemes in [14] involves keeping track of the dimensionality changes that come with MIMO, there are here modifications that are not trivial. These include changes in the way the scheme performs interference quantization as well as power and rate allocation, differences in decoding, as well as differences in the way the information is aggregated to achieve the corresponding DoF corner points. A particular extra challenge corresponding to the MIMO IC, has to do with the fact that now the signals must be sent by two independent transmitters. This will reflect on the power and rate allocation at each transmitter, and on the way common and private information is decoded at each receiver.

Before proceeding with the schemes, we again note that for the achievability proof of both BC and IC, we only focus on the case where $N < M \leq 2N$ simply because, for the case of having $M \leq N$, the optimal DoF can be achieved without any CSIT, while for the case of having $M \geq 2N$, we will consider it as having $M = 2N$, again just for the achievability proof. We also note that, for the case with sufficiently good delayed CSIT, having $M \geq 2N$ can be shown to be equivalent, in terms of DoF, with the case of having $M = 2N$ (cf. Theorem 2).

We first begin with the scheme description for the BC setting, while at the end we will describe the modifications required to achieve the result for the IC case. Section 3.4.1 will describe the encoding part, Section 3.4.2 the decoding part, and Section 3.4.3 will describe how we calibrate the parameters of this universal scheme to achieve the different DoF corner points.

The challenge here will be to design a scheme of large duration n, that utilizes the CSIT process $\{\hat{\boldsymbol{H}}_{t,t'}^{(1)}, \hat{\boldsymbol{H}}_{t,t'}^{(2)}\}_{t=1,t'=1}^{n}$. As in [14], the causal scheme will not require knowledge of future quality exponents, nor of predicted CSIT estimates of future channels. We remind the reader that the users are labeled so that $\bar{\alpha}^{(2)} \leq \bar{\alpha}^{(1)}$.

For notational convenience, we will use

$$\hat{\boldsymbol{H}}_t^{(1)} \triangleq \hat{\boldsymbol{H}}_{t,t}^{(1)}, \quad \hat{\boldsymbol{H}}_t^{(2)} \triangleq \hat{\boldsymbol{H}}_{t,t}^{(2)} \tag{3.43}$$

$$\check{\boldsymbol{H}}_t^{(1)} \triangleq \hat{\boldsymbol{H}}_{t,t+\eta}^{(1)}, \quad \check{\boldsymbol{H}}_t^{(2)} \triangleq \hat{\boldsymbol{H}}_{t,t+\eta}^{(2)} \tag{3.44}$$

to denote the current and delayed estimates of $\boldsymbol{H}_t^{(1)}, \boldsymbol{H}_t^{(2)}$, with the corresponding estimation errors being

$$\tilde{\boldsymbol{H}}_t^{(1)} \triangleq \boldsymbol{H}_t^{(1)} - \hat{\boldsymbol{H}}_t^{(1)}, \quad \tilde{\boldsymbol{H}}_t^{(2)} \triangleq \boldsymbol{H}_t^{(2)} - \hat{\boldsymbol{H}}_t^{(2)} \tag{3.45}$$

$$\ddot{\boldsymbol{H}}_t^{(1)} \triangleq \boldsymbol{H}_t^{(1)} - \check{\boldsymbol{H}}_t^{(1)}, \quad \ddot{\boldsymbol{H}}_t^{(2)} \triangleq \boldsymbol{H}_t^{(2)} - \check{\boldsymbol{H}}_t^{(2)}. \tag{3.46}$$

We will also use the notation

$$P_t^{(\boldsymbol{e})} \triangleq \mathbb{E}|\boldsymbol{e}_t|^2 \tag{3.47}$$

to denote the power of a symbol $\boldsymbol{e}_t$ corresponding to time-slot t, and we will use $r_t^{(\boldsymbol{e})}$ to denote the prelog factor of the number of bits $r_t^{(\boldsymbol{e})} \log P - o(\log P)$ carried by symbol $\boldsymbol{e}_t$ at time t.

3.4.1 Encoding

As in [14], we subdivide the overall time duration n, into S phases, each of duration of T, such that each phase s ($s = 1, 2, \cdots, S$) takes place over the time slots $t \in \mathcal{B}_s$

$$\mathcal{B}_s = \{\mathcal{B}_{s,\ell} \triangleq (s-1)2T + \ell\}_{\ell=1}^{T}, \quad s = 1, \cdots, S. \tag{3.48}$$

Naturally in the gap of what we define here to be consecutive phases, another message is sent, using the same exact scheme. Going back to the aforementioned assumption, T is sufficiently large so that

$$\frac{1}{T}\sum_{t\in\mathcal{B}_s}\alpha_t^{(i)}\to\bar{\alpha}^{(i)},\ \frac{1}{T}\sum_{t\in\mathcal{B}_s}\beta_t^{(i)}\to\bar{\beta}^{(i)},\ s=1,\cdots,S \tag{3.49}$$

$i=1,2$. For notational convenience we will also assume that $T>\eta$ (cf. (3.11)), although this assumption can be readily removed, as this was argued in [14]. Finally with n being infinite, S is also infinite.

Adhering to a phase-Markov structure which - in the context of imperfect and delayed CSIT, was first introduced in [8,9] - the scheme will quantize the accumulated interference of a certain phase s, broadcast it to both receivers over phase $(s+1)$, while at the same time it will send extra information to both receivers in phase s, which will help recover the interference accumulated in phase $(s-1)$.

We first describe the encoding for all phases except the last phase which will be addressed separately due to its different structure.

Phase s, for $s=1,2,\cdots,S-1$

In each phase, the scheme combines zero forcing and superposition coding, power and rate allocation, and interference quantizing and broadcasting. We proceed to describe these steps.

Zero forcing and superposition coding At time $t\in\mathcal{B}_s$ (of phase s), the transmitter sends

$$\boldsymbol{x}_t=\boldsymbol{W}_t\boldsymbol{c}_t+\boldsymbol{U}_t\boldsymbol{a}_t+\boldsymbol{U}_t'\boldsymbol{a}_t'+\boldsymbol{V}_t\boldsymbol{b}_t+\boldsymbol{V}_t'\boldsymbol{b}_t' \tag{3.50}$$

where $\boldsymbol{a}_t\in\mathbb{C}^{(M-N)\times 1},\boldsymbol{a}_t'\in\mathbb{C}^{N\times 1}$ are the vectors of symbols meant for receiver 1, $\boldsymbol{b}_t\in\mathbb{C}^{(M-N)\times 1},\boldsymbol{b}_t'\in\mathbb{C}^{N\times 1}$ are those meant for receiver 2, where $\boldsymbol{c}_t\in\mathbb{C}^{M\times 1}$ is a common symbol vector, where $\boldsymbol{U}_t=(\hat{\boldsymbol{H}}_t^{(2)})^{\perp}\in\mathbb{C}^{M\times(M-N)}$ is a unit-norm matrix that is orthogonal to $\hat{\boldsymbol{H}}_t^{(2)}$, where $\boldsymbol{V}_t=(\hat{\boldsymbol{H}}_t^{(1)})^{\perp}\in\mathbb{C}^{M\times(M-N)}$ is orthogonal to $\hat{\boldsymbol{H}}_t^{(1)}$, and where $\boldsymbol{W}_t\in\mathbb{C}^{M\times M},\boldsymbol{U}_t'\in\mathbb{C}^{M\times N},\boldsymbol{V}_t'\in\mathbb{C}^{M\times N}$ are predetermined randomly-generated matrices known by all nodes.

Power and rate allocation The powers and (normalized) rates during phase s time-slot t, are

$$\begin{array}{ll}
P_t^{(\boldsymbol{c})}\doteq P, & \\
P_t^{(\boldsymbol{a})}\doteq P^{\delta_t^{(2)}}, & r_t^{(\boldsymbol{a})}=(M-N)\delta_t^{(2)}\\
P_t^{(\boldsymbol{b})}\doteq P^{\delta_t^{(1)}}, & r_t^{(\boldsymbol{b})}=(M-N)\delta_t^{(1)}\\
P_t^{(\boldsymbol{a}')}\doteq P^{\delta_t^{(2)}-\alpha_t^{(2)}}, & r_t^{(\boldsymbol{a}')}=N(\delta_t^{(2)}-\alpha_t^{(2)})^+\\
P_t^{(\boldsymbol{b}')}\doteq P^{\delta_t^{(1)}-\alpha_t^{(1)}}, & r_t^{(\boldsymbol{b}')}=N(\delta_t^{(1)}-\alpha_t^{(1)})^+.
\end{array} \tag{3.51}$$

where $\{\delta_t^{(1)}, \delta_t^{(2)}\}_{t\in\mathcal{B}_s}$ are designed such that

$$\beta_t^{(i)} \geq \delta_t^{(i)} \quad i=1,2,\ t\in\mathcal{B}_s \tag{3.52}$$

$$\frac{1}{T}\sum_{t\in\mathcal{B}_s}\delta_t^{(1)} = \frac{1}{T}\sum_{t\in\mathcal{B}_s}\delta_t^{(2)} = \bar{\delta} \tag{3.53}$$

$$\frac{1}{T}\sum_{t\in\mathcal{B}_s}(\delta_t^{(i)} - \alpha_t^{(i)})^+ = (\bar{\delta} - \bar{\alpha}^{(i)})^+ \quad i=1,2 \tag{3.54}$$

for some $\bar{\delta}$ that will be bounded by

$$\bar{\delta} \leq \min\{1, \bar{\beta}^{(1)}, \bar{\beta}^{(2)}, \frac{N(1+\bar{\alpha}^{(1)}+\bar{\alpha}^{(2)})}{M+N}, \frac{N(1+\bar{\alpha}^{(2)})}{M}\} \tag{3.55}$$

and which will be set to specific values later on, depending on the DoF corner point we wish to achieve.

The exact solutions for $\{\delta_t^{(1)}, \delta_t^{(2)}\}_{t\in\mathcal{B}_s}$ satisfied (3.52),(3.53),(3.54) are shown in [14], and the rates of the common symbols $\{\boldsymbol{c}_{\mathcal{B}_{s,t}}\}_{t=1}^{T}$ are designed to jointly carry

$$T(N-(M-N)\bar{\delta})\log P - o(\log P) \tag{3.56}$$

bits.

To put the above allocation in perspective, we show the received signals, and describe under each term the order of the summand's average power. These signals take the form

$$\begin{aligned}\boldsymbol{y}_t^{(1)} = &\underbrace{\boldsymbol{H}_t^{(1)}\boldsymbol{W}_t\boldsymbol{c}_t}_{P} + \underbrace{\boldsymbol{H}_t^{(1)}\boldsymbol{U}_t\boldsymbol{a}_t}_{P^{\delta_t^{(2)}}} + \underbrace{\boldsymbol{H}_t^{(1)}\boldsymbol{U}_t'\boldsymbol{a}_t'}_{P^{\delta_t^{(2)}-\alpha_t^{(2)}}} + \underbrace{\boldsymbol{z}_t^{(1)}}_{P^0} \\ &+ \underbrace{\overbrace{\check{\boldsymbol{H}}_t^{(1)}(\boldsymbol{V}_t\boldsymbol{b}_t+\boldsymbol{V}_t'\boldsymbol{b}_t')}^{\check{\iota}_t^{(1)}}}_{P^{\delta_t^{(1)}-\alpha_t^{(1)}}} + \underbrace{\overbrace{\ddot{\boldsymbol{H}}_t^{(1)}(\boldsymbol{V}_t\boldsymbol{b}_t+\boldsymbol{V}_t'\boldsymbol{b}_t')}^{\iota_t^{(1)}-\check{\iota}_t^{(1)}}}_{P^{\delta_t^{(1)}-\beta_t^{(1)}}\leq P^0}\end{aligned} \tag{3.57}$$

$$\begin{aligned}\boldsymbol{y}_t^{(2)} = &\underbrace{\boldsymbol{H}_t^{(2)}\boldsymbol{W}_t\boldsymbol{c}_t}_{P} + \underbrace{\boldsymbol{H}_t^{(2)}\boldsymbol{V}_t\boldsymbol{b}_t}_{P^{\delta_t^{(1)}}} + \underbrace{\boldsymbol{H}_t^{(2)}\boldsymbol{V}_t'\boldsymbol{b}_t'}_{P^{\delta_t^{(1)}-\alpha_t^{(1)}}} + \underbrace{\boldsymbol{z}_t^{(2)}}_{P^0} \\ &+ \underbrace{\overbrace{\check{\boldsymbol{H}}_t^{(2)}(\boldsymbol{U}_t\boldsymbol{a}_t+\boldsymbol{U}_t'\boldsymbol{a}_t')}^{\check{\iota}_t^{(2)}}}_{P^{\delta_t^{(2)}-\alpha_t^{(2)}}} + \underbrace{\overbrace{\ddot{\boldsymbol{H}}_t^{(2)}(\boldsymbol{U}_t\boldsymbol{a}_t+\boldsymbol{U}_t'\boldsymbol{a}_t')}^{\iota_t^{(2)}-\check{\iota}_t^{(2)}}}_{P^{\delta_t^{(2)}-\beta_t^{(2)}}\leq P^0}\end{aligned} \tag{3.58}$$

where

$$\iota_t^{(1)} \triangleq \boldsymbol{H}_t^{(1)}(\boldsymbol{V}_t\boldsymbol{b}_t+\boldsymbol{V}_t'\boldsymbol{b}_t'),\ \iota_t^{(2)} \triangleq \boldsymbol{H}_t^{(2)}(\boldsymbol{U}_t\boldsymbol{a}_t+\boldsymbol{U}_t'\boldsymbol{a}_t') \tag{3.59}$$

TABLE 3.1 – Number of bits carried by private and common symbols, and by the quantized interference (phase s).

	Total bits ($\times \log P$)
Private symbols for user 1	$T((M-N)\bar{\delta} + N(\bar{\delta} - \bar{\alpha}^{(2)})^+)$
Private symbols for user 2	$T((M-N)\bar{\delta} + N(\bar{\delta} - \bar{\alpha}^{(1)})^+)$
Common symbols	$T(N-(M-N)\bar{\delta})$
Quantized interference	$TN((\bar{\delta} - \bar{\alpha}^{(1)})^+ + (\bar{\delta} - \bar{\alpha}^{(2)})^+)$

denote the interference at receiver 1 and receiver 2 respectively, and where

$$\check{\iota}_t^{(1)} \triangleq \check{\boldsymbol{H}}_t^{(1)}(\boldsymbol{V}_t \boldsymbol{b}_t + \boldsymbol{V}_t' \boldsymbol{b}_t'),\ \check{\iota}_t^{(2)} \triangleq \check{\boldsymbol{H}}_t^{(2)}(\boldsymbol{U}_t \boldsymbol{a}_t + \boldsymbol{U}_t' \boldsymbol{a}_t') \tag{3.60}$$

denote the transmitter's delayed estimates of $\iota_t^{(1)}, \iota_t^{(2)}$.

Quantizing and broadcasting the accumulated interference Before the beginning of phase $(s+1)$, the transmitter reconstructs $\check{\iota}_t^{(1)}, \check{\iota}_t^{(2)}$ for all $t \in \mathcal{B}_s$, using its knowledge of delayed CSIT, and quantizes these into

$$\bar{\check{\iota}}_t^{(1)} = \check{\iota}_t^{(1)} - \tilde{\iota}_t^{(1)}, \quad \bar{\check{\iota}}_t^{(2)} = \check{\iota}_t^{(2)} - \tilde{\iota}_t^{(2)} \tag{3.61}$$

using a total of $N(\delta_t^{(1)} - \alpha_t^{(1)})^+ \log P$ and $N(\delta_t^{(2)} - \alpha_t^{(2)})^+ \log P$ quantization bits respectively. This allows for bounded power of quantization noise $\tilde{\iota}_t^{(1)}, \tilde{\iota}_t^{(2)}$, i.e, allows for $\mathbb{E}|\tilde{\iota}_t^{(2)}|^2 \doteq \mathbb{E}|\tilde{\iota}_t^{(1)}|^2 \doteq 1$, since $\mathbb{E}|\check{\iota}_t^{(2)}|^2 \doteq P^{\delta_t^{(2)} - \alpha_t^{(2)}}$, $\mathbb{E}|\check{\iota}_t^{(1)}|^2 \doteq P^{\delta_t^{(1)} - \alpha_t^{(1)}}$ (cf. [39]). Then the transmitter evenly splits the

$$\begin{aligned} &\sum_{t \in \mathcal{B}_s} \left(N(\delta_t^{(1)} - \alpha_t^{(1)})^+ + N(\delta_t^{(2)} - \alpha_t^{(2)})^+ \right) \log P \\ &= TN \left((\bar{\delta} - \bar{\alpha}^{(1)})^+ + (\bar{\delta} - \bar{\alpha}^{(2)})^+ \right) \log P \end{aligned} \tag{3.62}$$

(cf. (3.54)) quantization bits into the common symbols $\{\boldsymbol{c}_t\}_{t \in \mathcal{B}_{s+1}}$ that will be transmitted during the next phase (phase $s+1$), and which will convey these quantization bits together with other new information bits for the receivers. These $\{\boldsymbol{c}_t\}_{t \in \mathcal{B}_{s+1}}$ will help the receivers cancel interference, as well as will serve as extra observations (see (3.63) later on) that will allow for decoding of all private information (see Table 3.1).

Finally, for the last phase S, the main target will be to recover the information on the interference accumulated in phase $(S-1)$. For large S, this last phase can focus entirely on transmitting common symbols.

This concludes the part of encoding, and we now move to decoding.

3.4.2 Decoding

In accordance to the phase-Markov structure, we consider decoding that moves backwards, from the last to the first phase. The last phase was specifically designed to allow decoding of the common symbols $\{\boldsymbol{c}_t\}_{t\in\mathcal{B}_S}$. Hence we focus on the rest of the phases, to see how - with knowledge of common symbols from the next phase - we can go back one phase and decode its symbols.

During phase s, each receiver uses $\{\boldsymbol{c}_t\}_{t\in\mathcal{B}_{s+1}}$ to reconstruct the delayed estimates $\{\bar{\bar{\iota}}_t^{(2)}, \bar{\bar{\iota}}_t^{(1)}\}_{t\in\mathcal{B}_s}$, to remove - up to noise level - all the interference $\iota_t^{(i)},\ t\in\mathcal{B}_s$, by subtracting the delayed interference estimates $\bar{\bar{\iota}}_t^{(i)}$ from $\boldsymbol{y}_t^{(i)}$.

Now given $\{\bar{\bar{\iota}}_t^{(2)}, \bar{\bar{\iota}}_t^{(1)}\}_{t\in\mathcal{B}_s}$, receiver 1 combines $\{\bar{\bar{\iota}}_t^{(2)}\}_{t\in\mathcal{B}_s}$ with $\{\boldsymbol{y}_t^{(1)} - \bar{\bar{\iota}}_t^{(1)}\}_{t\in\mathcal{B}_s}$ to decode $\{\boldsymbol{c}_t, \boldsymbol{a}_t, \boldsymbol{a}_t^{'}\}_{t\in\mathcal{B}_s}$ of phase s. This is achieved by decoding over all accumulated MIMO multiple-access channel (MIMO MAC) of the general form

$$\begin{bmatrix} \boldsymbol{y}^{(1)}_{\mathcal{B}_{s,1}} - \bar{\bar{\iota}}^{(1)}_{\mathcal{B}_{s,1}} \\ \bar{\bar{\iota}}^{(2)}_{\mathcal{B}_{s,1}} \\ \vdots \\ \boldsymbol{y}^{(1)}_{\mathcal{B}_{s,T}} - \bar{\bar{\iota}}^{(1)}_{\mathcal{B}_{s,T}} \\ \bar{\bar{\iota}}^{(2)}_{\mathcal{B}_{s,T}} \end{bmatrix} = \begin{bmatrix} \boldsymbol{H}^{(1)}_{\mathcal{B}_{s,1}} \boldsymbol{W}_{\mathcal{B}_{s,1}} & & \\ \boldsymbol{0} & & \\ & \ddots & \\ & & \boldsymbol{H}^{(1)}_{\mathcal{B}_{s,T}} \boldsymbol{W}_{\mathcal{B}_{s,T}} \\ & & \boldsymbol{0} \end{bmatrix} \begin{bmatrix} \boldsymbol{c}_{\mathcal{B}_{s,1}} \\ \vdots \\ \boldsymbol{c}_{\mathcal{B}_{s,T}} \end{bmatrix}$$
$$+ \begin{bmatrix} \begin{bmatrix} \boldsymbol{H}^{(1)}_{\mathcal{B}_{s,1}} \\ \check{\boldsymbol{H}}^{(2)}_{\mathcal{B}_{s,1}} \end{bmatrix} \begin{bmatrix} \boldsymbol{U}_{\mathcal{B}_{s,1}} & \boldsymbol{U}^{'}_{\mathcal{B}_{s,1}} \end{bmatrix} & & \\ & \ddots & \\ & & \begin{bmatrix} \boldsymbol{H}^{(1)}_{\mathcal{B}_{s,T}} \\ \check{\boldsymbol{H}}^{(2)}_{\mathcal{B}_{s,T}} \end{bmatrix} \begin{bmatrix} \boldsymbol{U}_{\mathcal{B}_{s,T}} & \boldsymbol{U}^{'}_{\mathcal{B}_{s,T}} \end{bmatrix} \end{bmatrix} \begin{bmatrix} \boldsymbol{a}_{\mathcal{B}_{s,1}} \\ \boldsymbol{a}^{'}_{\mathcal{B}_{s,1}} \\ \vdots \\ \boldsymbol{a}_{\mathcal{B}_{s,T}} \\ \boldsymbol{a}^{'}_{\mathcal{B}_{s,T}} \end{bmatrix} + \begin{bmatrix} \tilde{\boldsymbol{z}}^{(1)}_{\mathcal{B}_{s,1}} \\ -\tilde{\iota}^{(2)}_{\mathcal{B}_{s,1}} \\ \vdots \\ \tilde{\boldsymbol{z}}^{(1)}_{\mathcal{B}_{s,T}} \\ -\tilde{\iota}^{(2)}_{\mathcal{B}_{s,T}} \end{bmatrix} \tag{3.63}$$

where

$$\tilde{\boldsymbol{z}}_t^{(1)} = \ddot{\boldsymbol{H}}_t^{(1)}(\boldsymbol{V}_t\boldsymbol{b}_t + \boldsymbol{V}_t'\boldsymbol{b}_t') + \boldsymbol{z}_t^{(1)} + \tilde{\iota}_t^{(1)}$$

and where $\mathbb{E}|\tilde{\boldsymbol{z}}_t^{(1)}|^2 \doteq 1$. It can be readily shown (cf. [39]) that optimal decoding in such a MIMO MAC setting, allows user 1 to achieve the aforementioned rates in (3.51),(3.53),(3.54),(3.56) i.e., allows for $r^{*(\boldsymbol{a})}\log P = T\big((M-N)\bar{\delta} + N(\bar{\delta}-\bar{\alpha}^{(2)})^+\big)\log P$ bits to be reliably carried by

$$\begin{bmatrix} \boldsymbol{a}_{\mathcal{B}_{s,1}} & \boldsymbol{a}^{'}_{\mathcal{B}_{s,1}} & \cdots & \boldsymbol{a}_{\mathcal{B}_{s,T}} & \boldsymbol{a}^{'}_{\mathcal{B}_{s,T}} \end{bmatrix}^{\mathsf{T}}$$

as well as allows for $r^{*(\boldsymbol{c})}\log P = T\big(N-(M-N)\bar{\delta}\big)\log P$ bits to be carried by $\begin{bmatrix} \boldsymbol{c}_{\mathcal{B}_{s,1}} & \cdots & \boldsymbol{c}_{\mathcal{B}_{s,T}} \end{bmatrix}^{\mathsf{T}}$. Similarly receiver 2 can again accumulate enough received signals to construct a similar MIMO MAC, which will again allow

for decoding of its own private and common symbols at the aforementioned rates in (3.51),(3.56).

Now the decoders shift to phase $s-1$ and use $\{\boldsymbol{c}_t\}_{t\in\mathcal{B}_s}$ to decode the common and private symbols of that phase. Decoding stops after decoding of the symbols in phase 1.

3.4.3 Calibrating the scheme to achieve DoF corner points

We now describe how to regulate the scheme's parameters to achieve the different DoF points of interest. As previously discussed, we can focus - without an effect to our result [5] - on the case where $N < M \leq 2N$.

Focusing first on the DoF region of the outer bound in Lemma 3, we note that the DoF corner points that define this region, vary from case to case, as these cases are each defined by each of the following inequalities

$$\min\{\bar{\beta}^{(1)},\bar{\beta}^{(2)}\} \geq \min\{1, M-\min\{M,N\}, \frac{N(1+\bar{\alpha}^{(1)}+\bar{\alpha}^{(2)})}{\min\{M,2N\}+N}, \frac{N(1+\bar{\alpha}^{(2)})}{\min\{M,2N\}}\} \tag{3.64}$$

$$\min\{\bar{\beta}^{(1)},\bar{\beta}^{(2)}\} < \min\{1, M-\min\{M,N\}, \frac{N(1+\bar{\alpha}^{(1)}+\bar{\alpha}^{(2)})}{\min\{M,2N\}+N}, \frac{N(1+\bar{\alpha}^{(2)})}{\min\{M,2N\}}\} \tag{3.65}$$

$$\bar{\alpha}^{(1)} < \frac{N(1+\bar{\alpha}^{(2)})}{M} \tag{3.66}$$

$$\bar{\alpha}^{(1)} \geq \frac{N(1+\bar{\alpha}^{(2)})}{M} \tag{3.67}$$

$$\bar{\alpha}^{(1)}+\bar{\alpha}^{(2)} > \frac{M}{N} \tag{3.68}$$

$$\bar{\alpha}^{(1)}+\bar{\alpha}^{(2)} \leq \frac{M}{N}. \tag{3.69}$$

The set of all corner points (see also Figure 3.1) is as follows

$$A^* = \big(N, \frac{(M-N)N(1+\bar{\alpha}^{(2)})}{M}\big) \tag{3.70}$$

$$B^* = \big((M-N)\bar{\alpha}^{(2)}, N\big) \tag{3.71}$$

$$C^* = \big(\frac{MN}{M+N}(1+\bar{\alpha}^{(1)}-\frac{N}{M}\bar{\alpha}^{(2)}), \frac{MN}{M+N}(1+\bar{\alpha}^{(2)}-\frac{N}{M}\bar{\alpha}^{(1)})\big) \tag{3.72}$$

$$D^* = \big(N, (M-N)\bar{\alpha}^{(1)}\big) \tag{3.73}$$

$$E^* = \big(M-N\bar{\alpha}^{(2)},\ N\bar{\alpha}^{(2)}\big) \tag{3.74}$$

$$F^* = \big(N\bar{\alpha}^{(1)},\ M-N\bar{\alpha}^{(1)}\big). \tag{3.75}$$

To achieve the entirety of the outer bound, we need sufficiently good delayed CSIT, and specifically we need (3.64) to hold. Given (3.64), if (3.66) and

5. We clarify that the outer bound left open the possibility that $M > 2N$.

TABLE 3.2 – Outer bound corner points.

Cases	Corner points
(3.66) and (3.68)	D^*, B^*, E^*, F^*
(3.66) and (3.69)	D^*, B^*, C^*
(3.67)	B^*, A^*

(3.68) hold then the 'active' outer bound corner points are D^*, B^*, E^*, F^*, whereas if (3.66) and (3.69) hold, then the active corner points are D^*, B^*, C^*, while if (3.67) holds then the active outer bound corner points are B^*, A^* (see Table 3.2).

We proceed to show how the designed scheme achieves the above points. To do so, we will show how the scheme, in its general form, achieves a range of DoF points (see (3.80),(3.81) later on), which can be shifted to the DoF corner points of interest by properly adapting the power allocation and the rate splitting of the new information carried by the common symbols.

General DoF point

Remaining on the case where (3.64) holds, we see that the bound in (3.55) now implies that

$$\bar{\delta} \leq \min\{1, \frac{N(1+\bar{\alpha}^{(1)}+\bar{\alpha}^{(2)})}{M+N}, \frac{N(1+\bar{\alpha}^{(2)})}{M}\}. \tag{3.76}$$

Changing $\bar{\delta}$ - within the bounds of (3.76) - will achieve the different DoF points. Such changing of $\bar{\delta}$, amounts to changing the power allocation (cf. (3.51)) by changing $\{\delta_t^{(1)}, \delta_t^{(2)}\}_{t\in\mathcal{B}_s}$ which are a function of $\bar{\delta}$ (cf. (3.53),(3.54)).

The first step is to see that for any fixed $\bar{\delta}$, the rate allocation in (3.51) tells us that, the total amount of information, for user 1, in the *private symbols* of a certain phase $s < S$, is equal to

$$\big((M-N)\bar{\delta} + N(\bar{\delta}-\bar{\alpha}^{(2)})^+\big)T\log P \tag{3.77}$$

bits, while for user 2 this is

$$\big((M-N)\bar{\delta} + N(\bar{\delta}-\bar{\alpha}^{(1)})^+\big)T\log P \tag{3.78}$$

bits.

The next step is to see the amount of interference information bits accumulated in one phase. Given the power and rate allocation in (3.52), (3.53), (3.54), (3.55), it is guaranteed that the accumulated quantized interference in a phase $s < S$ has $\big(N(\bar{\delta}-\bar{\alpha}^{(1)})^+ + N(\bar{\delta}-\bar{\alpha}^{(2)})^+\big)T\log P$ bits (cf. (3.62)), which 'fit' into the common symbols of the next phase $(s+1)$ that can carry

a total of $\big(N-(M-N)\bar{\delta}\big)T\log P$ bits (cf. (3.56)). This leaves an extra space of $\Delta_{\text{com}}T\log P$ bits in the common symbols, where

$$\Delta_{\text{com}} \triangleq \big(N-(M-N)\bar{\delta}-N(\bar{\delta}-\bar{\alpha}^{(1)})^{+}-N(\bar{\delta}-\bar{\alpha}^{(2)})^{+}\big) \tag{3.79}$$

is guaranteed to be non-negative due to (3.52),(3.53),(3.54),(3.55). This extra space can be split between the two users, by allocating $\omega\Delta_{\text{com}}T\log P$ bits for the message of user 1, and the remaining $(1-\omega)\Delta_{\text{com}}T\log P$ bits for the message of user 2, for some $\omega\in[0,1]$.

Consequently, considering (3.77),(3.78), and given (3.64), the scheme allows for DoF performance in its general form [6]

$$d_1 = (M-N)\bar{\delta}+N(\bar{\delta}-\bar{\alpha}^{(2)})^{+}+\omega\Delta_{\text{com}} \tag{3.80}$$

$$d_2 = (M-N)\bar{\delta}+N(\bar{\delta}-\bar{\alpha}^{(1)})^{+}+(1-\omega)\Delta_{\text{com}}. \tag{3.81}$$

Again under the setting of (3.64), we can now move to the different cases, and set ω and $\bar{\delta}$ (and thus Δ_{com}) to achieve the different DoF corner points (cf. Table 3.2).

Case 1 - (3.64) *and* (3.66) *and* (3.68) *(points* D^*, B^*, E^*, F^**) :*

We first consider the case where (3.66) and (3.68) hold, and show how to achieve DoF corner points D^*, B^*, E^*, F^*. In this setting, (3.76) gives that $\bar{\delta}\leq 1$ because (3.66) implies that $\bar{\alpha}^{(2)}\leq\bar{\alpha}^{(1)}\leq\frac{N(1+\bar{\alpha}^{(1)}+\bar{\alpha}^{(2)})}{M+N}\leq\frac{N(1+\bar{\alpha}^{(2)})}{M}$ while at the same time (3.68) implies that $\frac{N(1+\bar{\alpha}^{(1)}+\bar{\alpha}^{(2)})}{M+N}\geq\frac{N(1+\frac{M}{N})}{M+N}=1$.

To achieve $E^*=\big(M-N\bar{\alpha}^{(2)},\ N\bar{\alpha}^{(2)}\big)$, we set $\bar{\delta}=1,\omega=0$ (cf. (3.80)), which gives

$$d_1 = (M-N)\bar{\delta}+N(\bar{\delta}-\bar{\alpha}^{(2)})^{+} \tag{3.82}$$

$$= M-N\bar{\alpha}^{(2)} \tag{3.83}$$

$$d_2 = (M-N)\bar{\delta}+N(\bar{\delta}-\bar{\alpha}^{(1)})^{+}+\Delta_{\text{com}} \tag{3.84}$$

$$=(M-N)+N(1-\bar{\alpha}^{(1)})^{+}+\big(N-(M-N)-N(1-\bar{\alpha}^{(1)})^{+}-N(1-\bar{\alpha}^{(2)})^{+}\big)$$

$$= N\bar{\alpha}^{(2)} \tag{3.85}$$

where (3.82) and (3.84) are directly from (3.80),(3.81) after setting $\omega=0$, and where (3.83) and (3.85) consider the value of Δ_{com} in (3.79) and the fact that $\bar{\delta}=1$.

To achieve $F^*=\big(N\bar{\alpha}^{(1)},\ M-N\bar{\alpha}^{(1)}\big)$, we set $\bar{\delta}=1$ and we set $\omega=$

6. This expression considers that S is large, and thus removes the effect of having a last phase that carries no new message information.

$\frac{N(1+\bar{\alpha}^{(1)}+\bar{\alpha}^{(2)})-(M+N)\bar{\delta}}{\Delta_{\text{com}}} = 1$, to get

$$d_1 = (M-N)\bar{\delta} + N(\bar{\delta}-\bar{\alpha}^{(2)})^+ + \omega\Delta_{\text{com}} \tag{3.86}$$
$$= (M-N) + N(1-\bar{\alpha}^{(2)})^+ + \Delta_{\text{com}} = N\bar{\alpha}^{(1)} \tag{3.87}$$
$$d_2 = (M-N)\bar{\delta} + N(\bar{\delta}-\bar{\alpha}^{(1)})^+ + (1-\omega)\Delta_{\text{com}} \tag{3.88}$$
$$= (M-N) + N(1-\bar{\alpha}^{(1)})^+ = M - N\bar{\alpha}^{(1)} \tag{3.89}$$

where again (3.86) and (3.88) are directly from (3.80),(3.81), and where (3.87) and (3.89) consider the value of Δ_{com} in (3.79), together with the fact that $\bar{\delta} = 1$.

To achieve $B^* = \big((M-N)\bar{\alpha}^{(2)}, N\big)$, we set $\omega = 0$ and $\bar{\delta} = \bar{\alpha}^{(2)}$, which - after recalling that we label the receivers so that $\bar{\alpha}^{(1)} \geq \bar{\alpha}^{(2)}$ - gives $\Delta_{\text{com}} = \big(N - (M-N)\bar{\alpha}^{(2)}\big)$, which in turn gives (cf. (3.80),(3.81))

$$d_1 = (M-N)\bar{\delta} + N(\bar{\delta}-\bar{\alpha}^{(2)})^+ = (M-N)\bar{\alpha}^{(2)} \tag{3.90}$$
$$d_2 = (M-N)\bar{\delta} + N(\bar{\delta}-\bar{\alpha}^{(1)})^+ + \Delta_{\text{com}} \tag{3.91}$$
$$= (M-N)\bar{\alpha}^{(2)} + N(\bar{\alpha}^{(2)}-\bar{\alpha}^{(1)})^+ + \big(N-(M-N)\bar{\alpha}^{(2)} - N(\bar{\alpha}^{(2)}-\bar{\alpha}^{(1)})^+\big)$$
$$= N. \tag{3.92}$$

To achieve $D^* = \big(N, (M-N)\bar{\alpha}^{(1)}\big)$, we set $\omega = \frac{N(1+\bar{\alpha}^{(1)}+\bar{\alpha}^{(2)})-(M+N)\bar{\delta}}{\Delta_{\text{com}}} = 1$ and $\bar{\delta} = \bar{\alpha}^{(1)}$, which gives $\Delta_{\text{com}} = \big(N-(M-N)\bar{\alpha}^{(1)} - N(\bar{\alpha}^{(1)}-\bar{\alpha}^{(2)})^+\big) = N - M\bar{\alpha}^{(1)} + N\bar{\alpha}^{(2)}$, which in turn gives (cf. (3.80),(3.81))

$$d_1 = (M-N)\bar{\delta} + N(\bar{\delta}-\bar{\alpha}^{(2)})^+ + \omega\Delta_{\text{com}}$$
$$= (M-N)\bar{\alpha}^{(1)} + N(\bar{\alpha}^{(1)}-\bar{\alpha}^{(2)})^+ + \Delta_{\text{com}} = N \tag{3.93}$$
$$d_2 = (M-N)\bar{\delta} + N(\bar{\delta}-\bar{\alpha}^{(1)})^+ + (1-\omega)\Delta_{\text{com}} = (M-N)\bar{\alpha}^{(1)}. \tag{3.94}$$

Case 2 - (3.64) *and* (3.66) *and* (3.69) *(points* D^*, B^*, C^**) :*

Again under the condition of (3.64), we now consider the case where (3.66) and (3.69) hold, and seek to achieve points D^*, B^*, C^*. For points D^*, B^*, we can use the same parameters $\omega, \bar{\delta}$ that we used before to achieve these same points (for B^* we set $\bar{\delta} = \bar{\alpha}^{(2)}, \omega = 0$, and for D^* we set $\bar{\delta} = \bar{\alpha}^{(1)}, \omega = \frac{N(1+\bar{\alpha}^{(1)}+\bar{\alpha}^{(2)})-(M+N)\bar{\delta}}{\Delta_{\text{com}}} = 1$). To achieve point C^*, we need to set $\omega = 0$ and $\bar{\delta} = \frac{N(1+\bar{\alpha}^{(1)}+\bar{\alpha}^{(2)})}{M+N}$ which, as before, gives $d_1 = (M-N)\bar{\delta} + N(\bar{\delta} - \bar{\alpha}^{(2)})^+ = \frac{MN}{M+N}(1+\bar{\alpha}^{(1)} - \frac{N}{M}\bar{\alpha}^{(2)})$ and $d_2 = (M-N)\bar{\delta} + N(\bar{\delta}-\bar{\alpha}^{(1)})^+ + \Delta_{\text{com}} = \frac{MN}{M+N}(1 + \bar{\alpha}^{(2)} - \frac{N}{M}\bar{\alpha}^{(1)})$.

Case 3 - (3.64) *and* (3.67) *(points* B^*, A^**) :*

Again given (3.64), we now move to the case where (3.67) holds, and seek to achieve points B^* and A^*. To achieve B^* we can use the same parameters as before, and thus set $\bar{\delta} = \bar{\alpha}^{(2)}, \omega = 0$. To achieve $A^* = (N, \frac{(M-N)N(1+\bar{\alpha}^{(2)})}{M})$

we simply set $\bar{\delta} = \frac{N(1+\bar{\alpha}^{(2)})}{M}$ and $\omega = \frac{N(1+\bar{\alpha}^{(2)})-M\bar{\delta}}{\Delta_{\text{com}}} = 1$.

We now focus on the DoF points in the inner bound of Proposition 2, corresponding to the setting where (3.65) holds, rather than (3.64). In addition to the aforementioned points D^* and B^*, we will seek to achieve the new points

$$E = \big(M\min\{\bar{\beta}^{(1)},\bar{\beta}^{(2)}\} - N\bar{\alpha}^{(2)},\ N\bar{\alpha}^{(2)} + N(1-\min\{\bar{\beta}^{(1)},\bar{\beta}^{(2)}\})\big) \quad (3.95)$$

$$F = \big(N\bar{\alpha}^{(1)} + N(1-\min\{\bar{\beta}^{(1)},\bar{\beta}^{(2)}\}),\ M\min\{\bar{\beta}^{(1)},\bar{\beta}^{(2)}\} - N\bar{\alpha}^{(1)}\big) \quad (3.96)$$

$$G = \big(N,\ (M-N)\min\{\bar{\beta}^{(1)},\bar{\beta}^{(2)}\}\big). \quad (3.97)$$

Before proceeding, we note that under (3.65), the bound on $\bar{\delta}$ in (3.55) now becomes

$$\bar{\delta} \le \min\{\bar{\beta}^{(1)},\bar{\beta}^{(2)}\}. \quad (3.98)$$

We proceed with the different cases, and now additionally consider the cases where

$$\min\{\bar{\beta}^{(1)},\bar{\beta}^{(2)}\} \ge \bar{\alpha}^{(1)} \quad (3.99)$$

$$\min\{\bar{\beta}^{(1)},\bar{\beta}^{(2)}\} < \bar{\alpha}^{(1)}. \quad (3.100)$$

Case 4a - (3.65) *and* (3.66) *and* (3.99) *(points* D^*, B^*, E, F*) :*

To achieve D^*, B^* we use the same parameters as before, where for B^* we set $\omega = 0, \bar{\delta} = \bar{\alpha}^{(2)}$, and for D^* we set $\bar{\delta} = \bar{\alpha}^{(1)}, \omega = 1$, all of which satisfy the conditions in (3.98) and (3.99).

To get point E, we set $\omega = 0$ and $\bar{\delta} = \min\{\bar{\beta}^{(1)},\bar{\beta}^{(2)}\}$, and calculate that

$$d_1 = (M-N)\bar{\delta} + N(\bar{\delta}-\bar{\alpha}^{(2)})^+ = M\min\{\bar{\beta}^{(1)},\bar{\beta}^{(2)}\} - N\bar{\alpha}^{(2)} \quad (3.101)$$

$$d_2 = (M-N)\bar{\delta} + N(\bar{\delta}-\bar{\alpha}^{(1)})^+ + \Delta_{\text{com}} \quad (3.102)$$

$$= (M-N)\bar{\delta} + N(\bar{\delta}-\bar{\alpha}^{(1)})^+ + \big(N - (M-N)\bar{\delta} - N(\bar{\delta}-\bar{\alpha}^{(1)})^+ - N(\bar{\delta}-\bar{\alpha}^{(2)})^+\big) \quad (3.103)$$

$$= N - N(\bar{\delta}-\bar{\alpha}^{(2)})^+ = N\bar{\alpha}^{(2)} + N(1-\min\{\bar{\beta}^{(1)},\bar{\beta}^{(2)}\}). \quad (3.104)$$

To get point F, we set $\bar{\delta} = \min\{\bar{\beta}^{(1)},\bar{\beta}^{(2)}\}$ and $\omega = 1$, and calculate that

$$d_1 = (M-N)\bar{\delta} + N(\bar{\delta}-\bar{\alpha}^{(2)})^+ + \omega\Delta_{\text{com}} \quad (3.105)$$

$$= (M-N)\min\{\bar{\beta}^{(1)},\bar{\beta}^{(2)}\} + N(\min\{\bar{\beta}^{(1)},\bar{\beta}^{(2)}\} - \bar{\alpha}^{(2)})^+ + \Delta_{\text{com}} \quad (3.106)$$

$$= N\bar{\alpha}^{(1)} + N(1-\min\{\bar{\beta}^{(1)},\bar{\beta}^{(2)}\}) \quad (3.107)$$

$$d_2 = (M-N)\bar{\delta} + N(\bar{\delta}-\bar{\alpha}^{(1)})^+ + (1-\omega)\Delta_{\text{com}} = M\min\{\bar{\beta}^{(1)},\bar{\beta}^{(2)}\} - N\bar{\alpha}^{(1)}. \quad (3.108)$$

Case 4b - (3.65) *and* (3.66) *and* (3.100) *(points* B^*, E, G*) :*

Again under (3.65), we now consider the case where (3.66) and (3.100) hold, and seek to achieve points B^*, E and G. To achieve B^* we set as before $\omega = 0, \bar{\delta} = \bar{\alpha}^{(2)}$, and for E we set as before $\omega = 0$ and $\bar{\delta} = \min\{\bar{\beta}^{(1)}, \bar{\beta}^{(2)}\}$, both in accordance with the conditions in (3.98) and (3.100).

To get point $G = \big(N,\ (M-N)\min\{\bar{\beta}^{(1)}, \bar{\beta}^{(2)}\}\big)$, we simply set $\bar{\delta} = \min\{\bar{\beta}^{(1)}, \bar{\beta}^{(2)}\}$ and $\omega = 1$, and the calculations follow immediately.

Case 4c - (3.65) *and* (3.67) *(points* B^*, E, G*) :*

In the last case where (3.65) and (3.67) hold, we can achieve points B^*, E, G using the same parameters as above.

Finally the DoF regions in the theorem and proposition are achieved by time sharing between the proper DoF corner points.

3.4.4 Modifications for the IC

We here briefly describe the modifications that adapt our scheme to the IC setting. In terms of notation, the role of $\hat{\boldsymbol{H}}_t^{(1)} \triangleq \hat{\boldsymbol{H}}_{t,t}^{(1)}$ is taken by $\hat{\boldsymbol{H}}_t^{(12)} \triangleq \hat{\boldsymbol{H}}_{t,t}^{(12)}$, of $\hat{\boldsymbol{H}}_t^{(2)} \triangleq \hat{\boldsymbol{H}}_{t,t}^{(2)}$ by $\hat{\boldsymbol{H}}_t^{(21)} \triangleq \hat{\boldsymbol{H}}_{t,t}^{(21)}$, of $\check{\boldsymbol{H}}_t^{(1)} \triangleq \hat{\boldsymbol{H}}_{t,t+\eta}^{(1)}$ by $\check{\boldsymbol{H}}_t^{(12)} \triangleq \hat{\boldsymbol{H}}_{t,t+\eta}^{(12)}$, and the role of $\check{\boldsymbol{H}}_t^{(2)} \triangleq \hat{\boldsymbol{H}}_{t,t+\eta}^{(2)}$ is taken by $\check{\boldsymbol{H}}_t^{(21)} \triangleq \hat{\boldsymbol{H}}_{t,t+\eta}^{(21)}$.

Many of the steps follow from the BC, with the main difference being that now the common symbols must be transmitted by two independent transmitters. For that we change the structure of the signaling (cf. (3.50)) and now consider that at time $t \in \mathcal{B}_s$ (phase s), transmitter 1 sends

$$\boldsymbol{x}_t^{(1)} = \boldsymbol{W}_t^{(1)} \boldsymbol{c}_t^{(1)} + \boldsymbol{U}_t \boldsymbol{a}_t + \boldsymbol{U}_t' \boldsymbol{a}_t' \tag{3.109}$$

and transmitter 2 sends

$$\boldsymbol{x}_t^{(2)} = \boldsymbol{W}_t^{(2)} \boldsymbol{c}_t^{(2)} + \boldsymbol{V}_t \boldsymbol{b}_t + \boldsymbol{V}_t' \boldsymbol{b}_t' \tag{3.110}$$

where $\boldsymbol{c}_t^{(i)} \in \mathbb{C}^{M\times 1}$ is the common information vector sent by transmitter i ($i = 1, 2$), where $\boldsymbol{U}_t$ is orthogonal to $\hat{\boldsymbol{H}}_t^{(21)}$, $\boldsymbol{V}_t$ is orthogonal to $\hat{\boldsymbol{H}}_t^{(12)}$, and where $\boldsymbol{W}_t^{(1)}, \boldsymbol{U}_t', \boldsymbol{W}_t^{(2)}, \boldsymbol{V}_t'$ are randomly picked precoding matrices. Finally $\boldsymbol{a}_t, \boldsymbol{a}_t', \boldsymbol{b}_t, \boldsymbol{b}_t'$ accept the same rate and power allocation previously described in (3.51).

In the above, the common symbol vectors $\{\boldsymbol{c}_{\mathcal{B}_{s,t}}^{(1)}\}_{t=1}^{T}$ convey information on the (quantized version of the) interference $\iota_t^{(2)} \triangleq \boldsymbol{H}_t^{(21)}(\boldsymbol{U}_t \boldsymbol{a}_t + \boldsymbol{U}_t' \boldsymbol{a}_t')$, (cf. (3.59)) accumulated during phase $(s-1)$. These symbols will carry

$$\big(\omega T \Delta_{\text{com}} + TN(\bar{\delta} - \bar{\alpha}^{(2)})^+\big) \log P - To(\log P) \tag{3.111}$$

bits, where Δ_{com} is defined in (3.79), and where $\omega \in [0, 1]$ will be set depending on the target DoF point. Similarly $\{\boldsymbol{c}_{\mathcal{B}_{s,t}}^{(2)}\}_{t=1}^{T}$ will carry the

$$\big((1-\omega) T \Delta_{\text{com}} + TN(\bar{\delta} - \bar{\alpha}^{(1)})^+\big) \log P - To(\log P) \tag{3.112}$$

bits of information corresponding to $\{\iota_t^{(1)}\}_{t\in\mathcal{B}_{s-1}}$ where we recall that $\iota_t^{(1)} = \boldsymbol{H}_t^{(12)}(\boldsymbol{V}_t\boldsymbol{b}_t + \boldsymbol{V}_t'\boldsymbol{b}_t')$ (cf. (3.59)). Jointly $\{\boldsymbol{c}_{\mathcal{B}_{s,t}}^{(1)}, \boldsymbol{c}_{\mathcal{B}_{s,t}}^{(2)}\}_{t=1}^{T}$ will carry $T(N-(M-N)\bar{\delta})\log P - o(\log P)$ bits, which matches the amount in the BC setting (cf. (3.56)).

Decoding is similar to the case of the BC, except that now the corresponding MIMO MAC (for receiver 1) takes the form

$$\begin{bmatrix} \boldsymbol{y}_{\mathcal{B}_{s,1}}^{(1)} - \bar{\bar{\iota}}_{\mathcal{B}_{s,1}}^{(1)} \\ \bar{\bar{\iota}}_{\mathcal{B}_{s,1}}^{(2)} \\ \vdots \\ \boldsymbol{y}_{\mathcal{B}_{s,T}}^{(1)} - \bar{\bar{\iota}}_{\mathcal{B}_{s,T}}^{(1)} \\ \bar{\bar{\iota}}_{\mathcal{B}_{s,T}}^{(2)} \end{bmatrix} = \begin{bmatrix} \boldsymbol{H}_{\mathcal{B}_{s,1}}^{(11)}\boldsymbol{W}_{\mathcal{B}_{s,1}}^{(1)} & & \\ \boldsymbol{0} & & \\ & \ddots & \\ & & \boldsymbol{H}_{\mathcal{B}_{s,T}}^{(11)}\boldsymbol{W}_{\mathcal{B}_{s,T}}^{(1)} \\ & & \boldsymbol{0} \end{bmatrix} \begin{bmatrix} \boldsymbol{c}_{\mathcal{B}_{s,1}}^{(1)} \\ \vdots \\ \boldsymbol{c}_{\mathcal{B}_{s,T}}^{(1)} \end{bmatrix}$$
$$+ \begin{bmatrix} \boldsymbol{H}_{\mathcal{B}_{s,1}}^{(12)}\boldsymbol{W}_{\mathcal{B}_{s,1}}^{(2)} & & \\ \boldsymbol{0} & & \\ & \ddots & \\ & & \boldsymbol{H}_{\mathcal{B}_{s,T}}^{(12)}\boldsymbol{W}_{\mathcal{B}_{s,T}}^{(2)} \\ & & \boldsymbol{0} \end{bmatrix} \begin{bmatrix} \boldsymbol{c}_{\mathcal{B}_{s,1}}^{(2)} \\ \vdots \\ \boldsymbol{c}_{\mathcal{B}_{s,T}}^{(2)} \end{bmatrix} + \begin{bmatrix} \tilde{\boldsymbol{z}}_{\mathcal{B}_{s,1}}'^{(1)} \\ -\tilde{\iota}_{\mathcal{B}_{s,1}}^{(2)} \\ \vdots \\ \tilde{\boldsymbol{z}}_{\mathcal{B}_{s,T}}'^{(1)} \\ -\tilde{\iota}_{\mathcal{B}_{s,T}}^{(2)} \end{bmatrix}$$
$$+ \begin{bmatrix} \begin{bmatrix} \boldsymbol{H}_{\mathcal{B}_{s,1}}^{(11)} \\ \check{\boldsymbol{H}}_{\mathcal{B}_{s,1}}^{(21)} \end{bmatrix} \begin{bmatrix} \boldsymbol{U}_{\mathcal{B}_{s,1}} & \boldsymbol{U}_{\mathcal{B}_{s,1}}' \end{bmatrix} & & \\ & \ddots & \\ & & \begin{bmatrix} \boldsymbol{H}_{\mathcal{B}_{s,T}}^{(11)} \\ \check{\boldsymbol{H}}_{\mathcal{B}_{s,T}}^{(21)} \end{bmatrix} \begin{bmatrix} \boldsymbol{U}_{\mathcal{B}_{s,T}} & \boldsymbol{U}_{\mathcal{B}_{s,T}}' \end{bmatrix} \end{bmatrix} \begin{bmatrix} \boldsymbol{a}_{\mathcal{B}_{s,1}} \\ \boldsymbol{a}_{\mathcal{B}_{s,1}}' \\ \vdots \\ \boldsymbol{a}_{\mathcal{B}_{s,T}} \\ \boldsymbol{a}_{\mathcal{B}_{s,T}}' \end{bmatrix} \tag{3.113}$$

where the effective noise term at the end can be shown to have bounded power. As before, the receivers recover the signals at the rates described in (3.51), (3.111), (3.112) (cf. [39]).

3.5 Conclusions

The work, extending on recent work on the MISO BC, considered the symmetric MIMO BC and MIMO IC, and made progress towards establishing and meeting the tradeoff between performance, and feedback timeliness and quality. Considering a general CSIT process, the work provided simple DoF expressions that reveal the role of the number of antennas in establishing the feedback quality associated to a certain DoF performance.

Chapter 4

Fundamental Performance and Feedback Tradeoff over the K-User MISO BC

This chapter considers the multiuser multiple-input single-output (MISO) broadcast channel (BC), where a transmitter with M antennas transmits information to K single-antenna users, and where - as expected - the quality and timeliness of channel state information at the transmitter (CSIT) is imperfect. Motivated by the fundamental question of how much feedback is necessary to achieve a certain performance, we seeks to establish bounds on the tradeoff between degrees-of-freedom (DoF) performance and CSIT feedback quality. Specifically, the work provides a novel DoF region outer bound for the general K-user $M \times 1$ MISO BC with partial current CSIT, which naturally bridges the gap between the case of having no current CSIT (only delayed CSIT, or no CSIT) and the case with full CSIT. The work then characterizes the minimum CSIT feedback that is necessary for any point of the sum DoF, which is optimal for the case with $M \geq K$, and the case with $M = 2,\ K = 3$.

4.1 Introduction

We consider the multiuser multiple-input single-output (MISO) broadcast channel (BC), where a transmitter with M antennas, transmits information to K single-antenna users. In this setting, the received signal at time

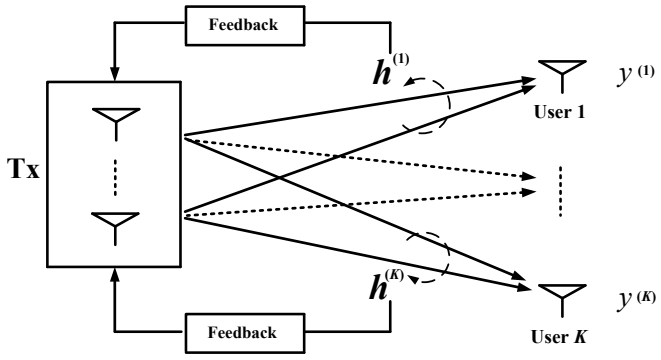

FIGURE 4.1 – System model of K-user MISO BC with CSIT feedback.

t, is of the form

$$y_t^{(k)} = \boldsymbol{h}_t^{(k)^{\mathsf{T}}} \boldsymbol{x}_t + z_t^{(k)}, \quad k = 1, \cdots, K \tag{4.1}$$

where $\boldsymbol{h}_t^{(k)}$ denotes the $M \times 1$ channel vector for user k, $z_t^{(k)}$ denotes the unit power AWGN noise, and where $\boldsymbol{x}_t$ denotes the transmitted signal vector adhering to a power constraint $\mathbb{E}[||\boldsymbol{x}_t||^2] \leq P$, for P taking the role of the signal-to-noise ratio (SNR or snr). We here consider that the fading coefficients $\boldsymbol{h}_t^{(k)}$, $k = 1, \cdots, K$, are independent and identically distributed (i.i.d.) complex Gaussian random variables with zero mean and unit variance, and are i.i.d. over time.

It is well known that the performance of the BC is greatly affected by the timeliness and quality of feedback; having full CSIT allows for the optimal $\min\{M, K\}$ sum degrees-of-freedom (DoF) (cf. [1]) [1], while the absence of any CSIT reduces this to just 1 sum DoF (cf. [2, 3]). This gap has spurred a plethora of works that seek to analyze and optimize BC communications in the presence of delayed and imperfect feedback. One of the works that stands out is the work by Maddah-Ali and Tse [4] which recently revealed the benefits of employing delayed CSIT over the BC, even if this CSIT is completely obsolete. Several interesting generalizations followed, including the work in [10] which showed that in the BC setting with $K = M + 1$, combining delayed CSIT with perfect (current) CSIT (over the last $\frac{K-1}{K}$ fraction of communication period) allows for the optimal sum DoF M corresponding to full CSIT. A similar approach was exploited in [46] which revealed that, to achieve the maximum sum DoF $\min\{M, K\}$, each user has to symmetrically feed back perfect CSIT over a $\frac{\min\{M,K\}}{K}$ fraction of the communication time,

1. We remind the reader that for an achievable rate tuple $(R_1, R_2, \cdots, R_K)$, where R_i is for user i, the corresponding DoF tuple $(d_1, d_2, \cdots, d_K)$ is given by $d_i = \lim_{P\to\infty} \frac{R_i}{\log P}$, $i = 1, 2, \cdots, K$. The corresponding DoF region $\mathcal{D}$ is then the set of all achievable DoF tuples $(d_1, d_2, \cdots, d_K)$.

and that this fraction is optimal. Other interesting works in the context of utilizing delayed and current CSIT, can be found in [5–8] which explored the setting of combining perfect delayed CSIT with immediately available imperfect CSIT, the work in [9,47] which additionally considered the effects of the quality of delayed CSIT, the work in [11] which considered alternating CSIT feedback, the work in [48] which considered delayed and progressively evolving (progressively improving) current CSIT, and the works in [19–24,49] and many other publications.

Our work here generalizes many of the above settings, and seeks to establish fundamental tradeoff between DoF performance and CSIT feedback quality, over the general K-user $M \times 1$ MISO BC.

4.1.1 CSIT quantification and feedback model

We proceed to describe the quality and timeliness measure of CSIT feedback, and how this measure relates to existing work. We here use $\hat{\boldsymbol{h}}_t^{(k)}$ to denote the current channel estimate (for channel $\boldsymbol{h}_t^{(k)}$) at the transmitter at timeslot t, and use

$$\tilde{\boldsymbol{h}}_t^{(k)} = \boldsymbol{h}_t^{(k)} - \hat{\boldsymbol{h}}_t^{(k)}$$

to denote the estimate error assumed to be mutually independent of $\hat{\boldsymbol{h}}_t^{(k)}$ and assumed to have i.i.d. circularly symmetric complex Gaussian entries with zero mean and power

$$\mathbb{E}\big[\|\tilde{\boldsymbol{h}}_t^{(k)}\|^2\big] \doteq P^{-\alpha_t^{(k)}},$$

for some CSI quality exponent $\alpha_t^{(k)} \in [0,1]$ describing the quality of this estimate. We note that $\alpha_t^{(k)} = 0$ implies very little current CSIT knowledge, and that $\alpha_t^{(k)} = 1$ implies perfect CSIT in terms of the DoF performance [2].

The approach extends over non-alternating CSIT settings in [4] and [5–8], as well as over an alternating CSIT setting (cf. [11, 46]) where CSIT knowledge alternates between perfect CSIT ($\alpha_t^{(k)} = 1$), and delayed or no CSIT ($\alpha_t^{(k)} = 0$).

In a setting where communication takes place over n such coherence periods (assuming that a single channel use per such coherence period, $t = 1, 2, \cdots, n$), this approach offers a natural measure of a per-user average feedback cost, in the form of

$$\bar{\alpha}^{(k)} \triangleq \frac{1}{n} \sum_{t=1}^{n} \alpha_t^{(k)}, \quad k = 1, 2, \cdots, K,$$

2. This can be readily derived, using for example the work in [17].

as well as a measure of current CSIT feedback cost

$$\mathsf{C}_{\mathrm{C}} \triangleq \sum_{k=1}^{K} \bar{\alpha}^{(k)}, \tag{4.2}$$

accumulated over all users.

Alternating CSIT setting

In a setting where delayed CSIT is always available, the above model captures the alternating CSIT setting where the exponents are binary ($\alpha_t^{(k)} = 0, 1$), in which case

$$\bar{\alpha}^{(k)} = \gamma_{\mathrm{P}}^{(k)}$$

simply describes the fraction of time during which user k feeds back perfect CSIT, with

$$\mathsf{C}_{\mathrm{C}} = \mathsf{C}_{\mathrm{P}} \triangleq \sum_{k=1}^{K} \gamma_{\mathrm{P}}^{(k)}$$

describing the *total perfect CSIT feedback cost.*

Symmetric and asymmetric CSIT feedback

Motivated by the fact that different users might have different feedback capabilities due to the feedback channels with different capacities and different reliabilities, symmetric CSIT feedback ($\bar{\alpha}^{(1)} = \cdots = \bar{\alpha}^{(K)}$) and asymmetric CSIT feedback ($\bar{\alpha}^{(k)} \neq \bar{\alpha}^{(k')}\ \forall\, k \neq k'$) are considered in this work.

4.1.2 Structure and summary of contributions

Section 4.2 provides the main results of this work :

- In Theorem 3 we first provide a novel outer bound on the DoF region, for the K-user $M \times 1$ MISO BC with partial current CSIT quantized with $\{\alpha_t^{(k)}\}_{k,t}$, which bridges the case with no current CSIT (only delayed CSIT, or no CSIT) and the case with full CSIT. This result manages to generalize the results by Maddah-Ali and Tse ($\alpha_t^{(k)} = 0,\ \forall t, k$), Yang et al. and Gou and Jafar ($K = 2,\ \alpha_t^{(k)} = \alpha,\ \forall t, k$), Maleki et al. ($K = 2,\ \alpha_t^{(1)} = 1, \alpha_t^{(2)} = 0,\ \forall t$), Chen and Elia ($K = 2,\ \alpha_t^{(1)} \neq \alpha_t^{(2)},\ \forall t$), Lee and Heath ($M = K+1,\ \alpha_t^{(k)} \in \{0, 1\},\ \forall t, k$), and Tandon et al. ($\alpha_t^{(k)} \in \{0, 1\},\ \forall t, k$).
- From Theorem 3, we then provide the upper bound on the sum DoF as a function of the current CSIT feedback cost, which is tight for the case with $M \geq K$ (cf. Theorem 4) and the case with $M = 2, K = 3$ (cf. Theorem 5, Corollary 5a).

– Furthermore, Theorem 6 characterizes the minimum total current CSIT feedback cost $\mathsf{C}_{\mathrm{P}}^{\star}$ to achieve the maximum sum DoF, where the total feedback cost $\mathsf{C}_{\mathrm{P}}^{\star}$ can be distributed among all the users with any (asymmetric and symmetric) combinations $\{\gamma_{\mathrm{P}}^{(k)}\}_k$.
– In addition, the work considers some other general settings of BC and provides the DoF inner bound as a function of the CSIT feedback cost.

The main converse proof, that is for Theorem 3, is shown in the Section 4.3 and appendix. Most of the achievability proofs are shown in the Section 4.4. Finally Section 4.5 concludes this work.

Throughout this work, we will consider communication over n coherence periods where, for clarity of notation, we will focus on the case where we employ a single channel use per such coherence period (unit coherence period). Furthermore, unless stated otherwise, we assume perfect delayed CSIT, as well as adhere to the common convention (see [4,6,7,11,33,46]), and assume perfect and global knowledge of channel state information at the receivers.

4.2 Main results

4.2.1 Outer bounds

We first present the DoF region outer bound for the general K-user $M\times 1$ MISO BC.

Theorem 3 (DoF region outer bound)**.** *The DoF region of the K-user $M\times 1$ MISO BC, is outer bounded as*

$$\sum_{k=1}^{K}\frac{d_{\pi(k)}}{\min\{k,M\}}\leq 1+\sum_{k=1}^{K-1}\left(\frac{1}{\min\{k,M\}}-\frac{1}{\min\{K,M\}}\right)\bar{\alpha}^{(\pi(k))} \tag{4.3}$$

$$d_k\leq 1,\quad k=1,2,\cdots,K \tag{4.4}$$

where π denotes a permutation of the ordered set $\{1,2,\cdots,K\}$, and $\pi(k)$ denotes the k th element of set π.

Proof. The proof is shown in Section 4.3. □

Remark 4. *It is noted that the bound captures the results in [4] ($\alpha_t^{(k)}=0,\ \forall t,k$), in [6, 7] ($K=2,\ \alpha_t^{(k)}=\alpha,\ \forall t,k$), in [33] ($M=K=2,\ \alpha_t^{(1)}=1,\alpha_t^{(2)}=0,\ \forall t$), in [8] ($K=2,\ \alpha_t^{(1)}\neq\alpha_t^{(2)},\ \forall t$), in [11, 46] ($\alpha_t^{(k)}\in\{0,1\},\ \forall t,k$), as well as in [26] ($M\geq K,\ \alpha_t^{(k)}=\alpha,\ \forall t,k$).*

Summing up from the above the K different bounds[3], we directly have the following upper bound on the sum DoF $d_\Sigma\triangleq\sum_{k=1}^{K}d_k$. In the following, we will use some notations given as

$$d_{\mathrm{MAT}}\triangleq\frac{K}{1+\frac{1}{\min\{2,M\}}+\frac{1}{\min\{3,M\}}+\cdots+\frac{1}{\min\{K,M\}}} \tag{4.5}$$

$$\Gamma\triangleq\frac{M}{\sum_{i=1}^{K-M}\frac{1}{i}(\frac{M-1}{M})^{i-1}+(\frac{M-1}{M})^{K-M}(\sum_{i=K-M+1}^{K}\frac{1}{i})}. \tag{4.6}$$

Corollary 3a (Sum DoF outer bound)**.** *For the K-user $M\times 1$ MISO BC, the sum DoF is outer bounded as*

$$d_\Sigma\leq d_{MAT}+\left(1-\frac{d_{MAT}}{\min\{K,M\}}\right)\sum_{k=1}^{K}\bar{\alpha}^{(k)}. \tag{4.7}$$

3. For bound k, $k=1,2,\cdots,K$, we have $\pi=\{\pi(i)=\mathrm{mod}(k+i-2)_K+1\}_{i=1}^{K}$, where $\mathrm{mod}(x)_K$ is the modulo operator.

The above then readily translates onto a lower bound on the minimum possible total current CSIT feedback cost $\mathsf{C}_{\mathrm{C}} = \sum_{k=1}^{K} \bar{\alpha}^{(k)}$ needed to achieve the maximum sum DoF [4] $d_{\Sigma} = \min\{K, M\}$.

Corollary 3b (Bound on CSIT cost for maximum DoF)**.** *The minimum* C_C *required to achieve the maximum sum DoF* $\min\{K, M\}$ *of the* K*-user* $M \times 1$ *MISO BC, is lower bounded as*

$$\mathsf{C}_C^{\star} \geq \min\{K, M\}. \tag{4.8}$$

Transitioning to the alternating CSIT setting where $\alpha_t^{(k)} \in \{0, 1\}$, we have the following sum-DoF outer bound as a function of the perfect-CSIT duration $\bar{\alpha}^{(k)} = \gamma_{\mathrm{P}}^{(k)} = \gamma_{\mathrm{P}},\ \forall\, k$. We note that the bound holds irrespective of whether, in the remaining fraction of the time $1 - \gamma_{\mathrm{P}}$, the CSIT is delayed or non existent.

Corollary 3c (Outer bound, alternating CSIT)**.** *For the* K*-user* $M \times 1$ *MISO BC, and given symmetric perfect-CSIT feedback cost* γ_P*, the sum DoF is outer bounded as*

$$d_{\Sigma} \leq d_{MAT} + \left(K - \frac{K d_{MAT}}{\min\{K, M\}}\right) \min\left\{\gamma_P, \frac{\min\{K, M\}}{K}\right\}. \tag{4.9}$$

4.2.2 Optimal cases of DoF characterizations

We now provide the optimal cases of DoF characterizations as a function of the current CSIT feedback cost. The case with $M \geq K$ is first considered in the following.

Theorem 4 (Optimal case, $M \geq K$)**.** *For the* K*-user* $M \times 1$ *MISO BC with* $M \geq K$*, and given symmetric perfect-CSIT feedback cost* γ_P*, the optimal sum DoF is characterized as*

$$d_{\Sigma} = (K - d_{MAT}) \min\{\gamma_P, 1\} + d_{MAT}. \tag{4.10}$$

Proof. The converse and achievability proofs are derived from Corollary 3c and Proposition 4 (shown in the next subsection), respectively. □

Remark 5. *It is noted that, for the special case with* $M = K = 2$*, the above characterization captures the result in [11].*

Moving to the case where $M < K$, we have the following optimal sum DoF characterizations for the case with $M = 2,\ K = 3$. The first interest is placed on the minimum $\mathsf{C}_{\mathrm{P}}^{\star}(d_{\Sigma})$ to achieve a sum DoF d_{Σ}, recalling that $\mathsf{C}_{\mathrm{P}}^{\star} = \sum_{k=1}^{K} \gamma_{\mathrm{P}}^{(k)}$ describes the total perfect CSIT feedback cost.

4. Naturally the result is limited to the case where $\min\{K, M\} > 1$.

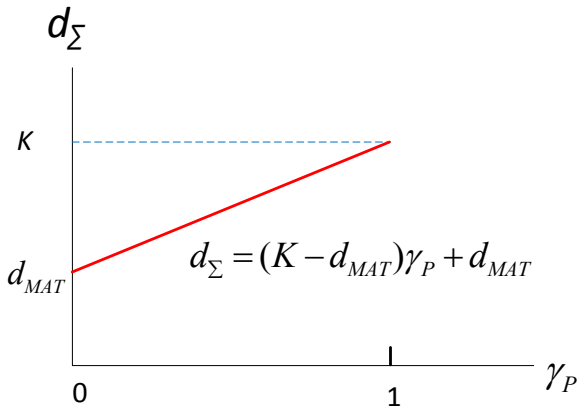

FIGURE 4.2 – Optimal sum DoF d_Σ vs. γ_P for the MISO BC with $M \geq K$.

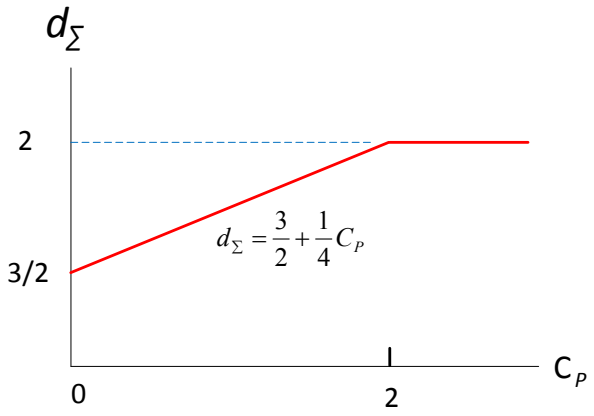

FIGURE 4.3 – Optimal sum DoF (d_Σ) vs. total perfect CSIT feedback cost (C_P) for three-user 2×1 MISO BC.

Theorem 5 (Optimal case, $M = 2, K = 3$)**.** *For the three-user* 2×1 *MISO BC, the minimum total perfect CSIT feedback cost is characterized as*

$$\mathsf{C}_P^\star(d_\Sigma) = (4d_\Sigma - 6)^+, \quad \forall\ d_\Sigma \in [0, 2] \tag{4.11}$$

where the total feedback cost $\mathsf{C}_P^\star(d_\Sigma)$ *can be distributed among all the users with some combinations* $\{\gamma_P^{(k)}\}_k$ *such that* $\gamma_P^{(k)} \leq \mathsf{C}_P^\star(d_\Sigma)/2$ *for any* k*.*

Proof. The converse proof is directly from Corollary 3a, while the achievability proof is shown in Section 4.4.2. □

Theorem 5 reveals the fundamental tradeoff between sum DoF and total perfect CSIT feedback cost (see Fig 4.3). The following examples are provided to offer some insights corresponding to Theorem 5.

Example 11. *For the target sum DoF $d_\Sigma = 3/2,\ 7/4,\ 2$, the minimum total perfect CSIT feedback cost is $\mathsf{C}_P^\star = 0,\ 1,\ 2$, respectively.*

Example 12. *The target $d_\Sigma = 7/4$ is achievable with asymmetric feedback $\boldsymbol{\gamma}_P = [1/6 \quad 1/3 \quad 1/2]$, and symmetric feedback $\boldsymbol{\gamma}_P = [1/3 \quad 1/3 \quad 1/3]$, and some other feedback such that $\mathsf{C}_P^\star(7/4) = 1$.*

Example 13. *The target $d_\Sigma = 2$ is achievable with asymmetric feedback $\boldsymbol{\gamma}_P = [1/3 \quad 2/3 \quad 1]$, and symmetric feedback $\boldsymbol{\gamma}_P = [2/3 \quad 2/3 \quad 2/3]$, and some other feedback such that $\mathsf{C}_P^\star(2) = 2$.*

Transitioning to the symmetric setting where $\gamma_{\mathrm{P}}^{(k)} = \gamma_{\mathrm{P}}\ \forall\, k$, from Theorem 5 we have the fundamental tradeoff between optimal sum DoF and CSIT feedback cost γ_{P}.

Corollary 5a (Optimal case, $M = 2, K = 3,\ \gamma_{\mathrm{P}}$)**.** *For the three-user 2×1 MISO BC with symmetrically alternating CSIT feedback, and given γ_P, the optimal sum DoF is characterized as*

$$d_\Sigma = \min\left\{\frac{3(2+\gamma_P)}{4}, 2\right\}. \tag{4.12}$$

Now we address the questions of what is the minimum $\mathsf{C}_{\mathrm{P}}^\star$ to achieve the maximum sum DoF $\min\{M, K\}$ for the general BC, and how to distribute $\mathsf{C}_{\mathrm{P}}^\star$ among all the users, recalling again that $\mathsf{C}_{\mathrm{P}}^\star$ is the total perfect CSIT feedback cost.

Theorem 6 (Minimum cost for maximum DoF)**.** *For the K-user $M \times 1$ MISO BC, the minimum total perfect CSIT feedback cost to achieve the maximum DoF is characterized as*

$$\mathsf{C}_P^\star(\min\{M,K\}) = \begin{cases} 0, & \text{if} \quad \min\{M,K\} = 1 \\ \min\{M,K\}, & \text{if} \quad \min\{M,K\} > 1 \end{cases}$$

where the total feedback cost $\mathsf{C}_P^\star$ can be distributed among all the users with any combinations $\{\gamma_P^{(k)}\}_k$.

Proof. For the case with $\min\{M, K\} = 1$, simple TDMA is optimal in terms of the DoF performance. For the case with $\min\{M, K\} > 1$, the converse proof is directly derived from Corollary 3b, while the achievability proof is shown in Section 4.4.1. □

It is noted that Theorem 6 is a generalization of the result in [46] where only symmetric feedback was considered. The following examples are provided to offer some insights corresponding to Theorem 6.

Example 14. *For the case where $M = 2,\ K = 4$, the optimal 2 sum DoF performance is achievable, with asymmetric feedback $\boldsymbol{\gamma}_P = [1/5 \quad 2/5 \quad 3/5 \quad 4/5]$, and symmetric feedback $\boldsymbol{\gamma}_P = [1/2 \quad 1/2 \quad 1/2 \quad 1/2]$, and any other feedback such that $\mathsf{C}_P^\star = 2$.*

Example 15. *For the case where $M = 3,\ K = 5$, the optimal 3 sum DoF performance is achievable, with asymmetric feedback $\boldsymbol{\gamma}_P = [1/5 \quad 2/5 \quad 3/5 \quad 4/5 \quad 1]$, and symmetric feedback $\boldsymbol{\gamma}_P = [3/5 \quad 3/5 \quad 3/5 \quad 3/5 \quad 3/5]$, and any other feedback such that $\mathsf{C}_P^\star = 3$.*

The following corollary is derived from Theorem 6, where the case with $\min\{M, K\} > 1$ is considered.

Corollary 6a (Minimum cost for maximum DoF)**.** *For the K-user $M \times 1$ MISO BC, where J users instantaneously feed back perfect (current) CSIT, with the other users feeding back delayed CSIT, then the minimum number J is $\min\{M, K\}$, in order to achieve the maximum sum DoF $\min\{M, K\}$.*

4.2.3 Inner bounds

In this subsection, we provide the following inner bounds on the sum DoF as a function of the CSIT cost, which are tight for many cases as stated.

Proposition 3 (Inner bound, $M = 2, K \geq 3$)**.** *For the $K(\geq 3)$-user 2×1 MISO BC, the sum DoF is bounded as*

$$d_\Sigma \geq \frac{3}{2} + \frac{K}{4} \min\{\gamma_P, \frac{2}{K}\}. \tag{4.13}$$

Proof. The proof is shown in Section 4.4.3. □

Proposition 4 (Inner bound, $M \geq K$ and $M < K$)**.** *For the K-user $M \times 1$ MISO BC, the sum DoF for the case with $M \geq K$ is bounded as*

$$d_\Sigma \geq (K - d_{MAT}) \min\{\gamma_P, 1\} + d_{MAT}, \tag{4.14}$$

while for the case with $M < K$, the sum DoF is bounded as

$$d_\Sigma \geq (K - \frac{K\Gamma}{M}) \min\{\gamma_P, \frac{M}{K}\} + \Gamma. \tag{4.15}$$

Proof. The proof is shown in Section 4.4.4. □

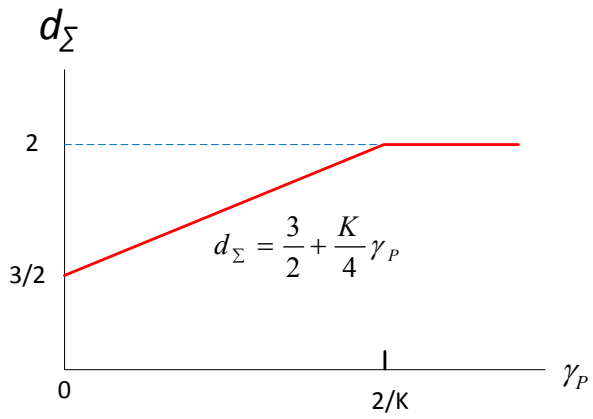

FIGURE 4.4 – Achievable sum DoF d_Σ vs. γ_P for the $K(\geq 3)$-user 2×1 MISO BC.

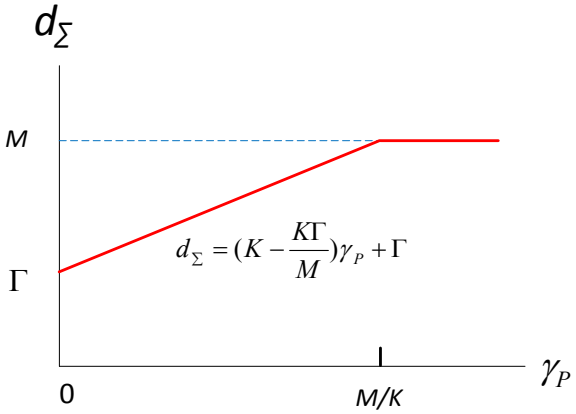

FIGURE 4.5 – Achievable sum DoF d_Σ vs. γ_P for the MISO BC with $M < K$.

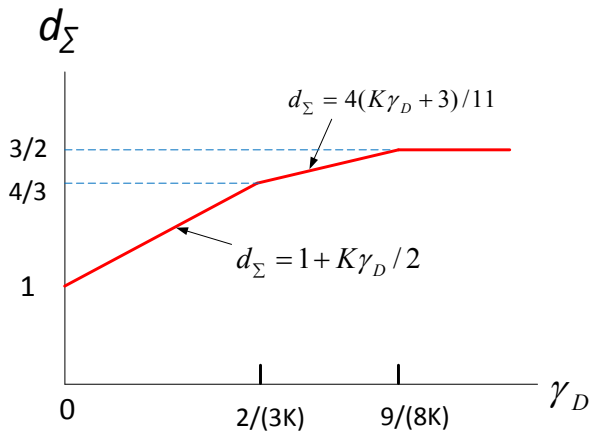

FIGURE 4.6 – Achievable sum DoF d_Σ vs. γ_D for the MISO BC with $K \geq 3, M = 2$, where $\gamma_\mathrm{P} = 0$.

Finally, we consider a case of BC with delayed CSIT feedback only, where $\gamma_\mathrm{P} = 0$. In this case, we use $\gamma_\mathrm{D}^{(k)}$ to denote the fraction of time during which CSIT fed back from user k is delayed, and focus on the case with $\gamma_\mathrm{D}^{(k)} = \gamma_\mathrm{D}, \ \forall k$.

Proposition 5 (Inner bound on DoF with delayed CSIT)**.** *For the $K(\geq 3)$-user 2×1 MISO BC, and for the case of $\gamma_P = 0$, the sum DoF is bounded as*

$$d_\Sigma \geq \min\left\{1 + \frac{K}{2}\gamma_D, \ \frac{12}{11} + \frac{4K}{11}\gamma_D, \ \frac{3}{2}\right\}. \tag{4.16}$$

Proof. The proof is shown in Section 4.4.5. □

Remark 6. *For the K-user MISO BC with current and delayed CSIT feedback, by increasing the number of users, the same DoF performance can be achievable with decreasing feedback cost per user. For example, for the K-user MISO BC with $M = 2$, by increasing K we can achieve any fixed DoF within the range of $(1, 2]$, with decreasing $\gamma_P \leq \frac{2}{K}$, and $\gamma_D \leq \frac{9}{8K}$, both of which approach to 0 as K is large.*

4.3 Converse proof of Theorem 3

We first provide the Proposition 6 to be used, where we drop the time index for simplicity.

Proposition 6. *Let*

$$\begin{aligned} y^{(k)} &= \boldsymbol{h}^{(k)\mathsf{T}}\boldsymbol{x} + z^{(k)}, \quad k = 1, 2 \cdots, K \\ \boldsymbol{y}_k &\triangleq [y^{(1)}\ y^{(2)}\ \cdots\ y^{(k)}]^{\mathsf{T}} \\ \boldsymbol{z}_k &\triangleq [z^{(1)}\ z^{(2)}\ \cdots\ z^{(k)}]^{\mathsf{T}} \\ \boldsymbol{H}_k &\triangleq [\boldsymbol{h}^{(1)}\ \boldsymbol{h}^{(2)}\ \cdots\ \boldsymbol{h}^{(k)}]^{\mathsf{T}} \\ \boldsymbol{H} &\triangleq [\boldsymbol{h}^{(1)}\ \boldsymbol{h}^{(2)}\ \cdots\ \boldsymbol{h}^{(K)}]^{\mathsf{T}} \\ \boldsymbol{H} &= \hat{\boldsymbol{H}} + \tilde{\boldsymbol{H}} \end{aligned}$$

where $\tilde{\boldsymbol{h}}^{(k)} \in \mathbb{C}^{M\times 1}$ *has i.i.d.* $\mathcal{N}_{\mathbb{C}}(0, \sigma_k^2)$ *entries. Then, for any* U *such that* $p_{X|U\hat{H}\tilde{H}} = p_{X|U\hat{H}}$ *and* $K \geq m \geq l$*, we have*

$$l'\, h(\boldsymbol{y}_m|U, \hat{H}, \tilde{H}) - m'\, h(\boldsymbol{y}_l|U, \hat{H}, \tilde{H}) \leq -(m' - l') \sum_{k=1}^{l} \log \sigma_k^2 + o(\log \mathsf{snr}) \tag{4.17}$$

where we define $l' \triangleq \min\{l, M\}$ *and* $m' \triangleq \min\{m, M\}$.

Proof. The proof is shown in the Section 4.6. □

Now giving the observations and messages of users $1, \ldots, k-1$ to user k, we establish the following genie-aided upper bounds on the achievable rates

$$nR_1 \leq I(W_1; y_{[n]}^{(1)} \,|\, \Omega_{[n]}) + n\epsilon \tag{4.18}$$

$$nR_2 \leq I(W_2; y_{[n]}^{(1)}, y_{[n]}^{(2)} \,|\, W_1, \Omega_{[n]}) + n\epsilon \tag{4.19}$$

$$\vdots$$

$$nR_K \leq I(W_K; y_{[n]}^{(1)}, y_{[n]}^{(2)}, \ldots, y_{[n]}^{(k)} \,|\, W_1, \ldots, W_{K-1}, \Omega_{[n]}) + n\epsilon \tag{4.20}$$

where we apply Fano's inequality and some basic chain rules of mutual information using the fact that messages from different users are independent, where we define

$$\begin{aligned} \boldsymbol{S}_t &\triangleq \left[\boldsymbol{h}_t^{(1)}\ \cdots\ \boldsymbol{h}_t^{(K)}\right]^{\mathsf{T}} & \hat{\boldsymbol{S}}_t &\triangleq \left[\hat{\boldsymbol{h}}_t^{(1)}\ \cdots\ \hat{\boldsymbol{h}}_t^{(K)}\right]^{\mathsf{T}} \\ \Omega_{[n]} &\triangleq \{\boldsymbol{S}_t, \hat{\boldsymbol{S}}_t\}_{t=1}^n & y_{[n]}^{(k)} &\triangleq \{y_t^{(k)}\}_{t=1}^n. \end{aligned}$$

Alternatively, we have

$$nR_1 \le h(y_{[n]}^{(1)} \,|\, \Omega_{[n]}) - h(y_{[n]}^{(1)} \,|\, W_1, \Omega_{[n]}) + n\epsilon \tag{4.21}$$

$$nR_2 \le h(y_{[n]}^{(1)}, y_{[n]}^{(2)} \,|\, W_1, \Omega_{[n]}) - h(y_{[n]}^{(1)}, y_{[n]}^{(2)} \,|\, W_1, W_2, \Omega_{[n]}) + n\epsilon \tag{4.22}$$

$$\vdots$$

$$\begin{aligned} nR_K \le\ & h(y_{[n]}^{(1)}, \ldots, y_{[n]}^{(K)} \,|\, W_1, \ldots, W_{K-1}, \Omega_{[n]}) \\ & - h(y_{[n]}^{(1)}, \ldots, y_{[n]}^{(K)} \,|\, W_1, \ldots, W_K, \Omega_{[n]}) + n\epsilon. \end{aligned} \tag{4.23}$$

Therefore, it follows that

$$\begin{aligned} & \sum_{k=1}^{K} \frac{n}{k'}(R_k - \epsilon) \\ & \le \sum_{k=1}^{K-1} \Bigg(\frac{1}{(k+1)'} h(y_{[n]}^{(1)}, \ldots, y_{[n]}^{(k+1)} \,|\, W_1, \ldots, W_k, \Omega_{[n]}) \\ & \qquad - \frac{1}{k'} h(y_{[n]}^{(1)}, \ldots, y_{[n]}^{(k)} \,|\, W_1, \ldots, W_k, \Omega_{[n]}) \Bigg) \\ & \qquad + h(y_{[n]}^{(1)} \,|\, \Omega_{[n]}) - \frac{1}{K'} h(y_{[n]}^{(1)}, \ldots, y_{[n]}^{(K)} \,|\, W_1, \ldots, W_K, \Omega_{[n]}) \qquad (4.24) \\ & \le \sum_{k=1}^{K-1} \sum_{t=1}^{n} \Bigg(\frac{1}{(k+1)'} h(y_t^{(1)}, \ldots, y_t^{(k+1)} \,|\, y_{[t-1]}^{(1)}, \ldots, y_{[t-1]}^{(k)}, W_1, \ldots, W_k, \Omega_{[n]}) \\ & \qquad - \frac{1}{k'} h(y_t^{(1)}, \ldots, y_t^{(k)} \,|\, y_{[t-1]}^{(1)}, \ldots, y_{[t-1]}^{(k)}, W_1, \ldots, W_k, \Omega_{[n]}) \Bigg) \\ & \qquad + n \log P + n\, o(\log P) \qquad (4.25) \\ & \le \log P \sum_{k=1}^{K-1} \sum_{t=1}^{n} \frac{(k+1)' - k'}{k'(k+1)'} \sum_{i=1}^{k} \alpha_t^{(i)} + n \log P + n\, o(\log P) \qquad (4.26) \\ & = n \log P \sum_{k=1}^{K-1} \frac{(k+1)' - k'}{k'(k+1)'} \sum_{i=1}^{k} \bar{\alpha}^{(i)} + n \log P + n\, o(\log P) \qquad (4.27) \\ & = n \log P \sum_{k=1}^{K-1} \Big(\frac{1}{k'} - \frac{1}{K'} \Big) \bar{\alpha}^{(k)} + n \log P + n\, o(\log P) \qquad (4.28) \end{aligned}$$

[5] where we define

$$k' \triangleq \min\{k, M\}; \tag{4.29}$$

the inequality (4.25) is due to 1) the chain rule of differential entropy, 2) the fact that removing condition does not decrease differential entropy,

5. We denote $y_0^{(i)}$ as an empty term, for all i.

3) $h(y_t^{(1)} \,|\, \Omega_{[n]}) \leq \log P + o(\log P)$, i.e., Gaussian distribution maximizes differential entropy under covariance constraint, and 4)

$$h(y_{[n]}^{(1)}, \ldots, y_{[n]}^{(K)} \,|\, W_1, \ldots, W_K, \Omega_{[n]}) = h(\{z_t^{(k)}\}_{t=1}^{n}{}_{k=1}^{K}) > 0;$$

(4.26) is from Proposition 6 by setting

$$U = \{y_{[n]}^{(1)}, \ldots, y_{[n]}^{(k)}, W_1, \ldots, W_k, \Omega_{[n]}\} \setminus \{\boldsymbol{S}_t, \hat{\boldsymbol{S}}_t\}, \quad H = \boldsymbol{S}_t, \quad \hat{H} = \hat{\boldsymbol{S}}_t;$$

the last equality is obtained after putting the summation over k inside the summation over i and some basic manipulations. Similarly, we can interchange the roles of the users and obtain the same genie-aided bounds. Finally, the single antenna constraint gives that $d_k \leq 1,\ k = 1, \cdots, K$. With this, we complete the proof.

4.4 Details of achievability proofs

In this section, we provide the details of the achievability proofs. Specifically, the achievability proof of Theorem 6 is first described in Section 4.4.1, which can be applied in parts for the achievability proof of Theorem 4.4.2 shown in Section 4.4.2, with the proposition proofs shown in the rest of this section.

4.4.1 Achievability proof of Theorem 6

We will prove that, the optimal sum DoF $d_\Sigma = \min\{M, K\}$ is achievable with any CSIT feedback cost $\boldsymbol{\gamma}_\mathrm{P} \triangleq [\gamma_\mathrm{P}^{(1)} \quad \gamma_\mathrm{P}^{(2)} \quad \cdots \quad \gamma_\mathrm{P}^{(K)}] \in \mathbb{R}^K$ such that $\mathsf{C}_\mathrm{P} = \sum_{k=1}^{K} \gamma_\mathrm{P}^{(k)} = \min\{M, K\}$. First of all, we note that there exists a minimum number n such that

$$\boldsymbol{\gamma}_\mathrm{P}{}' \triangleq [\gamma_\mathrm{P}^{(1)'} \quad \gamma_\mathrm{P}^{(2)'} \ \cdots \ \gamma_\mathrm{P}^{(K)'}] \triangleq n\boldsymbol{\gamma}_\mathrm{P} = [n\gamma_\mathrm{P}^{(1)} \quad n\gamma_\mathrm{P}^{(2)} \ \cdots \ n\gamma_\mathrm{P}^{(K)}] \in \mathbb{Z}^K$$

is an integer vector. The explicit communication with n channel uses is given as follows :

- Step 1 : Initially set time index $t = 1$.
- Step 2 : Permute user indices orderly into a set $\mathcal{U}$ such that $\gamma_\mathrm{P}^{(\mathcal{U}(1))'} \leq \gamma_\mathrm{P}^{(\mathcal{U}(2))'} \leq \cdots \leq \gamma_\mathrm{P}^{(\mathcal{U}(K))'}$, where $\mathcal{U}(k)$ denotes the k th element of set $\mathcal{U}$, and where $\mathcal{U}(k) \in \{1, 2, \cdots, K\}$.
- Step 3 : Select $\min\{M, K\}$ users to communicate : users $\mathcal{U}(K), \mathcal{U}(K-1), \cdots, \mathcal{U}(K - \min\{M, K\} + 1)$.
- Step 4 : Let selected users feed back perfect CSIT at time t, keeping the rest users silent.
- Step 5 : The transmitter sends $\min\{M, K\}$ independent symbols to those selected users respectively, which can be done with simple zero-forcing.
- Step 6 : Set $\gamma_\mathrm{P}^{(\mathcal{U}(k))'} = \gamma_\mathrm{P}^{(\mathcal{U}(k))'} - 1, \ k = K - \min\{M, K\} + 1, \cdots, K - 1, K$.
- Step 7 : Set $t = t + 1$. If renewed $t > n$ then terminate, else go back to step 2.

In the above communication with n channel uses, the algorithm guarantees that user i is selected by $\gamma_\mathrm{P}^{(k)'} = n\gamma_\mathrm{P}^{(k)}$ times totally, and that $\min\{M, K\}$ different users are selected in each channel use. As a result, the optimal sum DoF $d_\Sigma = \min\{M, K\}$ is achievable.

Now we consider an example with $M = 2, \ K = 3$, and $\boldsymbol{\gamma}_\mathrm{P} = [1/3 \quad 2/3 \quad 1]$, and show that the optimal sum DoF $d_\Sigma = 2$ is achievable with the following communication :

- Let $n = 3$. Initially $\gamma_\mathrm{P}^{(1)'} = n\gamma_\mathrm{P}^{(1)} = 1$, $\gamma_\mathrm{P}^{(2)'} = n\gamma_\mathrm{P}^{(2)} = 2$, $\gamma_\mathrm{P}^{(3)'} = n\gamma_\mathrm{P}^{(3)} = 3$.
- For $t = 1$, we have $\mathcal{U} = \{1, 2, 3\}$, and $\gamma_\mathrm{P}^{(\mathcal{U}(1))'} = 1$, $\gamma_\mathrm{P}^{(\mathcal{U}(2))'} = 2$, $\gamma_\mathrm{P}^{(\mathcal{U}(3))'} = 3$. Users 3 and 2 are selected to communicate.

TABLE 4.1 – Summary of the scheme for achieving $d_{\sum}^{*} = 2$ with $\mathsf{C}_{\mathrm{P}}^{\star} = 2$, where $M = 2,\ K = 3,\ \gamma_{\mathrm{P}}^{(1)} = 1/3,\ \gamma_{\mathrm{P}}^{(2)} = 2/3,\ \gamma_{\mathrm{P}}^{(3)} = 1$.

time t	1	2	3
$\mathcal{U}$	$\{1,2,3\}$	$\{1,2,3\}$	$\{2,1,3\}$
$\{\gamma_{\mathrm{P}}^{(\mathcal{U}(1))'},\ \gamma_{\mathrm{P}}^{(\mathcal{U}(2))'},\ \gamma_{\mathrm{P}}^{(\mathcal{U}(3))'}\}$	$\{1,2,3\}$	$\{1,1,2\}$	$\{0,1,1\}$
Active users	user 2, 3	user 2, 3	user 1, 3
Perfect CSIT feedback	user 3 : yes user 2 : yes user 1 : no	user 3 : yes user 2 : yes user 1 : no	user 3 : yes user 2 : no user 1 : yes
No. of transmitted symbols	2	2	2

– For $t = 2$, we update the parameters as $\mathcal{U} = \{1,2,3\}$, and $\gamma_{\mathrm{P}}^{(\mathcal{U}(1))'} = 1$, $\gamma_{\mathrm{P}}^{(\mathcal{U}(2))'} = 1$, $\gamma_{\mathrm{P}}^{(\mathcal{U}(3))'} = 2$. At this time, again user 3 and user 2 are selected to communicate.
– For $t = 3$, we update the parameters as $\mathcal{U} = \{2,1,3\}$, and $\gamma_{\mathrm{P}}^{(\mathcal{U}(1))'} = 0$, $\gamma_{\mathrm{P}}^{(\mathcal{U}(2))'} = 1$, $\gamma_{\mathrm{P}}^{(\mathcal{U}(3))'} = 1$. At this time, user 3 and user 1 are selected to communicate. After that the communication terminates.

In the above communication with three channel uses, the transmitter sends two symbols in each channel use, which allows for the optimal sum DoF $d_{\Sigma} = 2$ (see Table 4.1).

4.4.2 Achievability proof of Theorem 5

We proceed to show that, any sum DoF $d_{\Sigma} \in [3/2, 2]$ is achievable with the feedback

$$\gamma_{\mathrm{P}}^{(k)} \leq \frac{\mathsf{C}_{\mathrm{P}}}{2},\ k = 1,2,3, \quad \text{such that} \quad \mathsf{C}_{\mathrm{P}} = \sum_{k=1}^{3} \gamma_{\mathrm{P}}^{(k)} = 4d_{\Sigma} - 6.$$

First of all, we note that there exists a minimum number n such that

$$[2n\gamma_{\mathrm{P}}^{(1)}/\mathsf{C}_{\mathrm{P}} \quad 2n\gamma_{\mathrm{P}}^{(2)}/\mathsf{C}_{\mathrm{P}} \quad n2\gamma_{\mathrm{P}}^{(3)}/\mathsf{C}_{\mathrm{P}}] \in \mathbb{Z}^3, \quad \text{and} \quad 2n/\mathsf{C}_{\mathrm{P}} \in \mathbb{Z}.$$

The scheme has two blocks, with the first block consisting of n channel uses, and the second block consisting of

$$n^{'} = 2n/\mathsf{C}_{\mathrm{P}} - n$$

channel uses. In the first block, we use the algorithm shown in the Section 4.4.1 to achieve the full sum DoF in those n channel uses, during which user k feeds back perfect CSIT in $2n\gamma_{\mathrm{P}}^{(k)}/\mathsf{C}_{\mathrm{P}}$ channel uses, for $k = 1,2,3$. In

the second block, we use the Maddah-Ali and Tse scheme in [4] to achieve $3/2$ sum DoF in those $n^{'}$ channel uses, during which each user feeds back delayed CSIT only.

The communication with n channel uses for the first block is given as follows :

- Step 1 : Let $\gamma_{\mathrm{P}}^{(k)'} = 2n\gamma_{\mathrm{P}}^{(k)}/\mathsf{C}_{\mathrm{P}}$ for all k. Initially, set $t = 1$.
- The steps 2, 3, 4, 5, 6 are the same as those in the algorithm shown in Section 4.4.1, for $M = 2, K = 3$.
- Step 7 : Set $t = t + 1$. If renewed $t > n$ then terminate, else go back to step 2.

In the above communication with n channel uses, the algorithm guarantees that user k, $k = 1, 2, 3$, is selected by $\gamma_{\mathrm{P}}^{(k)'} = 2n\gamma_{\mathrm{P}}^{(k)}/\mathsf{C}_{\mathrm{P}}$ times. We note that $\gamma_{\mathrm{P}}^{(k)'} \leq n$ under the constraint $\gamma_{\mathrm{P}}^{(k)} \leq \mathsf{C}_{\mathrm{P}}/2$ for any k, and that $\sum_{k=1}^{K} \gamma_{\mathrm{P}}^{(k)'} = 2n$, to suggest that in each timeslot two different users are selected, which allows for the optimal 2 sum DoF in this block.

As stated, in the second block, we use the MAT scheme to achieve the $3/2$ sum DoF in those $n^{'}$ channel uses, during which each user feeds back delayed CSIT only. As a result, in the total $n + n^{'}$ channel uses communication, user $k = 1, 2, 3$ feeds back perfect CSIT in $2n\gamma_{\mathrm{P}}^{(k)}/(\mathsf{C}_{\mathrm{P}}(n+n^{'})) = \gamma_{\mathrm{P}}^{(k)}$ fraction of communication period, with achievable sum DoF given as

$$d_{\Sigma} = \frac{2n}{(n+n^{'})} + \frac{3n^{'}}{2(n+n^{'})} = \frac{3}{2} + \frac{1}{4}\mathsf{C}_{\mathrm{P}}.$$

We note that the achievability scheme applies to the case of having some $\gamma_{\mathrm{P}}^{(1)}, \gamma_{\mathrm{P}}^{(2)}, \gamma_{\mathrm{P}}^{(3)} \leq \mathsf{C}_{\mathrm{P}}/2$ such that $\mathsf{C}_{\mathrm{P}} = 4d_{\Sigma} - 6$, and allows to achieve any sum DoF $d_{\Sigma} \in [3/2, 2]$. Apparently, $\mathsf{C}_{\mathrm{P}} = 0$ allows for any sum DoF $d_{\Sigma} \in [0, 3/2]$, which completes the proof.

4.4.3 Proof of Proposition 3

The achievability scheme is based on time sharing between two strategies of CSIT feedback, i.e., delayed CSIT feedback with ${\gamma_{\mathrm{P}}}' = 0$ and alternating CSIT feedback with ${\gamma_{\mathrm{P}}}'' = \frac{2}{K}$, where the first strategy achieves $d_{\Sigma}' = 3/2$ by applying Maddah-Ali and Tse (MAT) scheme (see in [4]), with the second strategy achieving $d_{\Sigma}'' = 2$ by using alternating CSIT feedback manner (see in [46]).

Let $\Delta \in [0, 1]$ (resp. $1 - \Delta$) be the fraction of time during which the first (resp. second) CSIT feedback strategy is used in the communication. As a result, the final feedback cost (per user) is given as

$$\gamma_{\mathrm{P}} = {\gamma_{\mathrm{P}}}'\Delta + {\gamma_{\mathrm{P}}}''(1 - \Delta), \tag{4.30}$$

implying that

$$\Delta = \frac{{\gamma_{\mathrm{P}}}'' - \gamma_{\mathrm{P}}}{{\gamma_{\mathrm{P}}}'' - {\gamma_{\mathrm{P}}}'}, \tag{4.31}$$

with final sum DoF given as

$$\begin{aligned} d_{\Sigma} &= d'_{\Sigma}\Delta + d''_{\Sigma}(1-\Delta) \\ &= d''_{\Sigma} + \Delta(d'_{\Sigma} - d''_{\Sigma}) \\ &= d''_{\Sigma} + (d'_{\Sigma} - d''_{\Sigma})\frac{{\gamma_{\mathrm{P}}}'' - \gamma_{\mathrm{P}}}{{\gamma_{\mathrm{P}}}'' - {\gamma_{\mathrm{P}}}'} \\ &= \frac{3}{2} + \frac{K}{4}\gamma_{\mathrm{P}} \end{aligned} \tag{4.32}$$

which completes the proof.

4.4.4 Proof of Proposition 4

For the case with $M \geq K$, the proposed scheme is based on time sharing between delayed CSIT feedback with ${\gamma_{\mathrm{P}}}' = 0$ and full CSIT feedback with ${\gamma_{\mathrm{P}}}'' = 1$, where the first feedback strategy achieves $d_{\sum}^{'} = d_{\mathrm{MAT}}$ by applying MAT scheme, with the second one achieving $d_{\sum}^{''} = K$. As a result, following the steps in (4.30), (4.31), (4.32), the final sum DoF is calculated as

$$\begin{aligned} d_{\Sigma} &= d''_{\Sigma} + (d'_{\Sigma} - d''_{\Sigma})\frac{{\gamma_{\mathrm{P}}}'' - \gamma_{\mathrm{P}}}{{\gamma_{\mathrm{P}}}'' - {\gamma_{\mathrm{P}}}'} \\ &= (K - d_{\mathrm{MAT}})\gamma_{\mathrm{P}} + d_{\mathrm{MAT}} \end{aligned}$$

where $\gamma_{\mathrm{P}} \in [0,1]$ is the final feedback cost (per user) for this case.

Similar approach is exploited for the case with $M < K$. In this case, we apply time sharing between delayed CSIT feedback with ${\gamma_{\mathrm{P}}}' = 0$ and alternating CSIT feedback with ${\gamma_{\mathrm{P}}}'' = M/K$. In this case, the first feedback strategy achieves $d'_{\Sigma} = \Gamma$ by applying MAT scheme, with the second strategy achieving $d''_{\Sigma} = M$ by using alternating CSIT feedback manner. As a result, for $\gamma_{\mathrm{P}} \in [0, \frac{M}{K}]$ being the final feedback cost for this case, the final sum DoF is calculated as

$$\begin{aligned} d_{\Sigma} &= d''_{\Sigma} + (d'_{\Sigma} - d''_{\Sigma})\frac{{\gamma_{\mathrm{P}}}'' - \gamma_{\mathrm{P}}}{{\gamma_{\mathrm{P}}}'' - {\gamma_{\mathrm{P}}}'} \\ &= (K - \frac{K\Gamma}{M})\gamma_{\mathrm{P}} + \Gamma \end{aligned}$$

which completes the proof.

TABLE 4.2 – Summary of the achievability scheme for achieving $d_\Sigma = \frac{4}{3}$ with $\gamma_{\mathrm{D}} = \frac{2}{3K}$.

block index	1	2	$\cdots$	K
No. of channel uses	3	3	$\cdots$	3
Active users	user 1, 2	user 2, 3	$\cdots$	user K, 1
Delayed CSIT feedback fraction in a block	user 1 : 1/3 user 2 : 1/3 the rest : 0	user 2 : 1/3 user 3 : 1/3 the rest : 0	$\cdots$	user K : 1/3 user 1 : 1/3 the rest : 0
Sum DoF in a block	4/3	4/3	$\cdots$	4/3

4.4.5 Proof of Proposition 5

As shown in the Fig 4.6, the sum DoF performance has three regions :

$$d_\Sigma = \begin{cases} 1 + \frac{K}{2}\gamma_{\mathrm{D}}, & \gamma_{\mathrm{D}} \in [0, \frac{2}{3K}] \\ \frac{12}{11} + \frac{4K}{11}\gamma_{\mathrm{D}}, & \gamma_{\mathrm{D}} \in [\frac{2}{3K}, \frac{9}{8K}] \\ 3/2, & \gamma_{\mathrm{D}} \in [\frac{9}{8K}, 1]. \end{cases}$$

In the following, we will prove that the sum DoF $d_\Sigma = 1,\ \frac{4}{3},\ \frac{3}{2}$ are achievable with $\gamma_{\mathrm{D}} = 0,\ \frac{2}{3K},\ \frac{9}{8K}$, respectively. At the end, the whole DoF performance declared can be achievable by time sharing between those performance points.

The proposed scheme achieving $d_\Sigma = \frac{4}{3}$ with $\gamma_{\mathrm{D}} = \frac{2}{3K}$, is a modified version of the MAT scheme in [4]. The new scheme has K blocks, with each block consisting of three channel uses. In each block, four independent symbols are sent to two orderly selected users, which can be done with MAT scheme with each of two chosen user feeding back delayed CSIT in one channel use. As a result, $d_\Sigma = \frac{4}{3}$ is achievable with $\gamma_{\mathrm{D}} = \frac{2}{3K}$, using the fact that each of K users needs to feed back delayed CSIT twice only in the whole communication (see Table 4.2).

Similarly, the proposed scheme achieving $d_\Sigma = \frac{3}{2}$ with $\gamma_{\mathrm{D}} = \frac{9}{8K}$ has K blocks, with each block consisting of 8 channel uses. In each block, 3 out of K users are selected to communicate. In this case, 12 independent symbols are sent to the chosen users during each block, which can be done with another MAT scheme with each of chosen users feeding back delayed CSIT in 3 channel uses. As a result, $d_\Sigma = \frac{3}{2}$ is achievable with $\gamma_{\mathrm{D}} = \frac{9}{8K}$, using the fact that each of K users needs to feed back delayed CSIT 9 times only in the whole communication (see Table 4.3).

Finally, $d_\Sigma = 1$ is achievable without any CSIT. By now, we complete the proof.

TABLE 4.3 – Summary of the achievability scheme for achieving $d_\Sigma = \frac{3}{2}$ with $\gamma_{\mathrm{D}} = \frac{9}{8K}$.

block index	1	2	$\cdots$	K
No. of channel uses	8	8	$\cdots$	8
Active users	user 1, 2, 3	user 2, 3, 4	$\cdots$	user K, 1, 2
Delayed CSIT feedback fraction in a block	user 1 : 3/8 user 2 : 3/8 user 3 : 3/8 the rest : 0	user 2 : 3/8 user 3 : 3/8 user 4 : 3/8 the rest : 0	$\cdots$	user K : 3/8 user 1 : 3/8 user 2 : 3/8 the rest : 0
Sum DoF in a block	3/2	3/2	$\cdots$	3/2

4.5 Conclusions

This work considered the general multiuser MISO BC, and established inner and outer bounds on the tradeoff between DoF performance and CSIT feedback quality, which are optimal for many cases. Those bounds, as well as some analysis, were provided with the aim of giving insights on how much CSIT feedback to achieve a certain DoF performance.

4.6 Appendix - Proof details of Proposition 6

In the following, we will prove Proposition 6 used for the converse proof, as well as three lemmas to be used here. As stated, we will drop the time index for simplicity.

Lemma 4. [6] *Let $\boldsymbol{G} = \hat{\boldsymbol{G}} + \tilde{\boldsymbol{G}} \in \mathbb{C}^{m\times m}$ where $\tilde{\boldsymbol{G}}$ has i.i.d. $\mathcal{N}_c(0,1)$ entries, and $\tilde{\boldsymbol{G}}$ is independent of $\hat{\boldsymbol{G}}$. Then, we have*

$$\mathbb{E}_{\tilde{G}}\big[\log\det\left(\boldsymbol{G}^{\mathsf{H}}\boldsymbol{G}\right)\big] = \sum_{i=1}^{\tau}\log\big(\lambda_i(\hat{\boldsymbol{G}}^{\mathsf{H}}\hat{\boldsymbol{G}})\big) + o(\log\mathsf{snr}) \tag{4.33}$$

where $\lambda_i(\hat{\boldsymbol{G}}^{\mathsf{H}}\hat{\boldsymbol{G}})$ denotes the i th largest eigenvalue of $\hat{\boldsymbol{G}}^{\mathsf{H}}\hat{\boldsymbol{G}}$; τ is the number of eigenvalues of $\hat{\boldsymbol{G}}^{\mathsf{H}}\hat{\boldsymbol{G}}$ that do not vanish with snr (SNR), i.e., $\lambda_i(\hat{\boldsymbol{G}}^{\mathsf{H}}\hat{\boldsymbol{G}}) = o(1)$ when snr is large, $\forall\, i > \tau$.

Lemma 5. *For $\boldsymbol{P} \in \mathbb{C}^{m\times m}$ a permutation matrix and $\boldsymbol{A} \in \mathbb{C}^{m\times m}$, let $\boldsymbol{AP} = \boldsymbol{QR}$ be the QR decomposition of the column permuted version of $\boldsymbol{A}$. Then, there exist at least one permutation matrix $\boldsymbol{P}$ such that*

$$r_{ii}^2 \geq \frac{1}{m-i+1}\lambda_i(\boldsymbol{A}^{\mathsf{H}}\boldsymbol{A}), \quad i = 1,\ldots,m \tag{4.34}$$

where as stated $\lambda_i(\boldsymbol{A}^{\mathsf{H}}\boldsymbol{A})$ is the i th largest eigenvalue of $\boldsymbol{A}^{\mathsf{H}}\boldsymbol{A}$; r_{ii} is the i th diagonal elements of $\boldsymbol{R}$.

Lemma 6. *For any matrix $\boldsymbol{A} \in \mathbb{C}^{m\times m}$, there exists a column permuted version $\bar{\boldsymbol{A}}$, such that*

$$\det(\bar{\boldsymbol{A}}_{\mathcal{I}}^{\mathsf{H}}\bar{\boldsymbol{A}}_{\mathcal{I}}) \geq m^{-|\mathcal{I}|}\prod_{i\in\mathcal{I}}\lambda_i(\boldsymbol{A}^{\mathsf{H}}\boldsymbol{A}), \quad \forall\,\mathcal{I}\subseteq\{1,\ldots,m\} \tag{4.35}$$

where $\bar{\boldsymbol{A}}_{\mathcal{I}} = [A_{ji} :\ j\in\{1,\ldots,m\},\, i\in\mathcal{I}] \in \mathbb{C}^{m\times|\mathcal{I}|}$ is the submatrix of $\boldsymbol{A}$ formed by the columns with indices in $\mathcal{I}$.

4.6.1 Proof of Lemma 4

Let us perform a singular value decomposition (SVD) on the matrix $\hat{\boldsymbol{G}}$, i.e., $\hat{\boldsymbol{G}} = \boldsymbol{U}\begin{bmatrix}\boldsymbol{D}_1 & \\ & \boldsymbol{D}_2\end{bmatrix}\boldsymbol{V}^{\mathsf{H}}$ where $\boldsymbol{U},\boldsymbol{V}\in\mathbb{C}^{m\times m}$ are unitary matrices and $\boldsymbol{D}_1$ and $\boldsymbol{D}_2$ are $\tau'\times\tau'$ and $(m-\tau')\times(m-\tau')$ diagonal matrices of the singular values of $\hat{\boldsymbol{G}}$. Without loss of generality, we assume that the i th singluar value, $i = 1,\ldots,m$, scales with snr as snr^{b_i}, when snr is large. Moreover, the

6. We note that Lemma 4 is a slightly more general version of the result in [25, Lemma 6].

singular values in $\boldsymbol{D}_1$ are such that $b_i > 0$ and those in $\boldsymbol{D}_2$ verify $b_i \leq 0$. First, we have the following lower bound

$$
\begin{aligned}
&\mathbb{E}_{\tilde{G}}\big[\log\det\left(\boldsymbol{G}^{\mathsf{H}}\boldsymbol{G}\right)\big] \\
&\quad= \mathbb{E}_{\boldsymbol{M}}\left[\log\det\left(\left(\begin{bmatrix}\boldsymbol{D}_1 & \boldsymbol{D}_2\end{bmatrix}+\boldsymbol{M}\right)^{\mathsf{H}}\left(\begin{bmatrix}\boldsymbol{D}_1 & \boldsymbol{D}_2\end{bmatrix}+\boldsymbol{M}\right)\right)\right] && (4.36)\\
&\quad\geq \mathbb{E}_{\boldsymbol{M}}\left[\log\det\left(\left(\begin{bmatrix}\boldsymbol{D}_1 & 0\end{bmatrix}+\boldsymbol{M}\right)^{\mathsf{H}}\left(\begin{bmatrix}\boldsymbol{D}_1 & 0\end{bmatrix}+\boldsymbol{M}\right)\right)\right] && (4.37)\\
&\quad= \mathbb{E}_{\boldsymbol{M}}\Big[\log\big|\det\left(\boldsymbol{D}_1+\boldsymbol{M}_{11}\right)\det\big(\boldsymbol{M}_{22}-\underbrace{\boldsymbol{M}_{21}\left(\boldsymbol{D}_1+\boldsymbol{M}_{11}\right)^{-1}}_{\boldsymbol{B}}\boldsymbol{M}_{12}\big)\big|^2\Big] && (4.38)\\
&\quad= \log\big|\det\left(\boldsymbol{D}_1\right)\big|^2+\mathbb{E}_{\boldsymbol{M}_{11}}\Big[\log\big|\det\left(I+\boldsymbol{D}_1^{-1}\boldsymbol{M}_{11}\right)\big|^2\Big] \\
&\qquad+\mathbb{E}_{\boldsymbol{B}}\mathbb{E}_{\tilde{\boldsymbol{M}}}\big[\log\det(\tilde{\boldsymbol{M}}^H(I+\boldsymbol{B}\boldsymbol{B}^H)\tilde{\boldsymbol{M}})\big] && (4.39)\\
&\quad\geq \log\big|\det\left(\boldsymbol{D}_1\right)\big|^2+\mathbb{E}_{\boldsymbol{M}_{11}}\Big[\log\big|\det\left(I+\boldsymbol{D}_1^{-1}\boldsymbol{M}_{11}\right)\big|^2\Big] \\
&\qquad+\underbrace{\mathbb{E}_{\tilde{\boldsymbol{M}}}\big[\log\det(\tilde{\boldsymbol{M}}^H\tilde{\boldsymbol{M}})\big]}_{(\ln 2)^{-1}\sum_{l=0}^{m-\tau'-1}\psi(m-\tau'-l)=O(1)} && (4.40)
\end{aligned}
$$

where we define $\boldsymbol{M}\triangleq\boldsymbol{U}^{\mathsf{H}}\tilde{\boldsymbol{G}}\boldsymbol{V}=\left[\begin{smallmatrix}\boldsymbol{M}_{11} & \boldsymbol{M}_{12}\\ \boldsymbol{M}_{21} & \boldsymbol{M}_{22}\end{smallmatrix}\right]$ with $\boldsymbol{M}_{11}\in\mathbb{C}^{\tau'\times\tau'}$, and remind that the entries of $\boldsymbol{M}$, thus of $\boldsymbol{M}_{ij}$, $i,j=1,2$, are also i.i.d. $\mathcal{N}_c(0,1)$; (4.37) is from the fact that expectation of the log determinant of a non-central Wishart matrix is non-decreasing with in the "line-of-sight" component [50]; (4.38) is due to the identity

$$
\det\left(\left[\begin{smallmatrix}\boldsymbol{N}_{11} & \boldsymbol{N}_{12}\\ \boldsymbol{N}_{21} & \boldsymbol{N}_{22}\end{smallmatrix}\right]\right)=\det(\boldsymbol{N}_{11})\det(\boldsymbol{N}_{22}-\boldsymbol{N}_{21}\boldsymbol{N}_{11}^{-1}\boldsymbol{N}_{12})
$$

whenever $\boldsymbol{N}_{11}$ is square and invertible; in (4.39), we notice that, given the matrix $\boldsymbol{B}\triangleq\boldsymbol{M}_{21}\left(\boldsymbol{D}_1+\boldsymbol{M}_{11}\right)^{-1}$, the columns of $\boldsymbol{M}_{22}-\boldsymbol{B}\boldsymbol{M}_{12}$ are i.i.d. $\mathcal{N}_c(0,I+\boldsymbol{B}\boldsymbol{B}^H)$, from which $|\det(\boldsymbol{M}_{22}-\boldsymbol{B}\boldsymbol{M}_{12})|^2$ is equivalent in distribution to $\det(\tilde{\boldsymbol{M}}^H(I+\boldsymbol{B}\boldsymbol{B}^H)\tilde{\boldsymbol{M}})$ where $\tilde{\boldsymbol{M}}\in\mathbb{C}^{(m-\tau')\times(m-\tau')}$ has i.i.d. $\mathcal{N}_c(0,1)$ entries; the last inequality is from $\tilde{\boldsymbol{M}}^H(I+\boldsymbol{B}\boldsymbol{B}^H)\tilde{\boldsymbol{M}}\succeq\tilde{\boldsymbol{M}}^H\tilde{\boldsymbol{M}}$ and therefore $\det(\tilde{\boldsymbol{M}}^H(I+\boldsymbol{B}\boldsymbol{B}^H)\tilde{\boldsymbol{M}})\geq\det(\tilde{\boldsymbol{M}}^H\tilde{\boldsymbol{M}})$, $\forall\,\boldsymbol{B}$; the closed-form term in the last inequality is due to [51] with $\psi(\cdot)$ being Euler's digamma function. In the following, we show that $\mathbb{E}\big[\log\big|\det\left(I+\boldsymbol{D}_1^{-1}\boldsymbol{M}_{11}\right)\big|^2\big]\geq O(1)$ as well. To that end, we use the fact that the distribution of $\boldsymbol{M}_{11}$ is invariant to rotation, and so for $\boldsymbol{D}_1^{-1}\boldsymbol{M}_{11}$. Specifically, introducing $\theta\sim\mathrm{Unif}(0,2\pi]$ that

is independent of the rest of the random variables, we have

$$\begin{aligned}
&\mathbb{E}_{\boldsymbol{M}_{11}}\Big[\log\big|\det\left(I+\boldsymbol{D}_1^{-1}\boldsymbol{M}_{11}\right)\big|^2\Big] \\
&= \mathbb{E}_{\boldsymbol{M}_{11},\theta}\Big[\log\big|\det\left(I+\boldsymbol{D}_1^{-1}\boldsymbol{M}_{11}e^{j\theta}\right)\big|^2\Big] && (4.41)\\
&= \mathbb{E}_{\boldsymbol{M}_{11},\theta}\Big[\log\big|\det\left(e^{-j\theta}I+\boldsymbol{D}_1^{-1}\boldsymbol{M}_{11}\right)\big|^2\Big] && (4.42)\\
&= \sum_{i=1}^{\tau'}\mathbb{E}_J\mathbb{E}_\theta\big[\log|e^{-j\theta}+\underbrace{\lambda_i(\boldsymbol{D}^{-1}\boldsymbol{M}_{11})}_{J_i}|^2\big] && (4.43)\\
&= \sum_{i=1}^{\tau'}\mathbb{E}_J\mathbb{E}_\theta[\log(1+|J_i|^2+2|J_i|\cos(\theta+\phi(J_i)))] && (4.44)\\
&= \sum_{i=1}^{\tau'}\mathbb{E}_J\mathbb{E}_\theta[\log(1+|J_i|^2+2|J_i|\cos(\theta))] && (4.45)\\
&\geq \sum_{i=1}^{\tau'}\big[\mathbb{E}_J\big(\log(1+|J_i|^2)\big)-1\big] && (4.46)\\
&\geq -\tau' && (4.47)
\end{aligned}$$

where the first equality is from the fact that $\boldsymbol{M}_{11}$ is equivalent to $\boldsymbol{M}_{11}e^{j\theta}$ as long as θ is independent of $\boldsymbol{M}_{11}$ and that $\boldsymbol{M}_{11}$ has independent circularly symmetric Gaussian entries; (4.43) is due to the characteristic polynomial of the matrix $-\boldsymbol{D}^{-1}\boldsymbol{M}_{11}$; in (4.44) we define $\phi(J_i)$ the argument of J_i that is independent of θ; (4.45) is from the fact that $\mathrm{mod}(\theta+\phi)_{2\pi}\sim\mathrm{Unif}(0,2\pi]$ and is independent of ϕ, as long as $\theta\sim\mathrm{Unif}(0,2\pi]$ and is independent of ϕ, also known as the Crypto Lemma [52]; (4.46) is from the identity

$$\int_0^1\log(a+b\cos(2\pi t))\,\mathrm{d}t=\log\frac{a+\sqrt{a^2-b^2}}{2}\geq\log(a)-1,\forall\, a\geq b>0.$$

Combining (4.40) and (4.47), we have the lower bound

$$\mathbb{E}_{\tilde{G}}\big[\log\det\left(\boldsymbol{G}^{\mathsf{H}}\boldsymbol{G}\right)\big]\geq\log\big|\det\left(\boldsymbol{D}_1\right)\big|^2+O(1) \tag{4.48}$$

when snr is large. In fact, it has been shown that the $O(1)$ term here, sum of the $O(1)$ term in (4.40) and $-\tau'$ in (4.47), does not depend on snr at all.

The next step is to derive an upper bound on $\mathbb{E}\big[\log\det\left(\boldsymbol{G}^{\mathsf{H}}\boldsymbol{G}\right)\big]$. Following

Jensen's inequality, we have

$$\begin{aligned}
&\mathbb{E}_{\tilde{G}}\big[\log\det(\boldsymbol{G}^{\mathsf{H}}\boldsymbol{G})\big] \\
&\le \log\det\big(\mathbb{E}_{\tilde{G}}[\boldsymbol{G}^{\mathsf{H}}\boldsymbol{G}]\big) && (4.49)\\
&= \log\det\Big(\begin{bmatrix}\boldsymbol{D}_1^2 & \\ & \boldsymbol{D}_2^2\end{bmatrix} + \mathbb{E}[\boldsymbol{M}^{\mathsf{H}}\boldsymbol{M}]\Big) && (4.50)\\
&= \log|\det(\boldsymbol{D}_1)|^2 + \underbrace{\log\det\big(I + m\boldsymbol{D}_1^{-2}\big)}_{o(1)} + \underbrace{\log\det\big(mI + \boldsymbol{D}_2^2\big)}_{o(\log\mathsf{snr})} && (4.51)\\
&= \log|\det(\boldsymbol{D}_1)|^2 + o(\log\mathsf{snr}) && (4.52)
\end{aligned}$$

Putting the lower and upper bounds together, we have $\mathbb{E}\big[\log\det(\boldsymbol{G}^{\mathsf{H}}\boldsymbol{G})\big] = \log|\det(\boldsymbol{D}_1)|^2 + o(\log\mathsf{snr})$. Finally, note that, since $\lambda_i(\hat{\boldsymbol{G}}^{\mathsf{H}}\hat{\boldsymbol{G}}) \doteq \mathsf{snr}^0$, $i = \tau'+1,\ldots,\tau$, we have

$$\begin{aligned}
\log\big|\det(\boldsymbol{D}_1)\big|^2 &= \sum_{i=1}^{\tau'}\log\big(\lambda_i(\hat{\boldsymbol{G}}^{\mathsf{H}}\hat{\boldsymbol{G}})\big) && (4.53)\\
&= \sum_{i=1}^{\tau}\log\big(\lambda_i(\hat{\boldsymbol{G}}^{\mathsf{H}}\hat{\boldsymbol{G}})\big) - \sum_{i=\tau'+1}^{\tau}\log\big(\lambda_i(\hat{\boldsymbol{G}}^{\mathsf{H}}\hat{\boldsymbol{G}})\big) && (4.54)\\
&= \sum_{i=1}^{\tau}\log\big(\lambda_i(\hat{\boldsymbol{G}}^{\mathsf{H}}\hat{\boldsymbol{G}})\big) + o(\log\mathsf{snr}) && (4.55)
\end{aligned}$$

from which the proof is complete.

4.6.2 Proof of Lemma 5

The existence is proved by construction. Let $\boldsymbol{a}_j$, $j = 1,\ldots,m$, be the j th column of $\boldsymbol{A}$. We define j_1^* as the index of the column that has the largest Euclidean norm, i.e.,

$$j_1^* = \arg\max_{j=1,\ldots,m}\|\boldsymbol{a}_j\|. \tag{4.56}$$

Swapping the j_1^* and the first column, and denoting $\boldsymbol{A}_1 = \boldsymbol{A}$, we have

$$\boldsymbol{B}_1 \triangleq \boldsymbol{A}_1\boldsymbol{T}_{1,j_1^*} \tag{4.57}$$

where $\boldsymbol{T}_{ij} \in \mathbb{C}^{m\times m}$ denotes the permutation matrix that swaps the i th and j th columns. Now, let $\boldsymbol{U}_1 \in \mathbb{C}^{m\times m}$ be any unitary matrix such that the first column is aligned with the first column of $\boldsymbol{B}_1$, i.e., equal to $\frac{\boldsymbol{a}_{j_1^*}}{\|\boldsymbol{a}_{j_1^*}\|}$. Then, we can construct a block-upper-triangular matrix $\boldsymbol{R}_1 = \boldsymbol{U}_1^{\mathsf{H}}\boldsymbol{B}_1 = \boldsymbol{U}_1^{\mathsf{H}}\boldsymbol{A}_1\boldsymbol{T}_{1,j_1^*}$ with the following form

$$\boldsymbol{R}_1 = \begin{bmatrix} r_{11} & * \\ \boldsymbol{0}_{(m-1)\times 1} & \boldsymbol{A}_2\end{bmatrix} \tag{4.58}$$

where it is readily shown that

$$r_{11}^2 = \|\boldsymbol{a}_{j_1^*}\|^2 \tag{4.59}$$
$$\geq \frac{1}{m}||\boldsymbol{A}_1||_F^2 \tag{4.60}$$
$$\geq \frac{1}{m}\lambda_1(\boldsymbol{A}_1^{\mathsf{H}}\boldsymbol{A}_1). \tag{4.61}$$

Repeating the same procedure on $\boldsymbol{A}_2$, we will have $\boldsymbol{R}_2 = \boldsymbol{U}_2^{\mathsf{H}}\boldsymbol{B}_2 = \boldsymbol{U}_2^{\mathsf{H}}\boldsymbol{A}_2\boldsymbol{T}_{2,j_2^*}$ where all the involved matrices are similarly defined as above except for the reduced dimension $(m-1)\times(m-1)$ and

$$\boldsymbol{R}_2 = \begin{bmatrix} r_{22} & * \\ \boldsymbol{0}_{(m-2)\times 1} & \boldsymbol{A}_3 \end{bmatrix} \tag{4.62}$$

where it is readily shown that

$$r_{22}^2 \geq \frac{1}{m-1}\lambda_1(\boldsymbol{A}_2^{\mathsf{H}}\boldsymbol{A}_2) \tag{4.63}$$
$$\geq \frac{1}{m-1}\lambda_2(\boldsymbol{A}_1^{\mathsf{H}}\boldsymbol{A}_1). \tag{4.64}$$

Here, the last inequality is from the fact that, for any matrix $\boldsymbol{C}$ and a submatrix $\boldsymbol{C}_k$ by removing k rows or columns, we have [53, Corollary 3.1.3]

$$\lambda_i(\boldsymbol{C}_k^{\mathsf{H}}\boldsymbol{C}_k) \geq \lambda_{i+k}(\boldsymbol{C}^{\mathsf{H}}\boldsymbol{C}) \tag{4.65}$$

where we recall that λ_i is the i th largest eigenvalue. Let us continue the procedure on $\boldsymbol{A}_3$ and so on. At the end, we will have all the $\{\boldsymbol{U}_i\}$ and $\left\{\boldsymbol{T}_{i,j_i^*}\right\}$ such that

$$\underbrace{\begin{bmatrix} I_{m-1} & \\ & \boldsymbol{U}_m^{\mathsf{H}} \end{bmatrix}\cdots\begin{bmatrix} I_2 & \\ & \boldsymbol{U}_3^{\mathsf{H}} \end{bmatrix}\begin{bmatrix} 1 & \\ & \boldsymbol{U}_2^{\mathsf{H}} \end{bmatrix}\boldsymbol{U}_1^{\mathsf{H}}}_{\boldsymbol{Q}^{\mathsf{H}}}\boldsymbol{A}\underbrace{\boldsymbol{T}_{1,j_1^*}\begin{bmatrix} 1 & \\ & \boldsymbol{T}_{2,j_2^*} \end{bmatrix}\begin{bmatrix} I_2 & \\ & \boldsymbol{T}_{3,j_3^*} \end{bmatrix}\cdots\begin{bmatrix} I_{m-1} & \\ & \boldsymbol{T}_{m,j_m^*} \end{bmatrix}}_{\boldsymbol{P}}$$
$$= \underbrace{\begin{bmatrix} r_{11} & * & * & * \\ & r_{22} & * & * \\ & & \ddots & \vdots \\ & & & r_{mm} \end{bmatrix}}_{\boldsymbol{R}}$$

where it is obvious that $\boldsymbol{P}$ is a permutation matrix and $\boldsymbol{Q}$ is unitary. The proof is thus completed.

4.6.3 Proof of Lemma 6

Let $\bar{\boldsymbol{A}} \triangleq \boldsymbol{AP} = \boldsymbol{QR}$ with $\boldsymbol{P}$ a permutation matrix such that (4.34) holds. Then, we have

$$\begin{aligned}
\det(\bar{\boldsymbol{A}}_{\mathcal{J}}^{\mathsf{H}} \bar{\boldsymbol{A}}_{\mathcal{J}}) &= \det(\boldsymbol{R}_{\mathcal{J}}^{\mathsf{H}} \boldsymbol{Q}^{\mathsf{H}} \boldsymbol{Q} \boldsymbol{R}_{\mathcal{J}}) && (4.66)\\
&= \det(\boldsymbol{R}_{\mathcal{J}}^{\mathsf{H}} \boldsymbol{R}_{\mathcal{J}}) && (4.67)\\
&\geq \det(\boldsymbol{R}_{\mathcal{J}\mathcal{J}}^{\mathsf{H}} \boldsymbol{R}_{\mathcal{J}\mathcal{J}}) && (4.68)\\
&= \prod_{i\in\mathcal{J}} r_{ii}^2 && (4.69)\\
&\geq m^{-|\mathcal{J}|} \prod_{i\in\mathcal{J}} \lambda_i(\boldsymbol{A}^{\mathsf{H}}\boldsymbol{A}) && (4.70)
\end{aligned}$$

where the first inequality results from the Cauchy-Binet formula, and the last inequality is due to Lemma 5.

4.6.4 Proof of Proposition 6

The inequality (4.17) is trivial when $m \geq l \geq M$, i.e., $l' = m' = M$. From the chain rule

$$\begin{aligned}
h(\boldsymbol{y}_m \,|\, U, \hat{H}, \tilde{H}) &= h(\boldsymbol{y}_l \,|\, U, \hat{H}, \tilde{H}) + h(y^{(l+1)}, \ldots, y^{(m)} \,|\, \boldsymbol{y}_l, \hat{H}, \tilde{H}) && (4.71)\\
&= h(\boldsymbol{y}_l \,|\, U, \hat{H}, \tilde{H}) + o(\log \mathsf{snr}) && (4.72)
\end{aligned}$$

since with $l \geq M$, the observations $y^{(l+1)}, \ldots, y^{(m)}$ can be represented as a linear combination of $\boldsymbol{y}_l$, up to the noise error. In the following, we focus on the case $l \leq M$.

First of all, let us write

$$\begin{aligned}
&h(\boldsymbol{y}_m|U, \hat{H}, \tilde{H}) - \mu\, h(\boldsymbol{y}_l|U, \hat{H}, \tilde{H})\\
&= \mathbb{E}_{\hat{H}}\Big[\mathbb{E}_{\tilde{H}}[h(\boldsymbol{H}_m\boldsymbol{x} + \boldsymbol{z}_m \,|\, U, \hat{H} = \hat{\boldsymbol{H}}, \tilde{H} = \tilde{\boldsymbol{H}})]\\
&\qquad - \mu\, \mathbb{E}_{\tilde{H}}[h(\boldsymbol{H}_l\boldsymbol{x} + \boldsymbol{z}_l \,|\, U, \hat{H} = \hat{\boldsymbol{H}}, \tilde{H} = \tilde{\boldsymbol{H}})]\Big] && (4.73)
\end{aligned}$$

In the following, we focus on the term inside the expection over $\hat{H}$ in (4.73), i.e., for a given realization of $\hat{\boldsymbol{H}}$. Since $\boldsymbol{y}_l$ is a degraded version of $\boldsymbol{y}_m$, we can apply the results in [41, Corollary 4] and obtain the optimality of Gaussian input, i.e.,

$$\begin{aligned}
&\max_{\substack{p_{X|U\hat{H}}:\\ \mathbb{E}[\mathrm{tr}(XX^{\mathsf{H}})]\leq \mathsf{snr}}} \mathbb{E}_{\tilde{H}}\big[h(\boldsymbol{y}_m|U, \hat{H}=\hat{\boldsymbol{H}}, \tilde{H}=\tilde{\boldsymbol{H}})\big] - \mu\, \mathbb{E}_{\tilde{H}}\big[h(\boldsymbol{y}_l|U, \hat{H}=\hat{\boldsymbol{H}}, \tilde{H}=\tilde{\boldsymbol{H}})\big]\\
&= \max_{\boldsymbol{\Psi}\succeq 0:\mathrm{tr}(\boldsymbol{\Psi})\leq \mathsf{snr}} \mathbb{E}_{\tilde{H}}\big[\log\det\left(I + \boldsymbol{H}_m\boldsymbol{\Psi}\boldsymbol{H}_m^{\mathsf{H}}\right)\big] - \mu\, \mathbb{E}_{\tilde{H}}\big[\log\det\left(I + \boldsymbol{H}_l\boldsymbol{\Psi}\boldsymbol{H}_l^{\mathsf{H}}\right)\big] && (4.74)
\end{aligned}$$

for any $\mu \geq 1$. The next step is to upper bound the right hand side (RHS) of (4.74).

Next, let $\boldsymbol{\Psi} = \boldsymbol{V}\boldsymbol{\Lambda}\boldsymbol{V}^{\mathsf{H}}$ be the eigenvalue decomposition of the covariance matrix $\boldsymbol{\Psi}$ where $\boldsymbol{\Lambda}$ is a diagonal matrix and $\boldsymbol{V}$ is unitary. Note that it is without loss of generality to assume that all eigenvalues of $\boldsymbol{\Psi}$ are strictly positive, i.e., $\lambda_i(\boldsymbol{\Psi}) \geq c > 0$, $\forall i$, in the sense that

$$\begin{aligned}\log\det\left(I+\boldsymbol{H}\boldsymbol{\Psi}\boldsymbol{H}^{\mathsf{H}}\right) &\leq \log\det\left(I+\boldsymbol{H}(cI+\boldsymbol{\Psi})\boldsymbol{H}^{\mathsf{H}}\right)\\ &\leq \log\det\left(I+\boldsymbol{H}\boldsymbol{\Psi}\boldsymbol{H}^{\mathsf{H}}\right)+\log\det\left(I+c\boldsymbol{H}\boldsymbol{H}^{\mathsf{H}}\right). \quad (4.75)\end{aligned}$$

In other words, a constant lift of the eigenvalues of $\boldsymbol{\Psi}$ does not have any impact on the high SNR behavior. This regularization will however simplify the analysis. The following is an upper bound for the first term in the RHS of (4.74).

$$\begin{aligned}&\mathbb{E}_{\tilde{H}}\Big[\log\det\big(I+\boldsymbol{H}_m\boldsymbol{\Psi}\boldsymbol{H}_m^{\mathsf{H}}\big)\Big]\\ &= \mathbb{E}_{\tilde{H}}\Big[\log\det\Big(I_M+\boldsymbol{\Psi}^{\frac{1}{2}}\boldsymbol{H}_m^{\mathsf{H}}\boldsymbol{H}_m\boldsymbol{\Psi}^{\frac{1}{2}}\Big)\Big] &(4.76)\\ &\leq \mathbb{E}_{\tilde{H}}\left[\log\det\left(I_M+\boldsymbol{\Psi}^{\frac{1}{2}}\boldsymbol{U}^H\begin{bmatrix}\|\boldsymbol{H}_m\|_F^2 I_{m'} & \\ & 0\end{bmatrix}\boldsymbol{U}\boldsymbol{\Psi}^{\frac{1}{2}}\right)\right] &(4.77)\\ &= \mathbb{E}_{\tilde{H}}\Big[\log\det\big(I_{m'}+\|\boldsymbol{H}_m\|_F^2\,\tilde{\boldsymbol{\Psi}}\big)\Big] &(4.78)\\ &= \mathbb{E}_{\tilde{H}}\Big[\log\det\big(\tilde{\boldsymbol{\Psi}}\big)\Big]+\mathbb{E}_{\tilde{H}}\Big[\log\det\big(\tilde{\boldsymbol{\Psi}}^{-1}+\|\boldsymbol{H}_m\|_F^2 I\big)\Big] &(4.79)\\ &\leq \sum_{i=1}^{m'}\log\lambda_i(\boldsymbol{\Psi})+\underbrace{\log\det\big((c^{-1}+m+\|\hat{\boldsymbol{H}}_m\|_F^2)I\big)}_{o(\log\mathsf{snr})} &(4.80)\\ &\leq \log\det(\boldsymbol{\Lambda})+o(\log\mathsf{snr}) &(4.81)\end{aligned}$$

where $\boldsymbol{\Psi}^{\frac{1}{2}}$ is such that $\left(\boldsymbol{\Psi}^{\frac{1}{2}}\right)^2=\boldsymbol{\Psi}$; (4.77) is due to fact that $\boldsymbol{H}_m^H\boldsymbol{H}_m \preceq \boldsymbol{U}^H\begin{bmatrix}\|\boldsymbol{H}_m\|_F^2 I_{m'} & \\ & 0\end{bmatrix}\boldsymbol{U}$ with $\boldsymbol{U}$ being the matrix of eigenvectors of $\boldsymbol{H}_m^H\boldsymbol{H}_m$ and $\|\boldsymbol{H}_m\|_F$ being the Frobenius norm of $\boldsymbol{H}_m$, where $m' \triangleq \min\{m, M\}$; in (4.78), we define $\tilde{\boldsymbol{\Psi}}$ as the $m'\times m'$ upper left block of $\boldsymbol{U}\boldsymbol{\Psi}\boldsymbol{U}^{\mathsf{H}}$; the first term in (4.80) is due to $\det(\tilde{\boldsymbol{\Psi}})=\prod_{i=1}^{m'}\lambda_i(\tilde{\boldsymbol{\Psi}}) \leq \prod_{i=1}^{m'}\lambda_i(\boldsymbol{U}\boldsymbol{\Psi}\boldsymbol{U}^H)=\prod_{i=1}^{m'}\lambda_i(\boldsymbol{\Psi})$; the second term in (4.80) is from Jensen's inequality and using the fact that $\boldsymbol{\Psi}^{-1}\preceq c^{-1}I_M$ by assumption and that $\mathbb{E}_{\tilde{H}}(\boldsymbol{H}_m^H\boldsymbol{H}_m)=\sum_{k=1}^{m}\sigma_k^2 I_M+\hat{\boldsymbol{H}}_m^H\hat{\boldsymbol{H}}_m \preceq mI+\hat{\boldsymbol{H}}_m^H\hat{\boldsymbol{H}}_m$; the last inequality is from the assumption that every eigenvalue of $\boldsymbol{\Psi}$ is lower-bounded by some constant $c>0$ independent of snr. Now, we need to lower bound the second expectation in the RHS of

(4.74). To this end, let us write

$$\begin{aligned}
\det\left(I_l + \boldsymbol{H}_l\boldsymbol{\Psi}\boldsymbol{H}_l^{\mathsf{H}}\right) &= \det\left(I_l + \boldsymbol{H}_l\boldsymbol{V}\boldsymbol{\Lambda}\boldsymbol{V}^{\mathsf{H}}\boldsymbol{H}_l^{\mathsf{H}}\right) && (4.82)\\
&= \det\left(I_M + \boldsymbol{\Lambda}\boldsymbol{V}^{\mathsf{H}}\boldsymbol{H}_l^{\mathsf{H}}\boldsymbol{H}_l\boldsymbol{V}\right) && (4.83)\\
&= \det\left(I_M + \boldsymbol{\Lambda}\boldsymbol{\Phi}^{\mathsf{H}}\boldsymbol{\Sigma}^2\boldsymbol{\Phi}\right) && (4.84)\\
&= 1 + \sum_{\substack{\mathcal{I}\subseteq\{1,\ldots,M\}\\ \mathcal{I}\neq\emptyset}} \det(\boldsymbol{\Lambda}_{\mathcal{I}\mathcal{I}})\det(\boldsymbol{\Phi}_{\mathcal{I}}^{\mathsf{H}}\boldsymbol{\Sigma}^2\boldsymbol{\Phi}_{\mathcal{I}}) && (4.85)\\
&\geq \det(\boldsymbol{\Sigma}^2)\sum_{j=1}^{M}\det(\boldsymbol{\Lambda}_{\mathcal{I}_j\mathcal{I}_j})\det(\boldsymbol{\Phi}_{\mathcal{I}_j}^{\mathsf{H}}\boldsymbol{\Phi}_{\mathcal{I}_j}) && (4.86)\\
&\geq M\det(\boldsymbol{\Sigma}^2)\left(\prod_{j=1}^{M}\left(\det(\boldsymbol{\Lambda}_{\mathcal{I}_j\mathcal{I}_j})\det(\boldsymbol{\Phi}_{\mathcal{I}_j}^{\mathsf{H}}\boldsymbol{\Phi}_{\mathcal{I}_j})\right)\right)^{\frac{1}{M}} && (4.87)\\
&= M\det(\boldsymbol{\Sigma}^2)\det(\boldsymbol{\Lambda})^{\frac{l}{M}}\left(\prod_{j=1}^{M}\det(\boldsymbol{\Phi}_{\mathcal{I}_j}^{\mathsf{H}}\boldsymbol{\Phi}_{\mathcal{I}_j})\right)^{\frac{1}{M}} && (4.88)
\end{aligned}$$

where (4.83) is an application of the identity $\det(I+\boldsymbol{A}\boldsymbol{B}) = \det(I+\boldsymbol{B}\boldsymbol{A})$; in (4.84), we define

$$\boldsymbol{\Sigma} \triangleq \mathrm{diag}(\sigma_1,\ldots,\sigma_l),\ \boldsymbol{\Phi} \triangleq \boldsymbol{\Sigma}^{-1}\boldsymbol{H}_l\boldsymbol{V},\ \text{and}\ \hat{\boldsymbol{\Phi}} \triangleq \boldsymbol{\Sigma}^{-1}\hat{\boldsymbol{H}}_l\boldsymbol{V};$$

in (4.85), we define $\boldsymbol{\Phi}_{\mathcal{I}} \triangleq [\Phi_{ji}:\ j=1,\ldots,l,\ i\in\mathcal{I}] \in \mathbb{C}^{l\times|\mathcal{I}|}$ as the submatrix of $\boldsymbol{\Phi}$ with columns indexed in $\mathcal{I}$ and $\boldsymbol{\Lambda}_{\mathcal{I}\mathcal{I}} = [\Lambda_{ji}:\ i,j\in\mathcal{I}] \in \mathbb{C}^{|\mathcal{I}|\times|\mathcal{I}|}$, with $\mathcal{I}$ denoting a nonempty set; the equality (4.85) is an application of the identity [54]

$$\det(I+\boldsymbol{A}) = 1 + \sum_{\substack{\mathcal{I}\subseteq\{1,\ldots,M\}\\ \mathcal{I}\neq\emptyset}}\det(\boldsymbol{A}_{\mathcal{I}\mathcal{I}})$$

for any $\boldsymbol{A}\in\mathbb{C}^{M\times M}$; in (4.86), we define $\mathcal{I}_1,\ldots,\mathcal{I}_M$ as the so-called sliding window of indices

$$\mathcal{I}_1 \triangleq \{1,2,\cdots,l\},\ \mathcal{I}_2 \triangleq \{2,3,\cdots,l,l+1\},\ \cdots,\ \mathcal{I}_M \triangleq \{M,1,2,\cdots,l-1\} \tag{4.89}$$

$$\text{i.e.,}\ \mathcal{I}_j \triangleq \{\mathrm{mod}(j+i-1)_M+1:\ i=0,1,\cdots,l-1\},\ j=1,2,\cdots,M \tag{4.90}$$

with $\mathrm{mod}(x)_M$ being the modulo operator; (4.87) is from the fact that arithmetic mean is not smaller than geometric mean; in (4.88), we use the fact that $\prod_{j=1}^{M}\det(\boldsymbol{\Lambda}_{\mathcal{I}_j\mathcal{I}_j}) = \det(\boldsymbol{\Lambda})^l$.

Without loss of generality, we assume that the M columns of $\boldsymbol{H}_l\boldsymbol{V}$ are ordered in such a way that 1) the first l columns are linearly independent, i.e., $\hat{\boldsymbol{\Phi}}_{\mathcal{I}_1}$ has full rank, and 2) $\boldsymbol{A} = \hat{\boldsymbol{\Phi}}_{\mathcal{I}_1}$ satisfies Lemma 6. Note that the

former condition can almost always be satisfied since $\text{rank}(\hat{\mathbf{\Phi}}) = l$ almost surely. Hence, we have

$$\mathbb{E}_{\tilde{H}}\big[\log\det(\mathbf{\Phi}_{\mathcal{I}_j}^{\mathsf{H}}\mathbf{\Phi}_{\mathcal{I}_j})\big] = \sum_{i=1}^{\text{rank}(\hat{\mathbf{\Phi}}_{\mathcal{I}_j})} \log\big(\lambda_i(\hat{\mathbf{\Phi}}_{\mathcal{I}_j}^{\mathsf{H}}\hat{\mathbf{\Phi}}_{\mathcal{I}_j})\big) + o(\log \mathsf{snr}) \tag{4.91}$$

$$\geq \sum_{i=1}^{\text{rank}(\hat{\mathbf{\Phi}}_{\mathcal{I}_j \bigcap \mathcal{I}_1})} \log\big(\lambda_i(\hat{\mathbf{\Phi}}_{\mathcal{I}_j}^{\mathsf{H}}\hat{\mathbf{\Phi}}_{\mathcal{I}_j})\big) + o(\log \mathsf{snr}) \tag{4.92}$$

$$\geq \sum_{i=1}^{\text{rank}(\hat{\mathbf{\Phi}}_{\mathcal{I}_j \bigcap \mathcal{I}_1})} \log\big(\lambda_i(\hat{\mathbf{\Phi}}_{\mathcal{I}_j \bigcap \mathcal{I}_1}^{\mathsf{H}}\hat{\mathbf{\Phi}}_{\mathcal{I}_j \bigcap \mathcal{I}_1})\big) + o(\log \mathsf{snr}) \tag{4.93}$$

$$= \log\det(\hat{\mathbf{\Phi}}_{\mathcal{I}_j \bigcap \mathcal{I}_1}^{\mathsf{H}}\hat{\mathbf{\Phi}}_{\mathcal{I}_j \bigcap \mathcal{I}_1}) + o(\log \mathsf{snr}) \tag{4.94}$$

$$\geq \log \prod_{i \in \mathcal{I}_j \bigcap \mathcal{I}_1} \lambda_i(\hat{\mathbf{\Phi}}^{\mathsf{H}}\hat{\mathbf{\Phi}}) + o(\log \mathsf{snr}) \tag{4.95}$$

where (4.91) is from Lemma 4 by noticing that $\mathbf{\Phi}_{\mathcal{I}_j} = \hat{\mathbf{\Phi}}_{\mathcal{I}_j} + \tilde{\mathbf{\Phi}}_{\mathcal{I}_j}$ with the entries of $\tilde{\mathbf{\Phi}}_{\mathcal{I}_j} \triangleq \mathbf{\Sigma}^{-1}\tilde{\boldsymbol{H}}_l\boldsymbol{V}$ being i.i.d. $\mathcal{N}_c(0,1)$; (4.92) is from the fact that $\text{rank}(\hat{\mathbf{\Phi}}_{\mathcal{I}_j}) \geq \text{rank}(\hat{\mathbf{\Phi}}_{\mathcal{I}_j \bigcap \mathcal{I}_1})$; (4.93) is due to $\lambda_i(\hat{\mathbf{\Phi}}_{\mathcal{I}_j}^{\mathsf{H}}\hat{\mathbf{\Phi}}_{\mathcal{I}_j}) \geq \lambda_i(\hat{\mathbf{\Phi}}_{\mathcal{I}_j \bigcap \mathcal{I}_1}^{\mathsf{H}}\hat{\mathbf{\Phi}}_{\mathcal{I}_j \bigcap \mathcal{I}_1})$ where we recall that $\lambda_i(\boldsymbol{A}^{\mathsf{H}}\boldsymbol{A})$ is defined as the i th largest eigenvalue of $\boldsymbol{A}^{\mathsf{H}}\boldsymbol{A}$; and the last inequality is due to Lemma 6. Summing over all j, we have

$$\sum_{j=1}^{M} \mathbb{E}_{\tilde{H}}\big[\log\det(\mathbf{\Phi}_{\mathcal{I}_j}^{\mathsf{H}}\mathbf{\Phi}_{\mathcal{I}_j})\big] \geq \log\left(\prod_{j=1}^{M}\prod_{i \in \mathcal{I}_j \bigcap \mathcal{I}_1} \lambda_i(\hat{\mathbf{\Phi}}^{\mathsf{H}}\hat{\mathbf{\Phi}})\right) + o(\log \mathsf{snr}) \tag{4.96}$$

$$= \log\left(\left(\prod_{i \in \mathcal{I}_1} \lambda_i(\hat{\mathbf{\Phi}}^{\mathsf{H}}\hat{\mathbf{\Phi}})\right)^{l}\right) + o(\log \mathsf{snr}) \tag{4.97}$$

$$\geq l \log \prod_{i \in \mathcal{I}_1} \lambda_i(\hat{\mathbf{\Phi}}_{\mathcal{I}_1}^{\mathsf{H}}\hat{\mathbf{\Phi}}_{\mathcal{I}_1}) + o(\log \mathsf{snr}) \tag{4.98}$$

$$= l \log\det\left(\hat{\mathbf{\Phi}}_{\mathcal{I}_1}^{\mathsf{H}}\hat{\mathbf{\Phi}}_{\mathcal{I}_1}\right) + o(\log \mathsf{snr}) \tag{4.99}$$

$$= -l \log\det\left(\mathbf{\Sigma}^2\right) + o(\log \mathsf{snr}) \tag{4.100}$$

where (4.98) is due to $\lambda_i(\hat{\mathbf{\Phi}}^{\mathsf{H}}\hat{\mathbf{\Phi}}) \geq \lambda_i(\hat{\mathbf{\Phi}}_{\mathcal{I}_1}^{\mathsf{H}}\hat{\mathbf{\Phi}}_{\mathcal{I}_1})$, $\forall\, i = 1, \ldots, l$; the last equality is from the fact that $\hat{\mathbf{\Phi}}_{\mathcal{I}_1} = \mathbf{\Sigma}^{-1}\hat{\boldsymbol{H}}_l\boldsymbol{V}_{\mathcal{I}_1}$ and that $\hat{\boldsymbol{H}}_l\boldsymbol{V}_{\mathcal{I}_1}$ has full rank by construction. From (4.88) and (4.100), we obtain

$$\mathbb{E}_{\tilde{H}}\big[\log\det\left(I_l + \boldsymbol{H}_l\mathbf{\Psi}\boldsymbol{H}_l^{\mathsf{H}}\right)\big] \geq \frac{l}{M}\log\det(\mathbf{\Lambda}) + \frac{M-l}{M}\log\det(\mathbf{\Sigma}^2) + o(\log \mathsf{snr}) \tag{4.101}$$

and finally

$$\mathbb{E}_{\tilde{H}}\left[\log\det\left(I_m + \boldsymbol{H}_m\boldsymbol{\Psi}\boldsymbol{H}_m^{\mathsf{H}}\right)\right] - \frac{M}{l}\mathbb{E}_{\tilde{H}}\left[\log\det\left(I_l + \boldsymbol{H}_l\boldsymbol{\Psi}\boldsymbol{H}_l^{\mathsf{H}}\right)\right] \leq -\frac{M-l}{l}\log\det(\boldsymbol{\Sigma}^2) + o(\log\mathsf{snr}). \quad (4.102)$$

When $m < M$, the above bound (4.102) is not tight. However, we can show that, in this case, (4.102) still holds when we replace M with m. To see this, let us define $\boldsymbol{\Lambda}' \triangleq \mathrm{diag}(\lambda_1, \ldots, \lambda_m)$. First, note that when $m < M$, (4.81) holds if we replace $\boldsymbol{\Lambda}$ with $\boldsymbol{\Lambda}'$ on the RHS. Then, the RHS of (4.82) becomes a lower bound if we replace $\boldsymbol{\Lambda}$ with $\boldsymbol{\Lambda}'$ and $\boldsymbol{V}$ with $\boldsymbol{V}' \in \mathbb{C}^{M\times m}$, the first m columns of $\boldsymbol{V}$. From then on, every step holds with M replaced by m. (4.102) thus follows with M replaced by m. By taking the expectation on both sides of (4.102) over $\hat{\boldsymbol{H}}$ and plugging it into (4.73), we complete the proof of (4.17).

Chapter 5

On the Imperfect Global CSIR and Diversity Aspects

In this chapter we consider further aspects on the communications with imperfect, limited and delayed feedback.

The first focus in this chapter is placed on the aspect of having imperfect global CSIR, i.e., with imperfect receiver estimates of the channel of the other receiver, in the communication with limited feedback. It is motivated by the challenge of distributing global CSIR across the different receiving nodes, in addition to the challenge of communicating CSIT, over the resource links with limited capacity and limited reliability (cf. [35], [36]). Our work studies the multiple-input multiple-output (MIMO) broadcast channel (BC) communicating with imperfect delayed CSIT and with imperfect global CSIR, and proceeds to present schemes and degrees-of-freedom (DoF) bounds that are often tight, and to constructively reveal that even substantially imperfect delayed CSIT and imperfect global CSIR, are in fact sufficient to achieve the optimal DoF performance previously associated to perfect delayed CSIT and perfect global CSIR.

The second focus in this chapter is placed on the diversity aspect of the communication with delayed CSIT. Note that, most of the works considering communications with delayed CSIT, e.g., the works in [4–7,10,11,19–23], just focus on the DoF aspect. Besides the DoF aspect, another aspect so called *diversity* ([34]), corresponding to the characterizaiton of the communication reliability, is also very important for those delayed CSIT communication scenarios. Our work proposes a novel broadcast scheme which, over broadcast channel with delayed CSIT, employs a form of interference alignment to achieve both full DoF as well as full diversity.

5.1 On the Imperfect Global CSIR Aspect

5.1.1 Introduction

We here consider the two-user (M, N) multiple-input multiple-output (MIMO) broadcast channel (BC), where a M-antenna transmitter communicates information to two N-antenna receivers. In this setting, the channel model takes the form

$$\boldsymbol{y}_t^{(1)} = \boldsymbol{H}_t^{(1)}\boldsymbol{x}_t + \boldsymbol{z}_t^{(1)} \tag{5.1}$$

$$\boldsymbol{y}_t^{(2)} = \boldsymbol{H}_t^{(2)}\boldsymbol{x}_t + \boldsymbol{z}_t^{(2)} \tag{5.2}$$

where matrices $\boldsymbol{H}_t^{(1)}, \boldsymbol{H}^{(2)} \in \mathbb{C}^{N\times M}$ represent the transmitter-to-user 1 and the transmitter-to-user 2 channels respectively at time t, where $\boldsymbol{z}_t^{(1)}, \boldsymbol{z}_t^{(2)}$ represent unit power AWGN noise vectors at the two receivers, where $\boldsymbol{x}_t \in \mathbb{C}^{M\times 1}$ is the input signal vector at time t with power constraint $\mathbb{E}[||\boldsymbol{x}_t||^2] \leq P$, and where in this case, P also takes the role of the signal-to-noise ratio (SNR). In this work we assume that the elements of the channel matrices $\boldsymbol{H}_t^{(1)}$ and $\boldsymbol{H}_t^{(2)}$, are spatially and temporally i.i.d. Gaussian random variables, with zero mean and unit variance.

With channel state information at the transmitter (CSIT) being a crucial ingredient that facilitates improved performance, and with CSIT often being limited, imperfect and delayed, we here explore the effects of the *quality of delayed CSIT*, corresponding to how well the transmitter knows the channel $\boldsymbol{H}_t^{(1)}$ (resp. $\boldsymbol{H}_t^{(2)}$) after this channel state has fully changed. Naturally, reduced CSIT quality relates to limitations in the capacity and reliability of the feedback links. Similar issues, which additionally motivate this work, and which are addressed here, pertain to the *quality of delayed global CSIR*, i.e., to the quality of the estimates, at a given receiver, of the channel of the other receiver (see for example the work of [35], [36] on the challenge of obtaining such global CSIR).

5.1.2 Related work

It is well known that in the two-user (M, N) MIMO BC setting of interest, the presence of perfect CSIT allows for the optimal sum degrees-of-freedom (DoF) $\min\{M, 2N\}$ (this is with perfect global CSIR, cf. [1]), whereas the complete absence of CSIT causes a substantial degradation to just $\min\{M, N\}$ (cf. [3]) [1].

An interesting scheme that mitigates this degradation by utilizing partial CSIT knowledge, was recently presented in [4] by Maddah-Ali and Tse, which

1. We remind the reader that for an achievable rate pair (R_1, R_2), the corresponding DoF pair (d_1, d_2) is given by $d_i = \lim_{P\to\infty} \frac{R_i}{\log P},\ i = 1, 2$. The corresponding DoF region is then the set of all achievable DoF pairs.

showed that in the absence of current CSIT, delayed CSIT knowledge can still be useful in improving the DoF region of the multiple-input single-output (MISO) broadcast channel ($N = 1$). This result was later generalized by Vaze and Varanasi in [19] to the MIMO case (again, this is with perfect global CSIR). [2]

Our work extends the work in [19], and studies the general case of communicating with imperfect delayed CSIT and imperfect global CSIR. Specifically this work reveals that even substantially imperfect delayed-CSIT and imperfect global CSIR, are in fact sufficient to achieve the optimal DoF performance previously associated to perfect delayed CSIT and perfect global CSIR.

5.1.3 Quantification of CSI and CSIR quality

In this work we will consider the case without any current CSIT, but with imperfect delayed CSIT. In terms of delayed CSIT, we consider the case where the transmitter's (best) delayed estimates $\check{\boldsymbol{H}}_t^{(1)}, \check{\boldsymbol{H}}_t^{(2)}$ of channels $\boldsymbol{H}_t^{(1)}, \boldsymbol{H}_t^{(2)}$ come with estimation errors

$$\ddot{\boldsymbol{H}}_t^{(1)} = \boldsymbol{H}_t^{(1)} - \check{\boldsymbol{H}}_t^{(1)}, \quad \ddot{\boldsymbol{H}}_t^{(2)} = \boldsymbol{H}_t^{(2)} - \check{\boldsymbol{H}}_t^{(2)} \tag{5.3}$$

having independent and identically distributed (i.i.d.) Gaussian entries with power

$$\mathbb{E}[||\ddot{\boldsymbol{H}}_t||_F^2] \doteq \mathbb{E}[||\ddot{\boldsymbol{G}}_t||_F^2] \doteq P^{-\beta}$$

for some CSI quality exponent β describing the general quality of the delayed estimates. Without loss of generality, here we assume that the delayed estimates $\check{\boldsymbol{H}}_t^{(1)}, \check{\boldsymbol{H}}_t^{(2)}$ of channels $\boldsymbol{H}_t^{(1)}, \boldsymbol{H}_t^{(2)}$ become known to the transmitter with unit coherence delay, i.e., $\check{\boldsymbol{H}}_t^{(1)}, \check{\boldsymbol{H}}_t^{(2)}$ are available at time $(t+1)$.

In this setting, an increasing exponent β implies an improved delayed CSIT quality, with $\beta = 0$ implying very little delayed CSIT knowledge, and with $\beta = \infty$ implying perfect delayed CSIT.

In addition to the challenge of communicating CSIT over feedback channels with limited capacity and limited reliability, another known bottleneck is the non-negligible cost of distributing global CSIR across the different receiving nodes (see [35], [36]). For this reason, we explore the case where, in addition to limited and imperfect CSIT, we also have the additional imperfection of the global CSIR, which means that each user has imperfect estimates of the other user's channel, as well as, in this case, no access to

2. Other interesting works in the context of utilizing delayed and current CSIT, can be found in [6–8] which explored the setting of combining perfect delayed CSIT with immediately available imperfect CSIT, the work in [9] which additionally considered the effects of the quality of delayed CSIT for the MISO BC, the work in [48] which considered delayed and progressively evolving (progressively improving) current CSIT, and the works in [11, 21, 23] and many other publications.

the estimates of the transmitter. In the spirit of communicating global CSIR across feedback links ([35]) we also focus on the associated case of having imperfect delayed global CSIR corresponding to the same quality exponent β, and additionally having no receiver access to the CSIT estimates of the transmitter. With $\check{\check{\boldsymbol{H}}}_t^{(1)}$ denoting the delayed estimate of $\boldsymbol{H}_t^{(1)}$ at user 2, and $\check{\check{\boldsymbol{H}}}_t^{(2)}$ denoting the delayed estimate of $\boldsymbol{H}_t^{(2)}$ at user 1, we maintain as before that $\check{\check{\boldsymbol{H}}}_t^{(1)}, \check{\check{\boldsymbol{H}}}_t^{(2)}$ are available at time $(t+1)$, and that the estimation errors

$$\ddot{\boldsymbol{H}}_t^{(1)} = \boldsymbol{H}_t^{(1)} - \check{\check{\boldsymbol{H}}}_t^{(1)}, \quad \ddot{\boldsymbol{H}}_t^{(2)} = \boldsymbol{H}_t^{(2)} - \check{\check{\boldsymbol{H}}}_t^{(2)} \tag{5.4}$$

have i.i.d. Gaussian entries with power

$$\mathbb{E}[||\ddot{\boldsymbol{H}}_t^{(1)}||_F^2] \doteq \mathbb{E}[||\ddot{\boldsymbol{H}}_t^{(2)}||_F^2] \doteq P^{-\beta}$$

again for the same β as before, now also describing the quality of the global CSIR delayed estimates.

Remark 7. *We here note that without loss of generality, we can restrict our attention to the range* $0 \leq \beta \leq 1$ *(cf. [17]), where again* $\beta = 1$ *corresponds the case of perfect delayed CSIT.*

5.1.4 Conventions and structure

In Section 5.1.5, for the aforementioned two user MIMO BC, and for the general case of imperfect delayed CSIT and imperfect global-CSIR, we derive a DoF region inner bound, which turns out to be tight for any $\beta \geq \frac{N}{\min(M,2N)+N}$ previously associated to perfect delayed CSIT and perfect global-CSIR. Section 5.1.6 then presents the novel multi-phase precoding schemes associated to the aforementioned DoF regions.

Finally adhering to the common convention, we consider a unit coherence period, as well as assume that each receiver knows perfectly its own channel (perfect local CSIR).

5.1.5 DoF of the MIMO BC with Imperfect Delayed CSIT and Imperfect global-CSIR

It is noted that, for the case with $M \leq N$, the DoF region is characterized as $d_1 + d_2 \leq M$, which is achievable by TDMA scheme without any CSIT and without any global-CSIR. Thus in the following, we focus on the case with $M > N$.

Theorem 7. *For the* $(M > N, N)$ *MIMO BC with imperfect delayed CSIT and imperfect global-CSIR, the optimal DoF region takes the form*

$$\frac{d_1}{\min\{M,N\}} + \frac{d_2}{\min\{M,2N\}} \leq 1$$
$$\frac{d_2}{\min\{M,N\}} + \frac{d_1}{\min\{M,2N\}} \leq 1$$

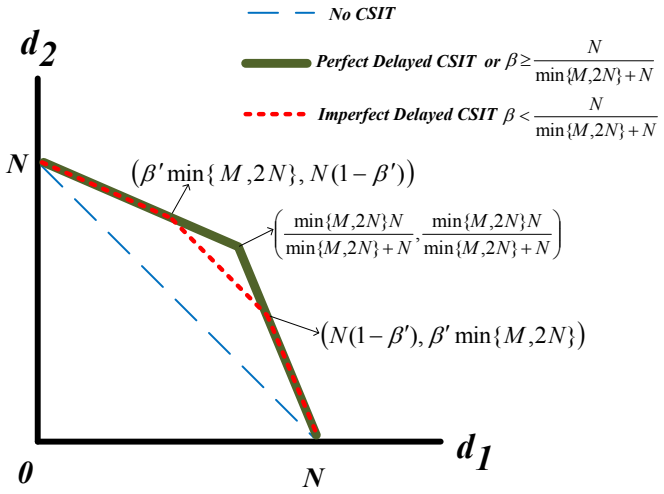

FIGURE 5.1 – DoF region of MIMO BC with imperfect delayed CSIT and imperfect global-CSIR ($M > N$).

when $\beta \geq \frac{N}{\min(M,2N)+N}$, *while when* $\beta < \frac{N}{\min(M,2N)+N}$ *this region is inner bounded by the achievable region*

$$\frac{d_1}{\min\{M,N\}} + \frac{d_2}{\min\{M,2N\}} \leq 1$$
$$\frac{d_2}{\min\{M,N\}} + \frac{d_1}{\min\{M,2N\}} \leq 1$$
$$d_1 + d_2 \leq \min\{M,N\} + \beta(\min\{M,2N\} - \min\{M,N\})$$

which, for $\beta' \triangleq \min\{\beta, \frac{N}{\min(M,2N)+N}\}$, *takes the form of a polygon with corner points* $\{(0,0),(0,N),(\min\{M,2N\}\beta', N(1-\beta')), (N(1-\beta'), \min\{M,2N\}\beta'), (N,0)\}$.

At this point we can draw an interesting conclusion on the amount of delayed CSIT and global CSIR needed to achieve a certain symmetric DoF performance d'. For all the cases considered here, the derived threshold value $\beta^* \triangleq \arg\min_\beta\{d(\beta) = d'\}$, accepts the simple form of

$$\beta^* = (d' - d(0))/(d(1) - d(0)) \tag{5.5}$$

describing the fraction of the DoF gap - between the no-CSIT-and-no-global-CSIR case and the perfect-delayed-CSIT-and-perfect-global-CSIR case - that is covered to reach d'.

As an example of this derived threshold quality, we see that for the case of the MIMO case with $N < M < 2N$, the target optimal $d' = d_1^* = MN/(M+N)$ (cf. [19]) corresponds to the aforementioned

$$\beta^* = \frac{d' - d(0)}{d(1) - d(0)} = \frac{MN/(M+N) - N/2}{M/2 - N/2} = \frac{N}{M+N}.$$

5.1.6 Schemes for MIMO BC with imperfect delayed CSIT and imperfect global CSIR

It is noted that in Chapter 3, a novel scheme has been proposed for the setting with imperfect CSIT but with perfect global CSIR. Here we proceed to describe a modified scheme that achieves the corresponding DoF corner points, and does so with imperfect delayed CSIT and imperfect global CSIR. In this specific setting, the encoding of this modified scheme is similar to the encoding of the previous general scheme in Chapter 3, by setting specific parameters for this setting, while the decoding here is lightly different from the decoding of the previous scheme, i.e., imperfect delayed global CSIR is sufficient for the decoding in this modified scheme. For

$$\beta^{'} \triangleq \min\{\beta, \frac{N}{\min(M, 2N) + N}\} \tag{5.6}$$

this modified scheme will achieve DoF corner points

$$E = (\min\{M, 2N\}\beta^{'}, N(1-\beta^{'})), \quad F = (N(1-\beta^{'}), \min\{M, 2N\}\beta^{'}) \tag{5.7}$$

both of which converge to the optimal DoF point

$$C = (\frac{\min\{M, 2N\}N}{\min\{M, 2N\} + N}, \frac{\min\{M, 2N\}N}{\min\{M, 2N\} + N})$$

when $\beta \geq \frac{N}{\min(M,2N)+N}$, recalling that we focus on the case with $M > N$. It is noted that, DoF corner point $(\min\{M, N\}, 0)$ and point $(0, \min\{M, N\})$ are easily achievable by single-user transmission scheme without any CSIT and without any global CSIR.

As in Chapter 3, the scheme has a forward-backward phase-Markov structure which, in the context of imperfect and delayed CSIT, was first introduced in [8, 9] to consist of four main ingredients that include

- block-Markov encoding
- spatial precoding
- interference quantization
- backward decoding.

In the scheme, the accumulated quantized interference bits of phase s can be broadcasted to both users inside the common information symbols of the next phase (phase $(s + 1)$), while also a certain amount of common information can be transmitted to both users during phase s, which will then help resolve the accumulated interference of phase $(s - 1)$.

As in Chapter 3, the scheme has infinite communication duration n, and in this setting each phase has one channel use.

Encoding

We first describe the encoding for $t = 1, 2, \cdots, n-1$ except the last channel use ($t = n$) which will be addressed separately due to its different structure.

Zero forcing and superposition coding At time $t = 1, 2, \cdots, n-1$, the transmitter sends

$$\boldsymbol{x}_t = \boldsymbol{c}_t + \boldsymbol{a}_t + \boldsymbol{b}_t \tag{5.8}$$

where $\boldsymbol{a}_t \in \mathbb{C}^{M\times 1}$ is a symbol vector meant for receiver 1, $\boldsymbol{b}_t \in \mathbb{C}^{M\times 1}$ is meant for receiver 2, where $\boldsymbol{c}_t \in \mathbb{C}^{M\times 1}$ is a common symbol vector.

Power and rate allocation For this setting, in order to achieve the DoF corner point E and point F (cf. (5.7)), the powers and (normalized) rates at time-slot t are set as

$$\begin{array}{ll} P_t^{(\boldsymbol{c})} \doteq P, & r_t^{(c)} = (N - (M-N)\beta') \\ P_t^{(\boldsymbol{a})} \doteq P^{\beta'}, & r_t^{(\boldsymbol{a})} = M\beta' \\ P_t^{(\boldsymbol{b})} \doteq P^{\beta'}, & r_t^{(\boldsymbol{b})} = M\beta'. \end{array} \tag{5.9}$$

where β' is defined in (5.6), where $P_t^{(\boldsymbol{e})} \triangleq \mathbb{E}|\boldsymbol{e}_t|^2$ denotes the power of a symbol vector $\boldsymbol{e}_t$ corresponding to time-slot t, and where $r_t^{(\boldsymbol{e})}$ denotes the prelog factor of the number of bits $r_t^{(\boldsymbol{e})} \log P - o(\log P)$ carried by symbol vector $\boldsymbol{e}_t$ at time t.

To put the above allocation in perspective, we show the received signals, and describe under each term the order of the summand's average power. These signals take the form

$$\boldsymbol{y}_t^{(1)} = \underbrace{\boldsymbol{H}_t^{(1)}\boldsymbol{c}_t}_{P} + \underbrace{\boldsymbol{H}_t^{(1)}\boldsymbol{a}_t}_{P^{\beta'}} + \underbrace{\overbrace{\check{\boldsymbol{H}}_t^{(1)}\boldsymbol{b}_t}^{\check{\iota}_t^{(1)}}}_{P^{\beta'}} + \underbrace{\overbrace{\ddot{\boldsymbol{H}}_t^{(1)}\boldsymbol{b}_t}^{\iota_t^{(1)}-\check{\iota}_t^{(1)}}}_{P^{\beta'-\beta}\leq P^0} + \underbrace{\boldsymbol{z}_t^{(1)}}_{P^0} \tag{5.10}$$

$$\boldsymbol{y}_t^{(2)} = \underbrace{\boldsymbol{H}_t^{(2)}\boldsymbol{c}_t}_{P} + \underbrace{\boldsymbol{H}_t^{(2)}\boldsymbol{b}_t}_{P^{\beta'}} + \underbrace{\overbrace{\check{\boldsymbol{H}}_t^{(2)}\boldsymbol{a}_t}^{\check{\iota}_t^{(2)}}}_{P^{\beta'}} + \underbrace{\overbrace{\ddot{\boldsymbol{H}}_t^{(2)}\boldsymbol{a}_t}^{\iota_t^{(2)}-\check{\iota}_t^{(2)}}}_{P^{\beta'-\beta}\leq P^0} + \underbrace{\boldsymbol{z}_t^{(2)}}_{P^0} \tag{5.11}$$

where

$$\iota_t^{(1)} \triangleq \boldsymbol{H}_t^{(1)}\boldsymbol{b}_t,\ \iota_t^{(2)} \triangleq \boldsymbol{H}_t^{(2)}\boldsymbol{a}_t \tag{5.12}$$

denote the interference at receiver 1 and receiver 2 respectively, and where

$$\check{\iota}_t^{(1)} \triangleq \check{\boldsymbol{H}}_t^{(1)}\boldsymbol{b}_t,\ \check{\iota}_t^{(2)} \triangleq \check{\boldsymbol{H}}_t^{(2)}\boldsymbol{a}_t \tag{5.13}$$

denote the transmitter's delayed estimates of $\iota_t^{(1)}, \iota_t^{(2)}$.

TABLE 5.1 – Number of bits carried by private and common symbols, and by the quantized interference (time t).

	Total bits ($\times \log P$)
Private symbols for user 1	$M\beta'$
Private symbols for user 2	$M\beta'$
Common symbols	$T(N-(M-N)\beta')$
Quantized interference	$2N\beta'$

Quantizing and broadcasting the accumulated interference Before the beginning of next phase (time $(t+1)$), the transmitter reconstructs $\check{\iota}_t^{(1)}, \check{\iota}_t^{(2)}$, using its knowledge of delayed CSIT, and quantizes these into

$$\bar{\tilde{\iota}}_t^{(1)} = \check{\iota}_t^{(1)} - \tilde{\iota}_t^{(1)}, \quad \bar{\tilde{\iota}}_t^{(2)} = \check{\iota}_t^{(2)} - \tilde{\iota}_t^{(2)} \tag{5.14}$$

using a total of $N\beta' \log P$ and $N\beta' \log P$ quantization bits respectively. This allows for bounded power of quantization noise $\tilde{\iota}_t^{(1)}, \tilde{\iota}_t^{(2)}$, i.e, allows for $\mathbb{E}|\tilde{\iota}_t^{(2)}|^2 \doteq \mathbb{E}|\tilde{\iota}_t^{(1)}|^2 \doteq 1$, since $\mathbb{E}|\check{\iota}_t^{(2)}|^2 \doteq P^{\beta'}$, $\mathbb{E}|\check{\iota}_t^{(1)}|^2 \doteq P^{\beta'}$ (cf. [39]). Then the transmitter evenly splits the

$$2N\beta' \log P$$

quantization bits into the common symbols $\boldsymbol{c}_{t+1}$ that will be transmitted during the next phase (at time $(t+1)$), and which will convey these quantization bits together with other new information bits for the receivers. These $\boldsymbol{c}_{t+1}$ will help the receivers cancel interference, as well as will serve as extra observations that will allow for decoding of all private information (see Table 5.1).

Finally, for the last phase at time $t = n$, the main target will be to recover the information on the interference accumulated in phase $(t-1)$. For large n, this last phase can focus entirely on transmitting common symbols.

This concludes the part of encoding, and we now move to decoding.

Decoding

As in Chapter 3, in accordance to the phase-Markov structure, we consider decoding that moves backwards, from the last to the first phase. The last phase (at time n) was specifically designed to allow decoding of the common symbols $\boldsymbol{c}_n$. Hence we focus on the rest of the phases, to see how - with knowledge of common symbols from the next phase - we can go back one phase and decode its symbols.

During phase t (at time t), each receiver uses $\boldsymbol{c}_{t+1}$ to reconstruct the delayed estimates $\{\bar{\tilde{\iota}}_t^{(2)}, \bar{\tilde{\iota}}_t^{(1)}\}$, to remove - up to noise level - all the interference

$\iota_t^{(i)}$, by subtracting the delayed interference estimates $\bar{\bar{\iota}}_t^{(i)}$ from $\boldsymbol{y}_t^{(i)}$, for $i = 1, 2$.

Now given $\bar{\bar{\iota}}_t^{(2)}, \bar{\bar{\iota}}_t^{(1)}$, receiver 1 combines $\bar{\bar{\iota}}_t^{(2)}$ with $(\boldsymbol{y}_t^{(1)} - \bar{\bar{\iota}}_t^{(1)})$ to decode $\boldsymbol{c}_t$ and $\boldsymbol{a}_t$ of phase t. This is achieved by decoding over a MIMO multiple-access channel (MIMO MAC) of the general form

$$\begin{bmatrix} \boldsymbol{y}_t^{(1)} - \bar{\bar{\iota}}_t^{(1)} \\ \bar{\bar{\iota}}_t^{(2)} \end{bmatrix} = \begin{bmatrix} \boldsymbol{H}_t^{(1)} \\ \boldsymbol{0} \end{bmatrix} \boldsymbol{c}_t + \begin{bmatrix} \boldsymbol{H}_t^{(1)} \\ \breve{\boldsymbol{H}}_t^{(2)} \end{bmatrix} \boldsymbol{a}_t + \begin{bmatrix} \tilde{\boldsymbol{z}}_t^{(1)} \\ \tilde{\boldsymbol{z}}_t^{'(2)} \end{bmatrix} \tag{5.15}$$

where

$$\tilde{\boldsymbol{z}}_t^{(1)} = \ddot{\boldsymbol{H}}_t^{(1)} \boldsymbol{b}_t + \boldsymbol{z}_t^{(1)} + \tilde{\iota}_t^{(1)}$$

and

$$\tilde{\boldsymbol{z}}_t^{'(2)} = (\ddot{\boldsymbol{H}}_t^{(2)} - \ddot{\boldsymbol{H}}_t^{(2)}) \boldsymbol{a}_t - \tilde{\iota}_t^{(2)}$$

and where $\mathbb{E}|\tilde{\boldsymbol{z}}_t^{(1)}|^2 \doteq \mathbb{E}|\tilde{\boldsymbol{z}}_t^{'(2)}|^2 \doteq 1$. It can be readily shown (cf. [39]) that optimal decoding in such a MIMO MAC setting - doing so with *imperfect global CSIR* $\breve{\boldsymbol{H}}_t^{(2)}$ - allows user 1 to achieve the aforementioned rates in (5.9), i.e., allows for decoding of $\boldsymbol{a}_t$ with $r_t^{(\boldsymbol{a})} = M\beta'$ and of $\boldsymbol{c}_t$ with $r_t^{(\boldsymbol{c})} = (N - (M-N)\beta')$, Similarly receiver 2 can construct a similar MIMO MAC, which will again allow for decoding of its own private and common symbols at the aforementioned rates in (5.9).

Now the decoders shift to phase $(t-1)$ and use $\boldsymbol{c}_t$ to decode the common and private symbols of that phase. Decoding stops after decoding of the symbols in phase 1.

It is noted that, the above construction in (5.15) is different from that in Chapter 3, and the construction in (5.15) allows us to handle the issue of the imperfection on global CSIR.

DoF calculation

We now describe, as in Chapter 3, how to regulate the scheme's parameters to achieve the DoF point E and point F (cf. (5.7)). The rate and power allocation in (5.9) tells us that, the total amount of information in the *private symbols* of a certain phase $t < n$, for user 1 is equal to $M\beta' \log P$ bits, while for user 2 this is also $M\beta' \log P$ bits (as shown in the table 5.1). Given the power and rate allocation in (5.9), it is guaranteed that the accumulated quantized interference in a phase $t < n$ has $2N\beta' \log P$ bits, which 'fit' into the common symbols of the next phase that can carry a total of $\big(N - (M-N)\beta'\big) \log P$ bits. This leaves an extra space of $\Delta_{\text{com}} \log P$ bits in the common symbols, where

$$\Delta_{\text{com}} \triangleq N - (M-N)\beta' - 2N\beta' = N - (M+N)\beta' \tag{5.16}$$

is guaranteed to be non-negative due to (5.9) and (5.6). This extra space can be split between the two users, by allocating $\omega\Delta_{\text{com}} \log P$ bits for the

message of user 1, and the remaining $(1-\omega)\Delta_{\text{com}} \log P$ bits for the message of user 2, for some $\omega \in [0,1]$.

Consequently, for large n, the scheme allows for DoF performance in the form

$$d_1 = M\beta^{'} + \omega\Delta_{\text{com}} = M\beta^{'} + \omega(N - (M+N)\beta^{'}) \tag{5.17}$$

$$d_2 = M\beta^{'} + (1-\omega)\Delta_{\text{com}} = M\beta^{'} + (1-\omega)(N - (M+N)\beta^{'}). \tag{5.18}$$

As a result, as in Chapter 3, setting $\omega = 0$ allows us to achieve the DoF corner point E, while setting $\omega = 1$ allows us to achieve the DoF corner point F, which completes the proof.

5.1.7 Conclusions

The work provided analysis and novel communication schemes for the setting of the two-user MIMO BC with imperfect delayed CSIT, as well as, in the presence of additional imperfections in the global CSIR. The derived DoF region is often optimal and, while corresponding to imperfect delayed CSIT and imperfect global CSIR, often matches the region previously associated to perfect delayed CSIT and perfect global CSIR. In addition to the theoretical limits and practical schemes, the work provided insight on how much delayed CSIT feedback and global CSIR feedback are necessary to achieve a certain target performance, offering possible advantages in the presence of feedback links with limited capacity and limited reliability.

5.2 Diversity

Maddah-Ali and Tse have recently shown that delayed transmitter channel state information (CSIT) can still be useful in increasing the degrees-of-freedom (DoF) over the MIMO broadcast channel. This was achieved by constructing a scheme that, in the presence of two transmit antennas, of two single-antenna receivers, and of CSIT that is delayed by one coherence time, manages to provide each user with 2/3 DoF, improving upon the 1/2 DoF corresponding to no CSIT. This same scheme though, as well as all subsequent pertinent schemes, achieve DoF gains by suppressing the inherent diversity of the broadcast parallel channel. The current work proposes a novel broadcast scheme which, over the above described setting of the delayed CSIT broadcast channel, employs a form of interference alignment to achieve both full DoF as well as full diversity.

5.2.1 Introduction

Many multiuser wireless communications settings are known to benefit greatly from the use of CSIT feedback. It is the case though that such feedback is often hard to obtain sufficiently fast, and as a result, efforts have been made to find ways to utilize delayed CSIT. One such case involves communication over the broadcast channel (BC), where recent advances by Maddah-Ali and Tse [4] have shown that stale CSIT can still allow for improvements in the channel's degrees-of-freedom (DoF) region. This same work in [4] developed a novel scheme that, in the specific setting of the multiple-input single-output (MISO) BC with 2 transmit antennas and 2 users each with a single receive antenna, can offer 2/3 DoF to each user, even when the CSIT is delayed by a coherence period.

While achieving the optimal DoF, this novel scheme, as well as subsequent pertinent techniques, neglect diversity considerations, thus resulting in substantial suboptimality with respect to diversity. This suboptimality naturally contributes to substantial performance degradation, and thus brings to the fore the need for novel designs that can combine the signal manipulations that allow for full diversity, with the signal manipulations that utilize stale CSIT to give full DoF. We here propose a novel design which employs interference alignment [55] techniques to provide, in the aforementioned two-user MISO BC with stale CSIT, full DoF and full diversity.

5.2.2 Outline

After describing the system model and briefly recalling the original MAT scheme, Section 5.2.5 describes the new DoF-optimal design, and Section 5.2.6 shows that the scheme achieves full diversity. As a side result, the interested reader can find in Appendix 5.2.8 an upper bound on the diversity-

multiplexing tradeoff (DMT) of the MAT scheme.

5.2.3 System model

As stated, we focus on the frequency-flat MISO BC with two transmit antennas and two users with a single receive antenna. We consider a coherence period of T_c channel uses, during which the channel remains the same. Specifically we consider communication over L coherence periods, or equivalently L phases, where each phase coincides with a coherence period. During phase l ($l = 1, \cdots, L$), the first user's channel is denoted as

$$\boldsymbol{h}_l = [h_{l,1}\ h_{l,2}]^{\mathsf{T}} \in \mathbb{C}^2$$

and the second user's as

$$\boldsymbol{g}_l = [g_{l,1}\ g_{l,2}]^{\mathsf{T}} \in \mathbb{C}^2.$$

For $\boldsymbol{x}_{l,t}$ denoting the transmitted signals during timeslot t of phase l, then the corresponding received signals at the first and second user respectively, take the form

$$y_{l,t}^{(1)} = \boldsymbol{h}_l^{\mathsf{T}} \boldsymbol{x}_{l,t} + z_{l,t}^{(1)}, \tag{5.19}$$

$$y_{l,t}^{(2)} = \boldsymbol{g}_l^{\mathsf{T}} \boldsymbol{x}_{l,t} + z_{l,t}^{(2)}, \tag{5.20}$$

($t = 1, 2, \cdots, T_c$), where $z_{l,t}^{(1)}, z_{l,t}^{(2)}$ denotes the AWGN noise. The fading coefficients are assumed to be i.i.d. circularly symmetric complex Gaussian $\mathbb{CN}(0,1)$ distributed, and are assumed to remain fixed during a phase and change independently from phase to phase. We let ρ denote the signal-to-noise ration (SNR), and we consider a short-term power constraint where $\mathbb{E}||\boldsymbol{x}^{\ell}(t)||^2 \leq \rho$. We also consider a communication rate of R bits per channel use, which is here taken to be the same for both users. We recall that the corresponding multiplexing gain (or equivalently DoF) takes the form

$$r = \lim_{\rho \to \infty} \frac{R_i}{\log \rho}$$

where r is also referred to as the multiplexing gain. Finally, for P_e denoting the probability that at least one user has decoded erroneously, we recall the notion of diversity to be

$$\mathbb{d} = -\lim_{\rho \to \infty} \frac{\log P_e}{\log \rho}$$

(cf. [34]).

Regarding knowledge of the channel state, we assume perfect channel state information at the receivers (perfect CSIR), but we only allow the transmitter perfect knowledge of CSIT with a delay of a single phase (single coherence time), and provide no knowledge of current CSIT.

We consider the minimum delay case where communication, just as in [4], takes place over $L = 3$ phases, and we note that naturally the achieved optimal DoF performance cannot further benefit from using $L > 3$ phases. The proposed design is presented here for simplicity only for the minimum phase-delay case ($L = 3$), for which it achieves the optimal diversity of 6 (3 coherence intervals, 2 transmit antennas). We note though that this design can be readily extended to the case where L is a multiple of 3, to again achieve the optimal diversity order of $2L$. We will henceforth consider that $L = 3$.

5.2.4 Original MAT scheme

The MAT scheme [4] applies irrespective of the coherence duration T_c, and it considers communication over $L = 3$ phases. Without consideration for the time index, in describing the scheme, we denote by $\{a_1, a_2\}$ the two symbols intended for the first user, and by $\{b_1, b_2\}$ the symbols for the second user. During the first, second and third phase, the transmitter sequentially sends $\boldsymbol{x}_1, \boldsymbol{x}_2, \boldsymbol{x}_3 \in \mathbb{C}^2$ where

$$\boldsymbol{x}_1 = \begin{bmatrix} a_1 \\ a_2 \end{bmatrix}, \ \boldsymbol{x}_2 = \begin{bmatrix} b_1 \\ b_2 \end{bmatrix}, \ \boldsymbol{x}_3 = \begin{bmatrix} \boldsymbol{h}_2^{\mathsf{T}}\boldsymbol{x}_2 + \boldsymbol{g}_1^{\mathsf{T}}\boldsymbol{x}_1 \\ 0 \end{bmatrix}. \tag{5.21}$$

Consequently the resulting input-output relationship seen by the first user, takes the form

$$\boldsymbol{y}^{(1)} = \begin{bmatrix} y_1^{(1)} \\ y_2^{(1)} \\ y_3^{(1)} \end{bmatrix} = \begin{bmatrix} \boldsymbol{h}_1^{\mathsf{T}} \\ \boldsymbol{0} \\ h_{3,1}\boldsymbol{g}_1^{\mathsf{T}} \end{bmatrix} \boldsymbol{x}_1 + \begin{bmatrix} \boldsymbol{0} \\ \boldsymbol{h}_2^{\mathsf{T}} \\ h_{3,1}\boldsymbol{h}_2^{\mathsf{T}} \end{bmatrix} \boldsymbol{x}_2 + \begin{bmatrix} z_1^{(1)} \\ z_2^{(1)} \\ z_3^{(1)} \end{bmatrix}$$

which is converted to the equivalent form

$$\breve{\boldsymbol{y}}^{(1)} \triangleq \begin{bmatrix} y_1^{(1)} \\ y_3^{(1)} - h_{3,1}y_2^{(1)} \end{bmatrix} = \breve{\boldsymbol{H}}\boldsymbol{x}_1 + \breve{\boldsymbol{z}}^{(1)}, \tag{5.22}$$

where

$$\breve{\boldsymbol{H}} = \begin{bmatrix} h_{1,1} & h_{1,2} \\ h_{3,1}g_{1,1} & h_{3,1}g_{1,2} \end{bmatrix}, \ \breve{\boldsymbol{z}}^{(1)} = \begin{bmatrix} z_1^{(1)} \\ z_3^{(1)} - h_{3,1}z_2^{(1)} \end{bmatrix}. \tag{5.23}$$

Noting that $\breve{\boldsymbol{H}}$ is almost surely of full rank, allows us to conclude that user 1 can achieve 2/3 DoF. Due to symmetry, the same holds for the second user.

Regarding the diversity of the MAT scheme, we have the following.

Proposition 7. *The MAT scheme gives diversity that is upper bounded by* 3.

This is shown in Appendix 5.2.8.

5.2.5 Interference alignment for achieving both full DoF and full diversity

We briefly note that the maximum achievable diversity that we can hope for is 6, simply because the transmitter has 2 antennas and because communication takes place over $L = 3$ statistically independent channel realizations ($L = 3$ phases).

The scheme applies to the case where the coherence period T_c is no less than 8. Without loss of generality, we will assume that $T_c = 8$, and that the entire coding duration is $LT_c = 24$ channel uses, spanning three different phases of 8 channel uses each. For $l = 1, \cdots, L,\ t = 1, \cdots, \frac{T_c}{2} = 4$, we denote by $\boldsymbol{x}_{l,2t-1}$ the vectors transmitted during odd timeslots of phase l (i.e., during timeslots $1, 3, 5, 7$ of phase l), and we denote by $\boldsymbol{x}_{l,2t}$ ($l = 1, \cdots, L,\ t = 1, \cdots, 4$) the vectors transmitted during even timeslots of phase l.

We assign 16 information symbols $\{a_{1,t}, a_{2,t}, a_{3,t}, a_{4,t}\}_{t=1}^{4}$ to the first user, and 16 symbols $\{b_{1,t}, b_{2,t}, b_{3,t}, b_{4,t}\}_{t=1}^{4}$ to the second user. Consequently for any given $t = 1, 2, 3, 4$, the transmitted signal vectors are designed as follows

$$\begin{aligned}
\boldsymbol{x}_{1,2t-1} =& [a_{1,t} + b_{1,t} \quad a_{3,t} + b_{3,t}]^{\mathsf{T}} \\
\boldsymbol{x}_{2,2t-1} =& \begin{bmatrix} \eta_3 \sum_{j=1}^{2} g_{1,j} a_{2j-1,t} + \eta_1 \sum_{j=1}^{2} h_{1,j} b_{2j-1,t} \\ 0 \end{bmatrix} \\
\boldsymbol{x}_{3,2t-1} =& \begin{bmatrix} \eta_4 \sum_{j=1}^{2} g_{1,j} a_{2j-1,t} + \eta_2 \sum_{j=1}^{2} h_{1,j} b_{2j-1,t} \\ 0 \end{bmatrix}
\end{aligned}$$

$$\begin{aligned}
\boldsymbol{x}_{1,2t} =& [a_{2,t} + b_{2,t} \quad a_{4,t} + b_{4,t}]^{\mathsf{T}} \\
\boldsymbol{x}_{2,2t} =& \begin{bmatrix} 0 \\ \eta_3 \sum_{j=1}^{2} g_{1,j} a_{2j,t} + \eta_1 \sum_{j=1}^{2} h_{1,j} b_{2j,t} \end{bmatrix} \\
\boldsymbol{x}_{3,2t} =& \begin{bmatrix} 0 \\ \eta_4 \sum_{j=1}^{2} g_{1,j} a_{2j,t} + \eta_2 \sum_{j=1}^{2} h_{1,j} b_{2j,t} \end{bmatrix}
\end{aligned} \tag{5.24}$$

where

$$\eta_i = \frac{1}{\phi_i + \sum_{j=1}^{2} |h_{1,j}|^2},\ i = 1, 2 \tag{5.25}$$

and

$$\eta_i = \frac{1}{\phi_i + \sum_{j=1}^{2} |g_{1,j}|^2},\ i = 3, 4, \tag{5.26}$$

for some positive constants $\{\phi_1, \phi_2, \phi_3, \phi_4\}$ that are specifically designed later on.

Due to symmetry, we can focus only on the first user. The received signals, accumulated at the first receiver, can be rearranged to take the form

$$\bar{\boldsymbol{y}}_t^{(1)} = \boldsymbol{H}_{AA} \boldsymbol{a}_t + \boldsymbol{H}_{AB} \boldsymbol{b}_t + \bar{\boldsymbol{z}}_t^{(1)},\ t = 1, \cdots, T_c/2, \tag{5.27}$$

where

$$\begin{aligned}
\bar{\boldsymbol{y}}_t^{(1)} &= \left[y_{1,2t-1}^{(1)}\ y_{2,2t-1}^{(1)}\ y_{3,2t-1}^{(1)}\ y_{1,2t}^{(1)}\ y_{2,2t}^{(1)}\ y_{3,2t}^{(1)}\right]^{\mathsf{T}} \\
\bar{\boldsymbol{z}}_t^{(1)} &= \left[z_{1,2t-1}^{(1)}\ z_{2,2t-1}^{(1)}\ z_{3,2t-1}^{(1)}\ z_{1,2t}^{(1)}\ z_{2,2t}^{(1)}\ z_{3,2t}^{(1)}\right]^{\mathsf{T}} \\
\boldsymbol{a}_t &= \left[a_{1,t}\ a_{3,t}\ a_{2,t}\ a_{4,t}\right]^{\mathsf{T}}, \\
\boldsymbol{b}_t &= \left[b_{1,t}\ b_{3,t}\ b_{2,t}\ b_{4,t}\right]^{\mathsf{T}},
\end{aligned} \tag{5.28}$$

and where

$$\boldsymbol{H}_{AA} = \begin{bmatrix}
h_{1,1} & h_{1,2} & 0 & 0 \\
h_{2,1}\eta_3 g_{1,1} & h_{2,1}\eta_3 g_{1,2} & 0 & 0 \\
h_{3,1}\eta_4 g_{1,1} & h_{3,1}\eta_4 g_{1,2} & 0 & 0 \\
0 & 0 & h_{1,1} & h_{1,2} \\
0 & 0 & h_{2,2}\eta_3 g_{1,1} & h_{2,2}\eta_3 g_{1,2} \\
0 & 0 & h_{3,2}\eta_4 g_{1,1} & h_{3,2}\eta_4 g_{1,2}
\end{bmatrix}$$

$$\boldsymbol{H}_{AB} = \begin{bmatrix}
h_{1,1} & h_{1,2} & 0 & 0 \\
h_{2,1}\eta_1 h_{1,1} & h_{2,1}\eta_1 h_{1,2} & 0 & 0 \\
h_{3,1}\eta_2 h_{1,1} & h_{3,1}\eta_2 h_{1,2} & 0 & 0 \\
0 & 0 & h_{1,1} & h_{1,2} \\
0 & 0 & h_{2,2}\eta_1 h_{1,1} & h_{2,2}\eta_1 h_{1,2} \\
0 & 0 & h_{3,2}\eta_2 h_{1,1} & h_{3,2}\eta_2 h_{1,2}
\end{bmatrix}.$$

Rewriting (5.27) we now get

$$\bar{\boldsymbol{y}}_t^{(1)} = \left[\boldsymbol{H}_{AA}\ \boldsymbol{H}_{AB}\right] \begin{bmatrix} \boldsymbol{a}_t \\ \boldsymbol{b}_t \end{bmatrix} + \bar{\boldsymbol{z}}_t^{(1)}. \tag{5.29}$$

Note that $\boldsymbol{H}_{AA} \in \mathbb{C}^{6\times 4}, \boldsymbol{H}_{AB} \in \mathbb{C}^{6\times 4}$, and that the rank of $[\boldsymbol{H}_{AA}\ \boldsymbol{H}_{AB}] \in \mathbb{C}^{6\times 8}$ can generally not support decoding of $[\boldsymbol{a}_t^{\mathsf{T}}\boldsymbol{b}_t^{\mathsf{T}}]^{\mathsf{T}} \in \mathbb{C}^8$. This problem is bypassed by the structure of the designed scheme which allows for aligning some of the interference at the first receiver (cf. Fig. 5.2), such that

$$\boldsymbol{H}_{AB}\boldsymbol{b}_t = \bar{\boldsymbol{H}}_{AB}\bar{\boldsymbol{b}}_t \tag{5.30}$$

where

$$\bar{\boldsymbol{H}}_{AB} = \begin{bmatrix}
h_{1,1} & 0 \\
h_{2,1}\eta_1 h_{1,1} & 0 \\
h_{3,1}\eta_2 h_{1,1} & 0 \\
0 & h_{1,1} \\
0 & h_{2,2}\eta_1 h_{1,1} \\
0 & h_{3,2}\eta_2 h_{1,1}
\end{bmatrix}, \quad \bar{\boldsymbol{b}}_t = \begin{bmatrix} b_{1,t} + \frac{h_{1,2}}{h_{1,1}} b_{3,t} \\ b_{2,t} + \frac{h_{1,2}}{h_{1,1}} b_{4,t} \end{bmatrix}.$$

Consequently we can rewrite (5.27) as

$$\bar{\boldsymbol{y}}_t^{(1)} = \bar{\boldsymbol{H}}_A \bar{\boldsymbol{x}}_t + \bar{\boldsymbol{z}}_t^{(1)}, \tag{5.31}$$

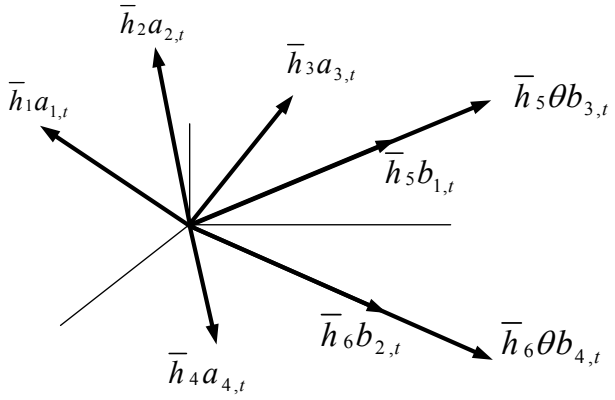

FIGURE 5.2 – Received signal space at user 1 after interference alignment. $\bar{\boldsymbol{h}}_i$ denotes the ith column of $\bar{\boldsymbol{H}}_A$, and $\theta = \frac{h_{1,2}}{h_{1,1}}$.

where

$$\bar{\boldsymbol{H}}_A = \left[\boldsymbol{H}_{AA}\ \bar{\boldsymbol{H}}_{AB}\right],\ \bar{\boldsymbol{x}}_t = \begin{bmatrix} \boldsymbol{a}_t \\ \bar{\boldsymbol{b}}_t \end{bmatrix}, \tag{5.32}$$

and where $\bar{\boldsymbol{H}}_A \in \mathbb{C}^{6\times 6}$, $\bar{\boldsymbol{x}}_A \in \mathbb{C}^6$.

At this point we randomly pick $\phi_1, \phi_2, \phi_3, \phi_4$ from the set of all possible numbers that guarantee

$$\frac{\eta_3}{\eta_4} \neq \frac{\eta_1}{\eta_2}$$

as well as guarantee that

$$\begin{aligned} \phi_3 \doteq \phi_4 &\doteq \max(|g_{1,1}|^2, |g_{1,2}|^2), \\ \phi_1 \doteq \phi_2 &\doteq \max(|h_{1,1}|^2, |h_{1,2}|^2). \end{aligned} \tag{5.33}$$

It is then easy to show that this random choice of $\phi_1, \phi_2, \phi_3, \phi_4$, while satisfying the power constraints, also guarantees that the rank of $\bar{\boldsymbol{H}}_A$ is full with probability 1. Simple zero-forcing (ZF) decoding guarantees the 2/3 DoF for both users.

5.2.6 Diversity analysis of the proposed scheme

We again focus, without loss of generality, on the first user, and consider joint ML decoding for the MAC channel corresponding to (5.31). We remind the reader that we are interested only in establishing the diversity of the scheme, i.e., we are interested in the case of $r = 0$ (R is fixed). Directly from [56] we know that the probability of error in this lightly loaded regime (cf. [56]) is dominated by the outage event

$$\mathcal{O} \triangleq \left\{ \bar{\boldsymbol{H}}_A : \frac{1}{6} I\left(\boldsymbol{a}_t; \bar{\boldsymbol{y}}_t^{(1)} | \bar{\boldsymbol{b}}_t, \bar{\boldsymbol{H}}_A\right) < R \right\}, \tag{5.34}$$

and as a result, the corresponding probability of error takes the form

$$\begin{aligned} P_e &\doteq Pr(\mathcal{O}) \\ &= Pr\left(\frac{1}{6} I(\boldsymbol{a}_t; \bar{\boldsymbol{y}}_t^{(1)} | \bar{\boldsymbol{b}}_t, \bar{\boldsymbol{H}}_A) < R\right) \\ &\doteq Pr\left(\frac{1}{6} \log\det(\mathbf{I} + \rho \boldsymbol{H}_{AA} \boldsymbol{H}_{AA}^{\mathsf{H}}) < R\right) \end{aligned}$$

where for the above we considered optimal Gaussian distributions for $\boldsymbol{a}_t$ and $\boldsymbol{b}_t$.

For

$$\boldsymbol{H}_{AA,j} = \begin{bmatrix} h_{1,1} & h_{1,2} \\ h_{2,j}\eta_3 g_{1,1} & h_{2,j}\eta_3 g_{1,2} \\ h_{3,j}\eta_4 g_{1,1} & h_{3,j}\eta_4 g_{1,2} \end{bmatrix}, \tag{5.35}$$

and

$$\Omega_j = \det\left(\mathbf{I} + \rho \boldsymbol{H}_{AA,j} \boldsymbol{H}_{AA,j}^{\mathsf{H}}\right), \text{ for } j = 1, 2, \tag{5.36}$$

and after considering that $\boldsymbol{H}_{AA}$ has a block-diagonal structure, we see that (5.35) implies that

$$P_e \doteq Pr(\log(\Omega_1 \Omega_2) < 6R). \tag{5.37}$$

Using the law of expansion of determinants by diagonal elements [54], and the Cauchy-Binet equation, we then have

$$\begin{aligned} \Omega_j = 1 + \sum_{n=1}^{2} \rho^n \sum_{\substack{J \subset \{1,2,3\} \\ |J|=n}} \sum_{\substack{S \subset \{1,2\} \\ |S|=n}} \det\left(([\boldsymbol{H}_{AA,j}]_{J,S})^{\mathsf{H}} [\boldsymbol{H}_{AA,j}]_{J,S}\right) \\ = 1 + \rho|h_{1,1}|^2 + \rho|h_{2,j}|^2|\eta_3|^2|g_{1,1}|^2 + \rho|h_{3,j}|^2|\eta_4|^2|g_{1,1}|^2 \\ + \rho|h_{1,2}|^2 + \rho|h_{2,j}|^2|\eta_3|^2|g_{1,2}|^2 + \rho|h_{3,j}|^2|\eta_4|^2|g_{1,2}|^2 \\ + \rho^2|h_{2,j}|^2|\eta_3|^2|h_{1,1}g_{1,2} - h_{1,2}g_{1,1}|^2 \\ + \rho^2|h_{3,j}|^2|\eta_4|^2|h_{1,1}g_{1,2} - h_{1,2}g_{1,1}|^2, \end{aligned}$$

where in the above, $[\mathbf{E}]_{J,S}$ denotes the submatrix of matrix $\mathbf{E}$ that includes the rows of $\mathbf{E}$ labeled by the elements of set J, and the columns labeled by the elements of set S. Continuing we get that

$$\begin{aligned} \Omega_j &\overset{(a)}{\doteq} 1 + \rho|h_{1,1}|^2 + \rho|h_{1,2}|^2 + \rho|h_{2,j}|^2 + \rho|h_{3,j}|^2 \\ &\quad + \rho^2(|h_{2,j}|^2 + |h_{3,j}|^2)|\eta_B|^2|h_{1,1}g_{1,2} - h_{1,2}g_{1,1}|^2 \\ &\geq 1 + \rho|h_{1,1}|^2 + \rho|h_{1,2}|^2 + \rho|h_{2,j}|^2 + \rho|h_{3,j}|^2 \end{aligned} \tag{5.38}$$

where in (a) we used that

$$\eta_A \triangleq \frac{1}{|h_{1,1}|^2+|h_{1,2}|^2}, \quad \eta_B \triangleq \frac{1}{|g_{1,1}|^2+|g_{1,2}|^2}, \tag{5.39}$$

and that (cf. (5.25),(5.33))

$$\eta_A \doteq \eta_1 \doteq \eta_2, \ \eta_B \doteq \eta_3 \doteq \eta_4.$$

Consequently (5.38) directly gives that

$$\begin{aligned} P_e \dot{\leq} Pr(\log(1+\rho|h_{1,1}|^2+\rho|h_{1,2}|^2+\rho|h_{2,1}|^2 \\ +\rho|h_{3,1}|^2+\rho|h_{2,2}|^2+\rho|h_{3,2}|^2) < 6R), \end{aligned}$$

which directly shows that the diversity of the scheme is 6 (again for $r = 0$). At this point we also note that the above design can be readily extended to the case where L is a multiple of 3. The proof for this is simple and it is omitted. The result is summarized in the following.

Proposition 8. *In the setting of the described two-user MISO BC with delayed CSIT, the proposed interference alignment based precoding scheme achieves full DoF and full diversity.*

5.2.7 Conclusions

In the setting of the two-user MISO broadcast channel with delayed CSIT, we designed the first scheme to achieve full DoF as well as full diversity. The scheme borrows from the techniques of interference alignment, which allow for combining the signal manipulations that increase the DoF with the signal manipulations that allow for full diversity. Future work can extend the result by analyzing the entire DMT behavior of the scheme, as well as extend the result to other BC settings.

5.2.8 Appendix - Proof of Proposition 7

In deriving the diversity achieved by the MAT scheme, we again focus, without loss of generality, on the performance of the first user.

From (5.22) we first recall that decoding is based on

$$\breve{\boldsymbol{y}}^{(1)} = \breve{\boldsymbol{H}}\boldsymbol{x}_1 + \breve{\boldsymbol{z}}^{(1)}.$$

Consequently, in the presence of Gaussian input $\boldsymbol{x}_1 = [a_1 \ a_2]^{\mathsf{T}}$ (cf. (5.21)), and noting that the noise term $\breve{\boldsymbol{z}}^{(1)}$ in (5.22) has zero mean and covariance

$$\mathbb{E}[\breve{\boldsymbol{z}}^{(1)}(\breve{\boldsymbol{z}}^{(1)})^{\mathsf{H}}] = \mathrm{diag}(\ 1\ ,\ 1+|h_{3,1}|^2),$$

we calculate the probability of outage to take the form

$$\begin{aligned} P_{\text{out}}(r) &= Pr\left(I(\boldsymbol{x}_1;\breve{\boldsymbol{y}}^{(1)}|\breve{\boldsymbol{H}}) < 3R\right) \qquad (5.40)\\ &\doteq Pr\left(\log\det(\mathbf{I}+\rho\breve{\boldsymbol{H}}\breve{\boldsymbol{H}}^{\mathsf{H}}) < 3R\right)\\ &= Pr(\log\Phi < 3r\log\rho), \qquad (5.41)\end{aligned}$$

where we used that

$$\Phi = \det\left(\mathbf{I}+\rho\breve{\boldsymbol{H}}\breve{\boldsymbol{H}}^{\mathsf{H}}\right),$$

and that

$$Pr(|h_{3,1}|^2 \geq \rho^{\epsilon}) = \exp(-\rho^{\epsilon}) \doteq 0,$$

for any positive ϵ. Consequently expanding the determinant and applying the Cauchy-Binet rule, gives

$$\begin{aligned}\Phi =& 1+\sum_{n=1}^{2}\rho^n \sum_{\substack{J\subset\{1,2\}\\|J|=n}}\sum_{\substack{S\subset\{1,2\}\\|S|=n}} \det\left([\breve{\boldsymbol{H}}]_{J,S}([\breve{\boldsymbol{H}}]_{J,S})^{\mathsf{H}}\right)\\ =& 1+\rho|h_{1,1}|^2+\rho|h_{1,2}|^2+\rho|h_{3,1}|^2|g_{1,1}|^2+\rho|h_{3,1}|^2|g_{1,2}|^2\\ &+\rho^2|h_{3,1}|^2|h_{1,1}g_{1,2}-h_{1,2}g_{1,1}|^2. \qquad (5.42)\end{aligned}$$

The fact that

$$\begin{aligned}|h_{1,1}g_{1,2}-h_{1,2}g_{1,1}|^2 \leq |h_{1,1}|^2|g_{1,2}|^2+|h_{1,2}|^2|g_{1,1}|^2\\ +2|h_{1,1}||g_{1,2}||h_{1,2}||g_{1,1}|,\end{aligned}$$

together with a change of variables where

$$h_{l,j} = \rho^{-\alpha_{l,j}}, \quad g_{l,j} = \rho^{-\beta_{l,j}},$$

and along with the fact that

$$Pr(\alpha_{l,j}) \doteq \begin{cases} \rho^{-\infty}, \text{ for } \alpha_{l,j} < 0 \\ \rho^{-\alpha_{l,j}}, \text{ for } \alpha_{l,j} \geq 0 \end{cases}, \qquad (5.43)$$

gives that the diversity $\mathtt{d}(r)$ of the MAT scheme is upper bounded as

$$\mathtt{d}(r) \leq \mathtt{d}_M(r) \triangleq \inf_{\mathcal{O}^M(r)} (\alpha_{1,1}+\alpha_{1,2}+\beta_{1,1}+\beta_{1,2}+\alpha_{3,1}) \qquad (5.44)$$

where

$$\mathcal{O}^M(r) = \left\{ \begin{array}{c} (1-\alpha_{1,1})^+ \leq 3r,\\ (1-\alpha_{1,2})^+ \leq 3r,\\ (1-\alpha_{3,1}-\beta_{1,1})^+ \leq 3r,\\ (1-\alpha_{3,1}-\beta_{1,2})^+ \leq 3r,\\ (2-\alpha_{3,1}-\alpha_{1,1}-\beta_{1,2})^+ \leq 3r,\\ (2-\alpha_{3,1}-\alpha_{1,2}-\beta_{1,1})^+ \leq 3r,\\ (2-\alpha_{3,1}-0.5\sum_{j=1}^{2}(\alpha_{1,j}+\beta_{1,j}))^+ \leq 3r \end{array} \right\}.$$

At this point it is easy to see that the diversity is upper bounded by 3 (see also Fig. 5.3). □

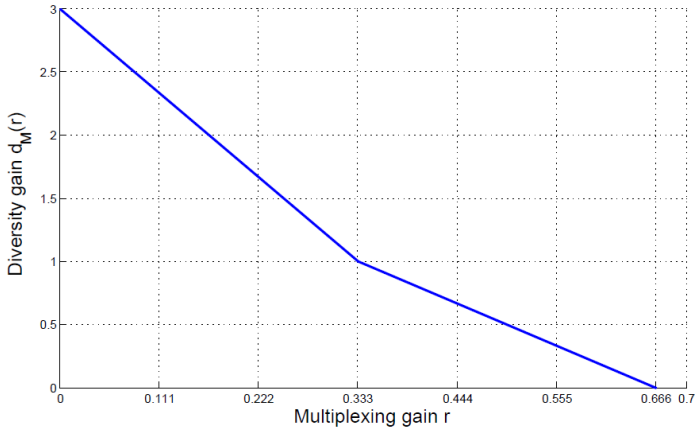

FIGURE 5.3 – DMT upper bound for the MAT scheme.

Chapter 6

Conclusions and Future Work

With a starting point that good feedback is crucial but hard and time-consuming to obtain, the main work in the thesis, sought to address the simple yet elusive and fundamental question of "HOW MUCH QUALITY of feedback, AND WHEN, must one send to achieve a certain performance in specific settings of multiuser communications".

The thesis first considered the two-user MISO BC, and made progress towards establishing and meeting the tradeoff between performance, and feedback timeliness and quality. Considering a general CSIT process, the work provided DoF expressions that are simple and insightful functions of easy to calculate parameters. The results - bounds and novel schemes- hold for a broad family of channel models spanning a large class of block fading and non-block fading channel models.

It also introduced the novel *periodically evolving feedback* setting over the quasi-static block fading channel, where a gradual accumulation of feedback bits results in a progressively increasing CSIT quality as time progresses across a finite coherence period. This powerful setting captures many of the engineering options relating to feedback, as well as captured many interesting settings previously considered.

The derived DoF expressions are a result of novel schemes and improved outer bounds. These derived expressions offer insight on practical questions on topics relating to how much feedback quality (delayed, current or predicted) allows for a certain DoF performance, relating to the usefulness of delayed feedback, the usefulness of predicted CSIT, the impact of imperfections in the quality of current and delayed CSIT, the impact of feedback timeliness and the effect of feedback delays, the interplay between timeliness and quality of feedback, and the benefit of having feedback symmetry by

employing comparable feedback links across users.

Interestingly, the above results can be extended to the two user MIMO BC and the two user MIMO IC, in the presence of feedback with evolving quality and timeliness. In addition to the progress towards describing the limits of using such imperfect and delayed feedback in MIMO settings, the work offers different insights that include the fact that, an increasing number of receive antennas can allow for reduced quality feedback, as well as that no CSIT is needed for the direct links in the IC.

Then, the work considered the general K-user MISO BC, and established inner and outer bounds on the tradeoff between DoF performance and CSIT feedback quality. For the general K-user BC with imperfect current CSIT, the work provided a novel outer bound on the DoF region, which naturally bridges the gap between the case of having no current CSIT and the case with full CSIT. In addition, the work characterized the minimum current CSIT feedback that is necessary for any point of the sum DoF, which is optimal for many cases.

A further work focused on the *global CSIR* aspect, and provided analysis and novel communication schemes for the two-user MIMO BC with imperfect delayed CSIT, as well as, in the presence of additional imperfections in the global CSIR. The derived DoF region is often optimal and, while corresponding to imperfect delayed CSIT and imperfect global CSIR, often matches the region previously associated to perfect delayed CSIT and perfect global CSIR.

Finally, the thesis focused on the *diversity* aspect of the communication with limited and delayed feedback. In the setting of two-user MISO BC with delayed CSIT, the first scheme was provided to achieve full DoF as well as full *diversity*. The scheme borrows from the techniques of interference alignment, which allow for combining the signal manipulations that increase the DoF gain and diversity gain.

In addition to the theoretical limits and novel encoders and decoders, the work provided interesting insights on many practical and fundamental questions. However, up to now a number of fundamental questions are still open, regarding to the communication scenarios with limited, imperfect and delayed feedback. For example, what is DoF region outer bound for the setting with low-quality delayed CSIT ? What is DoF region outer bound for the two-user MISO BC where, the transmitter has perfect and instantaneous CSIT for one user's channel, but never has CSIT for the other user's channel ? Moving to the other settings, such as the setting of X channel, and the settings with different topologies, what are the fundamental limits of communications with limited feedback ? Those are the interesting questions that will be explored in the future work.

Chapter 7

French Summary

Dans des nombreux scénarios de communication sans fil multi-utilisateurs, une bonne rétroaction est un ingrédient essentiel qui facilite l'amelioration des performances. Bien qu'étant utile, une rétroaction parfaite reste difficile et fastidieuse à obtenir. En considérant ce défi comme point de départ, les présents travaux cherchent à adresser la question simple et pourtant insaisissable et fondamentale suivante : " Quel niveau de qualité de la rétroaction doit-on rechercher, et à quel moment faut-il envoyer pour atteindre une certaine performance en degrés de liberté (DoF en anglais) avec des paramètres spécifiques de communications multi-utilisateurs".

L'accent est tout d'abord mis sur les communications à travers un canal de diffusion (BC en anglais) à deux utilisateurs, multi-entrées, unique sortie (MISO en anglais) avec informations imparfaites et retardées à l'émetteur de l'état du canal (CSIT en anglais), un paramètre pour lequel la présente thèse explore le compromis entre la performance et la rapidité et la qualité de la rétroaction. La présente étude considère un cadre général dans lequel la communication a lieu en présence d'un processus d'attenuation aléatoire, et en présence d'un processus de rétroaction qui, à tout moment, peut ou non fournir des estimations CSIT - d'une qualité arbitraire - pour toute réalisation passée, actuelle ou future du canal. Sous des hypothèses standard, dans cette thèse est dérivée la région DoF qui est optimale pour un large régime de qualité CSIT. Cette région capture de manière concise l'effet des corrélations de canaux, la qualité de la valeur prédite, la valeur courante et retardée du CSIT, et capture généralement l'effet de la qualité du CSIT fourni à n'importe quel moment, sur n'importe quel canal.

Les encadrements sont obtenus à l'aide de nouveaux schémas qui - dans le contexte de CSIT imparfait et retardé - sont présentés ici pour la première

fois, avec encodage et décodage sur structure de phase Markovienne. Les résultats sont validés pour une grande classe de modèles de canaux d'atténuation en bloc et non-bloc, et ils unifient et étendent de nombreuses tentatives antérieures de capture de l'effet de rétroaction imparfaite et retardée. Cette généralité permet également d'examiner de nouveaux paramètres pertinents, tels que la nouvelle technique de rétroaction à évolution périodique, où une accumulation progressive de bits de rétroaction améliore progressivement le CSIT avec le temps, ce dernier progressant à travers une période de cohérence finie.

Les résultats ci-dessus sont atteints dans le cas du MISO-BC à deux utilisateurs, et sont ensuite immédiatement étendus aux cas entrées multiples sorties multiples (MIMO) BC à deux utilisateurs et de canaux d'interférence MIMO (MIMO IC), encore une fois en présence de processus d'atténuation aléatoire, et en présence d'un processus de rétroaction qui, à tout moment, peut ou non fournir des estimations CSIT - d'une qualité arbitraire - pour toute réalisation passée, actuelle ou future du canal. Sous les hypothèses standard, et en présence de M antennes par émetteur et N antennes par récepteur, la région DoF, qui est optimale pour un large régime de qualité CSIT, est dérivée. En plus de présenter une avancée dans la description des limites d'utilisation de telles informations imparfaites et retardées dans les milieux MIMO, la presente étude propose différentes idées dont le fait qu'un nombre croissant d'antennes de réception peuvent causer la réduction de la qualité de la rétroaction, ainsi que le fait qu'aucun CSIT n'est requis pour les liens directs dans l'IC.

Dans un deuxieme temps, la thèse considère le cadre plus général de la chaîne de diffusion K-utilisateurs MISO, où un émetteur avec M antennes transmet des informations aux K utilisateurs à une seule antenne, et où, une nouvelle fois, la qualité et la rapidité du CSIT est imparfaite. Dans ce contexte multi-utilisateurs, la thèse établit des limites sur le compromis entre la performance du DoF et la qualité de la rétroaction CSIT. Plus précisément, elle fournit une nouvelle région de la borne externe DoF dans le cas general à K - utilisateurs MISO BC avec un CSIT à qualité imparfaite courante, ce qui naturellement comble le lien entre le cas sans CSIT courant (ou le CSIT est seulement retardé, ou sans CSIT) et le cas où l'on dispose d'un CSIT complet. Dans ce contexte, la présente étude caractérise alors la rétroaction CSIT à courant minimum nécessaire pour atteindre n'importe quel état de somme DoF. Cette caractérisation est optimale dans le cas où $M \geq K$, et le cas $M = 2, K = 3$.

Dans une autre perspective, l'étude considère également un autre aspect de la communication à rétroaction imparfaite et retardée : celui où une imperfection supplémentaire sur les estimations du récepteur sur le canal d'un autre récepteur (CSIR global) est présente, en plus de l' imperfection du CSIT. L'étude se concentre sur un canal de diffusion MIMO avec un CSIT de qualité donnée, imparfait et retardé, et un CSIR global imparfait et re-

tardé. Et des schémas, ainsi que des encadrements des DoFs, souvent précises, sont présentés. L'étude continue ensuite en révélant de manière constructive comment même des CSIT sensiblement imparfaits retardés et des CSIR globaux essentiellement imparfaits retardés sont en fait suffisants pour atteindre la performance optimale en DoF qui était précédemment associée au CSIT parfait retardé et au CSIR parfait global.

En s'aventurant plus loin encore, l'étude tient également compte de l'aspect diversité de la communication - entre deux utilisateurs MISO BC - avec CSIT retardé. Dans ce cadre, l'ouvrage propose un nouveau système de diffusion qui fait appel au CSIT retardé et à une forme d' alignement d'interférence pour obtenir à la fois le maximum DoF possible (2/3), ainsi qu'une diversité complète.

En plus de fournir des limites théoriques et des nouveaux encodeurs et décodeurs, l'étude s'applique à obtenir une meilleure comprehension sur des questions pratiques relatives à combien la qualité de rétroaction (différée, en cours ou prévue) influe sur les performances DoF. Sur des questions relatives à l'utilité de la rétroaction retardée, l'utilité du CSIT prédit, à l'impact des imperfections sur la qualité du CSIT courant et différé, l'impact de la rapidité de la rétroaction et l'effet des retards de rétroaction, l'avantage d'avoir de la symétrie dans la rétroaction en utilisant des liens de rétroaction comparables entre les utilisateurs, l'impact des imperfections sur la qualité des CSIR globaux. Finalement sur des questions relatives à la façon d'atteindre à la fois un DoF et une diversité complets.

7.1 Modèle Canal

Dans le cadre de scénarios de communication multi-utilisateurs (voir par exemple la figure 7.1 et la figure 7.2), nous allons examiner à entrées multiples et sortie unique canal de diffusion (MISO BC), multiple-input multiple-output BC (MIMO BC), ainsi comme canal MIMO interférence (MIMO IC).

7.1.1 MISO BC

Nous nous concentrons d'abord sur le canal de diffusion multi-utilisateur, avec un émetteur, et avec K utilisateurs, en présence d'imparfait et retardée évaluations de la CSIT.

Nous commençons avec deux-utilisateurs MISO BC où un émetteur communique à deux utilisateurs. $\boldsymbol{h}_t$ et $\boldsymbol{g}_t$ représentent ces canaux à l'instant t, pour la première et la deuxième utilisateur. $\boldsymbol{x}_t$ représentent le vecteur émis au moment t. Les signaux reçus correspondant à la première et deuxième

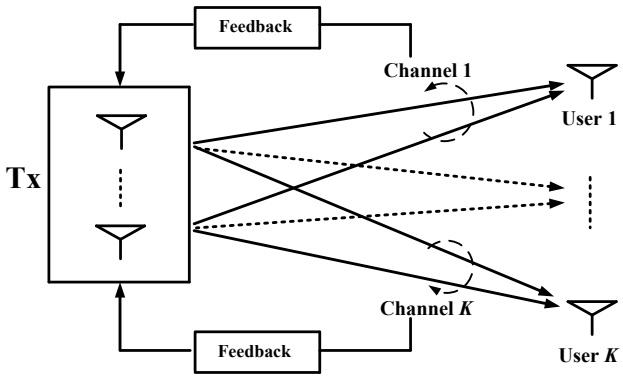

FIGURE 7.1 – Modèle de système de K-utilisateur MISO BC.

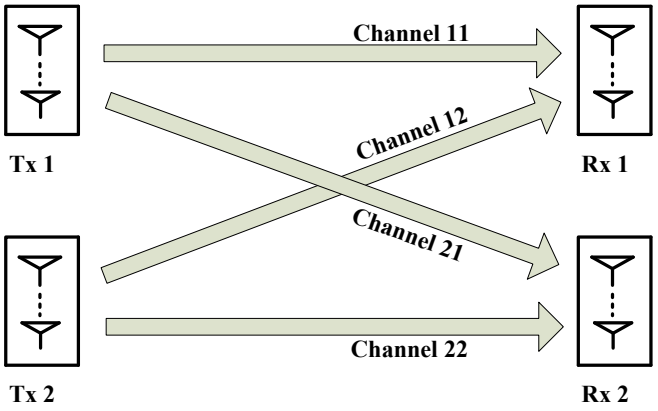

FIGURE 7.2 – Modèle de système de canal d'interfŕence de deux utilisateurs.

utilisateur prennent la forme

$$y_t^{(1)} = \boldsymbol{h}_t^{\mathsf{T}} \boldsymbol{x}_t + z_t^{(1)} \tag{7.1}$$

$$y_t^{(2)} = \boldsymbol{g}_t^{\mathsf{T}} \boldsymbol{x}_t + z_t^{(2)} \quad t = 1, 2, \cdots \tag{7.2}$$

$z_t^{(1)}, z_t^{(2)}$ sont le bruit AWGN, la puissance unitaire. Il existe une contrainte de puissance

$$\mathbb{E}[||\boldsymbol{x}_t||^2] \leq P = \rho$$

et P (ou ρ) prend le rôle du rapport signal-sur-bruit (SNR).

7.1.2 MIMO BC

Nous considérons également le MIMO BC. Dans ce cadre, le modèle canal prend la forme

$$\boldsymbol{y}_t^{(1)} = \boldsymbol{H}_t^{(1)}\boldsymbol{x}_t + \boldsymbol{z}_t^{(1)} \tag{7.3}$$
$$\boldsymbol{y}_t^{(2)} = \boldsymbol{H}_t^{(2)}\boldsymbol{x}_t + \boldsymbol{z}_t^{(2)} \tag{7.4}$$

$\boldsymbol{H}_t^{(1)} \in \mathbb{C}^{N\times M}, \boldsymbol{H}_t^{(2)} \in \mathbb{C}^{N\times M}$ représentent le premier et le deuxième canal du récepteur au temps t ; $\boldsymbol{z}_t^{(1)}, \boldsymbol{z}_t^{(2)}$ représentent le AWGN bruit, la puissance de l'unité ; $\boldsymbol{x}_t \in \mathbb{C}^{M\times 1}$ est le signal d'entrée, la contrainte de puissance $\mathbb{E}[||\boldsymbol{x}_t||^2] \leq P$.

7.1.3 MIMO IC

Nous considérons également le MIMO BC. Dans ce cadre, le modèle canal prend la forme

$$\boldsymbol{y}_t^{(1)} = \boldsymbol{H}_t^{(11)}\boldsymbol{x}_t^{(1)} + \boldsymbol{H}_t^{(12)}\boldsymbol{x}_t^{(2)} + \boldsymbol{z}_t^{(1)} \tag{7.5}$$
$$\boldsymbol{y}_t^{(2)} = \boldsymbol{H}_t^{(21)}\boldsymbol{x}_t^{(1)} + \boldsymbol{H}_t^{(22)}\boldsymbol{x}_t^{(2)} + \boldsymbol{z}_t^{(2)} \tag{7.6}$$

$\boldsymbol{H}_t^{(11)} \in \mathbb{C}^{N\times M}, \boldsymbol{H}_t^{(22)} \in \mathbb{C}^{N\times M}$ représentent les matrices de canal des liens directs, $\boldsymbol{H}_t^{(12)} \in \mathbb{C}^{N\times M}, \boldsymbol{H}_t^{(21)} \in \mathbb{C}^{N\times M}$ représentent les matrices de canal des liaisons transversales, au temps t.

7.2 Degrés de liberté

La thèse principale portera sur la performance degrés de liberté (DoF). Dans le régime de la haute-SNR, étant donné les taux réalisables

$$(R_1, R_2, \cdots, R_K)$$

le correspondant DoF est donnée par

$$d_i = \lim_{P\to\infty} \frac{R_i}{\log P},\ i = 1, 2, \cdots, K.$$

La région de la DoF $\mathcal{D}$ est l'ensemble de tous les DoF réalisable $(d_1, d_2, \cdots, d_K)$.

Lla analyse à haut SNR offre un bon aperçu de la performance au régime SNR modérée.

7.3 Effets et de qualité de retard de rétroaction

Comme dans de nombreux scénarios de communication sans fil multi-utilisateurs, la performance du canal de diffusion dépend de la rapidité et la qualité de la CSIT. Cette rapidité et la qualité peuvent être réduites par des liens de retour à capacité limitée, qui peuvent offrir une qualité d'évaluations basse, ou peut offrir des informations de bonne qualité qui vient si tard dans le processus de communication et peuvent donc être utilisés pour seulement une fraction de la durée de communication. La dégradation de performance correspondante, par rapport au cas de la rétroaction parfaite sans délai, la force de questions et de qualité de retard de la quantité d'informations qui est nécessaire, et lorsque, dans le but d'atteindre un certain rendement.

Ces effets et la qualité de retard de réaction, tombent naturellement entre les deux cas extrêmes de non CSIT et de plein CSIT (CSIT immédiatement disponible et parfait), avec CSIT complète permettant l'optimal 1 degrés de liberté par utilisateur (cf., [1]), tandis que l'absence de toute CSIT réduit ce nombre à seulement 1/2 DoF par l'utilisateur (cf., [2, 3]).

Un outil précieux en vue de combler cette lacune et de comprendre davantage les effets et la qualité de retard de réaction, est venu avec [4] montrant que les réactions retardées arbitrairement peut encore permettre l'amélioration des performances de l'affaire sans CSIT. Dans un cadre qui établit une distinction entre la CSIT courant et différé - CSIT tardive étant celle qui est disponible après l'écoulement du canal, soit après la fin de la période de cohérence correspondant à la voie décrite par cette réaction tardive, alors que CSIT actuelle correspondait aux commentaires reçus au cours de la période de la cohérence de la chaîne - le travail dans [4] a montré que parfait CSIT retardée, même sans CSIT actuel, permet une amélioration de 2/3 DoF par utilisateur.

Dans le même contexte de retard contre courant CSIT, le travail dans [5–8] a introduit des considérations de qualité de rétroaction, et a réussi à quantifier l'utilité de la combinaison parfaite CSIT retardé avec immédiatement disponible CSIT imparfait d'une certaine qualité qui est resté inchangé pendant toute la durée de la cohérence. Dans ce cadre les travaux ci-dessus montre un pont supplémentaire de l'écart de 2/3 à 1 DoF, en fonction de cette qualité CSIT actuel.

De nouveaux progrès est venu avec le travail dans [9] qui, en plus d'explorer les effets de la qualité de la CSIT actuel, également examiné les effets de la qualité de la CSIT retardée, permettant ainsi l'examen de la possibilité que l'ensemble nombre de bits de rétroaction (correspondant au retard en plus du courant CSIT) peut être réduite. Se concentrant à nouveau sur le réglage précis où la qualité de la CSIT courant est resté inchangé pour l'ensemble de la période de cohérence, ce travail a révélé entre autres que imparfaite CSIT retard peut atteindre le même optimalité qui a été précédemment attribué à perfectionner CSIT retard, donc équivalente montrant comment l'quantité

de feedback retard nécessaire, est proportionnelle à la quantité de retour de courant.

Une généralisation utile du paradigme de la CSIT retard par rapport courant, est venu avec le travail dans [10] qui s'écarte de l'hypothèse d'avoir la qualité de la CSIT invariant tout au long de la période de la cohérence, et a permis à la possibilité que CSIT courant peut être disponible uniquement après un certain retard, et en particulier seulement après une certaine fraction de la période de cohérence. Sous ces hypothèses, en présence de plus de deux utilisateurs, et en présence d'une parfaite CSIT retard, les travaux ci-dessus a montré que jusqu'à un certain retard, on peut atteindre la performance optimale correspondant à pleine CSIT (et immédiat).

Une autre généralisation intéressante est venu avec le travail dans [11] qui, pour le réglage de l'heure sélectif pour deux utilisateurs MISO BC, le CSIT pour le canal de l'utilisateur 1 et l'utilisateur 2, alterner entre les trois états extrêmes de la CSIT parfaite actuel, parfait CSIT retardé, et aucune CSIT.

Les paramètres ci-dessus, et de nombreux autres paramètres avec CSIT imparfait et retardée, comme ceux de [12, 13, 15–28, 48], a abordé différentes instances du problème plus général de la communication en présence de rétroaction avec des propriétés différentes et de qualité de retard, avec chacun de ces paramètres être motivé par le fait que CSIT parfaite peut être généralement difficile et fastidieux à obtenir, que la précision CSIT peut être améliorée au fil du temps, et que les retards de rétroaction et les imperfections coûte généralement en termes de performances. La généralisation ici pour la mise à CSIT imparfait, retardé et limité générale, intègre les considérations et motivations ci-dessus, et permet un aperçu sur les questions pertinentes telles que :

- Combien de qualité CSIT (retard, actuel ou prévu) permet une certaine performance DoF ?
- Imparfait CSIT retardé pouvez obtenir le même optimalité qui a été précédemment attribué à parfaite CSIT retard ?
- Quand est retardé commentaires inutiles ?
- On prévoit CSIT utile en termes de performances DoF ?
- Commentaires symétrique offre DoF peut bénéficier au cours de la réaction asymétrique ?
- Quel est l'impact du CSIR mondiale imparfaite (estimations de la réception imparfaites du canal de l'autre récepteur) ?
- Un système de communication permettant à la fois toute la diversité et la pleine DoF pour la mise à CSIT seulement retardé ?

7.4 Manche et processus de rétroaction

Ce travail se concentrera d'abord sur les deux - utilisateur MISO BC, et examinera la communication d'une durée infinie n (sauf avec l'argument spécifique), un processus de décoloration du canal aléatoire $\{\boldsymbol{h}_t, \boldsymbol{g}_t\}_{t=1}^n$ tirée d'une distribution statistique, et un processus de rétroaction qui fournit des estimations CSIT $\{\hat{\boldsymbol{h}}_{t,t'}, \hat{\boldsymbol{g}}_{t,t'}\}_{t,t'=1}^n$ (de canal $\boldsymbol{h}_t, \boldsymbol{g}_t$) en tout temps t' - avant, pendant ou après la matérialisation de $\boldsymbol{h}_t, \boldsymbol{g}_t$ au temps t - et le fait avec une certaine qualité

$$\{\mathbb{E}[||\boldsymbol{h}_t - \hat{\boldsymbol{h}}_{t,t'}||^2], \mathbb{E}[||\boldsymbol{g}_t - \hat{\boldsymbol{g}}_{t,t'}||^2]\}_{t,t'=1}^n.$$

7.5 Début, le courant et différé CSIT

Pour le canal $\boldsymbol{h}_t, \boldsymbol{g}_t$ au temps t, les estimations $\{\hat{\boldsymbol{h}}_{t,t}, \hat{\boldsymbol{g}}_{t,t}\}$, les estimations $\{\hat{\boldsymbol{h}}_{t,t'}, \hat{\boldsymbol{g}}_{t,t'}\}_{t'>t}$, et les estimations $\{\hat{\boldsymbol{h}}_{t,t'}, \hat{\boldsymbol{g}}_{t,t'}\}_{t'<t}$ forment ce que l'on peut décrire comme des estimations de la CSIT, les estimations de la CSIT retardés et les estimations de la CSIT début, respectivement. Contrairement à la CSIT estimations actuelles disponibles au moment de t, les estimations de la CSIT retardées sont disponibles au temps $t' > t$ en raison du retard, alors que les estimations de la CSIT premières sont disponibles au temps $t' < t$ attribué à la prédiction.

7.6 Exemples

Voici Prenons quelques exemples qui sont incorporés et pris en compte dans notre généralisation.

Example 16 (Envoi différé CSIT)**.** *Un des paramètre Incorporated est la CSIT retard (sans CSIT courant) de mise en [4]. étendue du réglage du CSIT retard dans [4], notre généralisation suit et révèle que imparfaite CSIT retard peut être aussi utile que parfait CSIT retardée.*

Example 17 (CSIT courant et différé Imperfect)**.** *Un des paramètre Incorporated est le réglage de la CSIT courant et différé imparfaite dans [6, 7].*

Example 18 (Asymmetric CSIT)**.** *Un des paramètre Incorporated est le réglage asymétrique de la CSIT dans [33], où les utilisateurs offerts parfait CSIT retard, mais où un seul utilisateur offert CSIT actuel parfait. Une telle asymétrie pourrait tenir compte des commentaires des liens avec des capacités différentes ou des retards différents.*

Example 19 (Not-so-retardé CSIT)**.** *Un des paramètre Incorporated est le réglage de la CSIT pas si retardé dans [10] correspond au canal à évanouissements par blocs avec retour périodique.*

Example 20 (Alternatif CSIT)**.** *Un des paramètre Incorporated est le réglage de la CSIT alternance dans [11] où alterne entre la CSIT parfait, retardée et ne CSIT Unis.*

Example 21 (Évolution CSIT)**.** *L'un des paramètre de nouveau considéré est le paramètre de rétroaction évolue périodiquement sur le canal avec évanouissement bloc quasi-statique, où une accumulation progressive des bits de rétroaction des résultats dans une qualité CSIT augmentant progressivement à mesure que le temps progresse à travers une période de cohérence finie. Ce paramètre puissant capte de nombreuses options d'ingénierie relatifs à la rétroaction, ainsi que capturé de nombreux paramètres intéressants considérés précédemment.*

7.7 Diversité

La thèse examine également l'aspect de la diversité de communiquer avec rétroaction limitée.

P_e est la probabilité d'erreur de la communication. La diversité est

$$\mathbb{d} = -\lim_{P\to\infty} \frac{\log P_e}{\log P}$$

(cf. [34]).

7.8 Global CSIR

En plus limitée CSIT, nous considérons également le Global CSIR limitée, chaque utilisateur dispose des estimations imparfaites de la chaîne de l'autre utilisateur.

7.9 Les contributions et les grandes lignes de la thèse

Comme indiqué précédemment, le principal travail de thèse vise à répondre à la question simple et pourtant insaisissable et fondamental de la "Combien qualité des commentaires, et quand faut-il envoyer pour atteindre un certain rendement dans des contextes spécifiques de communications multi-utilisateurs".

Dans le chapitre 2, le travail considère deux utilisateurs MISO BC avec CSIT imparfait et retardée, et explore le compromis entre la performance et la rétroaction rapidité et la qualité. Le travail estime un cadre large où la communication a lieu en présence d'un processus de décoloration aléatoire, et en présence d'un processus de rétroaction qui, à tout moment, peuvent ou non fournir des estimations CSIT - d'une certaine qualité arbitraire - pour tout

passé, la réalisation actuelle ou future canal. Sous les hypothèses habituelles, le travail vient de la région DoF, ce qui est optimal pour un grand régime de qualité CSIT. Cette région capte de manière concise l'effet des corrélations de canal, la qualité de la valeur prédite, le courant et différé CSIT, et capture généralement l'effet de la qualité de la CSIT offert à n'importe quel moment, sur n'importe quel canal. Les limites sont remplies avec de nouveaux régimes qui - dans le contexte de la CSIT imparfait et retardée - Introduire ici pour la première fois, l'encodage et le décodage d'une structure de phase Markov. Les résultats tiennent pour une large classe de bloc et modèles de canaux fading non - bloc, et qu'elles unifient et s'étendent de nombreuses tentatives antérieures pour capturer l'effet de rétroaction imparfait et retardée. Cette généralité permet également d'examiner les nouveaux paramètres pertinents, tels que le nouveau paramètre de rétroaction évoluer périodiquement, où une accumulation progressive de bits de rétroaction améliore progressivement CSIT que le temps progresse à travers une période de cohérence finie. Les résultats ont été publiés en partie à

- Jinyuan Chen and Petros Elia, "**Can Imperfect Delayed CSIT be as Useful as Perfect Delayed CSIT ? DoF Analysis and Constructions for the BC**", in *Proc. of 50th Annual Allerton Conf. Communication, Control and Computing (Allerton'12)*, October 2012.
- Jinyuan Chen and Petros Elia, "**Degrees-of-Freedom Region of the MISO Broadcast Channel with General Mixed-CSIT**", in *Proc. Information Theory and Applications Workshop (ITA'13)*, February 2013.
- Jinyuan Chen and Petros Elia, "**MISO Broadcast Channel with Delayed and Evolving CSIT**", in *Proc. IEEE Int. Symp. Information Theory (ISIT'13)*, July 2013.

et sera publié en partie à

- Jinyuan Chen and Petros Elia, "**Toward the Performance vs. Feedback Tradeoff for the Two-User MISO Broadcast Channel**", to appear in *IEEE Trans. Inf. Theory*, available on arXiv :1306.1751.
- Jinyuan Chen and Petros Elia, "**Optimal DoF Region of the Two-User MISO-BC with General Alternating CSIT**", to appear in *Proc. 47th Asilomar Conference on Signals, Systems and Computers (Asilomar'13)*, 2013, available on arXiv :1303.4352.

Dans le chapitre 3, étendant les résultats de réglage BC MISO deux utilisateurs, le travail explore la performance de l'utilisateur deux entrées multiples sorties multiples (MIMO) BC et les deux canal MIMO interférence de l'utilisateur (MIMO IC), en présence de rétroaction avec l'évolution qualité et la rapidité. Sous les hypothèses habituelles, et en présence de M antennes par émetteur et N antennes par récepteur, le travail vient de la région DoF, ce qui est optimal pour un grand régime de qualité CSIT. Cette région capte de manière concise l'effet d'avoir prédit, le courant et différé CSIT, ainsi que de façon concise capte l'effet de la qualité de la CSIT offert à n'importe quel

moment, sur n'importe quel canal. En plus de la progression vers décrivant les limites de l'utilisation de telles informations imparfait et retardée dans les milieux MIMO, l'ouvrage propose différentes idées qui incluent le fait que, un nombre croissant d'antennes de réception peuvent permettre de réduire la rétroaction de la qualité, ainsi que qu'aucune CSIT est nécessaire pour les liens directs dans l'IC. Les résultats ont été publiés en partie à

- Jinyuan Chen and Petros Elia, "**Symmetric Two-User MIMO BC and IC with Evolving Feedback**", June 2013, available on arXiv : 1306.3710.
- Jinyuan Chen and Petros Elia, "**MIMO BC with Imperfect and Delayed Channel State Information at the Transmitter and Receivers**", in *Proc. IEEE 14th Workshop on Signal Processing Advances in Wireless Communications (SPAWC'13)*, June 2013.

Dans le chapitre 4, le travail considère les K - utilisateur MISO BC, et établit des limites sur le compromis entre la performance et la qualité DoF de rétroaction CSIT. Plus précisément, pour le MISO BC général avec CSIT actuel imparfait, un roman DoF région externe lié est fourni, qui relie naturellement l'écart entre le cas de ne pas avoir CSIT actuelle et le cas de plein CSIT. Le travail caractérise alors le retour de la CSIT minimum qui est nécessaire pour n'importe quel point de la somme DoF, ce qui est optimal pour de nombreux cas. Les résultats seront publiés en partie à

- Jinyuan Chen, Sheng Yang, and Petros Elia, "**On the Fundamental Feedback-vs-Performance Tradeoff over the MISO-BC with Imperfect and Delayed CSIT**", in *Proc. IEEE Int. Symp. Information Theory (ISIT'13)*, July 2013.

Dans le chapitre 5, le travail considère en outre les autres aspects fondamentaux sur les communications avec les informations imparfait et retardée. Un autre travail est axé sur un canal de diffusion MIMO avec fixe de qualité imparfaite CSIT tardive et imparfaite CSIR global retardée (les estimations du récepteur de la chaîne de l'autre récepteur), et procède à des régimes actuels de géant DoF qui sont souvent serrés, et de manière constructive révéler comment voire sensiblement imparfaite CSIR retardée global retardée CSIT et essentiellement imparfait, sont en fait suffisante pour atteindre la performance optimale DoF précédemment associé à perfectionner CSIT retardée et CSIR global parfait. Encore d'autres études sur le travail de l'aspect de la diversité de la communication avec CSIT retardée. L'ouvrage propose un système de diffusion roman qui, sur le canal de diffusion avec CSIT retardée, emploie une forme d'alignement d'interférence pour obtenir à la fois DoF complet ainsi que toute leur diversité. Les résultats ont été publiés en partie à

- Jinyuan Chen, Raymond Knopp, and Petros Elia, "**Interference Alignment for Achieving both Full DoF and Full Diversity in the Broadcast Channel with Delayed CSIT**", in *Proc. IEEE Int. Symp. Information Theory (ISIT'12)*, July 2012.

– Jinyuan Chen and Petros Elia, "**MIMO BC with Imperfect and Delayed Channel State Information at the Transmitter and Receivers**", in *Proc. IEEE 14th Workshop on Signal Processing Advances in Wireless Communications (SPAWC'13)*, June 2013.

Chapitre 6 décrit enfin les conclusions et les travaux futurs.

En plus des limites théoriques et de nouveaux encodeurs et décodeurs, le travail s'applique à gagner idées sur des questions pratiques sur des sujets relatifs à combien la qualité de rétroaction (différée, en cours ou prévus) permet une certaine performance DoF, relative à l'utilité de la rétroaction retardée, l'utilité de la CSIT prévu, l'impact des imperfections dans la qualité de la CSIT courant et différé, l'impact des évaluations rapidité et l'effet des retards de rétroaction, l'avantage d'avoir des commentaires symétrie en utilisant les liens de rétroaction comparables entre les utilisateurs, l'impact des imperfections de la qualité des CSIR global relatif à la façon d'atteindre les deux DoF plein et la diversité.

En outre, dans additon aux résultats ci-dessus, certains autres résultats obtenus dans mon travail de thèse ont été publiés en partie à

– Jinyuan Chen, Petros Elia, and Raymond Knopp, "**Relay-Aided Interference Neutralization for the Multiuser Uplink-Downlink Asymmetric Setting**", in *Proc. IEEE Int. Symp. Information Theory (ISIT'12)*, July 2011.
– Jinyuan Chen, Arun Singh, Petros Elia and Raymond Knopp, "**Interference Neutralization for Separated Multiuser Uplink - Downlink with Distributed Relays**", in *Proc. Information Theory and Applications Workshop (ITA)*, February 2011.

7.10 Résumé du chapitre 2

7.10.1 Modèle canal

Dans ce chapitre, nous considérons les deux-utilisateur MISO BC avec un M-antenne d'émission ($M \geq 2$) émetteur communiqueant à deux utilisateurs reçevant avec une seule antenne de reception chacun. Le modèle de canal prend la forme de (2.1) et (2.2), ie,

$$y_t^{(1)} = \boldsymbol{h}_t^{\mathsf{T}} \boldsymbol{x}_t + z_t^{(1)}$$
$$y_t^{(2)} = \boldsymbol{g}_t^{\mathsf{T}} \boldsymbol{x}_t + z_t^{(2)}$$

où $\boldsymbol{h}_t, \boldsymbol{g}_t$ désigne le canal du premier et second utilisateur respectivement au temps t, et où $\boldsymbol{h}_t$ et $\boldsymbol{g}_t$ sont tirés d'une distribution aléatoire, de telle sorte que chacune a une moyenne nulle et de covariance d'identité (spatialement décorrélée), et de telle sorte que $\boldsymbol{h}_t$ est linéairement indépendant de $\boldsymbol{g}_t$ avec une probabilité.

7.10.2 Processus de canal et de feedback

Comme dans de nombreux scénarios de communication sans fil multi-utilisateurs, la performance du canal de diffusion dépend de la rapidité et de la qualité de l'information d'état de canal de l'émetteur (CSIT). Cette rapidité et qualité peuvent être réduites par des liens de feedback à capacité limitée, ce qui peut offrir un feedback avec toujours faible qualité et d'important retards, c'est à dire, le feedback qui offre une représentation inexacte de l'état réel du canal, comme feedback qui ne peut être utilisé pour une fraction suffisante de la durée de la communication. La dégradation de performance correspondante, par rapport au cas de feedback parfait sans délai, force la question de delai et de qualité de la quantité nécessaire de la qualité du feedback, dans le but d'atteindre un certain rendement.

Nous considérons ici la communication d'une durée infinie n, un processus de décoloration du canal $\{\boldsymbol{h}_t, \boldsymbol{g}_t\}_{t=1}^n$ tiré d'une distribution statistique, et un processus de feedback qui fournit des estimations de la CSIT $\{\hat{\boldsymbol{h}}_{t,t'}, \hat{\boldsymbol{g}}_{t,t'}\}_{t,t'=1}^n$ (du canal $\boldsymbol{h}_t, \boldsymbol{g}_t$) en tout temps t' - avant, pendant ou après la matérialisation de $\boldsymbol{h}_t, \boldsymbol{g}_t$ au temps t - et ce, avec une qualité définie par les statistiques de

$$\{(\boldsymbol{h}_t - \hat{\boldsymbol{h}}_{t,t'}), (\boldsymbol{g}_t - \hat{\boldsymbol{g}}_{t,t'})\}_{t,t'=1}^n \tag{7.7}$$

où l'on compte de ces erreurs d'estimation d'avoir de moyenne nulle circulairement symétriques d'entrées gaussiennes complexes.

7.10.3 Notation, conventions et hypothèses

Nous allons utiliser la notation

$$\alpha_t^{(1)} \triangleq -\lim_{P\to\infty} \frac{\log \mathbb{E}[||\boldsymbol{h}_t - \hat{\boldsymbol{h}}_{t,t}||^2]}{\log P} \tag{7.8}$$

$$\alpha_t^{(2)} \triangleq -\lim_{P\to\infty} \frac{\log \mathbb{E}[||\boldsymbol{g}_t - \hat{\boldsymbol{g}}_{t,t}||^2]}{\log P} \tag{7.9}$$

pour décrire l'exposant de la qualité actuelle pour les deux utilisateurs ($\alpha_t^{(1)}$ est de utilisateur 2), alors que nous allons utiliser

$$\beta_t^{(1)} \triangleq -\lim_{P\to\infty} \frac{\log \mathbb{E}[||\boldsymbol{h}_t - \hat{\boldsymbol{h}}_{t,t+\eta}||^2]}{\log P} \tag{7.10}$$

$$\beta_t^{(2)} \triangleq -\lim_{P\to\infty} \frac{\log \mathbb{E}[||\boldsymbol{g}_t - \hat{\boldsymbol{g}}_{t,t+\eta}||^2]}{\log P} \tag{7.11}$$

- pour toute suffisamment grand mais fini entier $\eta > 0$ - pour désigner la qualité des exposants différé pour chaque utilisateur. En d'autres termes, $\alpha_t^{(1)}$ mesures de la qualité de la CSIT (environ $\boldsymbol{h}_t$) qui est disponible à l'instant t, tandis que $\beta_t^{(1)}$ mesure la qualité (le meilleur) de la CSIT (environ $\boldsymbol{h}_t$) qui arrive strictement après le canal apparaît, c'est strictement après le temps t (même $\alpha_t^{(2)}, \beta_t^{(2)}$ pour le canal $\boldsymbol{g}_t$ du second utilisateur).

Il est facile de voir que, sans perte de généralité, dans le cadre DoF d'intérêt, nous pouvons limiter notre attention à la plage

$$0 \le \alpha_t^{(i)} \le \beta_t^{(i)} \le 1$$

où $\beta_t^{(i)} = 1$ correspond à avoir (asymptotiquement) parfait CSIT retard pour $\boldsymbol{h}_t, \boldsymbol{g}_t$, et où $\alpha_t^{(1)} = \alpha_t^{(2)} = 1$, correspond au cas optimal de la CSIT parfaite courante (complete).

En outre, nous allons utiliser la notation

$$\bar{\alpha}^{(i)} \triangleq \lim_{n\to\infty} \frac{1}{n} \sum_{t=1}^{n} \alpha_t^{(i)}, \quad \bar{\beta}^{(i)} \triangleq \lim_{n\to\infty} \frac{1}{n} \sum_{t=1}^{n} \beta_t^{(i)}, \quad i = 1, 2 \tag{7.12}$$

pour désigner la moyenne des exposants de qualité. A ce stade, nous constatons que nos résultats, en particulier la partie de faisabilité, tiendront sous l'hypothèse que toute suffisamment longue séquence $\{\alpha_t^{(1)}\}_{t=\tau}^{\tau+T}$ (respectivement $\{\alpha_t^{(2)}\}_{t=\tau}^{\tau+T}$, $\{\beta_t^{(1)}\}_{t=\tau}^{\tau+T}$, $\{\beta_t^{(2)}\}_{t=\tau}^{\tau+T}$) a une moyenne qui converge vers la moyenne à long terme $\bar{\alpha}^{(1)}$ (respectivement $\bar{\alpha}^{(2)}, \bar{\beta}^{(1)}, \bar{\beta}^{(2)}$), pour tout τ et, pour certains finie T qui peuvent être choisis pour être suffisamment large pour permettre la convergence ci-dessus.

Nous adhérons à la convention commune d'assumer une connaissance parfaite et globale de l'information d'état de canal au niveau des récepteurs (CSIR global parfait), où les récepteurs connaissent tous les Etats du canal et toutes les estimations. Nous adhérons également à la convention commune de supposer que l'erreur d'estimation actuelle est statistiquement indépendante des estimations actuelles et passées, et par conséquent le signal d'entrée est une fonction du message et de la CSIT. Cette hypothèse s'accorde bien avec

de nombreux modèles de canaux s'étendant du cqnql fast fading (i.i.d. dans le temps), au modèle de canal corrélé car cela est considéré dans [5], le modèle fading bloc quasi-statique où les estimations de CSIT sont successivement raffiné tandis que le canal reste statique. En outre, nous considérons que les entrées de chaque vecteur d'erreur d'estimation $\boldsymbol{h}_t - \hat{\boldsymbol{h}}_{t,t'}$ (de même de $\boldsymbol{g}_t - \hat{\boldsymbol{g}}_{t,t'}$) à i.i.d Gaussienne, précisant cependant que nous référons seulement aux M des entrées dans chaque vecteur spécifique $\boldsymbol{h}_t - \hat{\boldsymbol{h}}_{t,t'}$, et que nous ne suggérons pas que l'erreur des entrées sont i.i.d. dans le temps ou entre les utilisateurs.

7.10.4 Région DoF des deux-utilisateur MISO BC

Nous procédons avec les principaux résultats de DoF, dont il est prouvé dans la section 2.4 (intérieure bound) et la section 2.6 (externe lié).

Nous rappelons ici que le lecteur des séquences

$$\{\alpha_t^{(1)}\}_{t=1}^n, \{\alpha_t^{(2)}\}_{t=1}^n, \{\beta_t^{(1)}\}_{t=1}^n, \{\beta_t^{(2)}\}_{t=1}^n$$

de qualité des exposants, que ceux-ci ont été définis dans (7.8)-(7.11), ainsi que des moyennes correspondantes

$$\bar{\alpha}^{(1)}, \bar{\alpha}^{(2)}, \bar{\beta}^{(1)}, \bar{\beta}^{(2)}$$

de (7.12). Nous rappelons aussi au lecteur que nous considérons la communication sur une grande durée n. Nous appelons désormais les utilisateurs de sorte que $\bar{\alpha}^{(2)} \leq \bar{\alpha}^{(1)}$.

L'extension du travail dans [6] qui met l'accent sur CSIT avec une qualité invariante et symétrique, on procède d'abord par construire un nouveau DoF externe lié qui soutient notre réglage. La preuve se trouve dans la Section 2.6.

Lemma 7. *La région DoF des deux-utilisateur MISO BC avec un processus CSIT* $\{\hat{\boldsymbol{h}}_{t,t'}, \hat{\boldsymbol{g}}_{t,t'}\}_{t=1,t'=1}^n$ *de qualité* $\{(\boldsymbol{h}_t - \hat{\boldsymbol{h}}_{t,t'}), (\boldsymbol{g}_t - \hat{\boldsymbol{g}}_{t,t'})\}_{t=1,t'=1}^n$*, est supérieure délimitée comme*

$$d_1 \leq 1, \qquad d_2 \leq 1 \tag{7.13}$$

$$2d_1 + d_2 \leq 2 + \bar{\alpha}^{(1)} \tag{7.14}$$

$$2d_2 + d_1 \leq 2 + \bar{\alpha}^{(2)}. \tag{7.15}$$

Le théorème suivant fournit la DoF optimale pour un large intervalle de suffisamment bien différé CSIT.

Theorem 8. *La région optimal de la DoF des deux-utilisateur MISO BC avec un processus CSIT* $\{\hat{\boldsymbol{h}}_{t,t'}, \hat{\boldsymbol{g}}_{t,t'}\}_{t=1,t'=1}^n$ *de qualité* $\{(\boldsymbol{h}_t - \hat{\boldsymbol{h}}_{t,t'}), (\boldsymbol{g}_t -$

$\hat{\boldsymbol{g}}_{t,t'})\}_{t=1,t'=1}^{n}$ *est donnée par*

$$d_1 \leq 1, \quad d_2 \leq 1 \tag{7.16}$$

$$2d_1 + d_2 \leq 2 + \bar{\alpha}^{(1)} \tag{7.17}$$

$$2d_2 + d_1 \leq 2 + \bar{\alpha}^{(2)} \tag{7.18}$$

pour tout processus CSIT suffisamment bien différé tels que

$$\min\{\bar{\beta}^{(1)}, \bar{\beta}^{(2)}\} \geq \min\{\frac{1 + \bar{\alpha}^{(1)} + \bar{\alpha}^{(2)}}{3}, \frac{1 + \bar{\alpha}^{(2)}}{2}\}.$$

Figure 2.2 correspond au résultat principal dans le théorème. Le résultat ci-dessus est complété par la proposition suivante.

Proposition 9. *Pour un processus CSIT* $\{\hat{\boldsymbol{h}}_{t,t'}, \hat{\boldsymbol{g}}_{t,t'}\}_{t=1,t'=1}^{n}$ *par* $\min\{\bar{\beta}^{(1)}, \bar{\beta}^{(2)}\} < \min\{\frac{1+\bar{\alpha}^{(1)}+\bar{\alpha}^{(2)}}{3}, \frac{1+\bar{\alpha}^{(2)}}{2}\}$*, la région DoF est intérieure délimitée par le polygone décrit par*

$$d_1 \leq 1, \quad d_2 \leq 1 \tag{7.19}$$

$$2d_1 + d_2 \leq 2 + \bar{\alpha}^{(1)} \tag{7.20}$$

$$2d_2 + d_1 \leq 2 + \bar{\alpha}^{(2)} \tag{7.21}$$

$$d_1 + d_2 \leq 1 + \min\{\bar{\beta}^{(1)}, \bar{\beta}^{(2)}\}. \tag{7.22}$$

Figure 7.4 correspond au résultat de la Proposition 9.

Avant de procéder àdes corollaires spécifiques qui offrent un meilleur aperçu, il vaut la peine de faire un commentaire sur le fait que toute la complexité du problème est capturé au niveau de la qualité des exposants.

Feedback symétrique et asymétrique

Nous partons à la découverte du cas particulier de feedback symétrique où la qualité de feedback accumulé est similaire entre les utilisateurs, c'est à dire, lorsque les liens de feedback de l'utilisateur 1 et l'utilisateur 2 partagent les mêmes moyennes des exposants

$$\bar{\alpha}^{(1)} = \bar{\alpha}^{(2)} = \bar{\alpha}, \quad \bar{\beta}^{(1)} = \bar{\beta}^{(2)} = \bar{\beta}.$$

La plupart des ouvrages existants, avec une exception dans [33], relèvent ce paramètre. Ce qui suit tient directement du théorème 8 et la Proposition 9.

Corollary 8a (DoF en réaction symétrique)**.** *La région de la DoF optimale pour le cas symétrique prend la forme*

$$d_1 \leq 1, \quad d_2 \leq 1, \quad 2d_1 + d_2 \leq 2 + \bar{\alpha}, \quad 2d_2 + d_1 \leq 2 + \bar{\alpha}$$

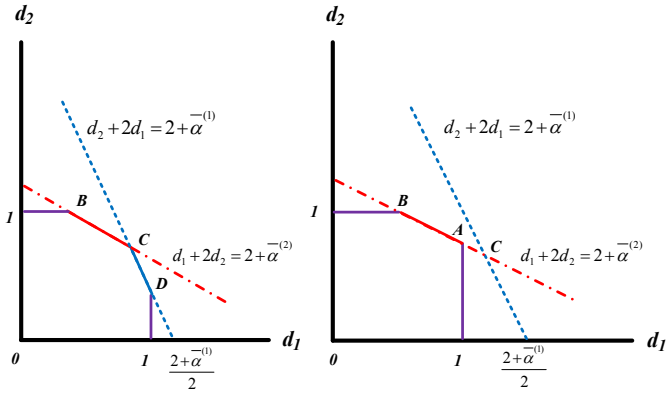

FIGURE 7.3 – Régions DoF optimal pour les deux utilisateurs MISO BC, pour le cas de $\min\{\bar{\beta}^{(1)}, \bar{\beta}^{(2)}\} \geq \min\{\frac{1+\bar{\alpha}^{(1)}+\bar{\alpha}^{(2)}}{3}, \frac{1+\bar{\alpha}^{(2)}}{2}\}$. Les points d'angle prennent les valeurs suivantes : $A = (1, \frac{1+\bar{\alpha}^{(2)}}{2})$, $B = (\bar{\alpha}^{(2)}, 1)$, $C = (\frac{2+2\bar{\alpha}^{(1)}-\bar{\alpha}^{(2)}}{3}, \frac{2+2\bar{\alpha}^{(2)}-\bar{\alpha}^{(1)}}{3})$, $D = (1, \bar{\alpha}^{(1)})$.

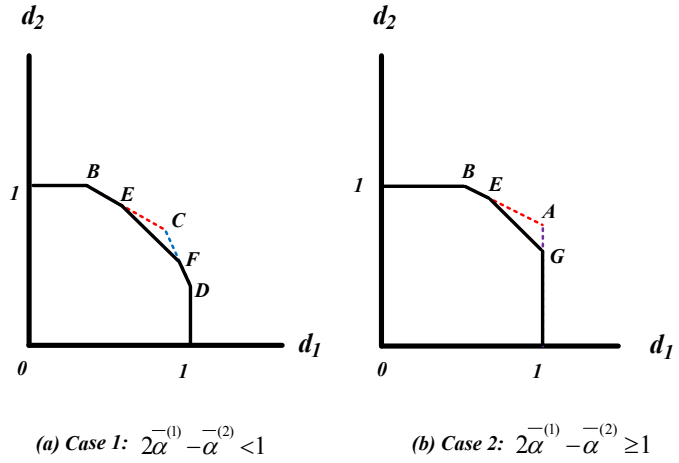

FIGURE 7.4 – Régions DoF pour les deux utilisateurs MISO BC avec $\min\{\bar{\beta}^{(1)}, \bar{\beta}^{(2)}\} \leq \min\{\frac{1+\bar{\alpha}^{(1)}+\bar{\alpha}^{(2)}}{3}, \frac{1+\bar{\alpha}^{(2)}}{2}\}$. Les points d'angle prennent les valeurs suivantes : $E = (2\bar{\delta} - \bar{\alpha}^{(2)}, 1 + \bar{\alpha}^{(2)} - \bar{\delta})$, $F = (1 + \bar{\alpha}^{(1)} - \bar{\delta}, 2\bar{\delta} - \bar{\alpha}^{(1)})$, $G = (1, \bar{\delta})$, $\bar{\delta} \triangleq \min\{\bar{\beta}^{(1)}, \bar{\beta}^{(2)}, \frac{1+\bar{\alpha}^{(1)}+\bar{\alpha}^{(2)}}{3}, \frac{1+\bar{\alpha}^{(2)}}{2}\}$.

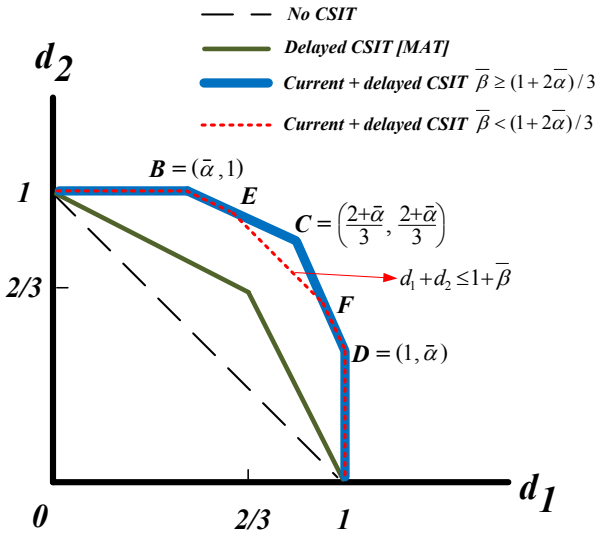

FIGURE 7.5 – Région DoF deux utilisateurs MISO BC avec feedback symétrique, $\bar{\alpha}^{(1)} = \bar{\alpha}^{(2)} = \bar{\alpha}, \bar{\beta}^{(1)} = \bar{\beta}^{(2)} = \bar{\beta}$. La zone optimale prend la forme d'un polygone avec des points d'angle $\{(0,0),(0,1),(\bar{\alpha},1),(\frac{2+\bar{\alpha}}{3},\frac{2+\bar{\alpha}}{3}),(1,\bar{\alpha}),(1,0)\}$ pour $\bar{\beta} \geq \frac{1+2\bar{\alpha}}{3}$. Pour $\bar{\beta} < \frac{1+2\bar{\alpha}}{3}$, la région dérivée prend la forme d'un polygone avec des points d'angle $\{(0,0),(0,1),(\bar{\alpha},1),(2\bar{\beta}-\bar{\alpha},1+\bar{\alpha}-\bar{\beta}),(1+\bar{\alpha}-\bar{\beta},2\bar{\beta}-\bar{\alpha}),(1,\bar{\alpha}),(1,0)\}$.

lorsque $\bar{\beta} \geq \frac{1+2\bar{\alpha}}{3}$, *tandis que* $\bar{\beta} < \frac{1+2\bar{\alpha}}{3}$ *cette région intérieure délimitée par la région réalisable*

$$d_1 \leq 1, \quad d_2 \leq 1 \tag{7.23}$$
$$2d_1 + d_2 \leq 2 + \bar{\alpha} \tag{7.24}$$
$$2d_2 + d_1 \leq 2 + \bar{\alpha} \tag{7.25}$$
$$d_2 + d_1 \leq 1 + \bar{\beta}. \tag{7.26}$$

Figure 7.5 représente la région DoF des deux-utilisateur MISO BC avec feedback symétrique.

Nous mesurons maintenant la mesure pour laquelle ayant un feedback symétrique offre un avantage sur le cas asymétrique où un utilisateur a généralement plus de feedback que l'autre. Différents travaux ont identifié des cas où ayant des offres de feedback symétriques (gains de symétrie) par rapport au cas asymétrique (cf. [11], [33]).

La comparaison générale qui suit se concentre sur le cas de parfaite CSIT différée, et oppose le cas symétrique $\bar{\alpha}^{(1)} = \bar{\alpha}^{(2)}$, au cas asymétrique $\bar{\alpha}^{(1)} \neq \bar{\alpha}^{(2)}$, sous une contrainte globale de feedback $\bar{\alpha}^{(1)} + \bar{\alpha}^{(2)} = \Delta$, pour tout $\Delta \in (0,2]$. La comparaison est en fonction de la somme-DoF optimal $d_1 + d_2$,

où, nous rappelons que les utilisateurs sont identifiés de sorte que $\bar{\alpha}^{(1)} \geq \bar{\alpha}^{(2)}$. La preuve est directe du théorème 8 et le corollaire 8a.

Corollary 8b (Rétroaction symétrique et asymétrique)**.** *Considérons tout* $\Delta \triangleq \bar{\alpha}^{(1)} + \bar{\alpha}^{(2)}$ *fixe dans l'intervalle* $(0, 2]$. *Si* $2\bar{\alpha}^{(1)} - \bar{\alpha}^{(2)} - 1 \leq 0$, *ayant un feedback symétrique* ($\bar{\alpha}^{(1)} = \bar{\alpha}^{(2)}$) *n'offre pas un gain somme-DoF sur le cas de feedback asymétrique, tandis que si* $2\bar{\alpha}^{(1)} - \bar{\alpha}^{(2)} - 1 > 0$, *il ya un gain somme-DoF symétrique et elle prend la forme* $\frac{2\bar{\alpha}^{(1)} - \bar{\alpha}^{(2)} - 1}{6}$.

Example 22. *Par exemple, sous la contrainte que* $\bar{\alpha}^{(1)} + \bar{\alpha}^{(2)} = \Delta = 1$, *l'asymétrie de* $\bar{\alpha}^{(1)} = 1, \bar{\alpha}^{(2)} = 0$ *donne une somme optimale DoF de* $d_1 + d_2 = 3/2$ *(Theorem 8 avec une parfaite CSIT différée), tandis que le symétrique* $\bar{\alpha}^{(1)} = \bar{\alpha}^{(2)} = 0.5$ *donne* $d_1 + d_2 = 5/3$, *et un gain somme DoF de* $5/3 - 3/2 = 1/6$.

Besoin d'informations retardé : CSIT Imparfait vs CSIT Retardé

Nous montrons ici que le CSIT imparfait retardé peut être aussi utile que le CSIT parfait retardé, et nous fournissons un aperçu de la qualité de la réaction globale (en temps opportun et en différé) qui est nécessaire pour atteindre un certain rendement du DoF.

Corollary 8c (CSIT imparfait vs parfait retardé)**.** *Un processus CSIT* $\{\hat{\boldsymbol{h}}_{t,t'}, \hat{\boldsymbol{g}}_{t,t'}\}_{t=1,t'=1}^{n}$ *qui offre*

$$\min\{\bar{\beta}^{(1)}, \bar{\beta}^{(2)}\} \geq \min\{\frac{1 + \bar{\alpha}^{(1)} + \bar{\alpha}^{(2)}}{3}, \frac{1 + \bar{\alpha}^{(2)}}{2}\} \tag{7.27}$$

Donne le même DoF qu'un processus CSIT qui offre un CSIT parfait retardé pour chaque réalisation de canal ($\beta_t^{(1)} = \beta_t^{(2)} = 1, \forall t$). *Pour le cas symétrique, avoir*

$$\bar{\beta} \geq \frac{1 + 2\bar{\alpha}}{3} \tag{7.28}$$

donne le même résultat.

Il est intéressant de noter que les expressions dans le corollaire ci-dessus correspondent au montant du CSIT retardé utilisé par les schemas de transmission dans le passé, même si ceux-ci n'ont pas été conçus dans le but explicite de réduire la quantité de CSIT retardé.

Besoin de CSIT prédit

Nous changeons maintenant l'accent du CSIT retardé pour l'autre extrême du CSIT prédit. Comme nous le rappelons, nous avons considéré un

processus de canal $\{\boldsymbol{h}_t, \boldsymbol{g}_t\}_t$ et un processus CSIT $\{\hat{\boldsymbol{h}}_{t,t'}, \hat{\boldsymbol{g}}_{t,t'}\}_{t,t'}$, composé d'estimations $\hat{\boldsymbol{h}}_{t,t'}$ - disponibles en tout temps t' - du canal $\boldsymbol{h}_t$ qui se matérialise en tout temps t. Nous avons également préconisé que nous pouvons supposer que $\mathbb{E}[||\boldsymbol{h}_t - \hat{\boldsymbol{h}}_{t,t'}||^2] \leq \mathbb{E}[||\boldsymbol{h}_t - \hat{\boldsymbol{h}}_{t,t''}||^2]$, pour tout $t' > t''$, tout simplement parce que l'on peut revenir à des estimations antérieures de statistiques de meilleure qualité. Cette hypothèse n'a cependant pas obstacle à l'utilité possible des premières estimations (prévue), même si ces estimations sont généralement de moindre qualité que les estimations actuelles (de moins bonne qualité que les estimations qui apparaissent pendant ou après le canal matérialise). Ce qui suit donne un aperçu sur ce sujet.

Corollary 8d (Besoin de CSIT prédit)**.** *Si le CSIT retardé vérifie*

$$\min\{\bar{\beta}^{(1)}, \bar{\beta}^{(2)}\} \geq \min\{\frac{1+\bar{\alpha}^{(1)}+\bar{\alpha}^{(2)}}{3}, \frac{1+\bar{\alpha}^{(2)}}{2}\}$$

il n'y a pas de gain de DoF à utiliser du CSIT prédit. Plus précisément - pour une qualité de CSIT, et afin de parvenir au DoF optimal - la transmission à un certain moment t^*, n'a pas besoin d'examiner toute estimation $\hat{\boldsymbol{h}}_{t,t'}$ d'un canal à venir $t > t^*$, où cette estimation est devenu disponible - naturellement par prédiction - à tout moment $t' \leq t^* < t$.

7.10.5 CSIT evoluant periodiquement

Nous nous concentrons ici sur des canaux variants par block, et considérons une accumulation progressive de CSIT qui se traduit par une qualité de CSIT augmentant progressivement lorsque le temps progresse à travers la période de la cohérence (T_c usages des canaux - CSIT courant), ou à tout moment après la fin de la période de la cohérence (CSIT retardé).

Cette amélioration progressive pourrait être recherchée dans les milieux FDD (Frequency Division Duplex) avec des liens de retour à capacité limitée qui peuvent être utilisés plus d'une fois au cours de la période de cohérence afin d'affiner progressivement le CSIT, ainsi que dans TDD (Time Division Duplex) les paramètres qui utilisent la réciprocité basé sur l'estimation qui améliore progressivement au fil du temps.

Dans ce cadre, le canal reste le même pour une durée limitée de T_c utilisations de canal, et l'indice de temps est agencé de telle sorte que

$$\boldsymbol{h}_{\ell T_c+1} = \boldsymbol{h}_{\ell T_c+2} = \cdots = \boldsymbol{h}_{(\ell+1)T_c}$$

$$\boldsymbol{g}_{\ell T_c+1} = \boldsymbol{g}_{\ell T_c+2} = \cdots = \boldsymbol{g}_{(\ell+1)T_c}$$

pour un entier non négatif ℓ. En outre la qualité de CSIT est maintenant périodique, comme cela se reflète dans les exposants de qualité courante CSIT où

$$\alpha_t^{(i)} = \alpha_{\ell T_c+t}^{(i)}, \forall \ell = 0, 1, 2, \cdots, \ i = 1, 2. \tag{7.29}$$

Nous nous concentrons ici principalement sur le cas symétrique. Dans ce cadre la qualité de rétroaction est maintenant représenté par le T_c courant CSIT qualité des exposants $\{\alpha_t\}_{t=1}^{T_c}$ et par le retard CSIT exposant β. Chaque α_t décrit la qualité des estimations du CSIT actuel au temps $t \leq T_c$, alors β capte la qualité des meilleures estimations de CSIT qui sont reçus après que le canal se soit écoulée, soit après la durée de cohérence du canal. Dans ce cadre nous avons que

$$0 \leq \alpha_1 \leq \cdots \leq \alpha_{T_c} \leq \beta \leq 1 \tag{7.30}$$

où une différence entre les deux exposants consécutifs est due à l'information qui a été reçu au cours de cette tranche de temps.

Ce même cadre saisit aussi le moment de ce retour périodique. Ayant par exemple $\alpha_1 = 1$ se réfère simplement pour le cas de parfaite (complète) CSIT, alors ayant $\alpha_{T_c} = 0$ signifie simplement qu'aucune rétroaction (ou très peu) est envoyée pendant la période de la cohérence du canal. Ayant même $\alpha_{\gamma T_c} = 0, \gamma \in [0,1]$ signifie simplement qu'aucune rétroaction (ou très peu) est envoyée au cours de la première γ fraction de la période de cohérence. Par exemple, avoir un processus de rétroaction périodique qui envoie par exemple des informations deux fois par période de cohérence, pour $t = \gamma_1 T_c + 1, t = \gamma_2 T_c + 1$ et plus jamais sur ce même canal, résulte en

$$\overbrace{0 = \alpha_1 = \cdots = \alpha_{\gamma_1 T_c}}^{\text{avant commentaires}} \leq \overbrace{\alpha_{\gamma_1 T_c + 1} = \cdots = \alpha_{\gamma_2 T_c}}^{\text{Après la première réaction}} \leq \underbrace{\alpha_{\gamma_2 T_c + 1} = \cdots = \alpha_{T_c} = \beta}_{\text{Après la deuxième réaction}} \tag{7.31}$$

tandis que si le même système de rétroaction ajoute quelques informations après l'écoulement du canal, puis nous avons tout simplement que $\beta \geq \alpha_{T_c}$.

On peut noter que la réduction de α_{T_c} implique une quantité réduite d'informations, sur un canal spécifique, qui est envoyé au cours de la période de la cohérence de ce même canal, tandis que la réduction de β implique une quantité réduite d'informations, au cours de ou après la période de la cohérence du canal. Le long de ces lignes, la réduction de $(\beta - \alpha_{T_c})$ implique une quantité réduite d'informations, sur un coefficient d'évanouissement spécifique, qui est envoyé après la période de cohérence du canal.

Les résultats suivant suivent directement à partir des résultats antérieurs dans ce travail, où nous avons maintenant simplement mis

$$\bar{\alpha} = \frac{1}{T_c} \sum_{t=1}^{T_c} \alpha_t. \tag{7.32}$$

Ce qui suit tient directement du corollaire 8a, dans le cas d'un processus de rétroaction avec évolution périodiquement sur un canal quasi-statique.

Corollary 8e (Commentaires sur l'évolution périodique)**.** *Pour un processus de rétroaction périodique avec* $\{\alpha_t\}_{t=1}^{T_c}$ *et parfait CSIT retardée (reçue à tout moment après la fin de la période de cohérence), la région de la DoF optimale sur un bloc-canal avec évanouissement est le polygone de sommets*

$$\{(0,0),(0,1),(\bar{\alpha},1),(\frac{2+\bar{\alpha}}{3},\frac{2+\bar{\alpha}}{3}),(1,\bar{\alpha}),(1,0)\}. \tag{7.33}$$

Cette même région optimal peut en fait être atteint même avec retard CSIT imparfait qualité, aussi longtemps que $\beta \geq \frac{1+2\bar{\alpha}}{3}$.

Remark 8 (Commentaires sur la dépendance qualité versus quantité)**.** *Bien que les résultats sont ici en termes de qualité de rétroaction plutôt qu'en termes de quantité de feedback, il ya des cas distincts où la relation entre les deux est bien défini. Tel est le cas lorsque les estimations de la CSIT sont calculés à l'aide de base - et pas nécessairement optimale - techniques de quantification scalaires [39]. Dans de tels cas, que nous mentionnons ici simplement pour offrir un aperçu, en consacrant* $\alpha \log P$ *de quantification par scalaire pour quantifier* $\boldsymbol{h}$ *en une estimation* $\hat{\boldsymbol{h}}$*, permet à une erreur quadratique moyenne [39]*

$$\mathbb{E}\|\boldsymbol{h}-\hat{\boldsymbol{h}}\|^2 \doteq P^{-\alpha}.$$

S'inspirant de cela, et de revenir à notre exemple précédent, considérons un processus de rétroaction périodique qui envoie raffinage informations deux fois par période de cohérence, en envoyant d'abord $\alpha' \log P$ bits d'informations par scalaire au temps $t = \gamma_1 T_c + 1$, puis l'envoi supplémentaire $\alpha'' \log P$ bits d'informations par scalaire au temps $t = \gamma_2 T_c + 1$, et où il envoie finalement $(\beta - (\alpha' + \alpha'')) \log P$ les bits supplémentaires de raffinage commentaires par scalaire, à n'importe quel moment après la période de la cohérence d'un canal. Cela aboutirait à avoir

$$\begin{aligned}\overbrace{0 = \alpha_1 = \cdots = \alpha_{\gamma_1 T_c}}^{\text{Before feedback}} &\leq \overbrace{\alpha' = \alpha_{\gamma_1 T_c+1} = \cdots = \alpha_{\gamma_2 T_c}}^{\text{After first feedback}} \\ &\leq \underbrace{\alpha' + \alpha'' = \alpha_{\gamma_2 T_c+1} = \cdots = \alpha_{T_c}}_{\text{After second feedback, before } T_c} \leq \underbrace{\beta}_{\text{After coherence period}}.\end{aligned} \tag{7.34}$$

À titre d'exemple, ayant évaluations périodiques qui envoie $\frac{4}{9} \log P$ bits d'informations par scalaire au temps $t = \frac{1}{3} T_c + 1$, puis envoie supplémentaire $\frac{1}{9} \log P$ bits d'informations par scalaire au temps $t = \frac{2}{3} T_c + 1$, se traduira par

$$\begin{aligned}\overbrace{0 = \alpha_1 = \cdots = \alpha_{\frac{1}{3}T_c}}^{\text{Before feedback}} &\leq \overbrace{\frac{4}{9} = \alpha_{\frac{1}{3}T_c+1} = \cdots = \alpha_{\frac{2}{3}T_c}}^{\text{After first feedback}} \\ &\leq \underbrace{\frac{5}{9} = \alpha_{\frac{2}{3}T_c+1} = \cdots = \alpha_{T_c}}_{\text{After second feedback, before } T_c}\end{aligned} \tag{7.35}$$

ce qui donne $\bar{\alpha} = (0 + 4/9 + 5/9)/3 = 1/3$, qui à son tour donne une région d'DoF optimale qui est définie par le polygone avec des points d'angle

$$\{(0,0),(0,1),(1/3,1),(7/9,7/9),(1,1/3),(1,0)\}. \tag{7.36}$$

On a sans doute remarqué qu'il n'y avait pas besoin de bits supplémentaires de (retardée) commentaires après la fin de la période de cohérence. C'est parce que le montant et le calendrier actuel des bits de rétroaction déjà autorisées pour

$$\beta = \alpha_{T_c} = 5/9 = \frac{1+2\bar{\alpha}}{3} = \frac{1+2/3}{3}$$

que nous avons vu dans le corollaire 1f soit aussi bon que parfait réaction retardée.

Placer notre focus sur la qualité des commentaires, nous procédons à un corollaire qui offre un aperçu sur la question de ce qu'est la qualité CSIT et le chronométrage suffisent pour atteindre un certain rendement du DoF. Pour faciliter l'exposé, nous nous concentrons sur le point DoF plus difficiles à atteindre $d_1 = d_2 = d$.

Corollary 8f (Suffisamment d'informations pour cible DoF)**.** *Avoir $\bar{\alpha} \geq 3d-2$ avec $\beta \geq 2d-1$, ou d'avoir $\bar{\alpha} \geq 3d-2$ avec $\alpha_{T_c} \geq 2d-1$ (et pas de retour retardé en sus), suffit à atteindre une cible symétrique DoF $d_1 = d_2 = d$.*

Un autre aspect pratique qui est abordé ici, a à voir avec les retards de rétroaction. Ces retards peuvent entraîner une dégradation des performances, ce qui pourrait être atténué si le retour, mais avec des retards, est de suffisamment bonne qualité. Le corollaire suivant donne un aperçu sur ces aspects, en décrivant les retards de rétroaction qui permettent pour une cible donnée symétrique DoF d en présence de contraintes sur les qualités CSIT courants et différés.

Nous serons particulièrement intéressés par le retard fractionnaire admissible de rétroaction (cf. [10])

$$\gamma \triangleq \arg\max_{\gamma'} \{\alpha_{\gamma' T_c} = 0\} \tag{7.37}$$

la fraction $\gamma \leq 1$ pour lesquels

$$\alpha_1 = \cdots = \alpha_{\gamma T_c} = 0, \alpha_{\gamma T_c + 1} > 0.$$

Nous sommes également intéressés de voir comment ce retard admissible réduit en présence d'une contrainte $\alpha_t \leq \alpha_{\max}\ \forall\ t$ sur la rétroaction en temps opportun, ou une contrainte sur β.

Corollary 8g (Délai de retour admissible)**.** *Sous une contrainte de qualité de la CSIT $\alpha_t \leq \alpha_{\max}$ $\forall t$, un DoF cible symétrique d peut être réalisé avec n'importe quel retard fractionnaire*

$$\gamma \leq \begin{cases} 1 - \frac{3d-2}{\alpha_{\max}} & si \;\; d \in [2/3, (2+\alpha_{\max})/3] \\ 1 & si \;\; d \in [0, 2/3] \end{cases}$$

alors que sous une contrainte $\beta \leq \beta_{\max}$, il peut être réalisé avec toute

$$\gamma \leq \begin{cases} 1 & si \;\; d \in [0, \frac{1+\min\{\beta_{\max}, 1/3\}}{2}] \\ \frac{1}{2}\left(\frac{1}{2d-1} - 1\right) & autre\ si \;\; d \in [\frac{1+\min\{\beta_{\max}, 1/3\}}{2}, \frac{1+\beta_{\max}}{2}] \end{cases}$$

Enfin depuis $\alpha_{\max} \leq \beta_{\max} \leq 1$, ce qui précède montre que sous aucune contrainte spécifique sur la qualité de la CSIT, d peut être réalisé avec

$$\gamma \leq \begin{cases} 3(1-d) & if \;\; d \in [2/3, 1] \\ 1 & if \;\; d \in [0, 2/3]. \end{cases}$$

Nous allons maintenant voir comment le réglage de rétroaction évoluer périodiquement, intègre différents paramètres existants d'intérêt.

7.10.6 Le réglage évolution périodiquement comme une généralisation de paramètres existants

Ce paramètre de rétroaction périodiquement l'évolution est puissante car elle capte les nombreuses options techniques que l'on peut avoir dans un cadre bloc-fading lorsque la nature des informations demeure largement inchangée à travers les périodes de cohérence. Il capture aussi et généralise les paramètres existants qui ont été d'un intérêt particulier, comme le Maddah-Ali et le réglage Tse dans [4], le Yang et al. et Gou et le réglage Jafar dans [6,7], le réglage Lee et Heath dans [10], et le réglage asymétrique dans [33]. Nous allons mettre en lumière certaines de ces généralisations pour différents paramètres existants d'intérêt.

CSIT seulement retardé - Maddah-Ali et Tse

Le réglage Maddah-Ali et Tse dans [4] correspond à la mise en évolution avec $\alpha_t = 0, t = 1, 2, \cdots, T_c$ et avec une parfaite CSIT retardée. Une généralisation directe de [4], qui s'inscrit dans le cadre évolutif actuel, est de considérer CSIT retardé par diminution de la qualité β. De cette généralisation, nous savons maintenant que la même performance DoF de $\{(0,0), (0,1), (\frac{2}{3}, \frac{2}{3}), (1,0)\}$, peut être atteint même si la CSIT retardé envoyé, est de qualité imparfaite, correspondant à toute $\beta \geq 1/3$.

CSIT retard avec CSIT actuel imparfait - Yang et al. et Gou et Jafar

De même, le Yang et al. et Gou et la mise en Jafar [6, 7], correspond à la mise en évoluant avec $\alpha_t = \alpha, t = 1, 2, \cdots, T_c$ et avec une parfaite CSIT retardée. Comme ci-dessus, une généralisation directe consiste à considérer la qualité imparfaite retardé CSIT, et pour cela, nous savons que la DoF optimal $\{(0,0), (0,1), (\frac{2+\alpha}{3}, \frac{2+\alpha}{3}), (1,0)\}$ peut être réalisé pour toute combinaison des exposants de qualité CSIT qui donnent $\bar{\alpha} = \alpha$, et même avec la qualité de la CSIT retard imparfait pour tout $\beta \geq (1+2\alpha)/3$.

Pas si retardé CSIT - Lee et Heath

La mise en [10] considère parfaite rétroaction retardée et rétroaction parfaite courant qui vient avec un retard fractionnaire $\gamma \in [0,1]$ de la période de la cohérence, c'est à dire, il considère que la rétroaction parfait arrive toujours γT_c canal utilise après la réalisation du canal. Ce paramètre - en mettant l'accent ici sur le cas de deux utilisateurs - puis des cartes au réglage de la CSIT évolution périodiquement avec une parfaite CSIT retard et avec

$$\underbrace{\alpha_1 = \cdots = \alpha_{\gamma T_c} = 0}_{\text{No feedback}}, \ \underbrace{\alpha_{\gamma T_c + 1} = \cdots = \alpha_{T_c} = 1}_{\text{Perfect CSIT}}. \tag{7.38}$$

Certaines généralisations pratiques ont été considérées dans le corollaire 1h qui décrit le retard maximal possible γ nécessaires pour réaliser une performance de DoF spécifique, sous des contraintes sur la qualité CSIT.

CSIT retardé par CSIT actuel pour un seul utilisateur - Maleki, Jafar et Shamai

Le réglage évolution peut être naturellement étendu à la création asymétrique où $\bar{\alpha}^{(1)} \neq \bar{\alpha}^{(2)}$ et où les exposants de la CSIT retard $\beta^{(1)}, \beta^{(2)}$ n'a pas besoin d'être égaux. Une telle configuration asymétrique donnerait une généralisation pour le réglage asymétrique de Maleki et al. dans [33], où les utilisateurs offerts parfait CSIT retard, et où seul le premier utilisateur offert CSIT de courant parfaite, résultant en une DoF optimale correspondant à DoF point d'angle $(1, 1/2)$ (somme DoF $d_1 + d_2 = 3/2$). Ce paramètre correspond à la création de la CSIT évolution périodiquement avec une parfaite CSIT retard et avec

$$\alpha_t^{(1)} = 1, \alpha_t^{(2)} = 0, \ \forall t.$$

Le corollaire suivant propose une généralisation du résultat correspondant à [33]. La preuve est directe depuis les suivantes adapte simplement le résultat dans le théorème principal, à la mise en évolution périodiquement. C'est nouveau pour la fixation d'assez bonne CSIT retardé par

$$\min\{\beta^{(1)}, \beta^{(2)}\} \geq \min\{\frac{1 + \bar{\alpha}^{(1)} + \bar{\alpha}^{(2)}}{3}, \frac{1 + \bar{\alpha}^{(2)}}{2}\}.$$

Corollary 8h (CSIT asymétrique et périodiques)**.** *La région de la DoF optimal est défini par des sommets* $B = (\bar{\alpha}^{(2)}, 1)$, $C = (\frac{2+2\bar{\alpha}^{(1)}-\bar{\alpha}^{(2)}}{3}, \frac{2+2\bar{\alpha}^{(2)}-\bar{\alpha}^{(1)}}{3})$, $D = (1, \bar{\alpha}^{(1)})$ *lorsque* $2\bar{\alpha}^{(1)} - \bar{\alpha}^{(2)} < 1$, *sinon par des sommets* $A = (1, \frac{1+\bar{\alpha}^{(2)}}{2})$ *Et* B.

Bibliography

[1] G. Caire and S. Shamai, "On the achievable throughput of a multiantenna Gaussian broadcast channel," *IEEE Trans. Inf. Theory*, vol. 49, no. 7, pp. 1691 – 1706, Jul. 2003.

[2] S. Jafar and A. Goldsmith, "Isotropic fading vector broadcast channels : The scalar upper bound and loss in degrees of freedom," *IEEE Trans. Inf. Theory*, vol. 51, no. 3, pp. 848 – 857, Mar. 2005.

[3] C. Huang, S. A. Jafar, S. Shamai, and S. Vishwanath, "On degrees of freedom region of MIMO networks without channel state information at transmitters," *IEEE Trans. Inf. Theory*, vol. 58, no. 2, pp. 849 – 857, Feb. 2012.

[4] M. A. Maddah-Ali and D. N. C. Tse, "Completely stale transmitter channel state information is still very useful," *IEEE Trans. Inf. Theory*, vol. 58, no. 7, pp. 4418 – 4431, Jul. 2012.

[5] M. Kobayashi, S. Yang, D. Gesbert, and X. Yi, "On the degrees of freedom of time correlated MISO broadcast channel with delayed CSIT," in *Proc. IEEE Int. Symp. Information Theory (ISIT)*, Jul. 2012.

[6] S. Yang, M. Kobayashi, D. Gesbert, and X. Yi, "Degrees of freedom of time correlated MISO broadcast channel with delayed CSIT," *IEEE Trans. Inf. Theory*, vol. 59, no. 1, pp. 315 – 328, Jan. 2013.

[7] T. Gou and S. Jafar, "Optimal use of current and outdated channel state information : Degrees of freedom of the MISO BC with mixed CSIT," *IEEE Communications Letters*, vol. 16, no. 7, pp. 1084 – 1087, Jul. 2012.

[8] J. Chen and P. Elia, "Degrees-of-freedom region of the MISO broadcast channel with general mixed-CSIT," in *Proc. Information Theory and Applications Workshop (ITA)*, Feb. 2013.

[9] ——, "Can imperfect delayed CSIT be as useful as perfect delayed CSIT ? DoF analysis and constructions for the BC," in *Proc. Allerton Conf. Communication, Control and Computing*, Oct. 2012.

[10] N. Lee and R. W. Heath Jr., "Not too delayed CSIT achieves the optimal degrees of freedom," in *Proc. Allerton Conf. Communication, Control and Computing*, Oct. 2012.

[11] R. Tandon, S. A. Jafar, S. Shamai, and H. V. Poor, "On the synergistic benefits of alternating CSIT for the MISO broadcast channel," *IEEE Trans. Inf. Theory*, vol. 59, no. 7, pp. 4106 – 4128, Jul. 2013.

[12] J. Chen and P. Elia, "MISO broadcast channel with delayed and evolving CSIT," in *Proc. IEEE Int. Symp. Information Theory (ISIT)*, Jul. 2013.

[13] J. Chen, S. Yang, and P. Elia, "On the fundamental feedback-vs-performance tradeoff over the MISO-BC with imperfect and delayed CSIT," in *Proc. IEEE Int. Symp. Information Theory (ISIT)*, Jul. 2013.

[14] J. Chen and P. Elia, "Toward the performance vs. feedback tradeoff for the two-user MISO broadcast channel," 2013, to appear in *IEEE Trans. Inform. Theory*.

[15] A. Lapidoth, S. Shamai, and M. A. Wigger, "On the capacity of fading MIMO broadcast channels with imperfect transmitter side-information," in *Proc. Allerton Conf. Communication, Control and Computing*, Sep. 2005.

[16] N. Jindal, "MIMO broadcast channels with finite-rate feedback," *IEEE Trans. Inf. Theory*, vol. 52, no. 11, pp. 5045 – 5060, Nov. 2006.

[17] G. Caire, N. Jindal, M. Kobayashi, and N. Ravindran, "Multiuser MIMO achievable rates with downlink training and channel state feedback," *IEEE Trans. Inf. Theory*, vol. 56, no. 6, pp. 2845 – 2866, Jun. 2010.

[18] G. Caire, N. Jindal, and S. Shamai, "On the required accuracy of transmitter channel state information in multiple antenna broadcast channels," in *Proc. Allerton Conf. Communication, Control and Computing*, Nov. 2007.

[19] C. S. Vaze and M. K. Varanasi, "The degrees of freedom region of two-user and certain three-user MIMO broadcast channel with delayed CSI," Dec. 2011, submitted to *IEEE Trans. Inf. Theory*, available on arXiv :1101.0306.

[20] A. Ghasemi, A. S. Motahari, and A. K. Khandani, "On the degrees of freedom of X channel with delayed CSIT," in *Proc. IEEE Int. Symp. Information Theory (ISIT)*, Jul. 2011.

[21] M. J. Abdoli, A. Ghasemi, and A. K. Khandani, "On the degrees of freedom of three-user MIMO broadcast channel with delayed CSIT," in *Proc. IEEE Int. Symp. Information Theory (ISIT)*, Jul. 2011.

[22] A. Ghasemi, A. S. Motahari, and A. K. Khandani, "Interference alignment for the MIMO interference channel with delayed local CSIT," Feb. 2011, available on arXiv :1102.5673v1.

[23] J. Xu, J. G. Andrews, and S. A. Jafar, "Broadcast channels with delayed finite-rate feedback : Predict or observe ?" *IEEE Trans. Wireless Commun.*, vol. 11, no. 4, pp. 1456 – 1467, Apr. 2012.

[24] Y. Lejosne, D. Slock, and Y. Yuan-Wu, "Degrees of freedom in the MISO BC with delayed-CSIT and finite coherence time : A simple optimal scheme," in *Proc. IEEE Int. Conf. on Signal Processing, Communications and Control (ICSPCC)*, Aug. 2012.

[25] X. Yi, S. Yang, D. Gesbert, and M. Kobayashi, "The degrees of freedom region of temporally-correlated MIMO networks with delayed CSIT," Nov. 2012, submitted to *IEEE Trans. Inform. Theory*, available on arXiv :1211.3322.

[26] P. de Kerret, X. Yi, and D. Gesbert, "On the degrees of freedom of the K-user time correlated broadcast channel with delayed CSIT," in *Proc. IEEE Int. Symp. Information Theory (ISIT)*, Jul. 2013.

[27] C. Hao and B. Clerckx, "Imperfect and unmatched CSIT is still useful for the frequency correlated MISO broadcast channel," in *Proc. IEEE Int. Conf. Communications (ICC)*, Jun. 2013.

[28] A. Vahid, M. A. Maddah-Ali, and A. S. Avestimehr, "Capacity results for binary fading interference channels with delayed CSIT," Jan. 2013, submitted to *IEEE Trans. Inform. Theory*, available on arXiv :1301.5309.

[29] A. Lozano, R. W. Heath Jr., and J. G. Andrews, "Fundamental limits of cooperation," *IEEE Trans. Inf. Theory*, vol. 59, no. 9, pp. 5213 – 5226, Sep. 2013.

[30] Y. Lejosne, D. Slock, and Y. Yuan-Wu, "NetDoFs of the MISO broadcast channel with delayed CSIT feedback for finite rate of innovation channel models," in *Proc. IEEE Int. Symp. Information Theory (ISIT)*, Jul. 2013.

[31] A. Zaidi and S. Shamai, "On cooperative multiple access channels with delayed CSI," in *Proc. IEEE Int. Symp. Information Theory (ISIT)*, Jul. 2013.

[32] M. J. Abdoli and S. Avestimehr, "On degrees of freedom scaling in layered interference networks with delayed CSI," in *Proc. IEEE Int. Symp. Information Theory (ISIT)*, Jul. 2013.

[33] H. Maleki, S. Jafar, and S. Shamai, "Retrospective interference alignment over interference networks," *IEEE Journal of Selected Topics in Signal Processing*, vol. 6, no. 3, pp. 228 – 240, Mar. 2012.

[34] L. Zheng and D. N. C. Tse, "Diversity and Multiplexing : A Fundamental Tradeoff in Multiple-Antenna Channels," *IEEE Trans. Inf. Theory*, vol. 49, no. 5, pp. 1073–1096, May 2003.

[35] A. Adhikary, H. C. Papadopoulos, S. A. Ramprashad, and G. Caire, "Multi-user MIMO with outdated CSI : Training, feedback and scheduling," in *Proc. Allerton Conf. Communication, Control and Computing*, Sep. 2011.

[36] M. Kobayashi and G. Caire, "On the net DoF comparison between ZF and MAT over time-varying MISO broadcast channels," in *Proc. IEEE Int. Symp. Information Theory (ISIT)*, Jul. 2012.

[37] A. Lapidoth and S. Shamai, "Fading channels : how perfect need "perfect side information" be ?" *IEEE Trans. Inf. Theory*, vol. 48, no. 5, pp. 1118 – 1134, May 2002.

[38] J. Chen and P. Elia, "MIMO BC with imperfect and delayed channel state information at the transmitter and receivers," in *Proc. IEEE Workshop on Signal Processing Advances in Wireless Communications (SPAWC)*, Jun. 2013.

[39] T. Cover and J. Thomas, *Elements of Information Theory*, 2nd ed. New York : Wiley-Interscience, 2006.

[40] O. El Ayach, A. Lozano, and R. W. Heath Jr., "On the overhead of interference alignment : Training, feedback, and cooperation," *IEEE Trans. Wireless Commun.*, vol. 58, no. 11, pp. 4192 – 4203, Nov. 2012.

[41] H. Weingarten, T. Liu, S. Shamai, Y. Steinberg, and P. Viswanath, "The capacity region of the degraded multiple-input multiple-output compound broadcast channel," *IEEE Trans. Inf. Theory*, vol. 55, no. 11, pp. 5011 – 5023, Nov. 2009.

[42] J. Boutros, E. Viterbo, C. Rastello, and J. C. Belfiore, "Good lattice constellations for both Rayleigh fading and Gaussian channels," *IEEE Trans. Inf. Theory*, vol. 42, no. 2, pp. 501 – 518, Mar. 1996.

[43] A. E. Gamal, "The feedback capacity of degraded broadcast channels," *IEEE Trans. Inf. Theory*, vol. 24, no. 3, pp. 379–381, Apr. 1978.

[44] S. A. Jafar and M. Fakhereddin, "Degrees of freedom for the MIMO interference channel," *IEEE Trans. Inf. Theory*, vol. 53, no. 7, pp. 2637 – 2642, Jul. 2007.

[45] C. Vaze and M. Varanasi, "The degree-of-freedom regions of MIMO broadcast, interference, and cognitive radio channels with no CSIT," *IEEE Trans. Inf. Theory*, vol. 58, no. 8, pp. 5254 – 5374, Aug. 2012.

[46] R. Tandon, S. A. Jafar, and S. Shamai, "Minimum CSIT to achieve maximum degrees of freedom for the MISO BC," Nov. 2012, available on arXiv :1211.4254v2.

[47] J. Chen and P. Elia, "Imperfect delayed CSIT can be as useful as perfect delayed CSIT : DoF and precoding schemes for BC," Oct. 2012, submitted to *IEEE Trans. Inform. Theory.*

[48] ——, "MISO broadcast channel with delayed and evolving CSIT," Nov. 2012, submitted to *IEEE Trans. Inform. Theory*, available on arXiv :1211.1622.

[49] R. Tandon, M. A. Maddah-Ali, A. Tulino, H. V. Poor, and S. Shamai, "On fading broadcast channels with partial channel state information

at the transmitter," in *Proc. Int. Symp. on Wireless Communication Systems (ISWCS)*, Aug. 2012.

[50] Y. H. Kim and A. Lapidoth, "On the log determinant of noncentral wishart matrices," in *Proc. IEEE Int. Symp. Information Theory (ISIT)*, Jul. 2003.

[51] R. J. Muirhead, *Aspects of Multivariate Statistical Theory.* New York : Wiley, 1982.

[52] G. D. Forney Jr., "On the role of MMSE estimation in approaching the information-theoretic limits of linear Gaussian channels : Shannon meets Wiener," in *Proc. Allerton Conf. Communication, Control and Computing*, Oct. 2003.

[53] R. A. Horn and C. R. Johnson, *Topics in Matrix Analysis.* Cambridge University Press, 1991.

[54] A. C. Aitken, *Determinants and Matrices*, 8th ed. Edinburgh : Oliver and Boyd, 1954.

[55] M. A. Maddah-Ali, A. S. Motahari, and A. K. Khandani, "Communication over MIMO X channels : Interference alignment, decomposition, and performance analysis," *IEEE Trans. Inf. Theory*, vol. 54, no. 8, pp. 3457 – 3470, Aug. 2008.

[56] D. N. C. Tse, P. Viswanath, and L. Zheng, "Diversity-multiplexing tradeoff in multiple-access channels," *IEEE Trans. Inf. Theory*, vol. 50, no. 9, pp. 1859–1874, Sep. 2004.